

Durham E-Theses

Algal biopolymers: Diversity of charophytic and chlorophytic cell walls

RAPIN, MARIE,NICOLE

How to cite:

RAPIN, MARIE,NICOLE (2023) *Algal biopolymers: Diversity of charophytic and chlorophytic cell walls*, Durham theses, Durham University. Available at Durham E-Theses Online:
<http://etheses.dur.ac.uk/14948/>

Use policy

The full-text may be used and/or reproduced, and given to third parties in any format or medium, without prior permission or charge, for personal research or study, educational, or not-for-profit purposes provided that:

- a full bibliographic reference is made to the original source
- a [link](#) is made to the metadata record in Durham E-Theses
- the full-text is not changed in any way

The full-text must not be sold in any format or medium without the formal permission of the copyright holders.

Please consult the [full Durham E-Theses policy](#) for further details.

Abstract - Algal biopolymers: Diversity of charophytic and chlorophytic cell walls – Marie Rapin

Charophytic green algae are an under-explored, widely diverse division of the streptophytes. Exploring their polysaccharides' properties could shine light on new under-exploited biomaterial sources. Initial experiments were performed on both early and late-diverging charophytic species; plus a bryophyte (*Anthoceros caucasicus*) and a chlorophyte (*Ulva linza*). They aimed at extracting and analysing, via classical 'land-plant methods', the different polysaccharide fractions (conventionally described as pectin, hemicellulose, and cellulose) present in algal cell walls. The bryophyte and the late-diverging charophytes (*Chara vulgaris*, Charales and *Coleochaete scutata*, Coleochaetales) showed similar features, both in terms of extractability and sugar residue compositions, to land plants. All the species were screened for the presence of the land-plant-specific polymers xyloglucan and rhamnogalacturonan-II, alongside species from the late-diverging charophytic order Zygnematales, via in vivo $^{14}\text{CO}_2$ labelling followed by enzymatic hydrolysis of their cell walls. Xyloglucan-like oligomers were visible in zygnemataleans, but the key dimer isoprimeverose could not be conclusively detected. An RG-II-like polymer was present in the cell walls of axenic *Chara* (Charales). During the initial experiment, early-diverging charophytes presented distinctive characteristics. Upon further characterisation, the extractability of the uronic acid-free 'pectic' polysaccharide in *Klebsormidium* was described. Some sections of the polymers were characterised, namely rhamnoxylan and galactoxylan. The basal species *Chlorokybus* showed the presence of the previously unknown dimer $\beta\text{-D-GlcpA-(1}\rightarrow\text{4)-L-Gal}$. Its 'pectic' fraction was found to be sulphated, contained L-Gal but not D-Gal, and was made up of two distinct polymers, different by their ionisation degree, sulphation degree, and susceptibility to hydrolysis. Finally, an investigation on the seaweed *Ulva* was conducted. In particular, the 'hemicellulosic' fraction was characterised using biochemical and spectroscopic methods: phyco-xyloglucan was found to be a linear $\beta\text{-(1,4)}$ -polymer of glucose and xylose, featuring xylose stretches up to four residues long, and with a much greater affinity for cellulose than that of many well-known land-plant-specific polymers. Overall, this work indicates the presence of previously unidentified polysaccharides in algal cell walls, making the harnessing of such widely available biomass possible and desirable.

Algal biopolymers: Diversity of charophytic and chlorophytic cell walls

Marie Rapin

A thesis prepared in fulfilment of the requirements for
the degree of Doctor of Philosophy (Ph.D.)

Department of Biosciences, Durham University

2022

Contents

Abstract - Algal biopolymers: Diversity of charophytic and chlorophytic cell walls – Marie Rapin	1
Contents	3
Tables	13
Annexes	14
Figures	14
Abbreviations.....	19
Declaration	22
Statement of copyright.....	23
Acknowledgements	24
1. Literature review	27
1.1. Background	28
1.2. About polysaccharides and land-plant cell walls.....	29
1.2.1. Cell wall polysaccharides	32
1.2.1.1. Cellulose	32
1.2.1.2. Hemicellulose	33
1.2.1.3. Pectin.....	35
1.2.1. Cell wall proteins.....	38
1.2.1.1. Generalities on cell wall proteins.....	38

1.2.1.2.	Plant cell wall enzymes	39
1.2.1.3.	Extensins	40
1.2.1.4.	Arabinogalactan proteins.....	40
1.2.1.5.	Proline-rich proteins	41
1.2.1.6.	Expansins.....	41
1.2.2.	Other cell wall biopolymers and solutes	42
1.2.2.1.	Lignin	42
1.2.2.2.	Plant cuticle.....	43
1.2.2.3.	Callose	43
1.2.3.	Plant cell wall: types, variations and organization	43
1.3.	A brief introduction to plant phylogeny. Focus on charophytic green algae... 47	
1.3.1.	From the primary endosymbiosis to plant diversity.....	47
1.3.2.	Phaeophytes (brown algae).....	50
1.3.3.	Rhodophytes (red algae).....	51
1.3.4.	Chlorophytes.....	52
1.3.5.	Charophytes.....	53
1.3.5.1.	Mesostigmales	55
1.3.5.2.	Chlorokybales.....	55
1.3.5.3.	Klebsormidiales	56
1.3.5.4.	Zygnematales	57

1.3.5.5.	Coleochaetales	58
1.3.5.6.	Charales	58
1.3.5.7.	Charophytic cell walls.....	60
1.3.5.8.	Genomes of the charophytes.....	65
1.3.6.	Bryophytes	66
1.3.7.	Lycophytes	68
1.3.8.	Pteridophytes (ferns)	70
1.3.9.	Gymnosperms	70
1.3.10.	Angiosperms: dicots.....	71
1.3.11.	Angiosperms: monocots	72
1.4.	Chemical analysis of plant cell walls: which tools?	75
1.5.	Modified plant cell walls: How and for what?.....	79
1.5.1.	Cellulose	80
1.5.2.	Hemicellulose.....	80
1.5.3.	Pectin	82
1.6.	Glossary.....	83
2.	Materials and Methods	86
2.1.	Materials	87
2.1.1.	Algae and <i>Anthoceros</i>	87
2.1.2.	Enzymes	88

2.1.3.	Chemicals and other consumables	88
2.2.	Methods.....	89
2.2.1.	Sequential extraction.....	89
2.2.2.	Hydrolysis.....	90
2.2.2.1.	Acid hydrolysis	90
2.2.2.2.	Enzymatic analysis.....	91
2.2.3.	Separation methods.....	93
2.2.3.1.	Thin-layer chromatography	93
2.2.3.1.	Paper chromatography	94
2.2.3.2.	Paper electrophoresis	94
2.2.3.3.	Gel electrophoresis	96
2.2.4.	Quantification assays.....	97
2.2.4.1.	Colorimetric test for total carbohydrates.....	97
2.2.4.2.	Colorimetric test for uronic acids.....	97
2.2.1.	Radiolabelling methodology	98
2.2.1.1.	<i>In vivo</i> ¹⁴ C radiolabelling	98
2.2.1.2.	Sodium borohydride radiolabelling	99
2.2.1.3.	Radioactivity measurement	101
3.	Sugar residue composition - semi-quantitative analysis.....	103
3.1.	Introduction.....	104

3.2.	Sequential extraction.....	105
3.3.	Monosaccharide analysis of plant extracts	107
3.4.	Pre-treatments of AIR.....	110
3.4.1.	Excessive glucose signals: de-starching plant AIR	110
3.4.1.1.	Amylase-solubilised sugars from plant AIR.....	114
3.4.1.2.	Sequential extraction on amylase-treated plant AIR.....	114
3.4.2.	Pre-solubilization of pectic carbohydrates	115
3.5.	Automated semi-quantification	119
3.5.1.	Needs for an automated analysis tool.....	119
3.5.2.	The algorithm.....	121
3.5.3.	Interpretation of the statistical analysis of the sugar contents of various plant species.....	124
3.5.3.1.	<i>Anthoceros caucasicus</i>	124
3.5.3.2.	<i>Ulva rigida</i>	128
3.5.3.3.	<i>Chara vulgaris</i>	131
3.5.3.4.	<i>Coleochaete scutata</i>	136
3.5.3.5.	<i>Klebsormidium fluitans</i>	139
3.5.3.6.	<i>Chlorokybus atmophyticus</i>	142
3.6.	Conclusion.....	144
4.	Characterization of novel cell-wall compounds and Study of <i>Chlorokybus atmophyticus</i> pectic and hemicellulosic fractions	151

4.1.	Introduction	152
4.2.	Extraction of monomers and small oligomers from cell-wall hydrolysates from preparative paper chromatograms	152
4.3.	Further chromatographic analysis of purified, non-identified eluates from PPC	155
4.3.1.	<i>Ulva</i> : electrophoretic and chromatographic analysis of fast-running cell-wall compounds	155
4.3.2.	<i>Anthoceros</i> : recognising a known cell-wall aldobiouronic acid	157
4.3.3.	<i>Klebsormidium</i> : fast-running monomers	158
4.3.4.	<i>Chlorokybus</i> : Characterization of new acidic compounds	159
4.4.	Focus on <i>Chlorokybus</i> cell-wall polysaccharides	163
4.4.1.	Pectic extract of <i>Chlorokybus</i>	163
4.4.1.1.	Enzymatic assays on <i>Chlorokybus</i> 'pectin'	165
4.4.1.2.	Separation on anion-exchange chromatography of <i>Chlorokybus</i> 'pectin'	166
4.4.2.	Hemicellulosic extract of <i>Chlorokybus</i>	170
4.4.2.1.	Enzymatic assays on 'hemicellulose' from <i>Chlorokybus</i>	170
4.4.2.2.	Mild hydrolysis assay of 'hemicellulose' from <i>Chlorokybus</i>	172
4.5.	Conclusion	173
5.	<i>Klebsormidium fluitans</i> - A fundamentally different cell wall	175
5.1.	Introduction	176

5.2.	Extractability of <i>Klebsormidium</i> 'pectin'	177
5.2.1.	Different temperatures and buffers	178
5.2.2.	Different pH and buffers	181
5.3.	Enzymatic assays on <i>Klebsormidium</i> 'pectic' extracts	184
5.3.1.	Results from pectin-specific enzymes on <i>Klebsormidium</i> 'pectic' extracts	186
5.3.2.	Results from hemicellulose-specific enzymes on <i>Klebsormidium</i> 'pectic' extracts	187
5.3.3.	Results from exo-enzymes (β -xylosidase and galactosidases) on <i>Klebsormidium</i> 'pectic' extracts	188
5.4.	Driselase dissection of <i>Klebsormidium</i> 'pectin'	189
5.4.1.	Preliminary tests of Driselase action on <i>Klebsormidium</i> 'pectin'	190
5.4.2.	Coupling α -amylase and Driselase for digestion of <i>Klebsormidium</i> 'pectin'	191
5.4.2.1.	Fraction Sol-Sol	193
5.4.2.2.	Fraction Sol-Res	193
5.4.2.3.	Fraction Res-Res	193
5.4.2.4.	Fraction Res-Sol	193
5.5.	Gel permeation chromatography for starch-freed, Driselase-digested <i>Klebsormidium</i> pectin	194

5.5.1.	Monomer composition of the oligomers produced by Driselase-digestion of <i>Klebsormidium</i> 'pectin'	195
5.5.2.	Chromatographic properties of the oligomers produced by Driselase-digestion of <i>Klebsormidium</i> 'pectin'	197
5.5.3.	Mild acid lability of the oligomers produced by Driselase-digestion of <i>Klebsormidium</i> 'pectin'	199
5.5.4.	Exo-enzyme tests on the oligomers produced by Driselase-digestion of <i>Klebsormidium</i> 'pectin'	200
5.6.	Partial acid hydrolysis of <i>Klebsormidium</i> 'pectin'	201
5.7.	Gel permeation chromatography for partially acid hydrolysed <i>Klebsormidium</i> 'pectin'	202
5.7.1.	Exo-enzymes assay on oligomers produced by partial hydrolysis of <i>Klebsormidium</i> 'pectin'	207
5.8.	Reductive radioactive labelling of reducing termini of the oligomers extracted from <i>Klebsormidium</i> 'pectin'	208
5.8.1.	Sugar monomers radiolabelling	209
5.8.2.	Sample radiolabelling	212
5.9.	Conclusion	213
6.	Land-plant-like polymers in charophytic algae	215
6.1.	Introduction	216
6.2.	Live radiolabelling: Measurements	217
6.2.1.	Radioactivity in ethanolic extracts	217

6.2.2.	Radioactivity in amylase-solubilised fractions.....	219
6.3.	XEG digestion.....	219
6.3.1.	Amounts of radioactivity extracted by XEG.....	219
6.3.2.	Analysis of XEG-solubilised oligomers	220
6.3.3.	Post-XEG extraction analysis.....	228
6.3.3.1.	Driselase dissection.....	228
6.3.3.2.	Acid hydrolysis	231
6.3.4.	Driselase product analysis for <i>Chara</i> and <i>Coleochaete</i>	234
6.3.5.	Enzymatic analysis of the alkali extracted fraction.....	238
6.4.	EPG assay.....	242
6.4.1.	Amounts of extracted radioactivity by EPG.....	242
6.4.1.1.	Chromatographic and electrophoretic analysis of EPG- released oligomers from <i>Chara</i>	244
6.5.	Conclusion.....	246
7.	<i>Ulva linza</i> cell wall: towards a modification of previous models	247
7.1.	Introduction	248
7.2.	Partial hydrolysis of <i>Ulva</i> pectic extract: characterisation of an unexpected oligomer.....	249
7.2.1.	Gel permeation chromatography of <i>Ulva</i> ‘pectin’– wide pores.....	249
7.2.2.	Gel permeation chromatography of <i>Ulva</i> ‘pectin’– small pores	251
7.2.3.	Characterisation of selected dimers extracted from <i>Ulva</i> ‘pectin’ ...	252

7.3.	<i>Ulva</i> hemicellulosic extract Hb: characterizing phyco-xyloglucan	254
7.3.1.	Xylanase assay on <i>Ulva</i> Hb.....	256
7.3.2.	Driselase assay on <i>Ulva</i> Hb	262
7.3.3.	Cellulase assays on <i>Ulva</i> Hb	269
7.3.4.	Behaviour of xylanase and cellulase	273
7.4.	<i>Ulva</i> hemicellulosic extract Hb: study of the affinity of phyco-xyloglucan for cellulose.....	277
7.4.1.	Measurement of hemicellulose/cellulose affinity.....	277
7.4.2.	Affinity of xylose for α -cellulose	279
7.5.	Conclusion.....	281
8.	Discussion: Botanical significance of unique algal polysaccharides features	283
8.1.	Charophytic and chlorophytic green algae – reminders and objectives of this thesis.....	284
8.2.	Extractability of polysaccharide fractions from plant AIR: general remarks..	286
8.3.	Features of the polysaccharide fractions from late-diverging charophytes and bryophyte	288
8.3.1.	Extractability of the polymeric fractions - link to their chemical nature..	288
8.3.2.	Presence of land-plant-like polymeric domains in ‘pectic’ fractions from late-diverging charophytes	289

8.3.3. Presence of key ‘hemicellulosic’ polymer in late-diverging charophytes.....	291
8.4. Features of the polysaccharide fractions from early-diverging charophytes and chlorophyte	292
8.4.1. <i>Chlorokybus atmophyticus</i> : study of a primordial ‘pectic’ fraction... 293	
8.4.2. <i>Klebsormidium fluitans</i> : characterisation and implication of a neutral ‘pectic’ fraction	295
8.4.3. Features of ulvan and ‘hemicellulose’ from <i>Ulva linza</i>	296
8.5. Conclusion.....	298
9. Appendix.....	300
10. Bibliography	311

Tables

Table 1: Presence of diverse polysaccharides in the different charophytes clades.	59
Table 2: Enzymes and conditions used to assay polysaccharide sugar contents	95
Table 3: Features of markers and of the main unknown compounds in both solvent mixtures.	147
Table 4: ¹ H and ¹³ C NMR spectral data of β-D-glucuronosyl-(1→4)-L-galactose.....	162
Table 5: Extractability of <i>Klebsormidium</i> “pectin”: Influence of temperature.	178
Table 6: Extractability of <i>Klebsormidium</i> “pectin”: Influence of pH.	182
Table 7: Enzymatic digestion of <i>Klebsormidium</i> pectic extract.	183
Table 8: Degradation of xylobioses with different linkages in alkali	253

Table 9: Summary of analysis of the oligomers produced by xylanase digestion of Hb <i>Ulva</i> and proposed structures.	262
Table 10: Summary of analysis of the oligomers produced by Driselase digestion of Hb <i>Ulva</i> and proposed structures.	266
Table 11: Summary of analysis of the oligomers produced by cellulase digestion of Hb <i>Ulva</i> and proposed structures.	273
Table 12: Final structures of the oligomers produced enzymatically from Hb <i>Ulva</i> and proposed structure for phyco-xyloglucan.	277

Annexes

Table a: 1H and 13C NMR spectral data of xylanase-produced oligomers from Hb <i>Ulva</i>	301
Table b: 1H and 13C NMR spectral data of Driselase-produced oligomers from Hb <i>Ulva</i>	305
Table c: 1H and 13C NMR spectral data of cellulase-produced oligomers from Hb <i>Ulva</i>	308

Figures

Figure 1: Chemical structure of the predominant building blocks of plant cell walls.	31
Figure 2: Plant plasma membrane and cell wall structure.	44
Figure 3: Main marine algae families, illustrated.	49
Figure 4: Simplified representation of general cell wall composition in the different groups of algae.	53
Figure 5: Evolution of the green plants lineage.	54
Figure 6: Main charophyte families, illustrated.	55

Figure 7: Extant members of bryophyte lineages, illustrated.....	67
Figure 8: Ferns and lycophytes occurring in China representing the morphological and ecological diversity, illustrated.....	69
Figure 9: Simplified 2D representation of general cell wall composition in the different groups of kingdom Plantae.	74
Figure 10: Scheme of the sequential extraction process.	89
Figure 11: Scheme of the live radiolabelling and de-starching processes.	100
Figure 12 : Quantities of plant extracts relative to the initial AIR quantity.	106
Figure 13: Thin layer chromatography (TLC) of the TFA-hydrolysed polymer fractions from different species.....	108
Figure 14: Ethanolic supernatants obtained from EPG, alkali and EPG, and amylase digestion of plant AIRs.	111
Figure 15: Quantities of plant extracts relative to the initial AIR quantity, after enzymatic and chemical pre-treatments.....	113
Figure 16 (see following double page) : Relative quantities of each sugar residue in the extracts from all six plants (<i>Anthoceros caucasicus</i> , <i>Chara vulgaris</i> , <i>Coleochaete scutata</i> , <i>Klebsormidium fluitans</i> , <i>Chlorokybus atmophyticus</i> , <i>Ulva linza</i>), following several pre-treatments.....	148
Figure 17: Preparative paper chromatography (PPC) of the selected algal hydrolysates.	154
Figure 18: Separation on TLC of the isolated unidentified compounds.	155
Figure 19: Analysis on paper electrophoresis of the extracts from <i>Ulva</i>	157
Figure 20: Separation of the hydrolysed and oxidised products from two aldobiouronic acids from <i>Anthoceros</i> and <i>Chlorokybus</i>	160
Figure 21: NMR spectra of β -D-glucuronosyl-(1 \rightarrow 4)-L-galactose.	163

Figure 22: Enzymatic digests of P2 of <i>Chlorokybus</i>	164
Figure 23: Separation of <i>Chlorokybus</i> P2 on anion-exchange chromatography.	169
Figure 24: Enzymatic assays on Hb of <i>Chlorokybus</i>	171
Figure 25: Mild hydrolysis assays on Hb from <i>Chlorokybus</i> , compared with starch and laminarin.....	172
Figure 26: Extractability of <i>Klebsormidium</i> 'pectin'. Influence of temperature, buffer and pH.	179
Figure 27: Separation of hydrolysed 'pectic' extracts from <i>Klebsormidium</i> AIR.	180
Figure 28: Enzymatic digestion of <i>Klebsormidium</i> 'pectic' extract with pectin specific enzymes.....	184
Figure 29: Enzymatic digestion of <i>Klebsormidium</i> 'pectic' extract with hemicellulose-specific enzymes.....	185
Figure 30: Enzymatic digestion of <i>Klebsormidium</i> 'pectic' extract with exo-enzymes.....	186
Figure 31: Driselase time-course on <i>Klebsormidium</i> 'pectin'.	191
Figure 32 : <i>Klebsormidium</i> 'pectin' digested successively with α -amylase and Driselase.....	192
Figure 33: De-starched, Driselase-digested <i>Klebsormidium</i> 'pectin' separated by gel permeation chromatography.....	195
Figure 34: Analytical TLC of GP-fractions from Driselase-digested pectin from <i>Klebsormidium</i> previously separated on preparative TLC.	196
Figure 35: Monomer composition of sub-fractions from preparative TLC.....	197
Figure 36: Chromatographic properties of sub-fractions from preparative TLC.	198
Figure 37: Acid lability of fraction 1 from preparative TLC.	200
Figure 38: <i>Klebsormidium</i> pectin hydrolysis at different acid concentrations and temperatures.....	203

Figure 39 : Separation of <i>Klebsormidium</i> pectin hydrolysate (80°C, 0.5 M TFA) by gel permeation chromatography	206
Figure 40: SEC-fractions from partially hydrolysed <i>Klebsormidium</i> pectin separated on preparative TLC, and their monomer composition revealed.....	207
Figure 41: Exo-enzyme assays on oligomers produced by enzymatic and acidic breakdown of <i>Klebsormidium</i> 'pectin'	208
Figure 42: Structures of sugars and their sodium-borohydride-reduced counterparts.	209
Figure 43: Preparation of NaB[³ H] ₄ -reduced monosaccharides.	210
Figure 44: Purification and hydrolysis of NaB[³ H] ₄ -reduced oligosaccharides extracted from <i>Klebsormidium</i> 'pectin'.....	211
Figure 45: Radioactivity released during AIR preparation and de-starching of radiolabelled algae.	218
Figure 46: Radioactivity released by XEG digestion of algal AIRs.	221
Figure 47: Separation of compounds in XEG1 extract.	223
Figure 48: Separation and hydrolysis of compounds in XEG2 to 5.	225
Figure 49: Driselase extracts of pre-XEG-digested AIR, and the impact of alkali treatment on these extracts.	230
Figure 50: Acid hydrolysis of pre-digested AIRs.....	232
Figure 51: In-depth analysis of Driselase extracts from XEG-pre-digested <i>Coleochaete</i> and <i>Chara</i>	237
Figure 52: Quantification of alkali-extracted biomass from radiolabelled AIR, and of enzyme-released oligomers from the alkali-extracted fraction.	239
Figure 53: Chromatography of enzymatic extracts from radiolabelled Hb.	242
Figure 54: Quantification of EPG-extracted oligomers from radiolabelled AIR.....	243

Figure 55: Analysis of EPG-digests from <i>Chara</i>	245
Figure 56: Gel-filtration of un-hydrolysed and partially hydrolysed pectin from <i>Ulva</i>	251
Figure 57: Gel-filtration of selected oligomers from partially hydrolysed pectin from <i>Ulva</i>	252
Figure 58: Hydrolysis and alkali assay of selected oligomers from <i>Ulva</i>	253
Figure 59: Stability of a commercial sulphated monosaccharide in acid and in alkali.	255
Figure 60: Xylanase assay on <i>Ulva</i> extracts.....	256
Figure 61: Bulk preparation of xylanase-digested Hb <i>Ulva</i>	258
Figure 62: Analysis of the oligomers produced by xylanase digestion of Hb <i>Ulva</i>	261
Figure 63: Driselase assay on Hb <i>Ulva</i> extract and hydrolysis of the released oligomers.....	263
Figure 64: Bulk preparation of Driselase-digested Hb <i>Ulva</i>	265
Figure 65: Analysis of the oligomers produced by Driselase digestion of Hb <i>Ulva</i>	268
Figure 66: Bulk preparation of cellulase-digested Hb <i>Ulva</i>	270
Figure 67: Analysis of the oligomers produced by cellulase digestion of Hb <i>Ulva</i>	272
Figure 68: Study of the behaviour of xylanase, Driselase and cellulase on commercial and <i>Ulva</i> -based oligomers.....	276
Figure 69: Study of the affinity of a range of polysaccharides for cellulose.....	278
Figure 70: Assessment of the xylose content in the α -cellulose fraction from <i>Ulva</i>	280
Figure 71: Extended phylogeny of the charophytic algae, showing the major pieces of work of this thesis.	287

Abbreviations

A	Alkali-treated AIR
A+E	Alkali-treated and EPG-digested AIR
AIR	Alcohol-insoluble residue
AGP	Arabinogalactan protein
Ara	Arabinose
B/A/W	Butan-1-ol / acetic acid / water (2:1:1 or 4:1:1, as specified)
Cell ₂ , Cell ₅	Cellobiose, cellopentaose
CGA	Charophytic green alga
2D	Two-dimensional
DP	Degree of polymerisation
Dris	Driselase
E	EPG-digested AIR
EPG	Endo-polygalacturonase
E/P/A/W	Ethyl acetate / pyridine / acetic acid / water 6:3:1:1
Fuc	Fucose
Gal	Galactose
GalA	Galacturonic acid
Genti	Gentiobiose
Glc	Glucose
GlcA	Glucuronic acid
Ha	Hemicellulose a
Hb	Hemicellulose b

HGA	Homogalacturonan
HVPE	High-voltage paper electrophoresis
IdA	Iduronic acid
IP	Isoprimeverose (α -D-xylopyranosyl-(1 \rightarrow 6)-D-glucose)
Lam ₂ , Lam ₃ , etc.	Laminaribiose, laminaritriose, etc.
Man	Mannose
ManA	Mannuronic acid
MeXyl	Methyl-xyloside
MH	Mild acid hydrolysis
MLG	Mixed-linkage glucan
Mlt ₂ , Mlt ₃ , etc.	Maltose, maltotriose, etc.
P1	Pectin 1 (rapidly solubilised from AIR)
P2	Pectin 2 (slowly solubilised from AIR)
PAGE	Polyacrylamide gel electrophoresis
PC	Paper chromatography
PPC	Preparative paper chromatography
Res	Insoluble residue
RG-I	Rhamnogalacturonan-I
RG-II	Rhamnogalacturonan-II
Rha	Rhamnose
Rib	Ribose
R _f	$\frac{\textit{distance travelled by compound}}{\textit{distance travelled by solvent}}$

R_{MeXyl}	$\frac{\textit{distance travelled by compound}}{\textit{distance travelled by MeXyl}}$
Sol	Soluble fraction
TFA	Trifluoroacetic acid
TLC	Thin-layer chromatography
W	Wash
XEG	Xyloglucan endo-glucanase
XGO	Xyloglucan oligosaccharide
XyG	Xyloglucan
Xyl	Xylose
Xyl ₂ , Xyl ₅	Xylobiose, xylopentaose
α A	α -amylase-digested AIR
α C (or AC)	α -cellulose

Declaration

This thesis has been composed by myself and the work of which it is a record has been carried out by myself. All collaborations and sources of information have been acknowledged and referenced.

Marie Rapin, Edinburgh, 2022

Statement of copyright

The copyright of this thesis rests with the author. No quotation from it should be published without the author's prior written consent and information derived from it should be acknowledged.

Acknowledgements

Firstly, I would like to thank my supervisors Prof Stephen Fry and Dr John Bothwell. Steve, I cannot be grateful enough for welcoming me into the laboratory in Edinburgh and for all the time spent reviewing multiple submissions and discussing numerous faulty experiments. John, thanks for the continuous support from afar and for continuously dealing with the pressures and the unplanned of the past four years.

This endeavour would not have been possible without SOFI CDT, who financed my research and provided a fantastic learning environment when I first arrived in the UK.

I am especially grateful to all the members of my SOFI cohort, and for the shared support and friendships that made this endeavour so enjoyable. Thanks should also go to my labmates and fellow students from IMPS, for all the stimulating discussions over countless lab meetings, coffees, and lunch breaks.

I would like to extend my acknowledgements to Dr. Ian Sadler and Dr. Lorna Murray, from the chemistry department, for their indispensable help. Without them, major parts of this thesis would simply not exist.

Finally, my deepest appreciation goes to the friends and many extraordinary people I have met along the way, starting with my housemates Sam and Veronica. The former for handling a two-person three-month-long lockdown, the latter for always being an example of determination and joy. I could never forget the many outdoor adventures shared with Holly, nor the unique friendship developed with Chris over the years. It would also be amiss not to mention Mike, who filled these last few months with happiness and optimism.

Lastly, none of this would have been possible without my family, their support, love and inspiration through the highs and lows encountered along the way.

To my parents

1.Literature review

1.1. Background

Plants are central in society, as they are used in a multitude of domains and for multiple applications.

The most obvious one is feeding, for both humans and animals. However, plants are also used in building, clothing, cosmetics, energy production . . . This wide range of applications encompasses only a fraction of the plant kingdom: the land plants. It is then understandable that the major part of plant science research has focused on those organisms. It is worth noting, however, that some algae have also received attention: the brown and red algae, which produce respectively alginates and carrageenans, are useful in pharmaceutical or rheological applications (Albersheim *et al.* 2011; Stiger-Pouvreau *et al.* 2016).

Many plant applications are based on specific sets of properties: mechanical, insulating, or gelling abilities for example. Those properties come from the plant cell walls. As a consequence, these cell walls have been widely studied over the past fifty years. Their biochemical architecture has been (partially) unravelled and their biosynthetic mechanisms studied. Land plants are considered, in this work, as the reference model for composition and interactions within the cell wall matrix.

The clade this review focuses on is the charophytic green algae. They are considered as the closest relatives to land plants, which is the main reason of their study (Popper *et al.* 2011). However, research on the matter is sparser than what one would expect. This can be

explained by the fact that charophytes do not currently have many uses for humans. They have been proposed a few times as phytoremediators or pollution indicators, as they are able to absorb appreciable quantities of heavy metal ions, but this remains marginal (Triboit *et al.* 2010; Sooksawat *et al.* 2016). Likewise, their ability to survive in harsh environments has been pointed out (Gyure *et al.* 1987; Karsten *et al.* 2013, 2016). A few studies have been conducted on their cell wall chemistry and indicate that surprising sidechain modifications and structures occur in certain algae, possibly of commercial value (Popper *et al.* 2003; O'Rourke *et al.* 2015). Such findings could lead to re-examining the use of charophytes by humans, as they represent a resilient and easy to sustain source of biomass.

In this review, the different components of plant cell walls and their respective roles will be detailed. Then basic plant phylogeny will be explained, in order to make the interest of charophytes clearer. The specific features of charophytic cell walls will be reviewed, as well as their links with land plants. Finally, a short summary of the available analytical methods will be provided.

1.2. About polysaccharides and land-plant cell walls

Polysaccharides are a class of materials widely produced by living organisms. They are biopolymers, which means that they are made of a high number of repeating units (sugars in this case) attached together by glycosidic linkages. Their structure is highly variable, as they

can be linear (e.g. cellulose), heavily branched (e.g. starch), of variable length, or even attached to other biopolymers such as proteins (Albersheim *et al.* 2011).

Because of this complexity, polysaccharides fulfil many different roles across the living world. For example, they are the most accessible energy storage resource for animals and plants, under two similar forms: glycogen and starch (Kaplan 1998). They also play essential roles in the cell metabolism, where they can act as adhesive agents or retention agents for example (Karunaratne 2012).

In plants and fungi, polysaccharides are the main component of the cell wall. Indeed, just like animal cells, plant and fungal cells are immersed in an extracellular matrix, which can either be described as the assembly of each individual cell coating, the cell walls, or as a continuum, the apoplast (Gow *et al.* 2017). The cell wall is distinct from the cell membrane, both in composition (polysaccharides versus lipids and proteins), and in thickness (0.1 to 10 μm versus under 0.01 μm) (Keegstra 2010; Fry 2017; Lampugnani *et al.* 2018). The cell wall participates in the cells' shaping and growth; it also acts to protect the organism from external stresses and plays a role in intercellular communication (Vorwerk *et al.* 2004; Wolf *et al.* 2012; Malinovsky *et al.* 2014). Cell walls in plants contain mainly polysaccharides, but also proteic biopolymers (in a lower proportion than fungal cell walls), as well as additional compounds detailed in Section 1.2.2.

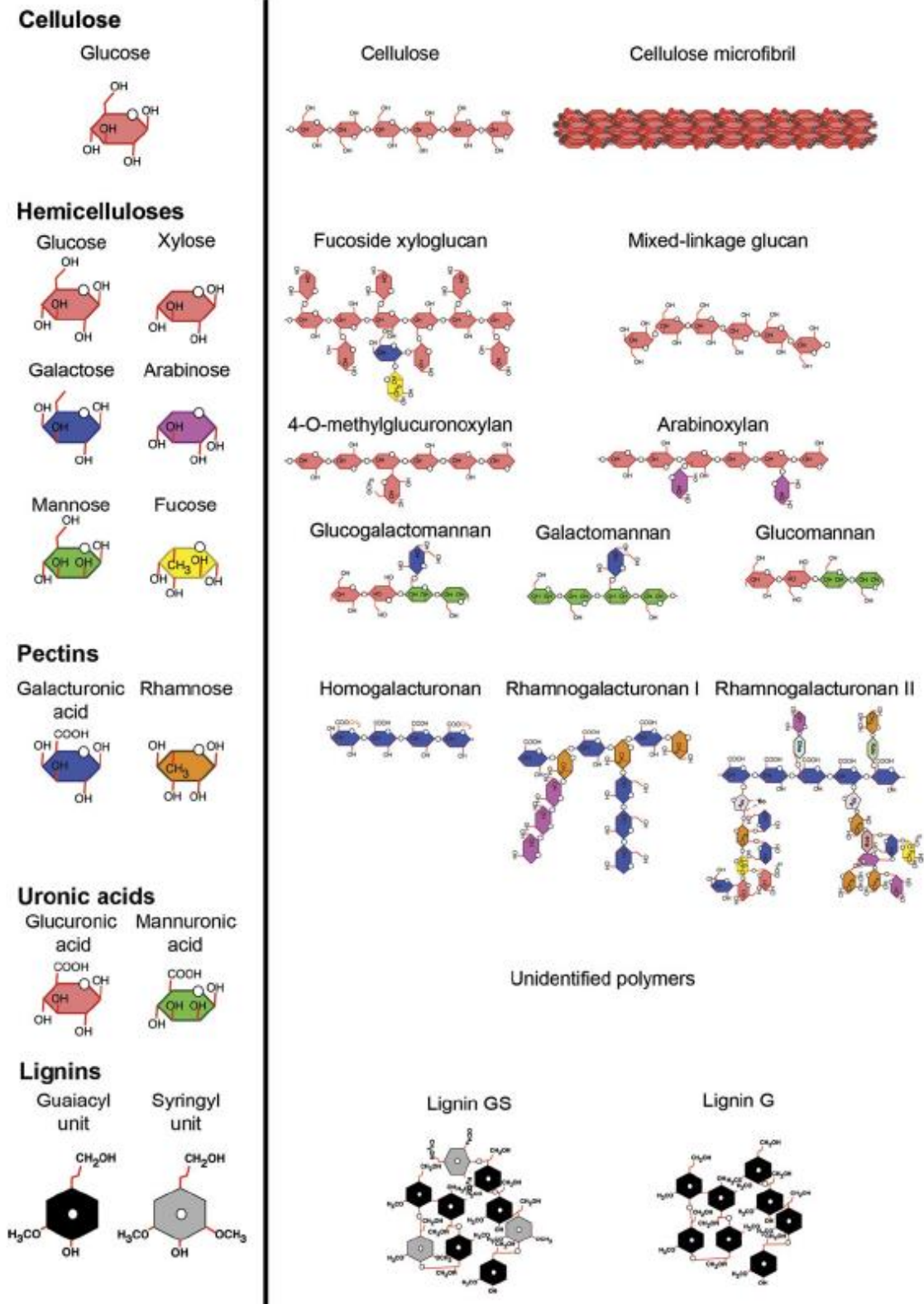


Figure 1: Chemical structure of the predominant building blocks of plant cell walls.
 Left panel: monomers. Right panels: polysaccharide domains. Reproduced from (Sarkar et al. 2009).

1.2.1. Cell wall polysaccharides

Cell wall polysaccharides from land plants can traditionally be divided into several classes, depending on their extractability in different solvents and/or their general chemical composition (Fry 2000; Albersheim *et al.* 2011). These classes, namely cellulose, hemicellulose and pectin, are described below. The main structures are visible on Figure 1.

1.2.1.1. Cellulose

Cellulose is the most abundant substance on Earth and the least soluble component of the cell wall, remaining solid after several extraction steps of the cell wall.

It is difficult to hydrolyse, and extremely resilient: crystalline cellulose presents an axial elastic modulus comparable to carbon fibres (about 150 GPa), and remains stable up to 300°C (Kim *et al.* 2010; Moon *et al.* 2011) It is responsible for providing strength and rigidity to the cell wall. From a mechanical point of view, it can be compared to the metal rods in reinforced concrete. Chemically, cellulose is a linear polymer made of β -D-Glc units, linked together via (1→4) glycosidic linkages. The polymer strands assemble into microfibrils and crystallize into straight fibres parallel to each other within a layer of the cell wall (Sarkar *et al.* 2009; Kim *et al.* 2010; Moon *et al.* 2011).

Cellulose synthesis is interesting, as the protein complex and genes (*CesA*) involved are similar across the plant kingdom and beyond. The *CesA* family originates from bacteria, and

in land plants the corresponding protein complex is always arranged in 6-units rosettes at the plasma membrane. The size of these rosettes define the thickness of the cellulose microfibrils: the more units, the more polymer strands, the thicker the microfibril. This arrangement differs in algae, ranging from linear arrays and stacked linear arrays in rhodophytes and chlorophytes for example (red and green algae), to a 9-units rosette in *Coleochaete* and even a 6-units rosette in *Nitella* (both charophytes)(Niklas 2004; Mikkelsen *et al.* 2014; Borowitzka *et al.* 2016).

1.2.1.2. Hemicellulose

Hemicelluloses, thanks to their neutral nature, interact strongly with the straight cellulose fibres and are thought to form a network to hold them together, whilst avoiding aggregation (Scheller and Ulvskov 2010). The specifics of those interactions are disputed: do hemicelluloses coat the microfibrils, or are they “sandwiched” in strategic mechanical hotspots? Are they interacting with cellulose only via hydrogen bonding, or are they also covalently linked (Cosgrove 2014)? From a biochemical point of view, hemicelluloses are diverse and involve in land plants a variety of different polysaccharides such as xyloglucans, xylans, mannans and mixed-linkage glucans (Scheller and Ulvskov 2010; Schultink *et al.* 2014). They are extractable by strong alkali solutions (Fry 2000).

1.2.1.2.1. Xyloglucan

Xyloglucan is made of a skeleton of β -(1→4)-D-Glc units, just like cellulose. This skeleton is highly substituted by D-xylose residues on O-6, but also by other characteristic groups

involving D-galactose and L-fucose, and much more rarely L-arabinose and D-galacturonic acid. It also displays acetyl ester groups, distributed along the Glc units of the backbone and the Gal sidechains. This composition varies widely between different groups and different species (Schultink *et al.* 2014). Xyloglucan was initially thought to be key for the cell's growth and structure, as it has been represented as the polymer cross-linking the cellulose fibres, hence fabricating a mechanically resistant 'tethered' network. However, this role might be more restricted than previously thought: some experiments on *Arabidopsis* tend to prove that modifications in plants growth are limited in the absence of detectable xyloglucan (Cavalier *et al.* 2008; Park and Cosgrove 2012; Schultink *et al.* 2014). The xyloglucan-cellulose interactions detected by NMR are sparse, while cellulose and pectin seem to have more extensive contact (Dick-Pérez *et al.* 2011). It is possible that xyloglucan, in flowering plants, is covalently linked to pectin, thus changing the widely accepted cell wall model (Popper and Fry 2005). Xyloglucan might have other functions, such as supplying energy for the seeds of plants and acting as a source of signalling molecules (Caffall and Mohnen 2009).

1.2.1.2.2. Xylan and derivatives

Xylans are the second most abundant hemicellulose in embryophyte primary cell walls. They are made of a skeleton of β -(1 \rightarrow 4)-D-Xyl units, sometimes acetylated on O-2 and O-3. They are substituted in land plants by various sugar residues such as L-arabinose and D-glucuronic acid or even 4-O-Me-D-glucuronic acid. These substituents are attached via (1 \rightarrow 3) glycosidic linkages to the backbone, and display acetyl groups. The resultant polysaccharides are often renamed, for example as arabinoxylan, glucuronoxylan, glucuronoarabinoxylan.

1.2.1.2.3. *Mannan and derivatives*

Mannans display a skeleton made of β -(1 \rightarrow 4) linked D-mannose residues. They can be substituted in many different ways. Glucose residues can be included in their backbone, making glucomannans. They can also be substituted by galactose residues, which makes them galactomannans. Non-substituted mannans have a structure similar to cellulose's, and are playing a similar structural role in some seaweeds (Caffall and Mohnen 2009).

1.2.1.2.4. *Mixed-linkage glucan*

Mixed-linkage glucans are made of glucose residues connected via glycosidic β -(1 \rightarrow 3) and β -(1 \rightarrow 4) linkages. They are often organised as trimers or tetramers of (1 \rightarrow 4)-Glc residues, interspersed with (1 \rightarrow 3) linkages. They are capable of forming gels (Lazaridou *et al.* 2004).

1.2.1.3. *Pectin*

Pectin is made of a variety of polysaccharide domains, and can amount for up to 50% of the dry weight of the cell wall (Albersheim *et al.* 2011). It is characterized by a particularly high proportion of galacturonic acid, and is capable of forming gels (Caffall and Mohnen 2009; Fraeye *et al.* 2010). It is extractable with chelating agents such as oxalate (Fry 2000). Pectin, with hemicelluloses, form the matrix of the plant cell wall. It is partly responsible for the shaping of the cell during its growth, is central in cell-cell adhesion and plays a role in the defence against pathogens (Jarvis *et al.* 2003; Wang *et al.* 2023). Pectin is considered the most complex class of carbohydrates, as it involves many sugar residues and domains, and fulfils numerous different roles. However, it is important to note that the term pectin does

not designate a variety of independent polysaccharides with similar properties, but rather the domains, linked to each other via covalent glycosidic bonds, of one giant polysaccharide molecule.

1.2.1.3.1. *Homogalacturonan*

Homogalacturonan is made of α -(1→4)-D-galacturonic acid residues, often methyl-esterified on C-6 carboxyl and acetylated on O-2 or O-3. It has the ability to form gels when combined with divalent cations such as Ca^{2+} , and is often used as such in foods. Indeed, stretches (more than 10) of non-substituted GalA bind to each other via those divalent cations in a so-called “egg box model”. It is then natural that the degree of substitution of homogalacturonan strongly impacts its mechanical behaviour (Fraeye *et al.* 2010). However, other factors might also influence pectin’s gelling, such as the presence of neutral sidechains from other pectic domains (Gawkowska *et al.* 2018). It is considered key in cell-cell adhesion, regulation of cell-wall pores and permeability, and cell-substrate adhesion (Domozych and Domozych 2014; Domozych *et al.* 2014). Some research has hinted that homogalacturonan might also be bound to other wall polysaccharides, such as xyloglucan (Popper and Fry 2005; Fry 2011).

1.2.1.3.2. *Rhamnogalacturonan-I*

Rhamnogalacturonans are especially important, as a major evolutionary feature of streptophytes (land plants). Rhamnogalacturonan I (RG-I) is a branched polysaccharide, with a backbone made of alternating units of galacturonic acid and rhamnose, \rightarrow 4)- α -D-GalA-(1→2)- α -L-Rha(1→. The acidic residues are often acetylated on O-2 or O-3. This

polysaccharide domain is highly substituted, mainly on the O-4 of the rhamnose residue, by galactose, arabinose and fucose residues, organized in more than 40 different sequences. The more abundant sidechains are arabinans α -(1→5) linked, galactans β -(1→4) linked, and arabinogalactans. RG-I structure varies widely across the land plants, suggesting adaptation to the species' requirements. RG-I might interact with cellulose, in a similar way xyloglucan does, and cross-link the microfibrils, via its neutral sidechains (Zykwinska *et al.* 2007, 2008).

1.2.1.3.3. *Rhamnogalacturonan-II*

Rhamnogalacturonan II (RG-II) is the most complex polysaccharide domain known. Its molecular mass is low (5 kDa) and it displays a backbone of α -(1→4)-D-galacturonic acid residues. It is substituted by at least eleven different glycosidic residues, the most common ones being D-galacturonic acid, D-glucuronic acid, L-rhamnose, D-galactose, L-arabinose, and L-fucose. They are organized in multiple different sequences. RG-II is known to form dimers through borate ester bonds, via the apiose residues on one of its larger sidechains. The absence of boron in the plant's media results in abnormal morphology and mechanical properties (O'Neill *et al.* 2004; Séveno *et al.* 2009). RG-II might be important for pectin's gelling ability, as it would reinforce and supplement the homogalacturonan "egg box" gel. Its structure is highly conserved through the land plants, suggesting that it plays a major role within the cell wall (Caffall and Mohnen 2009). RG-II is generally found close to the plasma membrane in cell walls, hence it probably does not play a major role in cell-cell adhesion (Jarvis *et al.* 2003).

1.2.1.3.4. *Substituted homogalacturonans*

Substituted homogalacturonans, which do not correspond to the well-known RG-II, can be found across the plant kingdom. The most well-known are xylogalacturonan and apiogalacturonans. Xylogalacturonan is made of an α -(1→4)-D-GalA backbone, generally substituted by xylose residues, either monomers or oligomers, on O-3. Apiogalacturonan display a similar backbone, substituted on O-2 and O-3 with apiose residues, either monomers or dimers (Caffall and Mohnen 2009). Those pectic domains can be considered as variations of the usual domains detailed above, useful for the species' specific needs. Indeed, the sidechains and lateral substitutions modulate the pectin's gelling capacities and interactions with other biopolymers (Gawkowska *et al.* 2018).

1.2.1. Cell wall proteins

1.2.1.1. Generalities on cell wall proteins

Plant cell walls also possess non-polysaccharide components, such as proteins, glycoproteins and proteoglycans. They represent about 5-10% of the dried cell wall, and fulfil a number of different roles, sometimes more than one at a time (Showalter 1993; Cassab 1998; Lee *et al.* 2004). Plant cell wall proteins can be classified in several different ways. Amongst these ways, their degree of interaction with other cell wall components is the simplest: soluble, unbound proteins that move freely in the extracellular space; weakly bound proteins (ionic bonds, Van der Waals interactions) that can be extracted from the cell wall with high ionic strength solvents; and proteins covalently linked to polysaccharides, much harder to access.

The difficulties of extraction and purification of cell wall proteins have been a source of trouble for scientists over the years (Jamet *et al.* 2006, 2008).

1.2.1.2. Plant cell wall enzymes

Plant cell wall enzymes are abundant, as they are primordial in polysaccharide turnover and reorganization, accompanying the stages of cell growth (Fry 2001; Minic 2008). Known cell wall enzymes are registered in the Carbohydrate-Active EnZymes (CAZy) database, based on the different roles they fulfil, all closely regulated *in vivo*: glycosidases, glycosyltransferases, peroxidases, esterases etc (Fry 1995; Gilbert 2010; Rose and Lee 2010).

Some of the most common cell-wall active enzymes include pectin methylesterases and pectin acetylerases, which are capable of changing the charges present on homogalacturonan, thus directly having an impact on the jellifying and mechanical properties of the cell wall (Sénéchal *et al.* 2014). These enzymes can be found throughout the charophytes, for examples in members of the genus *Chara* (Domozych *et al.* 2010). Other pectin-active enzymes can have a strong impact on plant tissues mechanic properties, such as pectate lyases during ripening and softening (Al Hinai *et al.* 2021).

Cell-wall modifying enzymes are usually active in very precise areas of the cell wall. For example, specific transglycanases are only presence in growth zones and at a certain age in land plants and in charophytic algae (Albersheim *et al.* 2011; Herburger *et al.* 2018).

However, the presence of cell wall-modifying enzymes is not always proof of their activities, as the conditions may be wrong (non-optimal pH for example), or the corresponding substract may be absent from the area or even from the plant. In charophytes in particular, land plant cell wall modifying enzyme may be present without the associated target

polymer, thus showing that the algae were pre-adapted to the transition to land plants (Mikkelsen *et al.* 2014). Thanks to the progress of genomics and the sequencing of new charophytes genomes, paired with transcriptomics, the list of known cell wall active enzymes in charophytes is becoming more precise and allow for a better comprehension of their similarities with land plants (Jiao *et al.* 2020).

1.2.1.3. Extensins

Extensins are amongst the major plant proteins, as they play an important structural role by strengthening the cell wall, both during and after cell growth and in response to pathogens and stress. They are hydroxyproline-rich glycoproteins (HRGPs), with about 50% of their weight as carbohydrates (Linskens and Jackson 1989). They present a rod-like helical structure, stabilized by their carbohydrate sidechains. Extensins' isoelectric point is approximately 9, which means that they are positively charged within the cell wall (opposite to the negative charge of de-esterified pectin) (Rose 2003). It is however unclear yet how extensins interact with the pectic matrix.

1.2.1.4. Arabinogalactan proteins

Arabinogalactan proteins (AGPs) also are glycoproteins, with only 1-10% of their weight being the amino-acid backbone (rich in hydroxyproline residues), the rest being carbohydrate sidechains. They are easily detectable thanks to their interaction with β -glycosyl Yariv reagent (Clarke *et al.* 1979; Lopes Leivas *et al.* 2016). "Classical" AGPs feature a GPI (glycosylphosphatidylinositol) anchor, which can be cleaved by phospholipases in order to release the protein into the extracellular matrix. "Non-classical" AGPs seem to lack this

feature; they are also less heavily glycosylated. Their structure is uncertain, as it might be either “wattle blossom”, globally spheroidal, or “twisted hairy rope”, implying a rod-like structure) (Rose 2003). They are important for cell-cell recognition, signalling and cell-cell adherence. They might also play a structural role by mediating pore size in the cell wall (Jarvis *et al.* 2003).

1.2.1.5. Proline-rich proteins

Proline-rich proteins (PRPs) are minimally, if not, glycosylated. They seem to play a role in wound responses and in cell growth and development, though it is not clear how. Glycine-rich proteins (GRPs) are not glycosylated and do not contain any hydroxyproline, by contrast with many other non-enzymatic wall proteins. They seem to be important in wound and cold responses (Cassab 1998; Rose 2003).

1.2.1.6. Expansins

Expansins, discovered in the nineties, play a major role in cell expansion by loosening interactions between hemicellulose and cellulose fibres within the cell wall. They work in close association with a wide range of enzymes acting on carbohydrates, such as glycosidases and transglycosidases (Cosgrove 1993, 2000a; b, 2015).

1.2.2. Other cell wall biopolymers and solutes

Cell walls also possess some additional polymers, only found in certain specific cases, depending on the cell function or the phylogenetic group the plant belongs to. Lignins and polyesters are the major categories of these additional components. Water can make up to 70% of the algal wall fresh weight, whereas its presence will be reduced to 40% in some woody tissues. Cell walls also contain a variety of mineral ions such as boron or calcium ions, which participate in biopolymer cross-linking.

1.2.2.1. Lignin

Lignins are aromatic compounds, covalently linked to certain cell wall polysaccharides (cellulose and hemicellulose). Chemically, lignin can be made of three different types of monomers: “H” unit, or *p*-hydroxy phenyl propanol, “G” unit, or guaiacyl propanol, and “S” unit, or syringyl alcohol (Ponnusamy *et al.* 2019). The ratio of those units change widely, depending on the clade studied. Lignins participate in keeping the plant’s mechanical integrity, protecting the cell wall’s polysaccharides against hydrolysis and protecting the plant against external stresses such as biological attacks (Albersheim *et al.* 2011; Popper *et al.* 2011; Cosgrove and Jarvis 2012). They are widely studied for their potential industrial applications, such as biofuels (Ghaffar and Fan 2013; Ponnusamy *et al.* 2019).

1.2.2.2. Plant cuticle

The plant cuticle is a layer found on the aerial parts of the plant (leaves, stems and flowers), useful to reduce non-stomatal water losses, but also as barriers against UV radiation, insect attack, and bacterial and fungal pathogens (Reina-Pinto and Yephremov 2009; Ahmad *et al.* 2015). They are made of a mixture of cell wall polysaccharides, cutin, cutan, waxes and aromatic compounds. Cutin is a polyester formed by the assembly of several long-chain aliphatic hydroxy-fatty acids, and cutan is of polymethylenic nature. Waxes possess both crystalline and amorphous domains and contain a wide variety of building blocks (long-chain aliphatics, such as alkanes, alcohols, aldehydes, fatty acids and esters, variable amounts of cyclic compounds such as triterpenoids) (Heredia-Guerrero *et al.* 2014; Serrano *et al.* 2014).

1.2.2.3. Callose

A more specific polysaccharide from plant cell walls is callose (linear β -(1 \rightarrow 3) glucan). It is thought to be key in developmental processes, intercellular communication and wound response (Piršelová and Matušíková 2013). Its presence is highly modulated by the external stresses the plant/alga is submitted to (Albersheim *et al.* 2011; Herburger and Holzinger 2015).

1.2.3. Plant cell wall: types, variations and organization

The relative quantities of the polymers described above vary widely depending on the stage of growth of the cell, its function and its species. Nevertheless, it is possible to distinguish

three main cell wall domains with distinctive features, as shown in the scheme displaying the overall organisation of cell wall compounds on Figure 2.

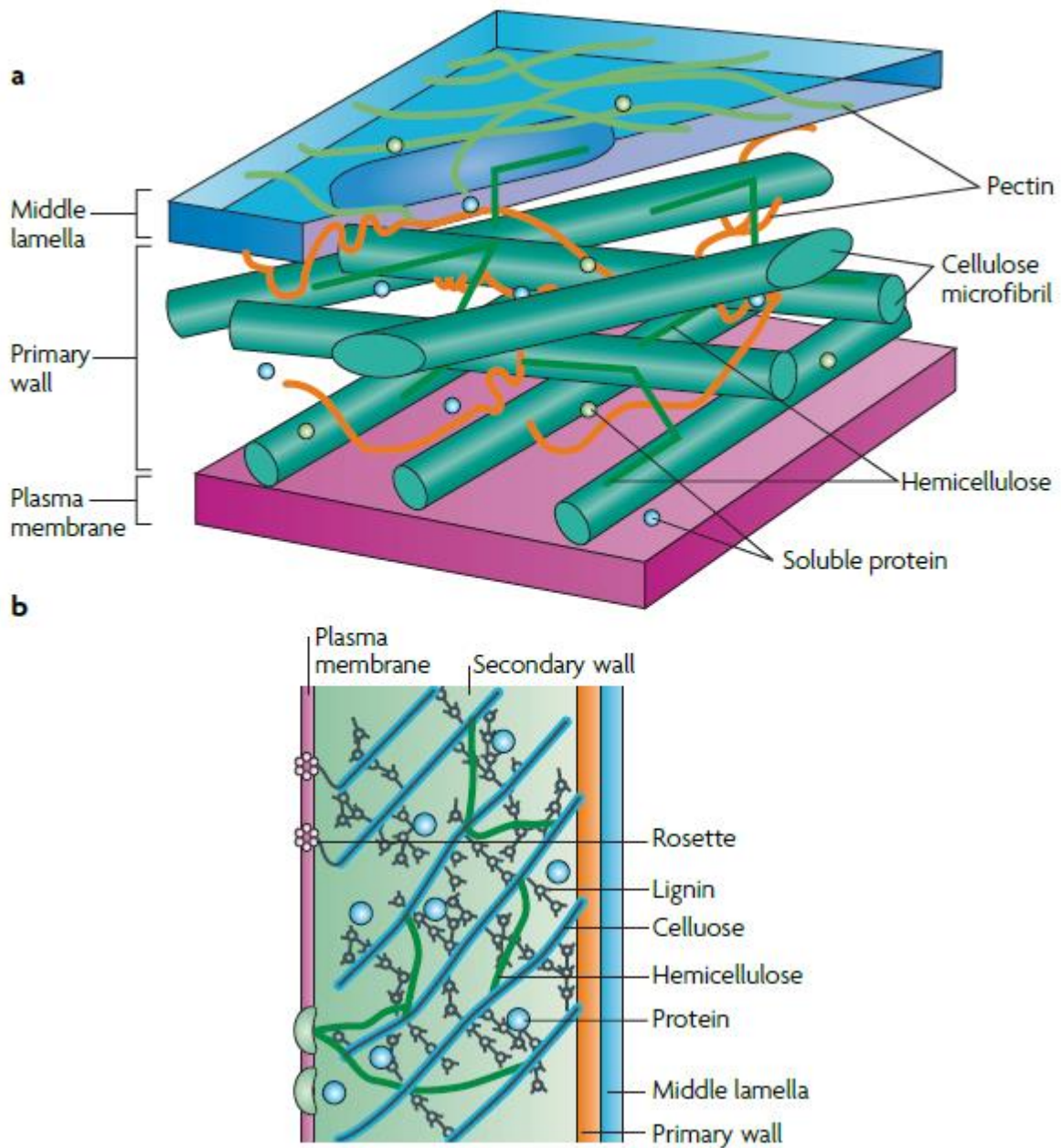


Figure 2: Plant plasma membrane and cell wall structure.

(a): Primary cell wall containing cellulose microfibrils, hemicellulose, pectin, lignin and soluble proteins. (b): Primary and secondary cell wall structure. Cellulose synthase enzymes are in the form of rosette complexes, which float in the plasma membrane. Reproduced and adapted from (Sticklen 2008).

Primary cell walls are built during the growth of the cell: they are capable of sustaining extension by taking in new material and stretching the pre-existent one, without bursting under turgor pressure. The primary cell wall is generally well hydrated and contains, approximately (on a dry weight basis) 30-50% pectins, 15-40% cellulose, 20-30% hemicellulose, and lesser amounts of proteins and glycoproteins. It can also become impregnated with lignin or waxes, once cell expansion has stopped (Somerville *et al.* 2004; Fry 2011; Cosgrove and Jarvis 2012).

The secondary cell wall is only present in certain cell types such as vessels, sclerenchyma and phellem in wood. It is built after the cell has stopped growing, it is therefore deposited on the inside of the primary cell wall. It thickens the cell wall and makes the cell stronger and inextensible, capable of withstanding both positive and negative pressures. The secondary cell wall is mainly made of cellulose, lignin (in certain cases) and hemicelluloses, and is much less hydrated than the primary cell wall (only about 30% water) (Fry 2011; Cosgrove and Jarvis 2012).

The middle lamella is the domain that binds two cells together; it is at the outer edge of the primary cell wall. It is particularly rich in pectin, primordial in cell-cell adhesion (Jarvis *et al.* 2003). Indeed, homogalacturonan and Ca^{2+} are co-localized in the middle lamella, and cell separation is induced by treatment with pectinases or Ca^{2+} chelating agents.

The key element to understanding the growth and the properties of the plant cell wall is its biochemical structure. How do the different elements described above interact with each other? Many models have been developed over the years, and they are in constant evolution. All of them agree in representing the cellulose microfibrils as the backbone of the cell wall, because of their length and their incomparable mechanical properties. The microfibrils would be cross-linked by hemicelluloses, and especially xyloglucan in primary cell walls. Finally, pectins make up a hydrogel in which this network is immersed. Extensins might form a secondary exoskeleton around the cell (Albersheim *et al.* 2011; Fry 2011).

However, the specifics of the interactions between these different elements are highly disputed. The degree of interaction between components is subject to questions. An early hypothesis represented all the polysaccharides as being covalently linked to each other (apart from cellulose) (Keegstra *et al.* 1973). Later, the widely accepted model became the tethered network model, with xyloglucan and cellulose interacting strongly to form a network, and pectin making up a gel around it. The interaction between cellulose and xyloglucan is controversial. It was initially thought that the microfibrils were coated by xyloglucan, in what is called the “sticky network model” (McCann and Roberts 1991; Carpita and Gibeaut 1993). It is now hypothesized, thanks to studies about cell expansion, that those interactions are reduced to mechanical hotspots where microfibrils and hemicellulose come in close contact (Park and Cosgrove 2012). Whether or not pectin itself interacts with cellulose and hemicellulose, either via hydrogen bonding or covalent linking, is another enigma to unravel (Popper and Fry 2005; Zykwincka *et al.* 2008; Wang and Hong 2016; Wang *et al.* 2016).

These are but a few examples of questions remaining about the structure of the plant cell wall. Moreover, the relative quantities and the way those interactions are regulated are subject to changes depending on the stage of growth of the cell, its environment, its function, and the localization with regard to the cell. The place of the organism studied in plant phylogeny also greatly influences the cell wall composition, leading to variations in chemical and physical interactions, and to different properties. The object of study of this thesis is the **charophytic green algae**, which occupy a very special place in the plant phylogenetic tree and whose wall features are not well described. These organisms will be described further, their cell wall particularities detailed.

1.3. A brief introduction to plant phylogeny. Focus on charophytic green algae

1.3.1. From the primary endosymbiosis to plant diversity

Plants can be defined as photosynthetic eukaryotes, meaning they have cells with a nucleus surrounded by a complex nuclear membrane and organelles, and are capable of using light as a source of energy for biomass production. Many other features define a photosynthetic eukaryote but these are the main and simplest ones. This definition includes many clades: brown algae, red algae, green algae and land plants (Niklas 2004; Popper *et al.* 2011). They are all thought to have evolved following a primary endosymbiotic event between a cyanobacterium (prokaryote organism capable of photosynthesis) and a eukaryotic cell. This

event, which happened about 1.5 billion years ago, gave birth to green and red algae. It is also believed that it brought the first bricks to cell wall history, in spite of major differences in cell wall compositions. Later on, an independent secondary endosymbiotic event gave birth to brown algae. Many studies have been conducted on red and brown algae, as they produce carrageenans and alginates, two polysaccharides widely studied for their applications in foods and medicine (as thickener or antibacterial for instance). We will focus here on green algae and their descendants, from bryophytes to vascular land plants. Green algae are also called Viridiplantae, and they are the only group of plants exclusively originating from primary endosymbiosis. They are divided into two classes, the chlorophytes and the streptophytes (i.e. charophytes and land plants), which diverged about a billion years ago (Stewart and Mattox 1975). Chlorophytes are green algae, found in marine, freshwater and dry environments. They form a widely diverse group of different sizes and morphologies. Examples of algae living in marine environments, from a variety of groups, is displayed in Figure 3.

Amongst streptophytes, all land plants are found: bryophytes, ferns, flowering plants. They are thought to have evolved from an aqueous environment to a dry one over 400 million years ago. The first plants to conquer dry earth are believed to have been small thalloid bryophytes, without vascularization (Harholt *et al.* 2016). It is disputed whether certain cell wall innovations, such as the invention of the pectic domain rhamnogalacturonan-II, followed or drove terrestrialization (Harholt *et al.* 2016). The vascularization of plants, and the appearance of seeds, fruits, and flowers led to the diversity of the vegetation observable nowadays. Most of the cell wall knowledge comes from the study of angiosperms and

gymnosperms. However, the few studies available on other land plant clades (bryophytes, pteridophytes, and lycopodiophytes) point towards similar compositions.

Charophytic green algae are also part of the monophyletic group Streptophyta. They are a group of green algae with low levels of cell differentiation, occupying a wide range of environments (Hall and Delwiche 2007). Charophytes and chlorophytes diverged about a million years ago, and the earliest charophytes were exclusively aquatic. Land plants have very probably evolved from these organisms, as many charophytes present land-plant features. Thus, charophytes are thought to be representative of the earliest embryophytes (Graham *et al.* 2012; Domozych *et al.* 2016).



Figure 3: Main marine algae families, illustrated.

Representatives of the major lineages of marine multicellular algae: (a) *Codium fragile*, Chlorophyceae; (b) *Chondrus crispus*, Rhodophyta; (c) *Porphyra umbilicalis*, Rhodophyta; and (d) *Ectocarpus siliculosus*, Phaeophyceae. Reproduced from (Popper *et al.* 2011).

The main groups of algae and land plants are described below, in order to give to the reader an overview of the relationships within the plant kingdom. In all these groups, cellulose plays a major role as the fibrillary component of the cell wall. However, the cellulose machinery and its degree of crystallinity is variable (Niklas 2004).

1.3.2. Phaeophytes (brown algae)

Brown algae are a class of about 2 000 species, most of them occupying marine environments. Only 7 are known to live in freshwater. They are multicellular organisms, either uniseriate, multiseriate or forming a crust from branched filaments. Their size varies from microscopic to several meters. Their colour is due to the presence of carotenoids and tannins, which might be useful in herbivorous or UV-light resistance. Brown algae storage carbohydrate is not starch, but laminarin, β -(1 \rightarrow 3)-glucan with β -(1 \rightarrow 6)-Glc branches. Brown algae can form extensive assemblies capable of contaminating beaches. They are considered phylogenetically independent from green algae and display important differences at several levels (Necchi 2016).

They have been extensively studied because of their cell wall polysaccharides. Cellulose represents less than 10% of the cell wall. The rest is made up by anionic polysaccharides, amongst which algin (or alginic acid), fucoidan and fucin. Algin, and its salt known as alginate, has attracted attention because of its medicinal properties and applications in food

industry. Fucoidan and fucin are both heavily sulphated fucose-containing polysaccharides (Sahoo and Seckbach 2015).

1.3.3. Rhodophytes (red algae)

Red algae, like brown algae, are primarily marine: only about 3% of their 6 500-10 000 species occupy freshwater habitats. They are considered as a sister group to Viridiplantae. Their size ranges from micrometric, up to about 1 m. Their colour is due to the presence of carotenoid compounds which hide the green colour of chlorophyll. Rhodophytes storage polysaccharide is floridean starch, or “semi-amylopectin”. It is more heavily branched than classical starch and can be found within the cytosol (instead of within plastids) (Stiger-Pouvreau *et al.* 2016).

Like brown algae, their cell wall has attracted attention. Cellulose is the main crystalline, fibrillary material of the cell wall. However, in some species it is replaced by fibrillary β -(1 \rightarrow 3)-linked xylan (Frei and Preston 1964). It is embedded in a matrix containing amorphous cellulose, sulphated galactan and mucilage (typically made of D-xylose, glucose, glucuronic acid and galactose). Red algae are commonly eaten in Eastern Asia (Kombu, Nori), and processed for the production of agar and carrageenans. Both those polysaccharides are found as sulphated galactans in the matrix phase of the cell wall. They find multiple food industry and pharmaceutical uses (Sahoo and Seckbach 2015; Hsieh and Harris 2019).

1.3.4. Chlorophytes

Chlorophytes comprise the vast majority of the green algae, however they are not part of the monophyletic group formed by the charophytes and land plants. They occupy both marine, freshwater and terrestrial environments. As for the previous groups, chlorophytes are extremely diverse, ranging from microscopic organisms to several meters long thalli, and presenting a huge variety of morphologies.

In most species, the fibrillary fraction of their cell wall is cellulose, embedded into an acidic matrix. Some of the marine species are able to produce sulphated polysaccharides, such as rhodophytes producing sulphated galactans, brown algae producing fucoidans (sulphated fucans), among others (Aquino *et al.* 2011). This trait is believed to be an adaptation to life in a highly ionic environment (seawater). Indeed, sulphated polysaccharides are also found in the extracellular matrices of vertebrate and invertebrate tissues, where they are thought to help coping with another type of highly ionic environment, the physiological saline serum (Popper and Tuohy 2010). Amongst chlorophytic algae, are found a considerable number of species that proliferate in eutrophicated coastal waters, such as species from the genus *Ulva*. *Ulva* spp. are an excellent example of the diversity existing amongst algae, as they present the classic cellulose fibres, but also unique pectin-like polymers known as ulvans: branched sulphated polysaccharides possessing, amongst other residues, high quantities of uronic acids and rhamnose (Lahaye and Robic 2007). A comparison of the main features of chlorophytes, red and brown algae is shown in Figure 4.

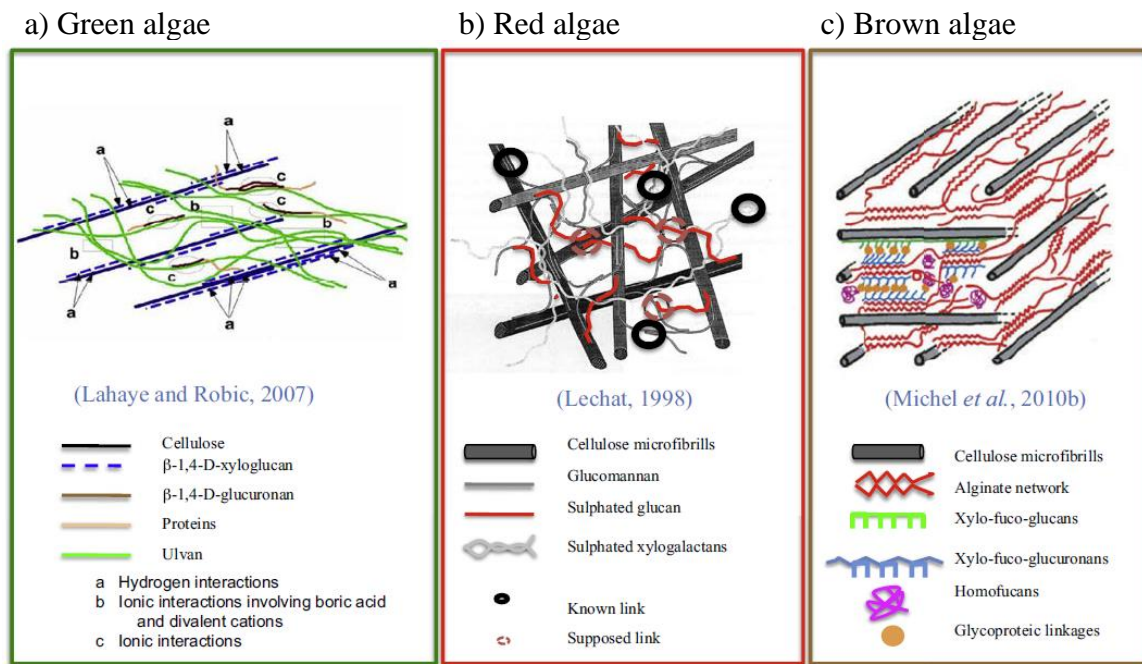


Figure 4: Simplified representation of general cell wall composition in the different groups of algae.

Schematic cell wall from green (a), red (b) and brown (c) seaweeds, with characteristic polysaccharides. Reproduced from (Stiger-Pouvreau *et al.* 2016).

1.3.5. Charophytes

Charophytes are, with land plant, part of the Streptophytes. They are green algae, living both in freshwater and terrestrial environments. Their phylogenetic position, between chlorophytes and land plants, is shown in Figure 5. They can be divided into two categories, the early divergent charophytes and the late ones (Sørensen *et al.* 2011). The first class, which includes the orders Klebsormidiales, Chlorokybales and Mesostigmatales, present more differences from land plants. The late divergent charophytic algae, Zygnematales, Charales and Coleochaetales, present considerable common features with land plants. However, it is not yet clear which one of these taxa is their closest living relative (Hall and Delwiche 2007). The different charophyte clades are detailed thereafter.

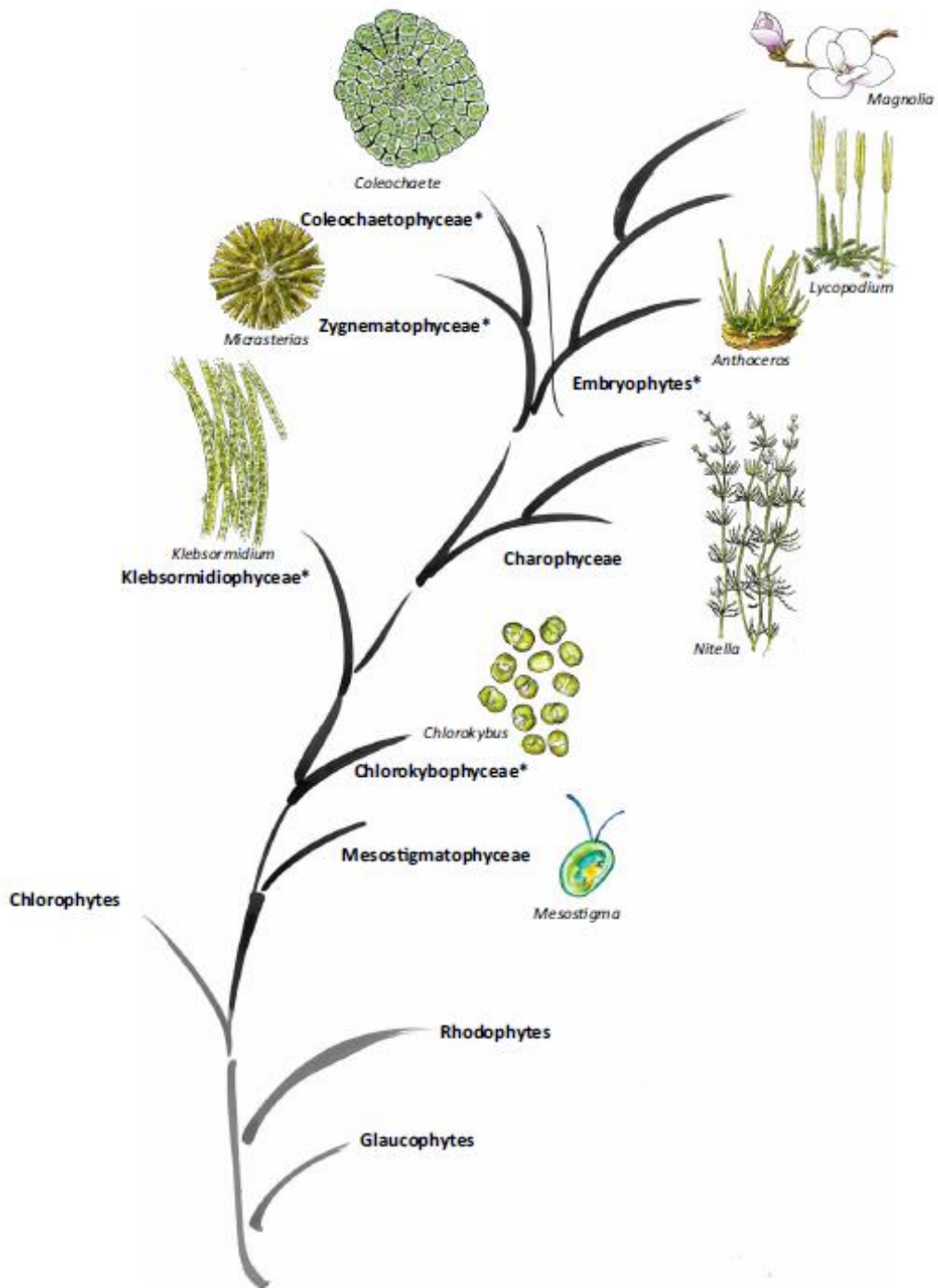


Figure 5: Evolution of the green plants lineage.

Classes with terrestrial or facultative terrestrial species are indicated with an asterisk. Classes in grey are algae, those in black are part of the Viridiplantae.

Mesostigmatophyceae, Chlorokybophyceae, Klebsormidiophyceae, Charophyceae, Zygmatophyceae and Coleochaetophyceae are charophytes. Reproduced from (Harholt et al. 2016).

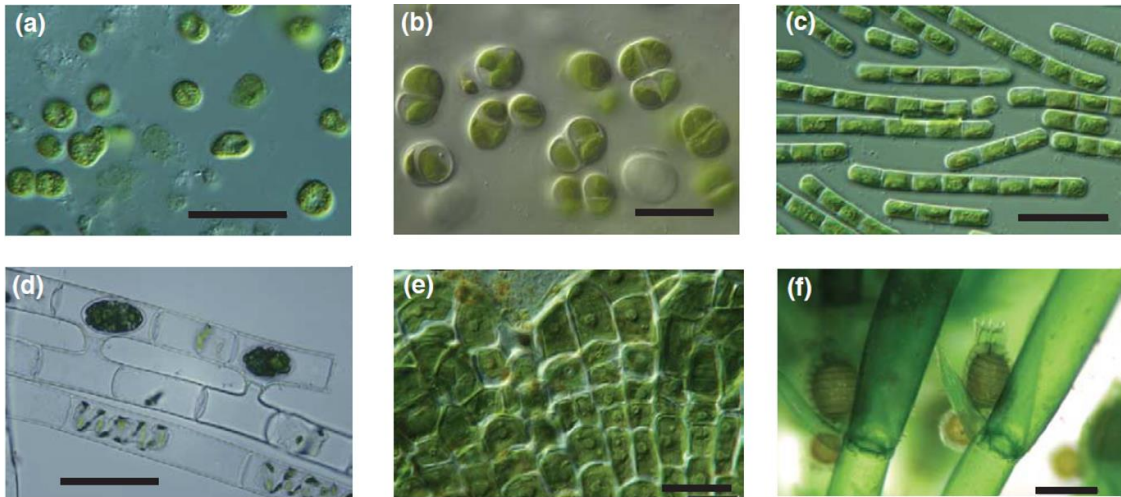


Figure 6: Main charophyte families, illustrated.

(a) Mesostigmatales (*Mesostigma viride*). Scale: bar=32 μ m. (b) Chlorokybales (*Chlorokybus atmophyticus*). Scale: bar=32 μ m. (c) Klebsormidiales (*Klebsormidium* sp.). Scale: bar=32 μ m. (d) Zygnematales (*Spirogyra* sp.) Scale: bar=64 μ m. (e) Coleochaetales (*Coleochaete pulvinata*). Scale: bar=32 μ m. (f) Charales (*Chara braunii*). Scale: bar=1 mm.). Reproduced from (McCourt et al. 2004).

1.3.5.1. Mesostigmales

This group only includes one genus, *Mesostigma* (Figure 6 (a)). It is a unicellular organism with an extracellular matrix made of 3 layers of mineralized scales (Domozych et al. 1991). Its phylogenetic position is not clear, as it has been successively grouped with the charophytes, prasinophyte, chlorophytes, or presented as a sister group to the streptophytes (Cracraft and Donoghue 2004; Lewis and McCourt 2004; McCourt et al. 2004). This clade is not investigated further in this work.

1.3.5.2. Chlorokybales

The most basal group of the charophytic green algae only presents one genus, *Chlorokybus*. *Chlorokybus* cells form small packets (two or four) embedded in mucilage, called sarcinoid thalli (Figure 6 (b)). They live in moist terrestrial habitats (Cracraft and Donoghue 2004; Necchi 2016; Cook and Graham 2017). They do possess a land-plant like cell wall, made

mainly of polysaccharides. However, those polysaccharides are clearly distinct from those found in land plants and need to be further studied (Kiemle 2010; Sørensen *et al.* 2011; O'Rourke *et al.* 2015).

1.3.5.3. Klebsormidiales

The Klebsormidiales form a group of filamentous algae, capable of surviving in a wide variety of environments, from alpine glaciers to African deserts and European cities (Figure 6 (c)). Commonly, the Klebsormidiales are considered to include two genera, *Klebsormidium* and *Entransia*, with about 30 species in total (Cracraft and Donoghue 2004; Cook and Graham 2017). *Klebsormidium* species are especially studied in this work. Differentiating one *Klebsormidium* species from another is not straightforward, as their simple morphology offers very few characters for identification, which sometimes contradict each other; their features change widely depending in the age and the conditions, and extensive molecular data are missing (Rindi *et al.* 2008; Ryšánek *et al.* 2016).

Klebsormidium species have developed a battery of adaptations to survive in harsh environments (Karsten *et al.* 2010; Holzinger and Pichrtová 2016).

For example, several species are believed to have evolved independently to deal with low pH environment (Škaloud *et al.* 2014). Some species produce callose as a way to fight desiccation stress, and some others produce specific metabolites to resist excessive ultraviolet irradiation or cold (Nagao *et al.* 2008; Kitzing *et al.* 2014; Herburger and Holzinger 2015; Míguez *et al.* 2020). They have also developed alternative strategies, such as self-shading, and they benefit from a highly tolerant photosynthetic machinery (Kaplan *et al.* 2012; Karsten *et al.* 2013; Karsten and Holzinger 2014). Most of the studies cited focus on

European alpine species; however, strains from other continents seem to display similar abilities (Elster *et al.* 2008; Karsten *et al.* 2016; Rippin *et al.* 2019).

1.3.5.4. Zygnematales

The Zygnematales are the most complex group amongst the charophytes: they present unicellular, colonial and filamentous morphologies, distributed between 10 000 species in some 54 genera (Figure 6 (d)). They are not very complex in terms of structure, and occupy media where they can exploit transient hydration, shallow waters, and interstitial moisture (Cracraft and Donoghue 2004; Delwiche and Cooper 2015; Sahoo and Seckbach 2015).

Some species have even adapted to survival into harsh environments with excessive light by producing phenolics and tannins (Aigner *et al.* 2013). The Zygnematales, also called conjugating green algae because of their reproductive system, were considered as two groups, the Desmidiaceae and the Zygnematales up until 1984. Zygnematales are, with Coleochaetales and Charales, candidates to be the closest sister group to land plants (Graham *et al.* 2012).

Amongst the Zygnematales, *Penium margaritaceum* is particularly well-described: it is indeed seen as an ideal plant model, because of its simplicity (it is a unicellular organism) and amenability to a range of manipulations. Its cell wall has been particularly well described through the use of immunolabelling techniques via a series of articles, showing how easily its pectic matrix can be manipulated (Palacio-López *et al.* 2020), how stable genetic manipulations can be (Sørensen *et al.* 2013), or demonstrating the premises of the advent of adhesive middle lamella in multicellular land plants (Domozych *et al.* 2014). Moreover, the use of glycan microarrays allowed for the study of cell wall characteristics during

reproduction in at least two Zygnematales species, *Mougeotia* sp. and *Spirogyra mirabilis* (Permann, Herburger, Felhofer, *et al.* 2021; Permann, Herburger, Nierdermeir, *et al.* 2021)

1.3.5.5. Coleochaetales

The Coleochaetales form a group of about 20 species and 2 genera, *Coleochaete* and *Chaetosphaeridium* (Figure 6 (e)).

They are found living worldwide, attached to submerged rocks or macrophytes in nearshore freshwater bodies (Cracraft and Donoghue 2004; Sahoo and Seckbach 2015; Cook and Graham 2017). *Coleochaete* presents several morphologies, erect branched system, prostrate branched systems with adherent filaments, and neatly arranged discs of cells. *Chaetosphaeridium* thalli are filamentous. *Coleochaete* surprisingly possess aromatic lignin-like compounds in their cell walls, which might have an antimicrobial and anti-UV action (Delwiche *et al.* 1989; Sørensen *et al.* 2011; Aigner *et al.* 2013).

1.3.5.6. Charales

Charales, also called stoneworts, are morphologically close to land plant (Figure 6 (f)). Indeed, they are attached via rhizoids to sandy and silty substrates at the bottom of quiet freshwater bodies, and their thalli are organised in unicellular nodes and internodes (Sahoo and Seckbach 2015). Charales vary widely in size, from a few centimetres to several decimetres in height. Several hundreds of species across six genera are included in this group, the most common ones being *Chara* and *Nitella*. Charalean thalli may become impregnated with calcium carbonate, hence the name stoneworts (Delwiche *et al.* 1989; Cracraft and Donoghue 2004).

Table 1: Presence of diverse polysaccharides in the different charophytes clades.

Others	Arabinogalactan	+	+/-	+	+	+
	Callose	+	+			+
Pectin	RG-II	-	-	-	-	-
	RG-I	-	-	+/-	+/-	+/-
	Homogalacturonan	+	+/-	+	+	+
Hemicellulose	Mannan	+	+	+	+	+
	Mixed-linkage-glucan	+	+	+/-	+/-	+
	Xylan	+	+	+	+	+
	Xyloglucan	-	-	+/-	+/-	+/-
	Chlorokybales		Klebsormidiales	Zygnematales	Coleochaetales	Charales

+ means that the polysaccharide has been detected several times by different methods; +/- means that its presence is disputed or has been shown only by one method; - means that it is considered absent from the clade. No sign means that it has not been examined.

1.3.5.7. Charophytic cell walls

Charophytic cell walls are only primary cell walls, thin and not extremely resistant mechanically. What is known of their cell wall composition is summarized in Table 1. In 2017, Mikkelsen et al. used CoMPP (comprehensive microarray polymer profiling, see 1.4) to assay a range of charophytes for land-plant-like polymers, producing a vast amount of data that can be used as a reference (Mikkelsen *et al.* 2021).

1.3.5.7.1. Cellulose

Cellulose is the main fibrillary compound of charophytes cell walls. It is found in every clade, and represents between 5 and 43% by dry weight of the algal alcohol-insoluble residue (Kiemle 2010; O'Rourke *et al.* 2015). The cellulose proportion in early-diverging charophytes is however especially low.

1.3.5.7.2. Hemicellulose

In land plant, cellulose generally interacts with hemicellulose, and more specifically xyloglucan. It seems that charophytes possess biosynthetic genes encoding the enzymes for xyloglucan synthesis, however direct proofs of xyloglucan presence in cell walls are sparse and often contradictory. Indeed, no isoprimeverose (dimer characteristic of xyloglucan) was detected in any charophyte clade (Popper and Fry 2004). The same way, xyloglucan seemed absent from Charales, Zygnematales, Klebsormidiales and Chlorokybales species, even though xyloglucan-like linkages were found in *Chara* spp. (Kiemle 2010). Finally, XET activity in *Chara* spp. was detected, even though xyloglucan was undetectable in the cell wall (Van Sandt *et al.* 2007). Later on, xyloglucan was detected by CoMPP in its un-fucosylated form in

several late-diverging charophytes (Sørensen *et al.* 2011). In *Chara corallina*, chemical and enzymatic digestion of vegetative cell walls did not yield any xyloglucan characteristic product, but antibody labelling yielded a positive result in vegetative and the antheridial cell walls (Popper and Fry 2003; Domozych *et al.* 2009, 2010). Xyloglucan was detected by both chemical digestion and antibody labelling in *Spirogyra* (Zygnematales), and might play a major role in cell-cell attachment (Ikegaya *et al.* 2008). It might be that charophytic algae do contain xyloglucan, though with a markedly different architecture than in land plants.

Since xyloglucan is either absent or present in small quantities in charophytic cell walls, the xylose residues commonly detected might be part of the hemicellulose xylan (Popper and Fry 2003). Xylans have been found to be substituted by α -Ara residues on O-2 and O-3 in *Klebsormidium flaccidum* (as in land plants), and to feature (1 \rightarrow 3) glycosidic linkages, which indicates mixed-linkage xylan. However, no GlcA substitution (common in embryophytes) was observed (Jensen *et al.* 2018). In *Chlorokybus*, 4-linked xylose residues were detected in the hemicellulose fraction, which might be indicative of xylan (Kiemle 2010). Xylan has also been detected, though probably in a highly substituted form in *Chara* cell walls (Domozych *et al.* 2010). Xylan biosynthesis genes may originate from before the divergence of red and green algae, since they are ubiquitous in rhodophytes, chlorophytes and streptophytes. However, it is important to note their glycosidic linkages are different between the different groups (Popper and Tuohy 2010). It has been proposed that, even though xylan is found across the charophytes, land-plant-like xylan (i.e. only (1 \rightarrow 4)-linked, with substitutions on C-2 and 3) is only found in embryophytes and certain charophytes (Jensen *et al.* 2018; Hsieh and Harris 2019).

Mannose has been detected extensively in charophytes, possibly involving the presence of mannans (Popper and Fry 2003; Scheller and Ulvskov 2010). It has been detected in *Chara* cell walls alkali-extractable portion (antheridium and vegetative cells) by antibody labelling (Domozych *et al.* 2009, 2010). It was detected in the same portion across the charophytes, though in variable quantities (Sørensen *et al.* 2011). It is considered almost ubiquitous in charophytes.

Mixed-linkage glucans have been thought for a long time to occur only in land-plant taxa, and especially grasses, where they can form gels (Lazaridou *et al.* 2004). They later were reported in a variety of organisms, including fungi, red algae and brown algae (Popper *et al.* 2011). They have also been reported in small quantities in late-divergent charophycean taxa (Domozych *et al.* 2012). MLGs were detected in Zygnematales species by CoMPP, however they were found to be absent from Charales and Coleochaetales when examined by enzymatic methods (Popper and Fry 2003; Sørensen *et al.* 2011). They might be present in Klebsormidiales, Chlorokybales, Charales and Zygnematales, even though their structure and base units are probably not identical to land plants' MLG (Kiemle 2010).

1.3.5.7.3. Pectin

Pectic domains form, with hemicelluloses, the matrix of the plant cell wall. Amongst them, homogalacturonan is the simplest. Galacturonic acid was detected in most charophytes examined, in higher concentrations than in land plants (Popper and Fry 2003). The polymer was detected by CoMPP across the charophytes, mostly with a low degree of esterification (Sørensen *et al.* 2011). Its presence, as well as evidence of cross-linking with Ca²⁺, was

confirmed by more specific studies, on Charales and Zygnematales species (Cherno *et al.* 1976; Domozych *et al.* 2007, 2009, 2010; Eder and Lütz-Meindl 2008, 2010; Anderson 2016). However, it seems to have been lost in some Klebsormidiales species (O'Rourke *et al.* 2015). Studies using immunolabelling of *Zygnema* sp. Cell walls have shown the link between homogalacturonan accumulation and desiccation-resistance, necessary to for land plants to survive (Herburger *et al.* 2019).

RG-I is present in all embryophytes (Fry 2000; Albersheim *et al.* 2011). It may be part of the cell wall of some late-diverging charophytes, as their sugar composition corresponds well to RG-I and rhamnose was released upon Driselase digestion (O'Rourke *et al.* 2015). The RG-I arabinan sidechain (α -(1→5)-Ara) has been detected in *Chara* spp., but the galactan sidechain was absent (Domozych *et al.* 2010). However, the full glycosidic sequence has not been found so far (Sørensen *et al.* 2011). RG-I signal from cell wall immunolabelling on Charales in Zygnematales was insufficient to claim its presence (Domozych *et al.* 2009, 2014).

RG-II appears to be a major innovation in land plants as it has not been reported in charophytes (Popper and Tuohy 2010; Sørensen *et al.* 2011; Domozych *et al.* 2014). However, some of the genes for RG-II synthesis are found in much more ancient organisms (bacteria), such as the gene coding for CMP-Kdo synthetase, a protein responsible for generating the activated sugar donor CMP-Kdo. Kdo, or 3-deoxy-D-manno-2-octulosonic acid, is a monosaccharide of RG-II. This indicate deep origins for the synthesis of RG-II segments (Popper *et al.* 2011).

1.3.5.7.4. *Arabinogalactan protein (AGP)*

Arabinogalactan proteins have been detected in charophytic algae. They are thought to be ubiquitous to the plant kingdom (Popper and Tuohy 2010; Popper *et al.* 2011). AGP epitopes were detected by immunolabelling in Charales species (Domozych *et al.* 2009, 2010). They were found by antibody labelling in Chlorokybales, Zygnematales and Coleochaetales species, where they seem to participate in cell-substrate adhesion (Palacio-López *et al.* 2019). Biochemical evidence of AGP was found in Chlorokybales, Klebsormidiales and Zygnematales (Kiemle 2010). Arabinogalactan was never detected by glycan microarray in *Klebsormidium* spp. (Klebsormidiales). However, charophytic AGPs might be only loosely related to the usual land plants' AGP, as they are not systematically detected and do not always react with β -Yariv reagent (Eder *et al.* 2008; Sørensen *et al.* 2011; Palacio-López *et al.* 2019).

1.3.5.7.5. *Other cell wall compounds*

Callose has been detected in various charophytic algae. It was detected several times in *Klebsormidium* (Klebsormidiales), both in vegetative cells and as a reaction to intensive desiccation stress in alpine strains (Sørensen *et al.* 2011; Herburger and Holzinger 2015). More generally, it was detected across the charophytes, and especially in *Chara* spp. (Charales) via immunolabelling methods (Domozych *et al.* 2010; Kiemle 2010).

Acofriose (3-O-Me-L-Rha) was found in both late and early-diverging charophytes, as well as in bryophyte cell walls. This sugar was undetectable in late-diverging plants (Popper *et al.* 2004). In the same way, 3-O-Me-D-galactose residues in pectic extracts have been found in

late-diverging charophytes. It appears that this sugar has been replaced by arabinose in bryophytes and late-diverging land plants (O'Rourke *et al.* 2015).

Phenolic compounds were found in some charophytes. Whereas lignins were thought to be restricted to late-diverging land plants, *Coleochaete* displays similar compounds, which might be the result of a convergent evolution (Delwiche *et al.* 1989). Some alpine Zygnematales species produce tannins, making them purple, which might help them resist high-UV exposures (Aigner *et al.* 2013).

Charophytic cell walls, due to their pivotal position in evolution, are very important to understand the phenomena leading to the birth of current vegetation. It is interesting to note that there are many more differences in cell wall architecture amongst non-charophytic algae than there are amongst streptophytes (charophytes and land plants) (Kirkwood 1974).

1.3.5.8. Genomes of the charophytes

Information about charophytic genomes are relatively new: the first species being sequenced was *Klebsormidium flaccidum* (Klebsormidiophyceae), in 2014. Since then, other charophytes have been sequenced, such as the early-diverging ones *Mesostigma viride* (Mesostigmatophyceae) in 2019 and several *Chlorokybus* (Chlorokybales) isolates in 2021, and the late diverging ones *Chara braunii* (Charales) in 2018, as well as *Spirogloea muscicola*, *Mesotaenium endlicherianum*, and *Penium maragaritaceum* (Zygnematophyceae) respectively in 2019, 2019 and 2020 (Domozych and Bagdan 2022).

These helped understanding the evolution of cell wall synthases, in particular specificities in the cellulose-synthase genes in basal charophytes (Wang et al. 2020). The presence of unique xylan synthases for cell wall biosynthesis in *Chara braunii* shows the remaining differences, even between higher charophytes and land plants (Nishiyama et al. 2018), while the detection of many land-plant like genes relating to cell wall synthesis in Zygnematophyceae emphasizes their similarities with land plants (Cheng et al. 2019). Finally, the study of the *Penium margaritaceum* genome provided answers about the comparative size of cell-wall related genomes between earlier and later-diverging charophytes (the first one being far smaller than the second), and the study of pre-existing land plant cell wall synthesis genes in charophytes (Jiao et al. 2020).

1.3.6. Bryophytes

Bryophytes are the earliest-diverging land plant group, with alternating life cycles (embryophytes) (Figure 7). They display low-levels of organization: they are not fully vascularised, their size is reduced and the availability of water is primordial for reproduction. Bryophytes can be divided into 3 categories: liverworts, fairly common in wet environments around the world (about 8 000 species and 330 genera), hornworts, living on bare soil or rocks on stream margins, or in humid cliffs and road cuts (fewer than 500 species in 5 or 6 genera), and mosses, ubiquitous around the globe (about 10 000 species in roughly 700 genera) (Cracraft and Donoghue 2004)(Figure 7).

Bryophytes' cell walls have not been extensively studied so far. As for charophytes, there is no distinction between primary and secondary cell wall. The presence of cellulose as fibrillary material is of course one of its trait. They seem to contain high quantities of mannose-rich cross-linking glycans (hemicellulose), uronic acids and 3-O-Me-Rha, as in charophytes. They also seem to contain xyloglucan and rhamnogalacturonan I and II, albeit in small proportions (Cracraft and Donoghue 2004; Matsunaga *et al.* 2004; Sarkar *et al.* 2009). However, the presence of xylan in bryophyte is reduced when compared to late-diverging land plants (Popper 2008). It is only present as highly substituted arabinoxylan in hornworts, indicating a close relationship of this clade with late-diverging land plants (Carafa *et al.* 2005). Hornwort display unique oligomers, such as the acid-resistant dimer α -D-glucuronosyl-(1 \rightarrow 3)-L-galactose, found in *Anthoceros caucasicus* (Popper and Fry 2003; Popper *et al.* 2003).

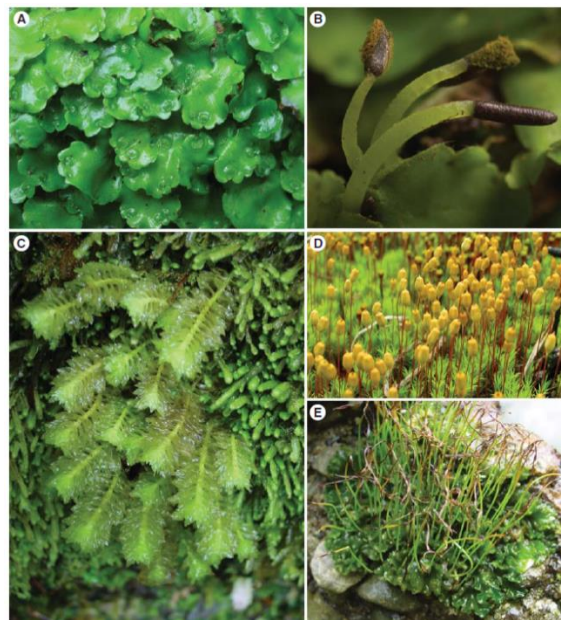


Figure 7: Extant members of bryophyte lineages, illustrated.

(A, B) *Monoclea forsteri* (complex thalloid liverworts), male gametophytes (A) and mature sporophytes (B). (C) *Schistochila alata* (leafy liverworts), gametophytes. (D) *Polytrichastrum formosum* (mosses), mature gametophytes and sporophytes. (E) *Phaeoceros carolinianus* (hornworts), gametophytes and sporophytes. Reproduced from (Ligrone *et al.* 2012)

1.3.7. Lycophytes

With the advent of the lycophytes comes the vascularisation of plants and the differentiation of aerial and subterranean components (shoot and root), which allowed organisms to get bigger and taller (Figure 8). This group and the ones described below thus form a monophyletic ensemble, the tracheophytes, characterised by the presence of specialized cells which conduct water and nutrients throughout the plant and provide structural support. It is interesting to note that this ability to transport solutes across a plant body has arisen twice within the photosynthetic eukaryotes, in tracheophytes and in brown algae (Cracraft and Donoghue 2004). Lignin appears in the plant cell wall (Popper *et al.* 2011). However, leaves are not completely differentiated (Ligrone *et al.* 2012).

Lycophytes, or Lycopodiophytes, represent less than 1% of the extant vascular plants. They can be divided into two groups, the homosporous and the advanced heterosporous (i.e. one or two types of spores). The homosporous species present more similarities with the bryophytes than the heterosporous ones, such as the presence of methylated hexoses (Me-Rha and Me-Gal) (Popper and Fry 2004; Popper 2008). Lycophytes in general contain amounts of RG-II and xyloglucan comparable to the ones found in later-diverging land plants (Matsunaga *et al.* 2004). They display lower quantities of uronic acids than earlier-diverging plants, and considerable amounts of xylan and mannan (Popper 2008).



Figure 8: Ferns and lycophytes occurring in China representing the morphological and ecological diversity, illustrated.

A, Epiphytic *Drynaria propinqua* showing leaf dimorphism (Polypodiaceae). B, Epiphytic nest-fern *Asplenium nidus* (Aspleniaceae). C, Rock fern *Woodsia* (*Cheilanthes*) *69ulvinat* (Woodsiaceae). D, Xerophytic rock fern *Aleuritopteris* (*Sinopteris*) *albofusca* (Pteridaceae). E, Climbing *Arthropteris palisotii* (Arthropteridaceae). F, Epiphytic *Elaphoglossum comforme* (Dryopteridaceae). G, *Cheiropleuria integrifolia* (Dipteridaceae) representing a basal lineage with dimorphic leaves. H, Apomictic *Polystichum* (*Cyrtogonellum*) *fraxinellum* (Dryopteridaceae). I, Thelypteroid *Stegnogramma* (*Dictyocline*) *saqittifolia* (Thelypteridaceae) illustrating the occurrence of complex venation patterns. J, Rock fern *Asplenium* (*Ceterachopsis*) *paucivenosum* (Aspleniaceae). K, Xerophytic *Selaginella 69ulvinat* (Selaginellaceae). L, Mangrove fern *Acrostichum aureum* (Pteridaceae). M, Mountain forest fern *Plagiogyria falcata* (Plagiogyriaceae) showing dimorphic leaves. N, *Botrychium yunnanense* (Ophioglossaceae), a representative of ferns with plesiomorphic eusporangia placed at the distinct spike. O, East Asian endemic *Blechnum* (*Struthiopteris*) *eburneum* (Blechnaceae). Species are labelled according to the taxonomy of Flora of China with one exception, *Stegnogramma saqittifolia*. Corresponding synonyms are given in brackets. Reproduced from (Liu 2016).

1.3.8. Pteridophytes (ferns)

The Pteridophytes, or ferns, can be divided into two groups. The leptosporangiate ferns are characterised by the fact that their sporangium (spore-producing organ) has just one cell layer. In contrary, the eusporangiates display two or more cell layers on their sporangium wall. They are thought to have diverged earlier than the leptosporangiates.

Both possess land-plant traits such as the presence of pectin, and specifically RG-II, xylan, and xyloglucan. Like the Lycophytes, they do not possess mixed-linkage glucans. The presence of methylated monosaccharides is considerably reduced (Popper 2008).

Methylated rhamnose was found in small quantities in their cell wall (Popper 2006). In contrary, leptosporangiates and late-diverging plants possess proanthocyanidins (flavonoid), which is absent from eusporangiates. Secondary lignin-containing cell walls are found in leptosporangiates, whereas eusporangiates cell walls are undifferentiated (Sarkar *et al.* 2009).

1.3.9. Gymnosperms

Gymnosperms are tall, woody plants and the earliest ones to bear seeds. They are, together with the later clades, spermatophytes. Gymnosperms are composed of different groups: cycads (about 130 species), *Ginkgo* (*G. biloba*, a single living species), conifers (about 550 species), and gnetophytes (about 70 species). The increase in size with the advent on

gymnosperm went with a decrease in reproduction rate and leaf biomass (Cracraft and Donoghue 2004).

Gymnosperms' cell walls are similar to those of leptosporangiates: presence of pectins, RG-II, xyloglucan and xylan, absence of MLG and reduced abundance of methylated sugar residues (Rha), uronic acids and mannans (Popper 2006, 2008). Xyloglucan and RG-II in gymnosperms are different from the ones in less evolved plants, as they are respectively more heavily fucosylated and bear less methylated side chains (Sarkar *et al.* 2009). Xylan is known to be the major cross-linking polysaccharide in spermatophytes.

Galactoglucomannans are major components of the cell walls of the woody tissues of both angiosperms and gymnosperms (Popper 2006).

1.3.10. Angiosperms: dicots

Angiosperms, or flowering plants, are the dominant clade of land plants, both in terms of number, diversity, and ecological importance. At least 260 000 species are known as angiosperms. As gymnosperms and all lignified plants, angiosperm do possess secondary lignified cell walls, albeit not in fruit or flowers. Lignin, present in woody tissues, is more chemically diverse in angiosperms than in lower land plants.

Dicots, or dicotyledons, form the major part of the angiosperm clade. They include magnoliids (magnolia, tulip, nutmeg for examples) and eudicots (more than 70% of all the

angiosperm species, amongst which poppies, sycamores, cacti, and clades such as rosids, saxifragales, asterids) (Cracraft and Donoghue 2004).

The cell walls of eudicots have been subjected to the most research, as they are the most economically relevant group. Overall their primary walls contain large proportions of pectin, smaller proportions of xyloglucans, and minor proportions of heteroxylans and heteromannans. Variations in the structure of those polysaccharides are important, for example the sidechains of RG-I (pectin) can be mostly arabinans (sugar beet) or galactans (potato) (Zykwinska *et al.* 2007). Xyloglucan in dicots is substituted with galactose and fucose, sometimes arabinose. Xyloglucan, in angiosperm, might be covalently linked to pectin, which would impact the current representations of the plant cell wall (Popper and Fry 2005). Heteroxylans and heteromannans are only found in very small quantities in dicots cell walls. Their secondary walls are heavily lignified, and possess in abundance 4-*O*-Me-glucuronoxylan and glucomannan. Their seeds cell walls display specific features, such as the presence of galactomannan and mannan, and non-fucosylated xyloglucan (Henry 2005).

1.3.11. Angiosperms: monocots

Monocots are a large angiosperm clade, encompassing about 65 000 species. They include groups such as poaleans (amongst which Poaceae (grasses and cereals)), palms, yams, gingers, lilies, and Asparagales (orchids, irises, and hyacinths). They can be divided into two groups, the commelinids, which are the most highly evolved (comprising palms and Poales amongst others) and the non-commelinids (comprising lilies and Asparagales for example) (Cracraft and Donoghue 2004).

The non-commelinids primary cell walls are close to dicots cell walls. They do contain a large pectic portion, with the RG-I fraction especially rich in galactan, and dicot-like xyloglucan. Some species amongst the non-commelinids possess apiogalacturonans such as sea grasses and duckweeds. Their secondary cell walls are of course lignified and appear to be close to dicots secondary cell walls.

The commelinids primary cell walls, and especially Poales, have been widely studied. Poales (comprising crops such as wheat and millet) are especially poor in classical pectin, but contain large amounts of glucuronoarabinoxylans (xylan backbone, substituted on C-2 and C-3 by Ara, GlcA or 4-*O*-Me-GlcA), and variable amounts of mixed-linkage glucans. It was originally thought that MLG only occurred in Poales, before it was discovered in other species. The Poales do display, albeit in small quantities, classical pectin, and low amounts of xyloglucan (non-fucosylated, and poor both in galactose and xylose) (Schultink *et al.* 2014). Other families of commelinids display higher abundances of “classical” pectin, possible fucosylation of xyloglucan, and lower amounts of glucuronoarabinoxylan. Commelinids secondary lignified cell walls are especially rich in glucuronoarabinoxylan and display small proportions of xyloglucans and mannans. It is worth noting that gymnosperm, non-grass monocots and dicots all have very similar cell wall composition (Henry 2005; Sarkar *et al.* 2009).

The diversity within the cell walls of previously described groups is displayed in Figure 9.

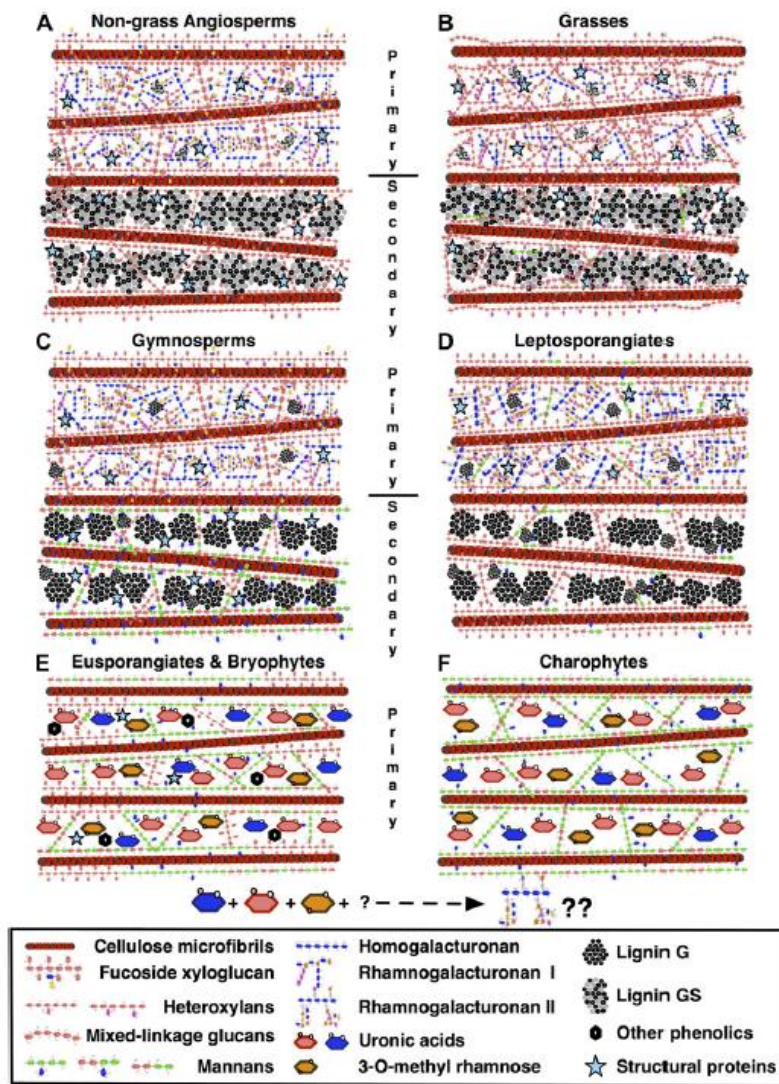


Figure 9: Simplified 2D representation of general cell wall composition in the different groups of kingdom Plantae.

All groups have cellulose microfibrils. Non-grass angiosperms (A) have high amount of hemicelluloses (fucoside xyloglucan, xylans, some mannans) and structural proteins. The primary walls have high amounts of pectins (homogalacturonans (HG), rhamnogalacturonan (RG) I and II) while the secondary walls have high amounts of lignins with guaiacyl (G) and syringyl (S) units. Xyloglucans, homogalacturonans and rhamnogalacturonans are lower in amount in grasses (B), which have higher amount of mixed-linkage glucans instead. Gymnosperms (C) have wall composition similar to non-grass angiosperms except they have higher amount of glucomannans and their lignins are homogeneous consisting primarily of guaiacyl units. Leptosporangiates (D) have low amounts of XGs, HGs and RGs, but have high amounts of xylans, mannans, uronic acids, 3-O-methyl rhamnose and lignins. In eusporangiates, bryophytes and charophytes (E, F), the cell walls are not clearly differentiated into primary and secondary walls. Eusporangiates and bryophytes (E), cell walls have compositions similar to leptosporangiate walls except they lack xylans and lignins. Phenolic compounds such as lignans are present instead of lignins. Only mannans, glucuronic acids, mannuronic acids and 3-O-methyl rhamnose have been detected from cell walls of charophytes (F) until now. Note: Spatial distribution, orientation, size and proportion of polymers in this diagram are not per scale. Reproduced from (Sarkar et al. 2009).

1.4. Chemical analysis of plant cell walls: which tools?

Multiple methods can be used for cell wall polysaccharide analysis, depending on the researcher's goal. Fractionation of the cell wall can be carried out via extractions in different solvents: e.g. chelating agent solution for pectins, and strong alkali for hemicelluloses. It is possible to break down the polysaccharides to examine their sugar composition, via acid hydrolysis for example. Depending on the pH and time of incubation chosen, it is possible to tailor this breakdown to one's needs (Fry 2000; Séveno *et al.* 2009). Methylation analysis entails functionalising free hydroxyl groups before hydrolysing the polymer, creating sugar residues with structures specific to their branching (Albersheim *et al.* 2011). It is also possible to use specific enzymes, which will be able to digest and extract extremely specific components. For example, endo-polygalacturonase digests exclusively non-methyl-esterified homogalacturonan, leading in classical pectins to the solubilisation of other pectic oligosaccharides (methyl-esterified oligogalacturonides, RG-I, RG-II). Batteries of enzymes from various microorganisms have been compiled, allowing for the production of specific oligosaccharides (Bauer *et al.* 2006; Nelson *et al.* 2008; McCleary *et al.* 2015; Ndeh *et al.* 2017).

Various chromatographic methods can be used to isolate the products of acid or enzymatic hydrolysis. Thin-layer and paper chromatography (respectively TLC and PC) both allow for multiple parallel separation, though with different elution parameter and quantities required. Paper and polyacrylamide gel electrophoresis (respectively PE and PAGE) allow for

separation of compounds based on their charge/mass ratio (Fry 2000). Gel electrophoresis is a valid method for a wide range of components, such as RG-II, proteins and DNA. Column chromatography is another powerful tool for compounds purification of compounds. This general term encompasses many techniques, such as gel permeation chromatography (GPC, also known as size-exclusion chromatography SEC), high-performance-liquid-chromatography (HPLC), gas-liquid chromatography etc. (Nagy *et al.* 2017). SEC, along with classical rheometry techniques, is useful for determining a biopolymer's size. Those techniques can generally be used for both detection and preparative purposes.

Detection tools need to be coupled to those separation methods. For TLC, PC, PE and PAGE, a range of staining methods with different sensitivities and selectivities are available. They need to be chosen carefully depending on the researcher's interest, and can be used in conjunction for optimal results (Fry 2000). Column chromatography is usually coupled to a detecting device. Common examples measure variations in refractive index or UV transparency. Mass spectrometry (MS) devices can also be coupled to chromatographic devices, allowing for immediate characterization of the separated products (Bruggink *et al.* 2005).

MS can also be used as a means to characterize a sample, independently of chromatography (Ashline *et al.* 2007; Bauer 2012; Kailemia *et al.* 2014). In the same way, nuclear magnetic resonance (NMR) helps characterizing sample structures. NMR presents the advantage of being non-destructive, but it requires a higher quantity of sample than MS. NMR, widely used in many domains of chemistry, is most often practised on a sample diluted in a solvent

such as D₂O. However, solid state NMR (SSNMR) also exists, and is particularly helpful for analysing the polymer-polymer interactions within the plant cell wall (Omarsdottir *et al.* 2006; Bothwell and Griffin 2011; Dick-Pérez *et al.* 2011; Wang and Hong 2016 p. 20; Wang *et al.* 2016).

Imaging techniques, in particular, bring to light many details about plant anatomy, as well as spatial and chemical processes regarding both plant cell walls and wider organisms (Geitmann 2023). They range from the use of classical optical microscopes, sometimes paired with fixation method to keep the sample in a viable state for longer, to the more modern X-ray based techniques. In particular, the use of lightsheet technology in confocal microscopy allows the production of 3D images through the acquisition of a series of 2D images; this technology can even be used in real time to obtain dynamic 3D imaging of plants (Van Oostende-Triplet *et al.* 2017). The use of X-ray techniques, imported from medical imaging, through for example X-ray microcomputed tomography, is another dynamic imaging technique available, this one based on density differences between different materials (Borsuk *et al.* 2022). Transmission electron microscopy, equally, allowed for the precise imaging of plants, allowing to classify charophytes as “basal streptophytes” (Mattox and Stewart 1984).

In order to make enhance the detection of particular structures or molecules via optical microscopy, the compounds of interest can be labelled so they are easy to visualize. This has historically been done through the use of histological stains, however, these are not overly specific and may give erroneous results. Immunohistochemical markers (i.e. the use of antibodies linked to fluorophores) are far more molecule-specific, but they require the

sample to previously be fixed and thus forbid the visualisation of dynamic processes (Geitmann 2023). The use of fluorescent labelling, which consists in introducing a GFP (green fluorescent protein) in the plant genome so that it produces the protein of interest with a fluorescent label attached, is an answer to the challenges posed by both previous approaches (Dhanoa *et al.* 2006). Furthermore, clearing solution can be used to enhance the images by getting rid of plant natural autofluorescences. The development of dedicated softwares for image processing, finally, is key for the production of high-quality digital dynamic images, sometimes allowing for direct quantification (Van Oostende-Triplet *et al.* 2017).

Immunohistochemical labelling may be useful in other contexts. For example, CoMPP, or comprehensive microarray polymer profiling, is a technique developed to enable the occurrence of cell-wall glycans to be systematically mapped throughout plants in a semi-quantitative high-throughput fashion (Moller *et al.*). It consists in sequentially extracting the different cell wall fractions, before generating microarrays, which are probed with monoclonal antibodies (mAbs) or carbohydrate-binding modules (CBMs) with specificities for cell-wall components. The array generated is then treated with an image processing software, allowing for the extraction of data and the production of a heat map of different polymers in different cell wall fractions. Immunolabelling is a field in constant movement, as new antibodies can be expressed and developed, making the method more precise and giving it a wider use (Rydahl *et al.* 2017; Zhou *et al.* 2018).

Finally, radioactive labelling consists in feeding plant cells radioactive isotopes, so that they produce radioactive polysaccharides. This method allows for enhanced detection of

compounds and biopolymers and discrimination between chemically identical substrates, through the use of all previously described biochemical methods (Domozych *et al.* 2014).

It is important to note that this selection of method is not, by far, exhaustive. New methods are constantly developed and transferred to the field of plant biology to facilitate wall analyses.

1.5. Modified plant cell walls: How and for what?

Polysaccharides are polymers. They behave in a similar way, and can be characterized as such. For example, their gyration radius, gelling ability, or persistence length can be studied. These parameters are linked to one another; they are also linked to the chemical structure of the polysaccharide. The presence of chemical modifications, such as acetylation, the branching, and the presence of side-chains strongly impact their behaviour (Oakenfull and Scott 1984; Rinaudo 2004; Morris and Ralet 2012; Gawkowska *et al.* 2018; Herburger *et al.* 2018).

These effects have been mostly studied *in vitro*. It is indeed much easier to do so, considering the extraordinary complexity of both polymeric structures and their interactions within the plant cell wall. Moreover, these *in vitro* studies are relevant when considering the industrial applications of carbohydrates: they are commonly isolated and chemically engineered before being integrated to the matrix of interest (in food for example).

1.5.1. Cellulose

The most widely used element of the cell wall is cellulose. Thanks to its remarkable stability and mechanical properties, cellulose finds uses in many areas, the paper and textile industries being maybe the most ancient ones. Cellulose is a unique polymer, and its chemical structure is identical across the plant kingdom. What differs is its organisation: size and length of the microfibrils, degree of crystallinity, degree of polymerisation, eventual interaction with other cell wall polysaccharides (Zykwinska *et al.* 2008; Wang and Hong 2016). An interesting feature of cellulose is that its glass transition temperature is superior to its degradation temperature: cellulose never presents viscoelastic features (in normal conditions). Synthetic derivatizations of cellulose are possible, given its numerous free hydroxyl groups. However, they are not studied in this work (Jedvert and Heinze 2017).

1.5.2. Hemicellulose

Hemicellulose is extracted from plant cell walls by strong alkali solutions. It is made of mostly neutral polymers, and is highly variable depending on the plant clade. It is not as widely used as other plant biopolymers, due to difficulties relating to its extraction, poor solubility and low molecular mass. Hemicellulose is used, amongst other things, as a base material for the production of biofuels and studied for applications in food packaging and drug delivery, and as hydrogels or tensioactives. It is also useful as gum in food industry, because of its thickening, emulsifying, stabilizing and gelling properties (Ebringerová 2005; Spiridon and Popa 2008).

Common side-chain modifications in hemicelluloses are lateral substitutions by a range of sugar residues. This includes biopolymers such as arabinoxylan, galactomannan and galactoglucomannans. In all cases, the solubility and oxygen permeability of the hemicellulose rises with the degree of substitution: the side-chains supposedly prevent intra and inter-chain interactions and decrease the solid-state packing of the backbones (Spiridon and Popa 2008; Kochumalayil and Berglund 2014; Naidu *et al.* 2018). The organization of these substitutions, either random or block-wise, is a significant factor in their influence over solubility (Ebringerová 2005). Backbone acetylation have a similar effect on glucuronoxylan and acetyl-galactoglucomannans (Willför *et al.* 2008; Naidu *et al.* 2018 p. 2). Mixed-linkage glucan extractability is, interestingly, linked to the ratio of C-3/C-4 linkages and their distribution along the backbone: the more consecutive C-4, the more MLG interacts with cellulose, the least extractable it is (Ebringerová 2005).

The rheological behaviour of hemicellulose solutions has been studied. Galactomannan, for example, forms gels (in conjugation with metal ions) or behaves like a liquid, depending on the source and the degree of branching. Variations in xyloglucan solutions behaviours, on the contrary, were explained by variations of their molecular weight. Gels from mixed-linkage glucans were influenced by the distribution of C-3 and C-4 linkages, since those govern interactions within and between the polysaccharide chains (Ebringerová 2005).

Hemicelluloses are often used in blends at the industrial level. Xylan, once separated from the rest of the biomass, is capable of forming films. However, their structure and properties are greatly influence by the polysaccharide structure and its interactions with other elements from the blend. It has been found that the use of de-branched xylan in films decreased both the moisture uptake and the tensile strength (by comparison with branched

xylan). This has been linked to the lower number of H-bond and a greater crystallinity in linear xylan (Kochumalayil and Berglund 2014; Naidu *et al.* 2018).

1.5.3. Pectin

Pectin has been especially studied with regards to its chemical modifications. This is due to its availability (pectin is abundant and easily extractable) and its wide range of applications, as gelling, thickening and emulsifying agent, especially in foods (Bonnin *et al.* 2014). The factors changing pectin properties in vitro have been studied.

First, the technique of pectin extraction has been examined: depending on the nature of the buffer used, its pH, the temperature and time of incubation, polysaccharides with different qualities (Mw, η) and compositions are extracted (Chen *et al.* 2014; Kaya *et al.* 2014).

Second, the functionalisation of pectin attracted interest. It appears that naturally occurring modifications (methylation, esterification, feruloylation) strongly impact its properties by modifying intra- and inter-chains interactions. This is especially important when it comes to gelling: highly methylated pectin only gels at pH<3.5 in presence of neutral sugars, whereas low methylated pectin gels at any pH in the presence of Ca²⁺(Oosterveld *et al.* 2002; Rinaudo 2004). Third, the composition in term of sugar residues of pectin was looked at. It appears that the presence of neutral side-chains can enhance its viscous properties for example (Morris and Ralet 2012; Ngouémazong *et al.* 2012).

Finally, pectin features within the cell wall have been studied, though not as widely. Characterizing their specificities and linking them to the properties of the plant is especially interesting. For example, pectin modifications may impact the plant response to pathogen invasions (Malinovsky *et al.* 2014). An example is the supposed influence of arabinan side-chains in desiccation resistance in resurrection plants (Moore *et al.* 2008). Especially in this field, it is important to note that pectin properties within the cell wall are not due only to the polymer's intrinsic properties. They are also governed by the physical structure of the cell wall material around it: surface area, pore size, particle size etc. (Chen *et al.* 2014).

1.6. Glossary

In order to make the contents of the following thesis accessible to any scientific reader, a glossary of the terms used in this thesis is presented.

Term	Definition
<i>Plant subgroup</i>	
Plant	Photosynthetic eukaryotes with carbohydrate cell walls (i.e. organisms made of cell(s) with a nucleus surrounded by a complex nuclear membrane and organelles, capable of using light as a source of energy for biomass production, and a cell wall made of polysaccharides).
Viridiplantae	Chlorophytes and streptophytes: Plants united by the absence of phycobilins, the presence of chlorophyll a and chlorophyll b (i.e. plants of this group are green), cellulose in the cell wall and the use of starch, stored in plastids, as a storage polysaccharide.

Chlorophyte	Group of green algae (mainly seaweeds) sharing the same pigments as land-plants, but distinct cell wall characteristics, amongst other defining traits.
Streptophyte	All land plants, plus charophytes. Characterised (amongst others) by the presence of certain enzymes (class I aldolase, Cu/Zn superoxide dismutase, glycolate oxidase, flagellar peroxidase),
Land plant / embryophyte	Complex multicellular eukaryotes with specialized reproductive organs mainly living in terrestrial habitats.
Bryophyte	Basal division of the embryophytes: group encompassing mosses, liverworts and hornworts. They are non-vascular plants, which means they have no roots or vascular tissue, but instead absorb water and nutrients from the air through their surface (e.g., their leaves).
Charophyte	Complex green algae that form a sister group to the Chlorophyta and within which the Embryophyta emerged.
<i>Plant polymer</i>	
Cellulose	Linear polymer made of β -D-Glc units, linked together via (1 \rightarrow 4) glycosidic linkages, responsible for providing strength and rigidity to the cell wall.
Hemicellulose	Diverse group of mainly neutral polysaccharides interacting strongly with cellulose, extractable from the cell wall with strong alkali.
Xyloglucan	Hemicellulosic polymer, mainly present in land plants, made of a backbone of β -(1 \rightarrow 4)-D-Glc units, highly substituted by D-xylose residues on O-6, and other monosaccharides depending on the species developmental stage of the plant.
Xylan	Hemicellulosic polymer with a skeleton of β -(1 \rightarrow 4)-D-Xyl units, sometimes acetylated on O-2 and O-3, and substituted.
Mixed-linkage glucan	Hemicellulosic polymer made of glucose residues connected via glycosidic β -(1 \rightarrow 3) and β -(1 \rightarrow 4) linkage, mainly present in grasses and pteridophytes.
Pectin	Negatively charged cell wall polysaccharide capable of gellification, extractable with chelating ions at high temperature.
Homogalacturonan	Pectic fraction, present in land plants and late-diverging charophytes, made of α -(1 \rightarrow 4)-D-galacturonic acid residues,

	often methyl-esterified on C-6 carboxyl and acetylated on O-2 or O-3.
Rhamnogalacturonan-I	Pectic fraction specific to land plants: branched polysaccharide, with a backbone made of alternating units of galacturonic acid and rhamnose, $\rightarrow 4)-\alpha\text{-D-GalA-(1}\rightarrow 2)-\alpha\text{-L-Rha(1}\rightarrow$, highly substituted with arabinan and galactan sidechains.
Rhamnogalacturonan-II	Pectic fraction specific to land plants: small and complex polysaccharide with a backbone of $\alpha\text{-(1}\rightarrow 4)\text{-D-galacturonic acid}$ residues, substituted by at least eleven different glycosidic residues.
Starch	Energy storage polymer in plants, made of $\alpha\text{-(1}\rightarrow 6)\text{-linked Glc}$ residues.
Aldobiouronic acid	Dimer of a uronic acid and a neutral sugar.

Chemical and biochemical terms

Hydrolysis	In this thesis, hydrolysis means the cleavage of chemical bonds by the addition of water.
Enzyme	Protein with catalytic properties. In this thesis, most of the enzymes used are glycosyl hydrolases (or glucanase) e.g. they provoke hydrolysis of glycosidic bonds.
Endo-enzyme	Endo-enzymes hydrolases randomly cleave the glycosidic linkages of polysaccharides.
Exo-enzyme	Exo-enzymes act from the nonreducing end of the polysaccharide.
Electrophoresis	Utilisation of an electric current going through a matrix (in this thesis, paper or gel) to separated substrates based on their size and electrical charge.

2. Materials and Methods

2.1. Materials

2.1.1. Algae and *Anthoceros*

Spirogyra varians, *Klebsormidium subtile*, *Klebsormidium fluitans* and *Chlorokybus atmophyticus* were purchased from CCAP (Culture Collection of Algae and Protozoa, SAMS, Scottish Marine Institute, Dunstaffnage, Argyll, UK, <https://www.ccap.ac.uk/>). These cultures were not axenic but each named algae was the only photosynthetic organism present. Axenic cultures of *Coleochaete scutata*, *Klebsormidium nitens*, *Penium margaritaceum*, *Zygnema circumcarinatum* were purchased from SAG (Göttingen University, <https://sagdb.uni-goettingen.de/>). An axenic culture of *Chara vulgaris* was kindly provided by Prof Burkhard Becker (Cologne University). Cultures of *Mesotaenium caldariorum* and *Netrium digitus* were kindly donated by Dr David Domozych, and received 25/3/2014. All cultures were grown at 25°C under constant light in 500 mL flasks, except for *Coleochaete scutata* which was also kept in flat horizontal bottles.

Anthoceros cell-suspension cultures were grown at pH 5.5 (fixed with sodium hydroxide 1 M) on their own specific culture medium (Gamborg's B5 basal salt medium (Sigma, 3.1 g.L⁻¹, sucrose (10 g.L⁻¹), *myo*-inositol (0.1 g.L⁻¹), nicotinic acid (10 mg.L⁻¹), pyridoxine HCl (10 mg.L⁻¹thiamine HCl (100 mg.L⁻¹)).

Chlorokybus was grown in soil medium (JM:SE2, 7:3).

All other algal species were grown on Bold basal medium (3N-BBM+V) (Bischoff et Bold 1963).

Ulva spp. harvested at North Berwick were kindly donated by Dr John Bothwell.

For isolation of polysaccharide-rich material, all plant and cell samples were stirred in 70–77% (v/v) ethanol at 20°C for 16 h, and centrifuged at 5000 g for 10 min. The resulting cell-wall-rich alcohol-insoluble residue (AIR) was washed several times in 70% ethanol, 96% ethanol, then acetone, and finally dried.

2.1.2. Enzymes

All enzymes were purchased from Megazyme (Auchincruive, United Kingdom), apart from α -amylase, Driselase, and D-galactose oxidase, which were purchased from Sigma-Aldrich (Poole, United Kingdom). Details of their respective sources, activities and use parameters are available in Table 2.

2.1.3. Chemicals and other consumables

All chemical reagents were purchased from Sigma Aldrich (Poole, United Kingdom), Fisher Scientific (Loughborough, United Kingdom), and VWR (Lutterworth, United Kingdom). All water used was deionised water unless otherwise stated. Silica TLC plates (plastic and aluminium-backed) were sourced from Merck. Films used for autoradiography and fluorography were sourced from Agfa.

Note the high concentration of NaOH used for the extraction of the hemicellulosic fraction ; the neutralisation of this fraction should be carried out carefully under a fume hood.

2.2.2. Hydrolysis

2.2.2.1. Acid hydrolysis

AIR or polysaccharide fractions (5 mg) were hydrolysed with 1 ml of 2 M trifluoroacetic acid (TFA) at 120°C for 1 h. The hydrolysate was dried, re-dissolved in water and chromatographed (published in O'Rourke *et al.* 2015). Alternatively, the polysaccharide fractions were hydrolysed following Saeman's protocol (Saeman *et al.* 1954). The dried sample was dissolved (1-2 h) to 50 mg.ml⁻¹ (less in case it was less soluble) in 72% (w/w) H₂SO₄. 21 times the initial volume was added as water, and the whole mixture was treated at 120°C for 1 h, then cooled on ice. An internal pH indicator was added (bromophenol blue), and the sample was neutralized with 0.18 M Ba(OH)₂. It was mixed vigorously, and a trace of H₂SO₄ was added to make the solution slightly acidic again. It was stirred overnight. A slight excess of solid BaCO₃ was added to neutralise the mixture, and left to stir. The solution was then centrifuged (15 min, 3000 g), the supernatant isolated, frozen overnight (-20°C), thawed and centrifugated again to get rid of the non-dissolved BaCO₃ and BaSO₄ (15 min, 3000 g). Finally the sample was dried, re-dissolved in water and chromatographed.

In this protocol, both TFA and sulfuric acid were used at fairly high concentrations and handled with care, only being heated in tightly shut Sarstedt tubes. Dispenses were carried out in a fume hood if more than a few milliliters were used.

2.2.2.2. Enzymatic analysis

2.2.2.2.1. *Solubilisation of homogalacturonan*

The samples were de-esterified by alkaline treatment. The AIR was suspended at 2.5 mg.ml⁻¹ in 1 M NaOH in 75% ethanol and incubated 10 minutes at room temperature, and centrifuged at 4000 g for 5 min. It was subsequently washed in 75% ethanol for 10–20 minutes, 100% ethanol for 10 to 20 minutes, and ethanol/0.5% acetic acid. At this point, the pH was verified (pH<7). It was finally washed with 100% acetone and dried in SpeedVac.

The samples were digested with endo-polygalacturonase (EPG). They were diluted to 20 mg.ml⁻¹ in EPG (Megazyme) at 2.5 U.ml⁻¹ in pyridine/acetic acid/water 1:1:98, pH 4.7. They were incubated 16 h at room temperature, on a shaker. Half the volume of water was added, the mixture was centrifuged and clear supernatant was transferred into a new tube. The operation was repeated on the insoluble residue.

2.2.2.2.2. *Solubilisation of starch*

The AIR was suspended at 10 mg.ml⁻¹ in 40 mM lutidine (OAc⁻) buffer, pH 6.7, in 0.25% (w/v) chlorobutanol, stirred at 100°C for 15 min (gelatinizing any starch), and cooled to 60°C. Next, 0.1 volumes of a solution of heat-stable α -amylase (*Bacillus amyloliquifaciens*; Sigma A7595 (Sigma-Aldrich, Poole, Dorset, UK); 10 ml of the commercial solution dialysed against water then diluted to 45 ml with the lutidine buffer) was added, and incubation was continued at 60°C for 72 h. Ethanol and ammonium formate were then added to give final concentrations of 70% (v/v) and 1% (w/v), respectively, and the suspension was incubated at 20°C for 16 h,

precipitating any water-soluble polysaccharides among the cell walls, which were thoroughly rinsed with 70% ethanol and dried.

No check was conducted to verify that all the starch had been solubilized.

2.2.2.2.3. Analysing polysaccharide content by enzymic dissection

Table 2 indicates the concentrations of stock solutions used for the enzymatic assays, as well as the durations and temperatures of the experiments and the enzyme activities. All the solutions were kept at -20°C.

Enzyme solution (10 µl) was mixed with 10 µl of polysaccharide suspension (or solution), and incubated for the indicated time, at the indicated temperature, under mild agitation.

Exceptions to those ratios include β-xylosidase (5 µl of enzyme solution was mixed with 25 µl of substrate solution), β-galactosidase (5 µl of enzyme solution + 10 µl of substrate solution and 15 µl of buffer), α-galactosidase (10 µl of enzyme solution + 10 µl of substrate solution and 10 µl of buffer), and Driselase (1.2 µl of enzyme solution + 30 µl of substrate solution).

After incubation, 420 µl of ethanol 80% was added. The mixture was left on the spinning wheel for at least 6 h. It was then centrifuged (3000 g, 3 min), 400 µl of supernatant was extracted. The solution was dried in the SpeedVac, diluted to the concentration of 5 µg/µl in water, and analysed as needed.

2.2.2.2.4. *Enzymatic determination of enantiomerism of Gal (O'Rourke, et al. 2015)*

Samples of authentic D-galactose, L-galactose, and 'U' (each at 0.25 mg.ml⁻¹) were incubated with D-galactose oxidase (4 U.ml⁻¹) in 0.3% collidine (OAc⁻) buffer, pH 6.0, for up to 96 h. At intervals, 16 µl of the reaction mixture (containing 4 µg substrate) was added to 10 µl of 50% formic acid, dried and analysed by TLC in BAW (4:1:1).

2.2.3. Separation methods

2.2.3.1. Thin-layer chromatography

Thin-layer chromatography (TLC) was on Merck aluminium- or plastic-backed silica-gel plates, usually in butan-1-ol/acetic acid/water (BAW, 4:1:1, v/v/v or BAW, 2:1:1), or ethyl acetate/pyridine/acetic acid/water (EPAW; 6:3:1:1) (Fry 2000); sugars were stained with thymol/H₂SO₄, which consisted in dipping the TLC plate in a mixture of sulfuric acid, ethanol and thymol (0.6% w/v thymol in 6% vol/vol sulfuric acid in ethanol), drying it, and heating it at 105°C for ten minutes (Jork *et al.* 1994).

Alternatively, preparative TLC was conducted on a glass-backed silica-gel plate, which allows for heavier loadings. The same solvent mixtures as above were used. The separate bands were transiently stained using iodine vapour.

The chromatography solvents were all volatile and their fumes might be harmful (especially from pyridine). Mixes and disposals were performed under a fume hood, and the remaining

solvents were disposed of carefully in specialised organic waste vials. Plates were left to dry in the fume hood.

Concerning the staining, it was entirely performed under a fume hood, as concentrated sulfuric acid was used at high temperature.

2.2.3.1. Paper chromatography

Preparative paper chromatography was performed on Whatman No. 1, usually in butan-1-ol/acetic acid/water (BAW; 12:3:5, v/v/v) for 16 h, or pyridine/acetic acid/water (PAW; 8:2:1 v/v/v) for 5h, or ethyl acetate/acetic acid/water (EAW; 10:5:6 v/v/v) for 30 h; markers and part of the sugars were stained with aniline hydrogen-phthalate. The selected portions (unstained) were cut off the sheet and extracted with 75% ethanol by centrifugation (Fry 2000).

Recommandations for solvent mixing and disposal are similar to those presented in the thin-layer chromatography section. Papers were left to dry in the fume hood.

2.2.3.2. Paper electrophoresis

Analytical paper electrophoresis was performed on Whatman No. 3, in acetic acid/pyridine/water (1:33:300, pH 6.5), at 3 kV for 100 min, and stained with AgNO₃ (Fry 2020).

Solvents used in paper electrophoresis were kept in the tank to be re-used later and therefore didn't need to be effectively disposed of. Papers were left to dry in the fume hood.

Table 2: Enzymes and conditions used to assay polysaccharide sugar contents

Enzyme	Source	Activity (U.mg ⁻¹)	Enzyme (U/mL)	Substrate (mg/mL)	Buffer	Incubation time	Incubation temperature
endo-1,4-β-xylanase	rumen microorganisms	~ 380	10	2.5	40 mM lutidine (acetate, pH 6.5)	16 h	20°C
endo-1,4-β-mannanase	<i>Bacillus</i> sp.	> 50	10	2.5	50 mM ammonia (acetate, pH 8.8)	1 h	20°C
endo-1,4-β-mannanase	<i>Aspergillus niger</i>	~ 50	10	2.5	0.25 mM pyridine (formic acid, pH 3.7)	1 h	20°C
endo-1,5-α-arabinanase	<i>Aspergillus niger</i>	~ 10	5	2.5	170 mM acetic acid (pyridine, pH)	1 h	20°C
endo-1,4-β-galactanase	<i>Aspergillus niger</i>	> 150	2.5	2.5	170 mM acetic acid (pyridine, pH 4)	1 h	25°C
endo-polygalacturonase	<i>Aspergillus aculeatus</i>	150	5	5	0.13 mM pyridine (acetate, pH 4.7)	16 h	25°C
β-xylosidase	<i>Selenomonas ruminantium</i>	~ 115	50	10	50 mM succinate (pH 5.5)	30 min	40°C
β-galactosidase	<i>Aspergillus niger</i>	~ 170	1	10	170 mM acetic acid (pyridine, pH 5)	48 h	25°C
α-galactosidase	guar	~ 50	100	2.5	170 mM acetic acid (pyridine, pH 5)	48 h	25°C
lichenase	<i>Bacillus subtilis</i>	~ 230	10	2.5	40 mM lutidine (acetate, pH 6.5)	1 h	40°C
XEG	<i>Paenibacillus</i> sp.	70	7	4	0.13 mM pyridine (acetate, pH 4.7)	16 h	25°C
Salivary amylase	Human saliva	N/A	N/A	N/A	40 mM lutidine (acetate, pH 6.5)	16 h	37°C
α-amylase	<i>Bacillus amyloliquifaciens</i>	>2500	N/A*	N/A*	40 mM lutidine (acetate, pH 6.7)	72 h	60°C
Driselase (mixture of enzymes)	<i>Irpex lacteus</i>	N/A	0.5%	10	0.13 mM pyridine (acetate, pH 4.7)	16-90 h	37°C
D-galactose oxidase	<i>Dactylium dendroides</i>	500	4	2.5	23 mM collidine (acetate, pH 6.0)	96 h	20°C

All the enzyme stock solutions were in buffer, all the polysaccharide stock solutions were in water. All enzymes are sourced from Megazyme, apart from amylase (laboratory-made), and Driselase (from Sigma). XEG is xyloglucan-specific endo-glucanase.

2.2.3.3. Gel electrophoresis

In a 50-ml tube, 834 μl of water, 834 μl of TRIS-HCl buffer (1.5 M, pH 8.8), 3.33 ml bis-acrylamide solution (40%) and 46.7 μl of ammonium persulfate solution (10% w/v, stored at 4°C) were mixed. Tetramethylethylenediamine (3.9 μl) was added, and the solution was transferred into a gel casting tray. It was left to polymerize. When set, it was submerged into the electrode buffer (6.057 g TRIS, 2.853 g glycine in 1 L water, pH 9.0). Samples were loaded (maximum volume 30 μl) into wells. They were mixed beforehand with 3 μl of loading buffer (4.2 ml TRIS-HCl buffer, 0.025 g bromophenol blue, 5 ml glycerol, 800 μl water). The electrophoresis is run for 15 minutes at 100 V, then about 1 h at 200 V.

The gel was routinely stained with silver nitrate. It was submerged for 30 minutes in 100 ml fixing solution (ethanol/acetic acid/water 4:1:5 v/v/v). It was rinsed three times in 100 ml water for 1 minute. It was submerged into 100 ml sensitizing solution (0.0632 g sodium thiosulfate in 1 L water) for 1 minute, and rinsed three times in 100 ml water for 1 minute. The gel was then submerged for 20 minutes into 100 ml freshly prepared staining solution (0.1019 g silver nitrate and 75.2 μl 37% formaldehyde into 100 ml water). It was rinsed twice in water for 20 s., and submerged in 100 ml stain stabilizer solution (29.677 g sodium carbonate, 20 ml sensitizing solution, 4.8 ml formaldehyde into 1 L water). The gel was then submerged into 100 ml stopping solution (40 g TRIS, 20 ml glacial acetic acid, 980 ml water). It was routinely scanned (while still wet) for analysis.

Further details about gel electrophoresis practicalities are given by Chormova et al. (Chormova *et al.* 2014).

The stained gel should always be manipulated with gloved hands, as the dye is harmful to human health.

2.2.4. Quantification assays

2.2.4.1. Colorimetric test for total carbohydrates

TLC plates were used for routine quantification assays.

An array of solutions of glucose in water was prepared, with a gradient of concentrations (for example 4%, 2%, 1%, 0.5%, 0.25%, 0%, w/v). Aliquots (2 μ l) of each solution and samples were loaded in triplicate on a labelled TLC plate. The plate was left to dry for about 10 min, then stained with thymol/H₂SO₄ (as described in Section 2.2.3.1). The plate was scanned, and the intensity of each spot measured via ImageJ. A standard curve was created from the standards array. Sample concentrations were calculated with the standard equation of the curve.

2.2.4.2. Colorimetric test for uronic acids

An array of solutions of galacturonic acid in water was prepared, with a gradient of concentrations (for example 4%, 2%, 1%, 0.5%, 0.25%, 0%). 20 μ l of each solution and samples were loaded in triplicate into a 96-wells PCR plate. Borax solution (100 μ l) was added to each well and mixed properly (0.5 g borax in 100 ml concentrated H₂SO₄, kept in the dark). The plate was incubated at 100°C for 5 minutes. The samples and standards were transferred into a 96-well flat-bottomed reading plate. The absorbances at 540 nm were read. *m*-Hydroxybiphenyl solution (2 μ l) was added in each well and mixed (0.15 g *m*-hydroxybiphenyl, 1.0 g NaOH in 100 ml water, kept in the dark). The plate was incubated at room temperature for 5 minutes. The absorbances at 540 nm were read. Absorbances pre *m*-hydroxybiphenyl were subtracted from absorbances post *m*-hydroxybiphenyl. A standard

curve was created from the standards array. Sample concentrations were calculated with the standard equation of the curve (Carpita and Filisetti-Cozzi 1991).

Again, concentrated sulfuric acid was used in this assay. It was therefore systematically performed under the fume hood.

2.2.1. Radiolabelling methodology

All dispensation of radioactive material was thoroughly traced, both through the University's online waste management system and through written records. Disposals were recorded either as volatile substances (carbon respired by the plants), aqueous waste, or solid/non-water miscible waste in specialised bins.

2.2.1.1. *In vivo* ^{14}C radiolabelling

In 15-ml transparent Falcon tubes, 5 ml of culture medium containing suspended algae were mixed with 50 μL of 200 mM MES buffer (morpholinoethanesulfonic acid, Na^+), pH 5.0.

Radioactive NaHCO_3 solution (50 μL ; 1 MBq) were added and the tubes were mixed (Fry 2000). They were incubated with lids tightly screwed shut for five days under the fume hood in constant direct light on a rocker (30 rpm). The lids were taken off and the tubes were incubated, standing, for two more days in constant darkness. Acidified ethanol (9 ml, about 0.7% formic

acid in 96% ethanol, freshly prepared) was added in each tube, and well mixed. The tubes were left open for about 8 hours. They were centrifuged at 18 g for 5 minutes. Supernatant 1 was collected. More ethanol was added, the tubes were mixed, centrifuged and the

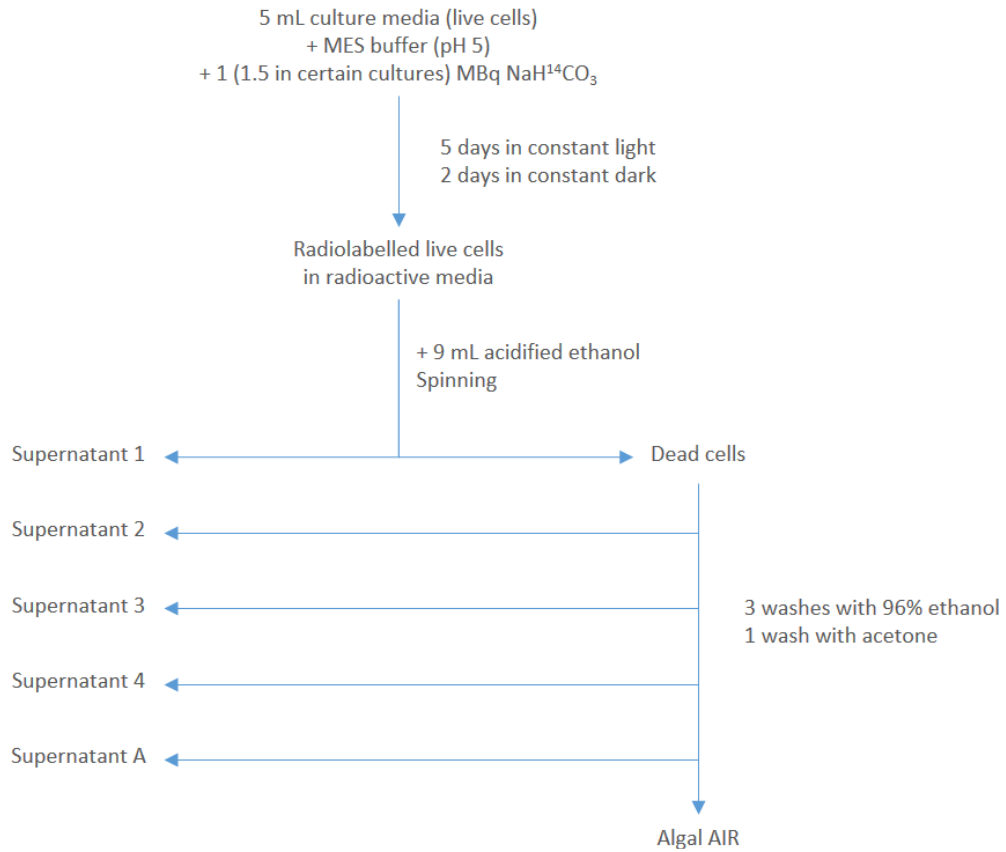
supernatant separated three more times. This was repeated once with acetone. The pellets were finally left to dry under the fume hood, making radiolabelled alcohol-insoluble algal residue (AIR).

The AIR was de-starched by digestion with salivary amylase. Each AIR sample (around 10 mg) was incubated at 37°C for 16 h with salivary amylase in 4 ml lutidine buffer (40 mM, adjusted with acetate to pH 6.5). Ethanol was added up to 75% v/v, the mixture was centrifuged at 18 g for 5 minutes, and the supernatant was rejected. The remaining solid residue was washed two more times with 5 ml of 70% ethanol. The pellets were left to dry under the fume hood (Figure 11).

2.2.1.2. Sodium borohydride radiolabelling

To 200 µg of sugar (either monosaccharide or oligosaccharide), 11 µL of 0.01 M tritiated sodium borohydride (about 32 MBq/ µmol) in 15% ammonium hydroxide were added. The mixture was incubated in sealed tubes for 72 h at room temperature. The tubes were open under the fume hood and left to dry for 24 h. The reduced sugars were re-dissolved in 10 µL of 10% acetic acid (Fry 1983).

(a)



(b)

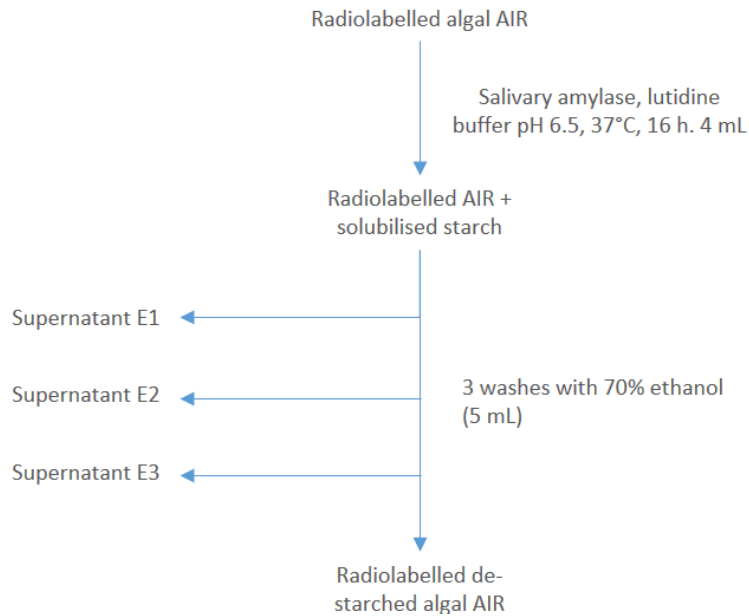


Figure 11: Scheme of the live radiolabelling and de-starching processes. (a) shows the radiolabelling process. (b) shows the de-starching process.

2.2.1.3. Radioactivity measurement

2.2.1.3.1. *Autoradiography and fluorography*

A radiolabelled sample was loaded and developed following previously described methods on paper or on thin-layer chromatography.

If the sample was labelled with ^{14}C , the plate/paper was directly set into a cassette, facing a film. It was kept in the dark for various amounts of time (3 days to a month) and developed.

If the sample was labelled with ^3H , the plate was dipped in 7% PPO in diethyl ether and hung to dry for about ten minutes. It was then placed into a cassette, facing a pre-flashed film.

This was kept in the dark at -80°C for 3 days to a month, and developed.

The result from these methods is a replicate of the film/paper, where the presence of radioactive compounds is indicated by the presence of dark stains (Fry 2000).

2.2.1.3.2. *Scintillation counter*

If the sample was soluble, it was diluted to the appropriate concentration in 0.1 to 1 ml of water in a scintillation vial. Ten times the volume of aqueous scintillation liquid (Meridian Biotechnologies Ltd, 1 to 10 ml) was added, the vial was mixed vigorously.

If the sample was solid (adsorbed on paper, insoluble in water), the appropriate amount of non-aqueous scintillation liquid was added. The tube was mixed well, so that the entire sample was covered in liquid.

The radioactivity in each tube was counted on the scintillation counter: the output is the number of flashes emitted per minute (CPM) by the scintillation liquid. This can be

converted into a measure of radioactivity, depending on the counting efficiency, simply by following the equation:

$$\text{Radioactivity}(Bq) = (CPM_{\text{sample}} - CPM_0) \div (60 \times CE)$$

CE is the counting efficiency, roughly equal to 0.9 for ^{14}C and 0.35 for ^3H .

The scintillation counter also measures H#, the quench number for each sample (Fry 2000).

2.2.1.3.3. *Scanner*

For a plate or paper on which radioactive compounds have been separated (loading above 0.4 kBq), it is possible to directly detect radioactivity by scanning it.

The output of the scanner is a profile of radioactive counting along the length of the plate (Xin *et al.*).

3. Sugar residue composition - semi-quantitative analysis

3.1. Introduction

A range of plants was selected for studying their cell wall sugar residue compositions. The aim in this chapter is to give an overview of their cell walls. Further studies were developed, based on those results, in other chapters.

Four algae from across the charophyte clade were selected: *Chlorokybus atmophyticus* (Chlorokybales), *Klebsormidium fluitans* (Klebsormidiales), *Chara vulgaris* (Charales), *Coleochaete scutata* (Coleochaetales). They were compared to plants from neighbouring groups: *Ulva rigida* (Ulvales, chlorophyte clade) and *Anthoceros caucasicus* (Anthocerotales, bryophyte).

They were submitted to sequential extraction, in order to separate what in land-plants would be called pectic, hemicellulosic and cellulosic fractions from one another. Each fraction was acid hydrolysed and the products were analysed by chromatographic methods.

These analyses were rendered less representative than expected by two phenomena: strong glucose bands were observed in the majority of extracts, probably coming from starch that was extracted alongside cell wall polysaccharides, and insufficient separation of pectin and hemicellulose, which might be due to incomplete pectin extraction. In order to solve these problems, a second set of experiments was set up, within which the algal and land-plant ethanol-insoluble residues (AIRs) were submitted to a range of chemical and enzymatic treatments prior to sequential extraction. These included α -amylase incubation, alkaline degradation coupled with endo-polygalacturonase (EPG) digestion, and controls included solely alkaline degradation and solely EPG treatment. These experiments were run in

triplicate, which allowed for statistical quantification of the sugar residues within cell wall fractions.

3.2. Sequential extraction

The land-plant/algal material, which had been produced in the laboratory and stored freeze-dried over several years, was first washed several times with 75% ethanol to produce alcohol-insoluble residue (AIR), containing all cellular polymers. The AIR was about 60 to 80% of the initial cell dry weight. Initially, this step was the only one prior to sequential extraction, and the samples could therefore have contained non-cell-wall polymers such as starch and glycoproteins.

The different polysaccharides were then extracted sequentially (Figure 12). The total yield was between 40 and 50% of the initial dry weight. The “pectic” portion, extractable with a chelating agent at high temperature (here oxalate), represented at the very least 40% of the total extracted mass. It was extracted in two steps: the solubilized products were separated after 2 h, giving the fraction P1, and again after 18 h, giving the fraction P2. The extractability of plant pectin was evaluated by the ratio P1/P2, a high ratio indicating that most of the pectin was easily extracted by a short heat treatment. It varied between species, and seemed to be higher in *Anthoceros* and the later-divergent CGAs than in the earlier-divergent CGAs and *Ulva*. The “hemicellulose” portions (extractable in concentrated alkali), and the “ α -cellulose” (final insoluble residue) represented the other major part of the AIR. Most of the hemicellulose remained soluble in neutral aqueous buffer, but a minor part

precipitated (giving respectively Hb and Ha fractions). The α -cellulose proportion varied appreciably between the different plants, ranging from 5 to 45% of the total AIR. A portion, “Wash”, was obtained by extraction with a slightly acidic acetate buffer from the alkali-inextractable residue and constituted a minor part of the total extracts.

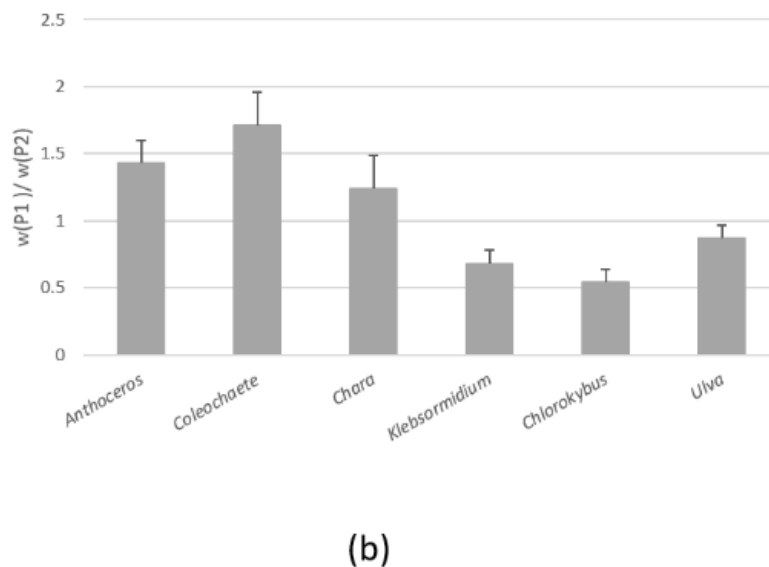
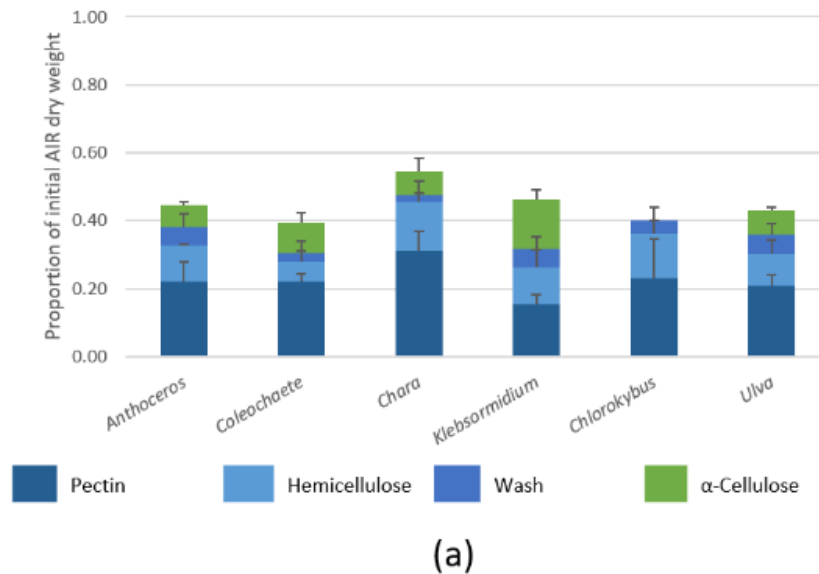


Figure 12 : Quantities of plant extracts relative to the initial AIR quantity.
 (a) : Proportions of the different extracts, in various plants. (b) : Ratio of the weights of pectin 1 over pectin 2, for each plant. The experiment was run in triplicate, allowing for statistical analysis. Error bars = SE, n = 3.

In total, the mass of the recovered polymer fractions only represented about half the initial AIR mass. This result is surprising, as the sequential protocol is tailored to optimise polysaccharide recovery. This loss is due to the dialysis step. Indeed, in order to get rid of the ions and chemicals used for solubilisation (oxalate, acetate, sodium), the extracts were dialysed three times against water with 12-kDa molecular-weight-cut-off (MWCO) tubing. This size corresponds to molecules about 60 Glc units long. It is thought to be a good compromise for efficient separation and minimal losses. However, 12-kDa MWCO is probably too high and smaller polymers are lost in solution.

Overall, those results were comparable to previous findings (O'Rourke *et al.* 2015).

3.3. Monosaccharide analysis of plant extracts

Each polymer fraction was TFA-hydrolysed and analysed by thin-layer chromatography (TLC) to isolate the individual sugars (Figure 13). The TLCs were run in duplicate in two different solvent systems, one being more efficient for the separation of neutral sugars (EPAW 6:3:1:1) and the other more efficient to resolve the different uronic acids (BAW 4:1:1). Markers were run alongside the samples, to help with the identification of the compounds: they were chosen because they are the most commonly found in plant cell walls. However, some algae presented thymol-staining compounds which did not match the usual markers. These are discussed in the next chapter.

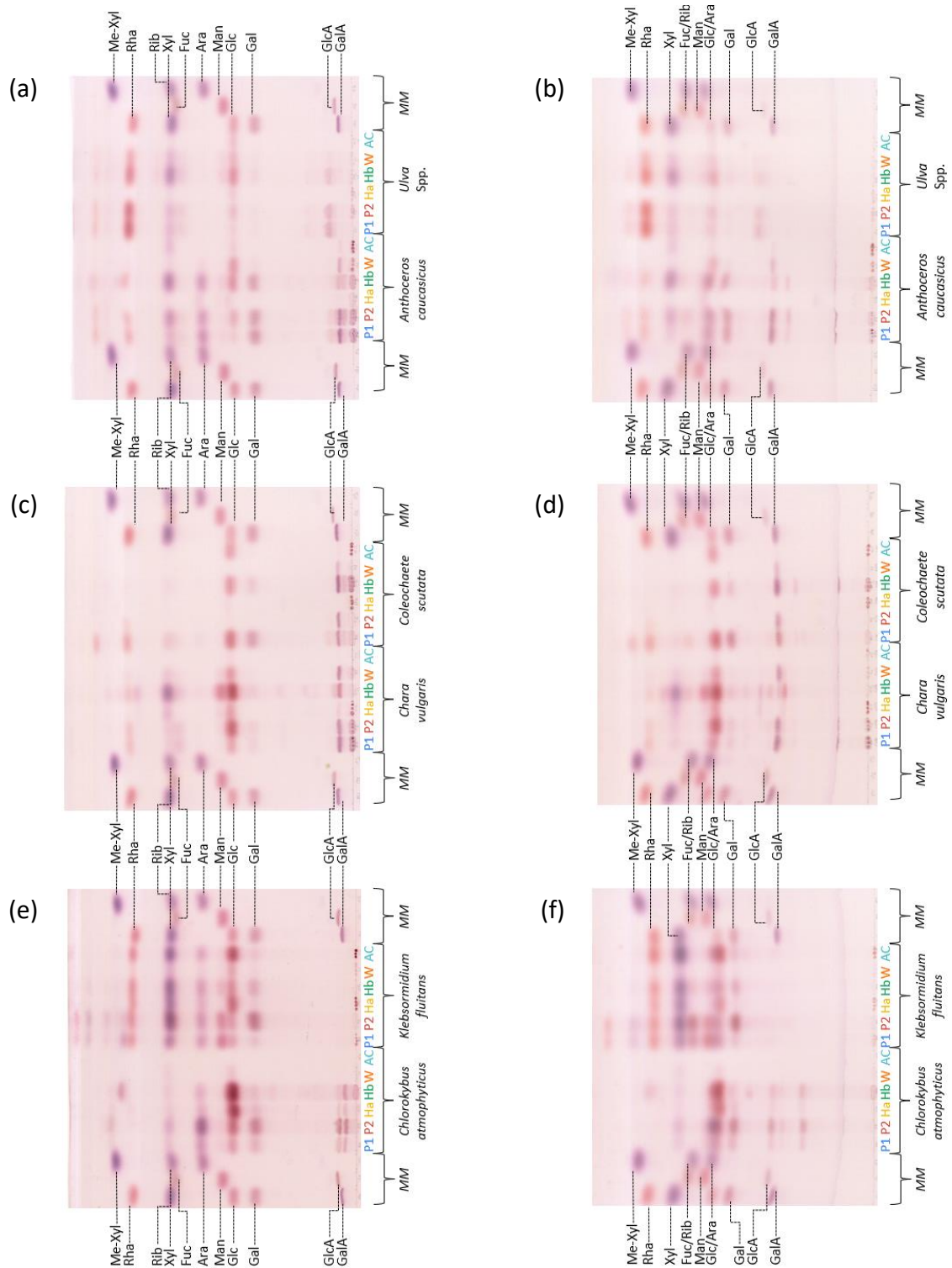


Figure 13: Thin layer chromatography (TLC) of the TFA-hydrolysed polymer fractions from different species.

Left: Developed in EPAW (ethyl acetate/pyridine/acetic acid/water 6:3:1:1), two ascents, on plastic-backed silica-gel plates. Right: Developed in BAW (butan-1-ol/acetic acid/water 4:1:1), two ascents, on plastic-backed silica-gel plates. Each hydrolysate was loaded as 15 μg , and each marker sugar was loaded as 3 μg .

The main points of this screening were:

- The presence of a putative aldobiouronic acid in *Chlorokybus*, which was extracted (visible in Figure 13 (f)). Structural analysis is presented in Section 4.
- The peculiarity of the pectic extract from *Klebsormidium*, as it did not yield any detectable uronic acid (Figure 13 (e) and (f)). This polysaccharide is investigated more in-depth in Section 5.
- *Chara* was especially rich in galacturonic acid and globally matched the expected composition of plant cell wall extracts (Figure 13 (c) and (d)).
- *Coleochaete* behaved in a similar way (Figure 13 (c) and (d)).
- *Anthoceros* (bryophyte and the only land plant of the study), was used as a comparator: it was used to check the viability of the method. A known aldobiouronic acid was detected and its sugar fingerprint was similar to previously reported ones (Popper *et al.* 2003) (Figure 13 (b)).
- *Ulva* (chlorophytic green alga), was analysed alongside the others. The similarity between the *Ulva* fractions was remarkable (Figure 13 (a) and (b)).

This introductory work was later repeated in order to confirm the presence of unusual compounds, and quantify more precisely the different fractions and the sugars constituting them.

It is remarkable that Hb is, in several plants, very similar to the pectic fractions: this could be the result of the pectin extraction protocol not being extensive enough for the polysaccharides (Benassi *et al.* 2021). Additionally, almost all the extracts present high quantities of glucose. Such high rates could come from starch, naturally stored in plant cells

(Busi *et al.* 2014). Further work was conducted to solve those extraction and detection issues.

3.4. Pre-treatments of AIR

In order to answer the questions that arose from the analysis of monosaccharides in the different polysaccharide fractions, the extracts were submitted to several enzymatic and chemical treatments. All the experiments were run in triplicate in order to provide a statistically significant set of data, including the initial one (described above).

3.4.1. Excessive glucose signals: de-starching plant AIR

It has been mentioned that glucose was a major component of almost all the extracts, and it is suspected of coming from starch stored in the plant. In order to test this hypothesis, algal AIR was digested with α -amylase prior to sequential extraction and acid hydrolysis. This process involves heating plant AIR to 100°C (in aqueous solution, pH 6.7, 15 minutes), and incubating it for 72 h at 60°C with α -amylase (Figure 14 (c)).

Seven extracts per plant were produced: the ethanol-soluble portion from α -amylase digestion, and the six polysaccharide fractions, P1, P2, Ha, Hb, W and α -C (Figure 15).

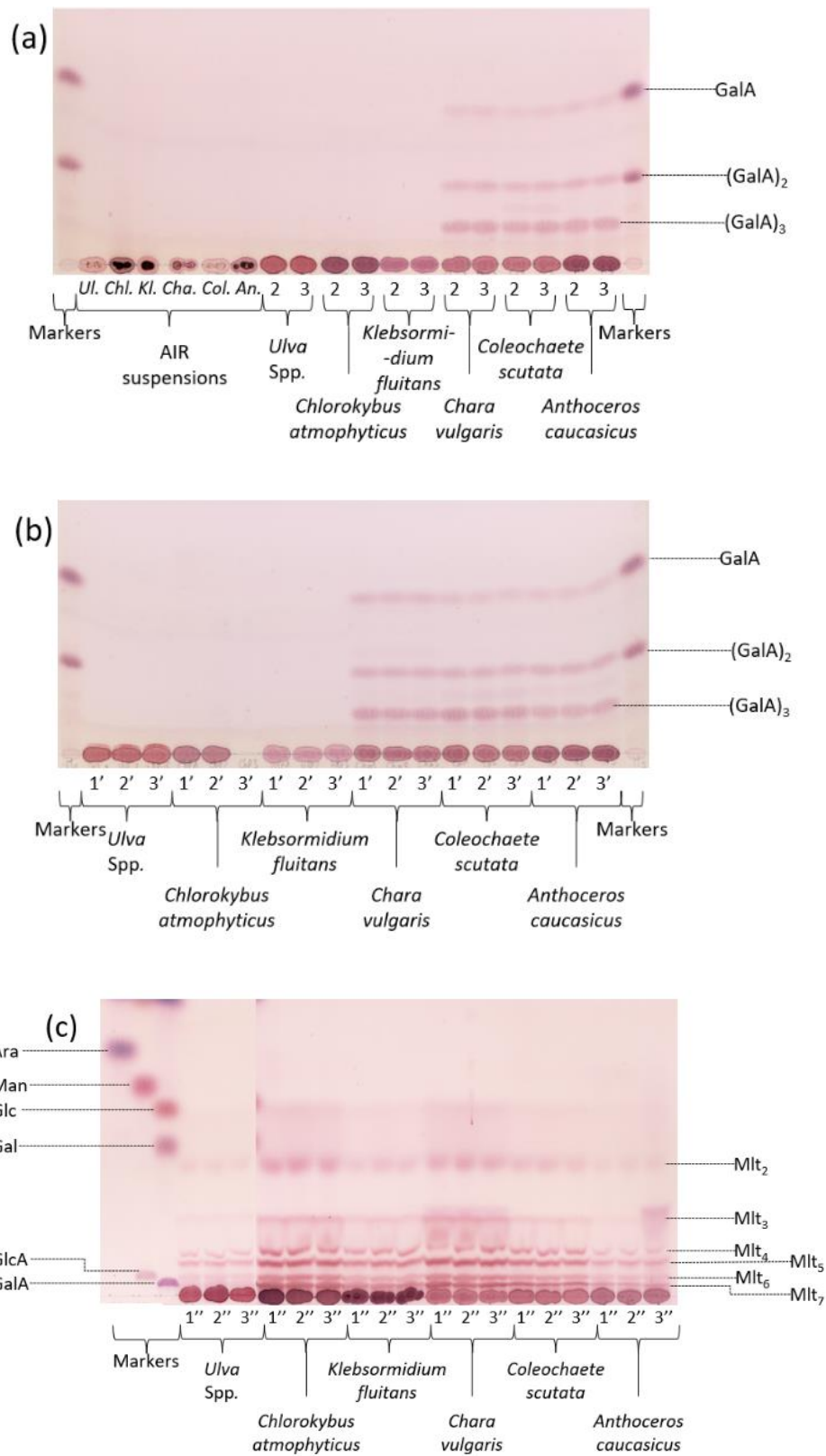
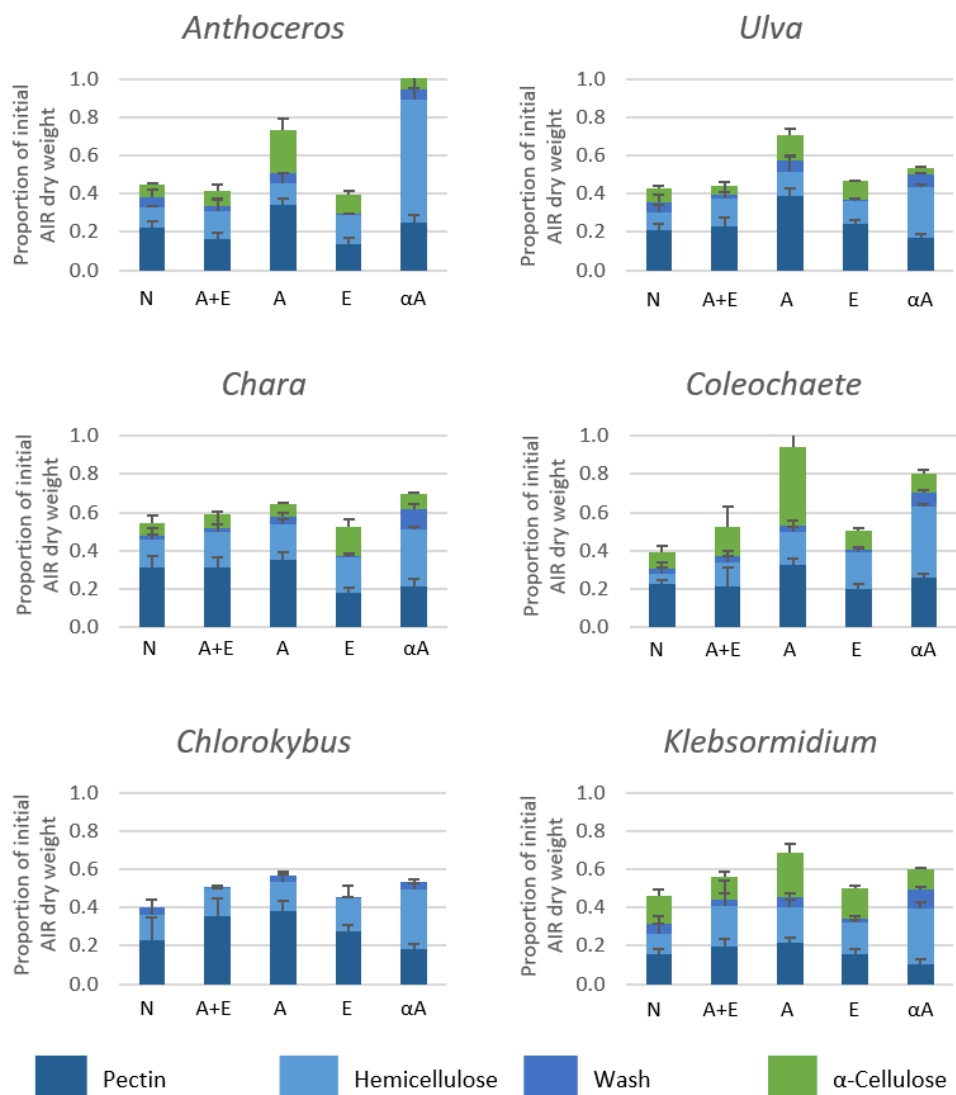


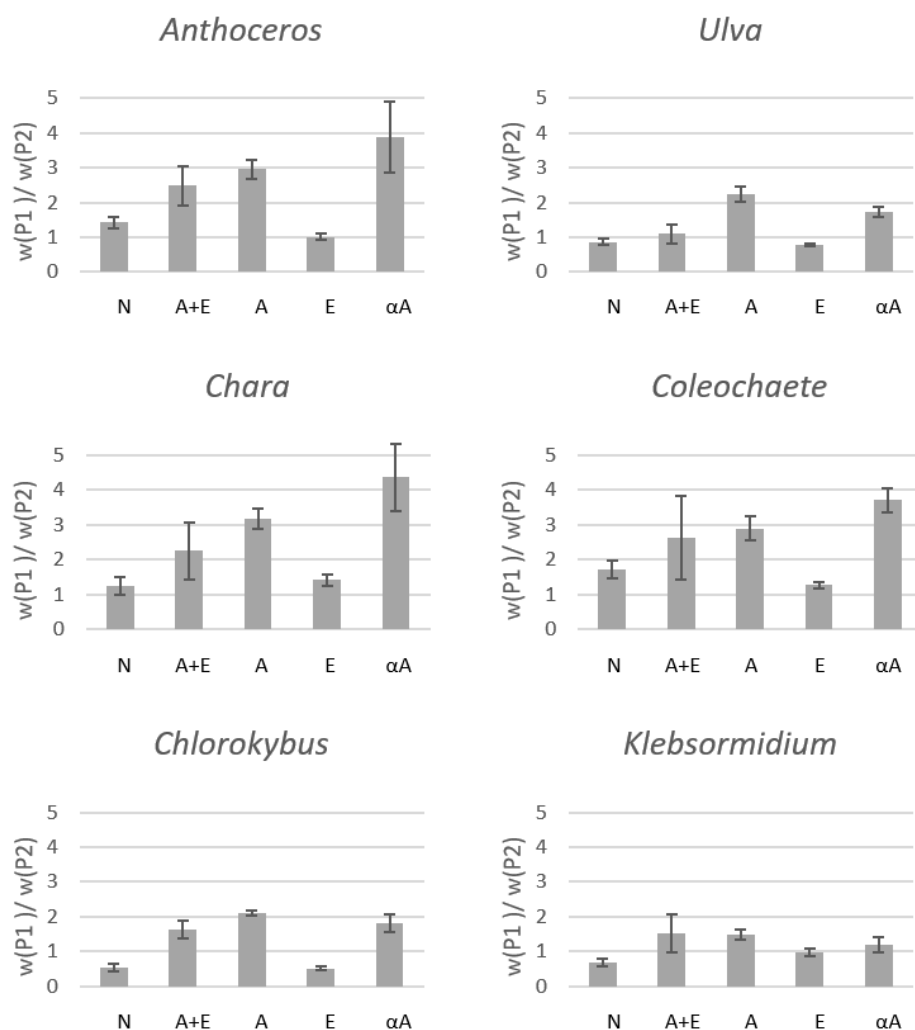
Figure 14: Ethanolic supernatants obtained from EPG, alkali and EPG, and amylase digestion of plant AIRs.

(a): TLC of replicates 2 and 3 of the aqueous supernatants obtained after successive alkaline and EPG digestion from different species. The first six lanes were loaded with plant AIR suspended in water. Ul. stands for *Ulva*, Chl. for *Chlorokybus*, Kl. for

Klebsormidium, *Cha. for Chara*, *Col. for Coleochaete*, *An. for Anthoceros*. (b): TLC of replicates 1', 2' and 3' of the aqueous supernatants obtained after EPG digestion from different species. (c): TLC of replicates 1'', 2'' and 3'' of the ethanolic supernatants obtained after α -amylase digestion of AIR from different species. The labels Mlt2, Mlt3, etc., stand for maltose, maltotriose, etc., which are characteristic of starch digests. (a) and (b) were developed in B/A/W 4:1:1 (butan-1-ol/acetic acid/water), one ascent, on aluminium-backed silica-gel plates. (c) was developed in E/P/A/W 6:3:1:1 (ethyl acetate/pyridine/acetic acid), two ascents, on plastic-backed silica-gel plates.



(a)



(b)

Figure 15: Quantities of plant extracts relative to the initial AIR quantity, after enzymatic and chemical pre-treatments.

(a): Proportions of the different extracts, in various plants, following a variety of pre-treatments, as proportion of the initial un-treated AIR weight. (b): Ratio of the weights of pectin 1 over pectin 2, for each plant with each pre-treatment. In both (a) and (b), the letters correspond to the treatments applied to the AIR prior to sequential extraction: N is for no treatment, A is for alkali digestion (1M NaOH in 75% ethanol, 25°C, 10 minutes, rinsed with ethanol, neutralised with acetic acid), E is for EPG digestion (2.5 U/ml in pyridinium acetate buffer pH 4.7, 25°C, 16h, rinsed with water several times) A+E is for alkali and EPG digestion, applied sequentially (alkali as above, the AIR was rinsed with acetone and dried after neutralisation, then EPG as above), αA is for α-amylase digestion (heating at 100°C, in lutidine buffer pH 6.7, for 15 minutes, followed by incubation with heat-resistant dialysed α-amylase, 60°C, 72h, and rinsed several times with ethanol, the first one containing ammonium formate). After each treatment, the remaining residue was rinsed with acetone and dried, then the new AIR was fractionated into pectin (P1 and P2), hemicellulose (Ha and Hb), wash (W), and cellulose (α-C).

3.4.1.1. Amylase-solubilised sugars from plant AIR

The low-molecular-weight α -amylase products were separated on TLC (Figure 14(c)). All plants showed signals of glucose, which is the monosaccharide constituent of starch. Therefore, they all seemed to contain starch, which is expected since starch production and storage is shared amongst members of the Viridiplantae (Busi *et al.* 2014; Sahoo and Seckbach 2015; Necchi 2016). However, the quantity of sugar that was released did vary. The chlorophyte *Ulva* showed the weakest glucose signals, pointing at it containing the smallest proportion of starch. In the same way, the bryophyte *Anthoceros* presented relatively low signals. Amongst the CGA, *Chlorokybus* and *Chara* were the most starch-rich, while *Klebsormidium* and *Coleochaete* displayed similarly low abundances. These variations in starch contents may come from the growth stage at which the different cultures were harvested, which would have corresponded to a higher or lower starch accumulation as energy backup for the algae/plant.

3.4.1.2. Sequential extraction on amylase-treated plant AIR

Following starch solubilisation and ethanolic precipitation of wall polysaccharides that had dissolved in the aqueous amylase solution, the AIRs were submitted to sequential extraction. Each one of the extracts (P1, P2, HA, HB, W, α -C) was weighed, and the results are presented in Figure 15. In all plants, the overall yield was higher than for sequential extraction upon amylase-un-treated AIR (comparing bar graphs labelled N and α A (Figure 15 (a))).

In particular, the hemicellulosic fraction was more abundant than in extracts produced from un-treated plant AIR. It is possible that heating the polysaccharides (pH 6.7, 100°C, 15

minutes) changed their conformation, loosening the interactions between polymers and making them more easily extractable.

Pectin extractability was highly impacted in all plants, apart from *Klebsormidium*. The ratio P1/P2 more than doubled in plants displaying uronic acid-containing pectic fractions. It is however unclear whether this is due to heating prior to extraction, which might have helped unravel the polysaccharides' network, or to the elimination of starch, which might allow a more efficient extraction. *Klebsormidium* is the only plant for which pectin extractability did not seem to be affected. It is also the only one with a non-ionised pectic fraction at pH 6.7, which might explain this fundamentally different behaviour. Indeed, uronic acid-containing pectic extracts are negatively charged in these conditions.

Each extract was hydrolysed with TFA, and the resulting sugar mixture separated on TLC as before. The results are analysed further on in this chapter.

3.4.2. Pre-solubilization of pectic carbohydrates

One of the flaws of the initial experiment was the incomplete separation of pectin from hemicellulose. Breaking down some parts of the pectin might help it solubilize and enhance the extraction process to follow (hot ammonium oxalate). Endo-polygalacturonase (EPG) was used, in order to hydrolyse (and thus solubilize) the galacturonan fraction. As EPG is not efficient on esterified GalA residues, the AIR must previously be treated with an alkali such as sodium hydroxide. This double treatment was conducted on all plants, followed by

sequential extraction and acid hydrolysis of each extract. In order to evaluate the impact of each step of this treatment, two control experiments were set up.

The first one was digestion with EPG prior to sequential extraction, without alkaline de-esterification. This should solubilize stretches of naturally un-esterified homogalacturonan.

The other control experiment is alkaline de-esterification, without EPG treatment prior to sequential extraction. In that case, all cell wall sugar residues should be de-esterified, but no domain or sugar residue should be extracted, as the alkaline treatment is conducted in 75% ethanol, which keeps polymers from solubilising.

The products yielded by EPG digestion, with and without previous alkaline treatment, were separated on TLC (Figure 14 (a) and (b)). In both cases, neither the chlorophyte *Ulva*, nor the 'lower' charophytes (*Chlorokybus* and *Klebsormidium*) yielded oligomers. It was not surprising for *Ulva*: homogalacturonan has not been detected in its cell wall so far (Ray and Lahaye 1995; Ray 2006). Its phylogenetic position, distant from land plants is reason enough for its cell wall to be chemically distinct. The results from *Klebsormidium* confirmed previous findings: no uronic acid was detectable in its AIR fractions, hence no homogalacturonan (O'Rourke *et al.* 2015). However, the absence of oligomers released by digestion of *Chlorokybus* was unexpected. It was previously established that this algae contains uronic acid, most certainly galacturonic and glucuronic (Figure 14). Those residues might be organized within the polysaccharide(s) in a different fashion than expected. The higher charophytes *Chara* and *Coleochaete*, and the bryophyte *Anthoceros* all yielded galacturonides, both with and without alkaline digestion. This is not surprising: it has been established that they contain galacturonic acid, and their similarity, or belonging, to land

plants certainly should be reflected in their cell walls (Sørensen *et al.* 2011; O'Rourke *et al.* 2015). However, no notable difference was visible between the alkali pre-treated samples and the others. Previous results concerning homogalacturonan functionalisation in *Chara* and *Coleochaete* showed that they were only marginally, or not at all, esterified (Cherno *et al.* 1976; Sørensen *et al.* 2011).

The results from *Anthoceros*, however, could not be explained or compared as it is unclear whether hornwort's pectin is esterified or not (Kremer *et al.* 2004).

EPG digestion was operated at ambient temperature, pH 4.7, making it highly unlikely for methyl and acetyl groups to be released from the sugar residues by non-enzymic hydrolysis during the incubation process. The absence of mobile thymol-stainable compound in AIR (Figure 14 (a)) confirmed that all the compounds detected had been released following incubation and digestion.

As previously, plant AIRs were submitted to sequential extraction following pre-treatment, and each extract was weighed. The yields were compared to the ones measured from untreated AIR samples (Figure 15).

In all plants, the EPG treatment alone resulted in almost no variation in the relative weights of extracted material, nor in total amount recovered, by comparison with non-previously treated AIR (comparing bar graphs labelled N and E in Figure 15 (a)).

The sodium hydroxide treatment on its own allowed a total higher polysaccharides recovery: it was doubled in *Anthoceros* and *Coleochaete*, augmented substantially in *Ulva*, *Chlorokybus*

and *Klebsormidium* (comparing bar graphs labelled N and A in Figure 15 (a)). The pectic fraction was augmented by NaOH most in *Anthoceros* and *Ulva*. In *Coleochaete*, the insoluble final residue (α -cellulose) represented half the total recovered AIR, which was unexpected. In other plants, the relative quantities between fractions changed relatively little.

The extracts from AIRs which had been submitted sequentially to alkaline and EPG digestions were not very different from untreated samples (comparing bar graphs labelled N and A+E in Figure 15 (a)). In *Ulva*, *Anthoceros* and *Chara*, they were basically identical. In *Coleochaete* and *Klebsormidium*, the hemicellulosic fraction had become more abundant after alkali-EPG pre-treatment. In *Chlorokybus*, the pectic fraction was augmented substantially.

It is surprising that the effects from the incubation with sodium hydroxide were not preserved after EPG incubation (sole alkaline treatment previously led to a much higher polysaccharide recovery, and a higher pectin recovery in some cases). This might be due to the subsequent enzymatic incubation at a slightly acidic pH, resulting in a reorganisation of the polysaccharides.

Another surprising finding, both from EPG and alkali+EPG pre-treatments experiments, was the fact that the oxalate-extractable pectin content did not drop, even in the 'higher' charophytes which possess homogalacturonan. Indeed, a considerable quantity of homogalacturonan was released during the digestion: since it is expected to be a major part of pectin, it would have been expected to see the pectin content drop. This might be due to

an incomplete digestion by the EPG, with only a small impact to the cell wall's global composition.

The pectin extractability was measured for each of these experiments. The EPG pre-treatment alone had a very limited effect on the efficiency of pectin solubilisation by hot oxalate. On the contrary, alkaline incubation made the pectin much more extractable, in every plant: the ratio P1/P2 more or less doubled. This might be due to the loosening of interactions between the cell wall's biopolymers, or to the partial depolymerisation of polysaccharides via alkaline peeling. The combination of alkaline and EPG treatment, however, was harder to assess as the results were very dispersed. In *Ulva* and the higher charophytes, it was not markedly different from the untreated (and EPG-only treated) samples. In *Anthoceros* and the lower charophytes, it was slightly superior, though not enough to draw any reasonable conclusion. Once more, it seems that the effect of the alkaline treatment was counterbalanced during the enzymatic incubation.

Each one of the extracts was hydrolysed with TFA, and the resulting sugar mixture were separated on TLC as before. The results are analysed further on in this chapter.

3.5. Automated semi-quantification

3.5.1. Needs for an automated analysis tool

The total number of extracts generated from the set of experiments previously described was high. Six plant species were analysed in total. Each plant AIR was submitted to a range of five pre-treatments (none, α -amylase, alkali, EPG, alkali+EPG) , in triplicate, generating 30 pre-treated AIRs. Each of these AIRs was submitted to sequential extraction, producing six different extracts, meaning 180 extracts in total. Each extract was run twice on TLC (in two different solvent systems). This meant that 360 TLC tracks needed to be analysed. The aim, however, was to get a global view on composition variations and possible irregularities. In order to do this, semi-quantification of each extract was seen as essential. However, doing so by systematic manual measurement via ImageJ would have been unnecessarily lengthy and repetitive. An automatic algorithm was set up for this project, using Matlab as a support.

Matlab is a tool that "combines a desktop environment tuned for iterative analysis and design processes with a programming language that expresses matrix and array mathematics directly". More directly, it is a user-friendly programming environment, especially efficient for treating sets of data in parallel. Matlab includes a variety of toolboxes, allowing for more specific applications. Amongst them, the Image Processing Toolbox provides a set of tools for image processing, analysis, visualization, and algorithm development. It was particularly useful here, as stained TLCs were to be analysed. The Signal Processing Toolbox was equally essential, as it contains pre-implemented functions that were extensively used.

The code developed in the laboratory, in order to analyse the previously described data, aimed to detect, identify and semi-quantify the sugar residues in each extract. It was able to synthesize the results from the 3 replicates of the experiment in order to get average percentages as well as standard deviations.

3.5.2. The algorithm

Two versions of the code were created. The simplest version analyses one plate at a time, "App1Plate".

The input is a scan of one TLC plate, organised, from left to right, as follows:

- The first "track" contains the marker mixture number 1 (MM1, GalA, Gal, Glc, Xyl, Rha), the second track contains the marker mixture number 2 (MM2, GlcA, Man, Fuc), the third track the marker mixture number 3 (MM3, Ara, Rib, Me-Xyl). These are tracks 1 to 3.
- The next six tracks (4 to 9) contains the extracts P1, P2, Ha, Hb, W and α -C of one plant species, with one specific pre-treatment. For example, *Anthoceros*, alkali-treated.
- The next six tracks (10 to 15) contains the same thing, for a different plant species, with the same pre-treatment. For example, *Ulva* spp., alkali-treated. Plants were usually paired up as follows: lower charophytes *Chlorokybus* and *Klebsormidium*, higher charophytes *Chara* and *Coleochaete* and others *Anthoceros* and *Ulva*.
- The final three tracks (16 to 18) are a repeat of the first three, containing MM1, MM2 and MM3.

The user is asked to choose certain parameters: the marker mixture set to be used as reference (left, i.e. tracks 1 to 3, or right, i.e. tracks 16 to 18, chosen depending on the evenness of the solvent front) and the minimum contrast of the bands for detection (numerical value, also called prominence).

The output of "App1Plate" is a series of 12 histograms, displaying the relative intensities of staining of each sample.

The algorithm starts by pre-treating the input: the coloured image (RGB) is transformed into a grey-level file.

The intensity profile of each sample is extracted and filtered via the Matlab-encoded Savitzky-Golay filter.

This filter was created in order to smooth noisy signals. It can be seen as a variation of the moving average method. Practically, it consists of fitting successive intervals of data points with low degree polynomials by the method of linear least squares (i.e. the coefficients of the model are calculated so that the squared difference between the fit and the data is minimal). If the data points are equally spaced, a single set of "convolution coefficients" can be found. This set, applied to any data sub-set, gives an estimate of the smoothed signal at the centre of each interval (i.e. data sub-set). The parameters of the filter are the order of the fit (3 here) and the number of points in each data sub-set (11 here).

The intensity peaks are then detected via the Matlab-encoded "findpeaks" function. It is made to detect local maxima and returns their position, their value at the top, their width and their prominence. Criteria for detection can be the prominence of the peak or its height. Here the prominence, or contrast, is set up for each plate, as relative intensities are not identical between plates. The height criterion (i.e. absolute intensity of the band) is not employed.

At this stage, all the necessary information has been extracted from the image. The user has defined which set of markers they want to use (left or right, depending on the solvent front). The set that is going to be used is isolated into a reference table. The areas of the peaks are

computed by approximating the peaks by Gaussian curves: $A = P \times w \times \sqrt{\pi}$ with P the prominence, w the width of the peak. It is assumed that the intensity of the peaks and the abundance of each sugar residue follow a consistent linear trend.

The peaks in the samples are matched to the MM peaks and labelled. If they do not correspond to any marker, they are labelled "Unknown1", "Unknown2", etc. The areas are normalized so that their sum is 1. Histograms displaying those relative intensities are drawn, and numbered 1 to 12.

The second version was developed specifically for my experiment, which required running triplicates, "AppTriplicate". The input for this algorithm is three scans of TLC plates, organised as described before. These three plates each display a replicate of the same experiment, for example NaOH-treated *Chlorokybus* and *Klebsormidium*, replicates 1, 2 and 3.

The information is extracted from each plate in the same way as in the "App1Plate" algorithm. The data from the three plates are then compiled, and the sugar relative intensities are averaged between the plates. The standard deviation is calculated for each sugar residue in each extract.

The app returns 12 histograms, presenting the average relative quantities of sugars in each fraction as well as their standard deviations. Each histogram is named by the extract it corresponds too, for example P1, *Chara*, NaOH-treated.

The pitfalls of this method are the possible peaks misidentifications (for example, if the intensity threshold used was inappropriate), which can be fixed by changing the selection

parameters, and the mismatches between the plates (visible on the final histograms as non-interpretable data).

3.5.3. Interpretation of the statistical analysis of the sugar contents of various plant species

For all six species studied in this chapter, sequential extraction and hydrolysis of each polysaccharide fraction were performed in triplicate. The hydrolysates were run on TLC in two solvent systems and the relative quantities of each sugar in each extract were measured following the automatised process described above (Figure 16). For each plant, comments are provided on the presence – or absence – of key identifiable and non-identifiable sugars.

3.5.3.1. *Anthoceros caucasicus*

3.5.3.1.1. *Anthoceros pectin*

The two pectin fractions were found to be almost identical, both when separated with BAW and with EPAW. Chromatography in BAW allowed for a clearer separation of the different acidic compounds: the one termed “Unknown1” on Figure 16 probably corresponds to the aldobiouronic acid previously analysed (Popper *et al.* 2003). This will be studied more closely in 4.3.2.

Galacturonic acid was one of the main components, making up to 30% of the total sugar residues. This was not surprising, as it is the main pectic sugar in land plants, present in homogalacturonan, RG-I and RG-II (Fry 2011).

Galactose represented 10 to 20% of the total sugars. In land plants, galactose is usually found in RG-I and RG-II sidechains.

The glucose contribution was highly variable. As expected, 'pectic' glucose dropped drastically when the AIR was de-starched: in EPAW, it went from 10 to ~0%. In BAW, it was impossible to differentiate glucose and arabinose, as they almost co-migrate (Table 3). However, it was clear that the so-called "Glc-Ara" contribution dropped after α -amylase digestion, from 40% to only 20%, supporting the idea that Glc is only present in contaminating starch and is not part of the pectic polysaccharide chain.

Arabinose made up to 20% of the pectic sugar residues. Arabinose is, like galactose, present in RG-I and RG-II sidechains.

Xylose was a minor component, present in both pectic extracts. In BAW, it was found to contribute for 5 to 15% of the pectic extracts. Xylose is part of the pectic domain xylogalacturonan in land plants. In EPAW solvent system, xylose could not be differentiated from ribose and fucose. However, these two sugars were only detected marginally in the BAW solvent system. The "Xyl-Rib-Fuc" contribution was found to be around 20% in EPAW. Ribose is sometimes found in the plant cell wall hydrolysate, this sugar residue being present in RNA, which is extracted when preparing plant AIR. The extra 5% detected (by comparison with the 15% of xylose measured in BAW) could be attributed to a variable proportion of fucose, which is known to be involved in the RG-II sidechains of pectin (Matsunaga *et al.*

2004). It is however difficult to give a definite explanation to this phenomenon, given the undetectable quantities of Fuc and Rib detected in BAW.

Rhamnose, finally, contributed around 10% to the total sugars. Rhamnose is very much expected in pectic extracts, as it is a major component of both RG-I and RG-II (respectively in the backbone and the sidechains).

A fast-migrating sugar, staining pink, was detected in many of the extracts, termed either “Me-Xyl” or “Unknown1” on the histograms. It was visible on many TLCs, though not always quantifiable. This sugar may correspond to the previously detected, in bryophytes and higher charophytes, acofriose (or 3-*O*-Me-Rha) (Popper *et al.* 2004). However, it is difficult to confirm as the chromatographic data available for acofriose relates to paper chromatography and not TLC. This compound has been identified in the minor RG-II pectic fraction of bryophytes, as a replacement for un-methylated rhamnose (Matsunaga *et al.* 2004).

3.5.3.1.2. *Anthoceros hemicellulose a*

Hemicellulose a was not always quantifiable. It is indeed a minor component of the AIR, and it was not always possible to load enough sample. However, the few measurable extracts were all very similar to each other, made of xylose and glucose, in about the same quantities. The main hemicellulose component in land plant primary cell walls, including early-divergent ones, is xyloglucan, which is made of a glucosyl backbone, bearing numerous xylosyl residues, and marginally galactosyl and fucosyl residues (Nothnagel and Nothnagel 2007; Albersheim *et al.* 2011). Hornworts are known to contain land-plant-resembling xyloglucan polysaccharides (Peña *et al.* 2008). However, xylose could also be part of the

hemicellulosic polysaccharide xylan, and glucose could be part of mixed-linkage glucan (Fry 2011).

3.5.3.1.3. *Anthoceros hemicellulose b*

Uronic acids were detected in hemicellulose b from untreated AIR, but not in any other sample. This could be due to a more efficient separation of fractions: acidic sugar residues are mostly expected to be found in pectin.

Galactose was present in all hemicellulose b extracts, about 10% in most and about 20% in de-starched extracts. In land plants hemicellulose, galactose is usually found as a substituent of xyloglucan.

Xylose and glucose were present in about the same quantities (see the separation on EPAW), each contributing about 25 to 30% to the hemicellulose sugar residues. The glucose quantity did not change much after α -amylase digestion, suggesting that most starch, if present, was extracted with the pectin.

Arabinose made up for 15% of the hemicellulose b sugar. It is a usual substituent to xylan in land plants.

No mannose was detected in *Anthoceros* cell wall, which contradicts previous findings (Popper and Fry 2003; Nothnagel and Nothnagel 2007).

3.5.3.1.4. *Anthoceros wash*

As for hemicellulose a, the wash fraction was only minor, and not always quantifiable. It was mainly made of glucose residues. As for hemicellulose b, uronic acids were detectable only in

the extract from untreated AIR, and galactose was a minor component. Xylose was sometimes detectable, as well as arabinose. This composition overall resembles that of hemicellulose b, even though glucose's contribution is much greater.

3.5.3.1.5. *Anthoceros* α -cellulose

As expected, most α -cellulose extracts were made of glucose residues. However, xylose and fast-migrating sugars were also detectable in the α C fraction from untreated AIR. The presence of xylose could be due to an incomplete separation of the xyloglucan or xylan chains from the cellulose microfibrils .

3.5.3.1.6. *Anthoceros* cell wall: summary

The composition of the bryophyte's polymer fractions did not vary much with the different pre-treatments the AIR had been subjected to, apart from the glucose from starch (Popper and Fry 2003). The two pectic fractions were always very similar to each other, containing a previously described aldobiouronic acid and a range of sugars typical of land-plant pectin, as well as acofriose (or 3-O-Me-Rha) (Matsunaga *et al.* 2004). The presence of xylose and other neutral monomers in hemicellulosic and cellulosic fractions fits with the expected presence of xyloglucan in *Anthoceros* cell walls (Bartels *et al.* 2017).

3.5.3.2. *Ulva rigida*

Ulva is a chlorophyte: its composition is expected to be markedly different from that of the other plants tested here.

3.5.3.2.1. *Ulva pectin*

Ulva spp. are known to contain a considerable proportion of the polysaccharide ulvan, extractable at high temperature (80 to 90°C) with a chelating agent such as oxalate. Those conditions match the pectin extraction conditions: ulvan should be extracted. It is a sulphated biopolymer made, in decreasing order of abundance, of glucuronic acid, rhamnose, xylose and iduronic acid oxalate (Lahaye and Robic 2007).

The pectic fraction contained a wide band around the uronic acid zone, labelled GlcA in this work. It probably corresponds to both GlcA and IdoA.

Rhamnose and xylose made up respectively about 40 and 10% of the pectic extract. The rhamnose abundance was higher than expected. Since the rhamnose was not accompanied by GalA, it cannot be from land-plant-like rhamnogalacturonan-I. Overall, the expected ulvan composition was visible in this pectic extract.

Glucose made up 10 to 20% of the pectic extracts, apart for the extracts from de-starched AIR, where it was only 5-10% of the total sugars. This remaining presence might be due to an incomplete amylase incubation (Prabhu *et al.* 2019).

3.5.3.2.2. *Ulva hemicellulose a*

The Ha fraction was not quantifiable in the untreated sample. In all others however, it was made of glucose and xylose in roughly even quantities. As *Ulva* has been found to contain phyco-xyloglucan, this is expected (Ray and Lahaye 1995).

3.5.3.2.3. *Ulva hemicellulose b*

The Hb fractions from untreated, NaOH, NaOH-EPG and EPG treated samples all resembled the pectic fractions, with less uronic acids and rhamnose. Their composition was about 10% uronic acid, 45% glucose, 25% xylose and 10% rhamnose.

However, the α -amylase digested samples were markedly different, made almost only of glucose and xylose in even quantities.

3.5.3.2.4. *Ulva wash*

Wash fractions from untreated and alkali-treated samples were made of glucose, xylose and rhamnose, respectively around 60, 20 and 20% of the total sugar residues.

Mainly glucose was detectable in wash from EPG and NaOH-EPG treated samples.

The extract from de-starched AIR was made of half glucose and half xylose, as were the two hemicellulose fractions from *Ulva*.

3.5.3.2.5. *Ulva α -cellulose*

The final insoluble residues were mostly made of glucose, as expected since *Ulva* is known to contain cellulose. However, xylose (and rhamnose in smaller quantities) was also detectable in some extracts, making up to 20% of the extract. As previously, this might be due to an incomplete separation of the fractions, and especially to difficulties in disrupting the hemicellulose–cellulose interactions. This similarity to land plants is worth noting, as opposed to the extreme difference between the hot oxalate-extractable fractions.

3.5.3.2.6. *Ulva cell wall: summary*

As expected, the oxalate-extractable fractions from *Ulva* contained the sugars that make up ulvan, even though the amounts of rhamnose detected are higher than expected (Lahaye and Robic 2007). The hemicellulosic extracts, even though they were still contaminated by ulvan in most cases, contained high amounts of xylose and glucose, indicative of the presence of phyco-xyloglucan (Ray and Lahaye 1995). The presence of xylose (on top of the expected glucose in the cellulosic fraction) indicates the strong affinity of the hemicellulosic and cellulosic polymers, which will be studied later on in this thesis (Section 7.4).

3.5.3.3. *Chara vulgaris*

Chara is a late-diverging charophyte, which means that it is expected to resemble land plants in terms of sugar residue composition and polysaccharide organisation. However, some key land plant polysaccharide structures are known to be absent (or present in minor amounts) of its cell wall, such as xyloglucan or RG-II (Popper and Tuohy 2010; Schultink *et al.* 2014).

3.5.3.3.1. *Chara pectin*

Chara's pectic fraction was, unsurprisingly, rich in galacturonic acid. In all extracts, GalA represented about 30% of P1 and 15% of P2. This alga was previously found to be rich in homogalacturonan, while other pectic domains seem to be only minor (Sørensen *et al.* 2011).

Traces of galactose were detected, especially in the de-starched samples, as the prolonged incubation may have solubilised more of the neutral polysaccharides. Galactose and

arabinose are key components in the major RG-I sidechains. The quasi-absence of these two sugar residues shows the quasi-absence of RG-I in the cell wall.

Glucose was a major compound found in *Chara*'s pectin. It contributed up to 70% of the total sugars in all samples but the de-starched one. In the α -amylase digested fraction, it was only around 25-30%. This contribution is still considerable. It could be due to an incomplete digestion of starch, which is made unlikely by the total elimination of glucose in the model case of *Anthoceros*. The other option would be that glucose is part of the pectic biopolymer of *Chara*. This would be surprising as glucose is not known to be part of land-plant pectin. A third explanation could be that separation from the other fractions (hemicellulose for example) was incomplete, and a different polymer's sugar composition is being described here.

Mannose is only detected in the de-starched samples. With other treatments, it is also found in the Hb fraction. It could be that a mannose-containing polysaccharide is made more labile during the α -amylase incubation. Mannose is not usually part of land plants' pectin.

However, it was found to be part of *Chara*'s pectin (O'Rourke *et al.* 2015).

Xylose and rhamnose were found in all pectic extracts, however they were discrepancies in their relative quantities.

In the BAW solvent system, the xylose contribution ranged from traces to around 10%. In the EPAW solvent system, it was between 10 and 25% for most extracts, and around 25-30% for the de-starched samples. The higher xylose contribution in the latter might be explained by a partial solubilisation of neutral (hemicellulosic) fractions, in the same way mannose's presence could be explained. It could also be that xylose-containing polysaccharides (and/or

mannose) are covalently linked to *Chara*'s pectin. It is worth noting that no xylogalacturonan was detected in charophytes (Sørensen *et al.* 2011).

The rhamnose contribution measurements also yielded different results depending on the solvent system. In EPAW, it was around 10%, apart from P2 extracted from untreated samples. In BAW, it was undetected in EPG-treated, NaOH-EPG-treated, and P2 from NaOH-treated samples. When looking at the TLC plates, however, it was always present if not always quantifiable. Rhamnose is known to be part of the pectic polysaccharide domains RG-I and RG-II. The presence of these polysaccharide domains in charophytes is contested (Sørensen *et al.* 2011; Palacio-López *et al.* 2019).

3.5.3.3.2. *Chara hemicellulose a*

This extract was only quantifiable in two cases, in the solvent system EPAW for the EPG-treated and the NaOH-EPG-treated samples. In both cases, they were approximately made of half xylose and half glucose, in this respect a surprising similarity between *Chara*, *Anthoceros* and *Ulva*.

3.5.3.3.3. *Chara hemicellulose b*

Many Hb extracts, when analysed on BAW, presented either a surprising ladder pattern in the uronic acids zone or unidentified compounds between the uronic acid and neutral sugars zone. Galacturonic acid was detected in all extracts, both when the sample was analysed in BAW and in EPAW. In land plants, galacturonic acid can be found in hemicelluloses as a sidechain of xyloglucan, xylan or mannan (Peña *et al.* 2008; Albersheim *et al.* 2011). It is

possible that some of those sidechains were resistant to hydrolysis (in various degrees), which would explain the ladder patterns.

Glucose was the main Hb component, contributing about 40% to the total sugar composition of the extracts. Glucose usually occurs in the alkali-extractable mixed-linkage glucan or in callose. Mixed-linkage glucan has been demonstrated to be part of the cell wall of *Chara corallina* (Kiemle 2010).

It was followed closely by xylose, which represented about 30% of all Hbs. Xylose can be part of the hemicellulosic polymers xyloglucan, xylan or arabinoxylan. However, xyloglucan is only found - if at all - in limited quantities in charophytic cell walls, and arabinose has not been detected in *Chara* at all. Xylan is thought to be the main xylose-containing polysaccharide in the Hb fraction from *Chara* (Domozych *et al.* 2010).

Mannose was equally detected in almost all cases in EPAW and made up 10 to 15% of the Hb (Nothnagel and Nothnagel 2007). Given that it migrated close to Ara and Glc in BAW, it was difficult to detect it for certain. Mannose is known to be an important component of some land plant hemicelluloses, as mannan or substituted mannan (glucomannans for example) (Scheller and Ulvskov 2010). Heteromannans have been detected previously in *Chara corallina* cell walls (Domozych *et al.* 2010).

Finally, some traces of rhamnose and fast-migrating compounds were sometimes detected in the extracts. Their presence was highly variable.

3.5.3.3.4. *Chara wash*

The wash fraction overall resembled Hb's composition, though with a higher glucose contribution.

3.5.3.3.5. *Chara α -cellulose*

The main component of those extracts was, unsurprisingly, glucose. However, it was not the only one.

In most α -cellulose extracts, traces of galacturonic acid were detectable. Mannose and xylose were also found in minor amounts. These could come from an incomplete separation of the cell wall fractions and indicates particularly strong interactions between the different polysaccharides.

3.5.3.3.6. *Chara cell wall: summary*

Chara 'pectin' resembles land plant pectin to a limited extent, in the way it contains high amounts of GalA (associated with homogalacturonan) but low amounts of RG-I-specific sugars. These findings corroborate the results from immunoassays performed previously (Sørensen *et al.* 2011). The presence of Man and Glc, especially in amylase-treated samples, indicate a pre-solubilisation of hemicelluloses during the de-starching process. Xylose and glucose, however, were the key compounds of the hemicellulosic extracts from most samples.

3.5.3.4. *Coleochaete scutata*

Coleochaete is the second 'higher' charophyte analysed in this study. Like *Chara*, it is expected to biochemically resemble land plants.

3.5.3.4.1. *Coleochaete pectin*

As expected, galacturonic acid was a major component of *Coleochaete*'s pectin. On the BAW solvent system, its contribution was evaluated to about 30% for P1, and about 15% for P2.

This was true for most pectic fractions, apart from the untreated samples, where more GalA was detected in P2 than in P1: pre-treatments may have made the galacturonic acid-rich cell wall fraction easier to extract by disturbing the ionic interactions of the GalA residues with the rest of the cell wall. On the EPAW system, these numbers were about 10 percentage points lower, which was simply due to detection issues. As GalA is extremely slow migrating, it was sometimes hard to properly quantify it in EPAW.

Galactose was found in all pectic extracts. It made up about 10% of the pectin in most cases. However, the de-starched samples displayed a much higher galactose content: around 20% in P1 and 30% in P2. Galactose is a major component of RG-I sidechains.

Glucose represented minimum 20% of the total sugars in pectic extracts. This went down to about 10% in the de-starched samples. As for *Chara*, it is unsure whether this remaining glucose is due an incomplete α -amylase digestion or a genuine contribution to the cell wall.

Arabinose was detected in all pectic extracts: its contribution was minor (around 5%) compared with the land-plant *Anthoceros*, but higher in *Chara*.

Ribose and/or fucose were equally detected in all samples, making up around 5% of the total extract. As explained before, ribose is unlikely to be present in detectable quantities in plants AIR. The sugar residue truly measured here is probably fucose. Fucose is mostly found in RG-I and RG-II sidechains, as well as in xyloglucan sidechains.

No xylose seemed to be detected in the extracts in BAW, although the trio Xyl-Rib-Fuc contributed around 10% of the total sugars in EPAW. Fuc was probably the main sugar being detected here.

Rhamnose was present in all extracts, contributing for about 5 to 10% to the total composition. This contribution seems quite limited. However, the presence, of rhamnose, coupled to the presence of galactose and arabinose, points towards the presence of RG-I within *Coleochaete* cell wall.

Finally, a fast-migrating compound was detected in almost all the extracts. It was termed “MeXyl” or “Unknown1” on the graphs. This compound, staining pink, co-migrated with Me-xylose in BAW and ran slightly faster in EPAW. It is probably the 3-O-Me-Rha previously detected in higher charophytes and lower land plants (Popper *et al.* 2004).

3.5.3.4.2. *Coleochaete hemicellulose a*

Ha is only measurable in the EPG-digested extracts, and is made of 50% glucose and 50% xylose, as found in other algae. This consistent feature may point to a form of phyco-xyloglucan in charophytic cell walls.

3.5.3.4.3. *Coleochaete hemicellulose b*

In *Coleochaete*, Hb extracts presented uronic acid compounds in various amounts. As in *Chara*, they might be part of hemicellulose's sidechains. Galactose, a major constituent of land plant pectin, contributed about 5% of the sugars in the untreated samples, and 20 to 30% in all others. This gap is unexplained.

Glucose was the major constituent of *Coleochaete* Hb, with its contribution ranging from 30 to 70% of the extract. In many cases, minor contributions of xylose, fucose, rhamnase and 3-*O*-Me-Rha were measured. It is worth noting that xylose is not as abundant as it is in other previously analysed plant extracts: the hemicellulose from *Coleochaete* is clearly different from that in *Anthoceros* and *Chara*.

3.5.3.4.4. *Coleochaete wash*

The wash fractions varied from completely identical to Hb, to glucose-enriched Hb.

3.5.3.4.5. *Coleochaete α -cellulose*

The major component of this last fraction was glucose (80 to 100%). However, in almost all extracts, galactose was detected on the EPAW solvent system.

Xylose and other fast-migrating compounds were also measured, though not systematically. Their presence is probably due to incomplete extract separation.

3.5.3.4.6. *Coleochaete* cell wall: summary

The pectic extracts in *Coleochaete* contained both high amounts of GalA and of the RG-I-specific sugars, pointing towards the presence of both HGA and RG-I in *Coleochaete* cell wall. Glucose was the main compound of the hemicellulosic and cellulosic extracts. Xylose seemed to be absent, contrary to the previous results from *Chara* and *Anthoceros*.

3.5.3.5. *Klebsormidium fluitans*

Klebsormidium is the first of the early-diverging charophytes examined here. This preliminary study led to further investigations, due the unusual nature of this alga's cell walls (see Section 5).

3.5.3.5.1. *Klebsormidium* pectin

The first remark that can be made concerning *Klebsormidium* pectic extract is the absence of uronic acids. Those residues are indeed primordial in usual land plants pectin, as explained earlier. Their absence implies a fundamentally different cell wall chemistry, and maybe different properties (Figure 13).

Galactose was one of the major components of this pectin, making up 10 to 30% of the sugar residues. There was more galactose in P2 than in P1 in almost all cases. Glucose made up about 15% of the pectic sugar residues. The glucose residue content did not drop with α -amylase digestion: it is possible that the cells only contained minor amounts of starch. Glucose might be part of the "pectic" matrix. Arabinose was present in all pectic extract, between 5 and 10%. Mannose and fucose, were detectable in all extracts, as minor compounds accounting for maximum 10% of the sugar residues. Xylose made up 20 to 40%

of the sugar residues. With galactose, it was the main 'pectin' component. Rhamnose made up 10 to 20% of the sugar residues. In almost all extracts, some fast-migrating compounds, staining purple and light pink, were spotted visually. However, they were not always quantifiable because they were only present as traces.

This highly unusual composition deserves particular attention: the usual polysaccharide domains (homogalacturonan, RG-I, RG-II) cannot be found. It would be useful to clarify the structures found here, as they imply very different cell-wall mechanisms. For example, the homogalacturonan "egg box model" for pectin gelation is not valid here, some other mechanisms must guarantee pectic integrity.

3.5.3.5.2. *Klebsormidium hemicellulose a*

The Ha extracts contained galactose in only very low quantities. The main sugar residues were glucose and xylose (the second and third compounds of *Klebsormidium* pectin). Arabinose, rhamnose, mannose and galactose were also detectable.

3.5.3.5.3. *Klebsormidium hemicellulose b*

The Hb extracts were surprising, as they highly resembled the pectic extracts, minus the galactose and the mannose. They were made of, in order of abundance: glucose, xylose, rhamnose, and arabinose.

3.5.3.5.4. *Klebsormidium wash*

The wash fractions were again very similar to the pectic fractions, minus the galactose, mannose, and fucose. The minor fast-migrating sugars were not detectable. Wash fractions were made of glucose, xylose, rhamnose and arabinose, at respectively about 40%, 40%, 15% and 5% w/w.

3.5.3.5.5. *Klebsormidium α -cellulose*

The α -cellulose fraction looked very much like a replicate of the wash fractions. However, it has been demonstrated that *Klebsormidium* does contain cellulose in its cell walls (Herburger and Holzinger 2015). The results of this study might indicate that cellulose interacts extremely closely with other polysaccharides and is thus difficult to isolate.

3.5.3.5.6. *Klebsormidium cell wall: summary*

Klebsormidium 'pectin' was unique and new, as it did not contain any uronic acid and was instead made up of Gal, Glc, Ara, Man, Fuc, Xyl and Rha, as well as fast-migrating sugars (further studied in Sections 5.4 to 5.8). Its hemicellulosic, wash and cellulose fractions were all very similar. They contained almost the same sugars as the pectic extract bar galactose and mannose, pointing toward particularly strong interactions between the cell wall components.

3.5.3.6. *Chlorokybus atmophyticus*

Chlorokybus is the second early-diverging charophyte of this study. It is expected to be different from classical land plants.

3.5.3.6.1. *Chlorokybus pectin*

Chlorokybus pectic extracts all displayed up to 25% of uronic acids (especially visible in the BAW solvent system). However, it was complicated to qualify them properly. The compound termed “Unknown1” migrated much slower than uronic acid monomers. It is probably an aldobiouronic acid, possibly resembling the α -D-glucuronosyl-(1 \rightarrow 3)-L-galactose from *Anthoceros*. It will be further analysed in Chapter 4. Two other uronic acids migrated at about the same speeds as GalA and GlcA. However, they were not always clearly distinct nor did they always match the markers.

Three neutral sugars constituted the bulk of *Chlorokybus* pectic extracts: galactose, glucose and arabinose, which respectively made up around 10, 30 and 30% of the sugar residues in P1, and around 10, 35, and 25% in P2. As for *Klebsormidium*, the amount of glucose did not drop after α -amylase digestion.

Xylose was a minor compound of *Chlorokybus* pectin, and was not always quantifiable.

A fast-migrating compound, staining brown, galactose-like, was visible in pectin when separated in the EPAW solvent system. It was however not always quantifiable. When run in BAW, it was detectable only on certain plates, and hardly quantifiable.

3.5.3.6.2. *Chlorokybus hemicellulose a*

The Ha samples were quantifiable in some cases. In the first case, only glucose was detectable. In the EPG and NaOH-EPG-treated samples, glucose and xylose were detected in similar amounts.

3.5.3.6.3. *Chlorokybus hemicellulose b*

The Hb extracts were all mostly made of glucose. It was the only compound in Hb from α -amylase-treated AIR extracts. It has been demonstrated that mixed-linkage glucan is present in *Chlorokybus atmophyticus*, which could be an explanation for this high glucose content (Kiemle 2010).

Some galactose and acidic compounds were detectable in the untreated sample, but not in others. This probably comes from an incomplete separation from pectin.

Xylose and fast-migrating sugars made up about 10% of the extracts from NaOH, EPG and NaOH-EPG treated AIR.

3.5.3.6.4. *Chlorokybus wash & α -cellulose*

It was difficult to separate the wash and α -cellulose fractions during sequential extraction, due to the low amounts of *Chlorokybus* biomass available. Only the wash fractions were analysed here. As expected, they contained mainly glucose, with minor compounds identical to the ones found in the pectic fraction (uronic acid, xylose, fast-migrating sugar).

3.5.3.6.5. *Chlorokybus cell wall: summary*

Chlorokybus 'pectin' was more similar to land plant pectin than *Klebsormidium*'s, as it did contain high amounts of uronic acids. However, *Chlorokybus* also displayed a new compound resembling an aldobiouronic acid, which was unknown and will be characterised in the next section of this thesis (Chapter 4). Galactose, glucose and arabinose are present in high amounts in *Chlorokybus* 'pectin', which may or may not point towards an RG-I-like structure in the algal cell wall. Glucose made up for most of the measurable hemicellulose, wash and cellulose fractions, pointing towards the presence of previously detected mixed-linkage glucan and cellulose (Kiemle 2010). It might also be that the alga contains callose, occurring in early-diverging charophytes (Herburger and Holzinger 2015).

3.6. Conclusion

In this first results chapter, one bryophyte, two late-diverging CGAs, two early-diverging CGAs, and a chlorophyte were studied for their cell wall extractability and composition.

In all six species, pectin represented the major part of the cell wall polysaccharides, followed by hemicellulose and then cellulose. It was found that pectin was more easily extractable in the bryophyte (*Anthoceros*) and late-diverging CGAs (*Chara* and *Coleochaete*) than in the early diverging charophytes (*Klebsormidium* and *Chlorokybus*) and the chlorophyte (*Ulva*).

All extracts (P1, P2, Ha, Hb, W, AC) from the six species were assayed for their sugar residue compositions. The presence in the *Anthoceros* pectic extract of a previously characterised aldobiouronic acid compound, and of the expected sugars, confirmed the validity of the method. Higher charophytes presented compositions similar to those of land-plants and

contained high amounts of GalA in their pectic fractions, as expected. Lower charophytes were more surprising, *Klebsormidium* cell walls containing no detectable uronic acid in any fraction, and *Chlorokybus* presenting an aldobiouronic acid-like band in its pectic hydrolysates. *Ulva* presented the neutral sugars expected to be found in ulvan (Rha, Xyl), as well as a range of ill-defined uronic acids. However, the separation between pectic extracts and others was unclear.

As all species presented strong glucose signals in their pectic fractions when the AIR was directly submitted to sequential extraction, an alternative method was attempted. The plant AIR were de-starched with α -amylase before proceeding to the sequential extraction. Following this, the analysis of sugar components in each fraction was repeated. All plants did contain digestible starch, *Chlorokybus* and *Chara* being the species containing the most. In all species apart from *Klebsormidium*, the P1/P2 ratio doubled after amylase digestion, thus the pectin was made more easily extractable by the de-starching process. More hemicellulose (by comparison with untreated samples) was extracted.

All species were submitted to land-plant-like pectin extraction, via the use of an alkali treatment of the AIR (aimed at de-esterifying GalA residues), followed by digestion with EPG (only active on non-esterified GalA residues). Controls were included, where the AIR was either only alkali-treated or only EPG-digested. Lower charophytes and *Ulva* did not release any sugars upon EPG digestion, by contrast with *Anthoceros*, *Coleochaete* and *Chara*. These last three plants released oligogalacturonides, irrespective of whether or not they had been alkali-treated beforehand, thus suggesting that they were not heavily, if at all, esterified. Surprisingly, the amount of extracted pectin did not change massively in any species after the EPG enzymatic treatment. The alkali treatment alone allowed a higher recovery of all

cell-wall fractions, and a more easily extractable pectin fraction (increased P1:P2 ratio) in all species.

The sequence of pre-treatment, sequential extraction, and sugar analysis was repeated on all species three times, in order to generate enough data to create a reliable bank. The sugar contents of each extract were analysed using a Matlab-encoded script, giving series of histograms showing the average proportions of each sugar in each pre-treated extract.

Table 3: Features of markers and of the main unknown compounds in both solvent mixtures.

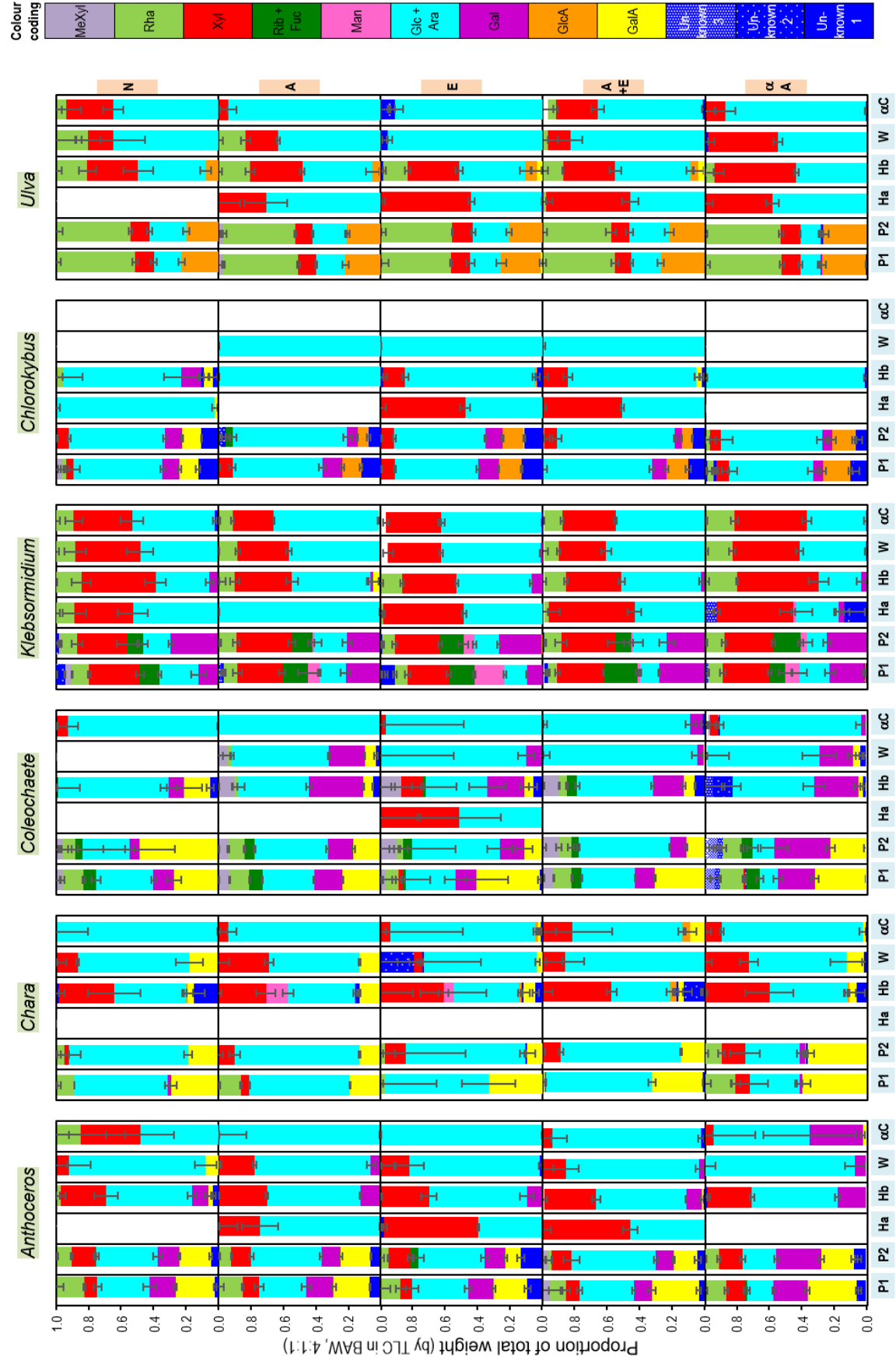
Sugar	R_{MeXyl} in BAW	R_{MeXyl} in EPAW	Colour of staining with thymol
Me-Xyl	1.00	1.00	Purple
Rha	0.96	0.91	Light pink
Xyl	0.85	0.75	Purple
Rib	0.77	0.75	Purple
Fuc	0.79	0.74	Brown
Man	0.72	0.54	Pink
Ara	0.69	0.62	Purple
Glc	0.68	0.49	Pink
Gal	0.61	0.41	Brown
GlcA	0.46	0.07	Brown
GalA	0.42	0.06	Purple
U1(BAW) <i>Anthoceros</i>	0.191		Brown
U1(BAW) <i>Ulva</i>	1.019		Light pink
U1(BAW) <i>Chlorokybus</i>	0.137		Brown
U1(BAW) <i>Klebsormidium</i>	1.113		Light pink
U1(BAW) <i>Coleochaete</i>	1.074		Light pink
U1(EPAW) <i>Anthoceros</i>		1.037	Light pink
U1(EPAW) <i>Ulva</i>		1.036	Light pink
U1(EPAW) <i>Coleochaete</i>		1.051	Light pink

R_{MeXyl} was calculated with reference to the MeXyl spot, the furthest migrating marker in the mixtures of reference.

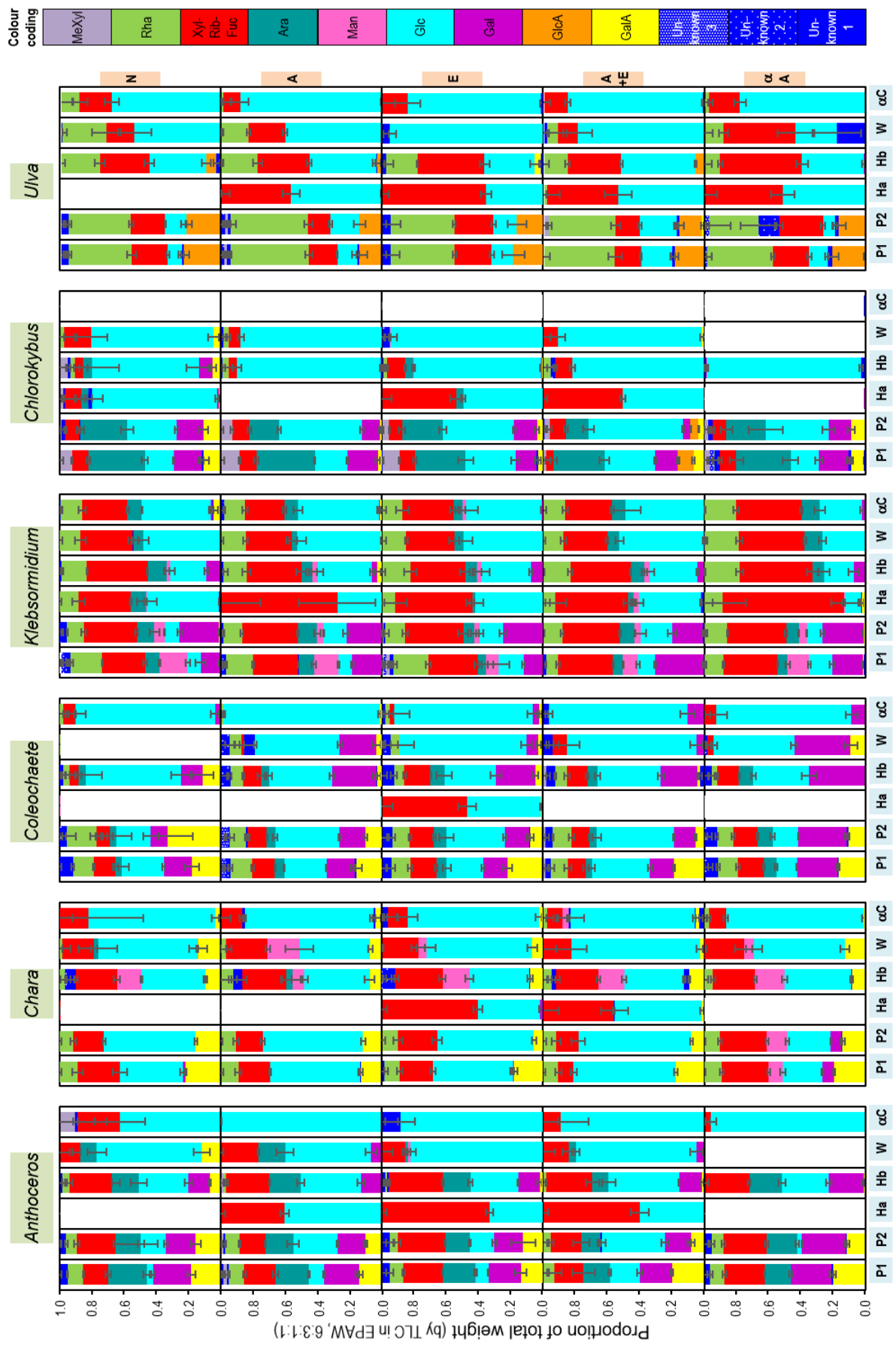
Figure 16 (see following double page) : Relative quantities of each sugar residue in the extracts from all six plants (*Anthoceros caucasicus*, *Chara vulgaris*, *Coleochaete scutata*, *Klebsormidium fluitans*, *Chlorokybus atmophyticus*, *Ulva linza*), following several pre-treatments.

They were measured from TLC plates run in (a) BAW 4:1:1, 2 ascents (first panel), or in (b) EPAW 6:3:1:1, 2 ascents (second panel). The blank spaces were impossible to quantify. The letters on the right correspond to the treatments applied prior to sequential extraction : N is for no treatment, A is for alkali treatment, E is for EPG digestion, A+E is for alkali treatment followed by EPG digestion, and α A is for α -amylase digestion. The error bars indicate the standard deviation of the quantity of each sugar (SD, $n = 3$, n being the number of analysed polysaccharide fraction from the same AIR sample). The 'unknown' sugars are the ones could not be identified with the markers and were numbered in order of growing R_{MeXyl} , independently in (a) and (b).

(a)



(b)



4. Characterization of novel cell-wall
compounds and Study of
Chlorokybus atmophyticus pectic
and hemicellulosic fractions

4.1. Introduction

Some of the extracts from the previous chapter were selected for further studies because they presented some unusual features, more specifically some of their sugar residues did not match the markers. For each species, data could be gathered about these unusual substrates. In particular, extra data were collected about the bryophyte *Anthoceros*, the chlorophyte *Ulva* and both early-diverging charophytes *Klebsormidium* and *Chlorokybus*. *Chlorokybus* displayed an aldobiouronic acid, which was clearly different from that of *Anthoceros* and was fully characterised here by pairing enzymatic and spectroscopic tools. The particular composition of the *Chlorokybus* cell wall, as well as its indigestibility by land-plant polysaccharide-specific hydrolases, and the identification of the aldobiouronic acid, made it particularly interesting. The pectic extract from *Chlorokybus* was investigated further using anion-exchange chromatography and an array of colorimetric assays. Its hemicellulosic extract Hb, containing exclusively Glc residues (see Section 3.5.3.6 *Chlorokybus atmophyticus*), was studied in comparison with other known glucans, using a combination of chemical, chromatographic, and spectroscopic methods.

4.2. Extraction of monomers and small oligomers from cell-wall hydrolysates from preparative paper chromatograms

Hydrolysates from the fractions obtained by sequential extraction were separated on TLC, and their main features have been detailed in the previous chapter. However, some compounds could not be identified, as they did not correspond to the most common sugar residues used as markers. Several extracts containing those unknown chemicals were selected:

- Pectic extracts (P1 and P2) from *Klebsormidium*, which yielded upon acidic hydrolysis fast-migrating compounds.
- Pectic extracts (P1 and P2) and hemicellulose (Hb) from *Ulva*, which also yielded fast-migrating compounds.
- Hemicellulose Hb from *Anthoceros*, which yielded a slow-migrating sugar.
- Pectic extract (P2) from *Chlorokybus*, which also yielded a slow-migrating sugar.

All seven of these extracts were submitted to acid hydrolysis (2M TFA, 1 h at 120°C) and their products were separated on preparative paper chromatography (PPC, Figure 17). The paper was partially stained with Wilson's dip, in order to detect the unknown sugars. The colour of the staining depended on the nature of the reducing terminus: uronic acids stained orange, neutral hexoses stained brown, and neutral pentoses stained red. Each extract was named systematically, for example as P2U-M2, the first two characters indicating the polysaccharide of provenance (P1, P2 etc.), the third character being the plant it comes from (U for *Ulva* etc.). The last two characters identify their positions on the PPC: A ('anion') for acidic compounds, M ('methy and/or deoxy') for fast-migrating compounds, U ('unknown') for other non-directly identifiable compounds; 1-4 for differentiating between similar compounds. The acid hydrolysis products were eluted

from the paper, and run on TLC to verify their purity and chromatographic properties (Figure 18).

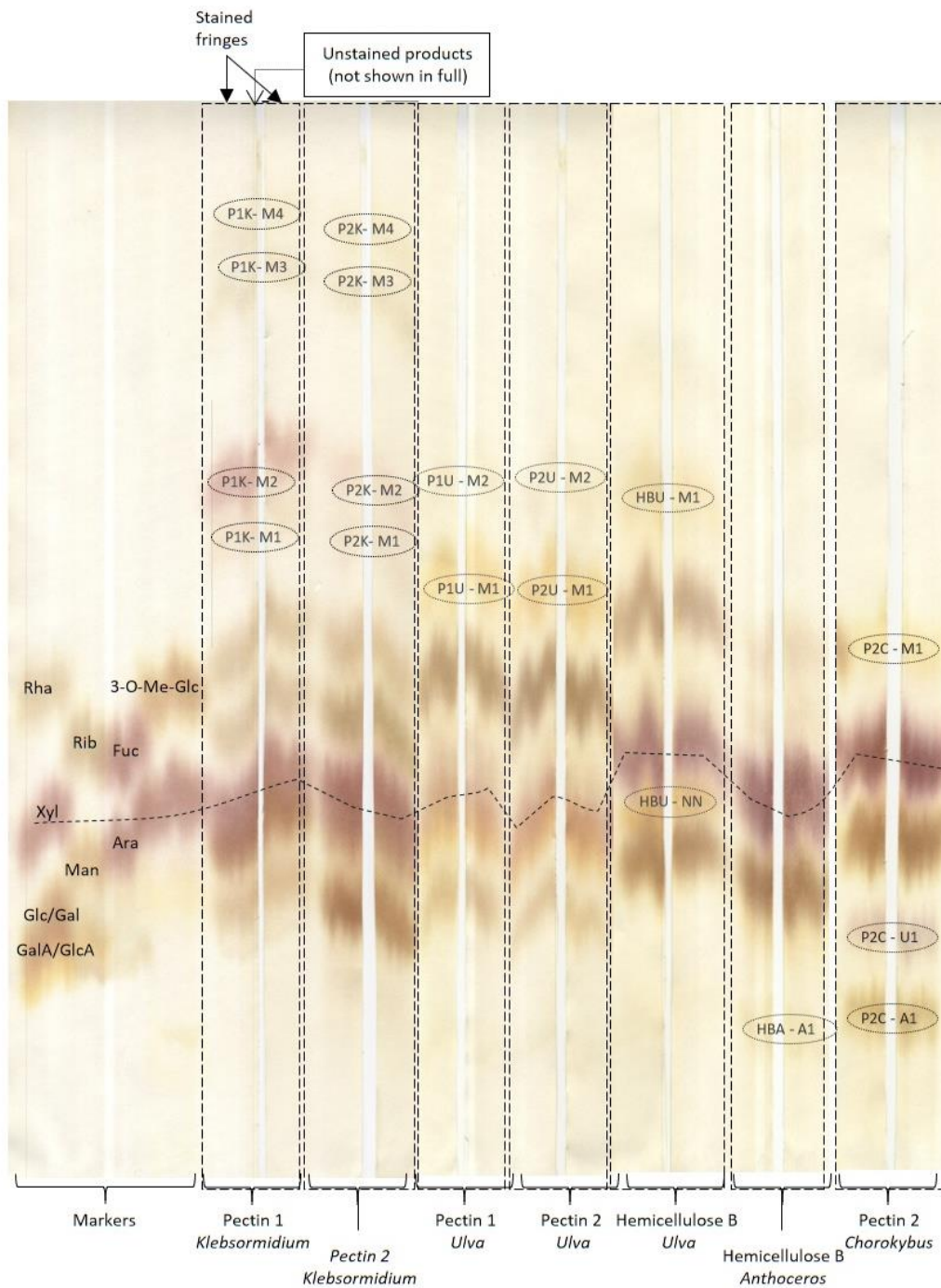


Figure 17: Preparative paper chromatography (PPC) of the selected algal hydrolysates. All seven algal cell wall fractions were hydrolysed with 2 M TFA for 1 h at 120°C. The solvent for paper chromatography was BAW (butan-1-ol/acetic acid/water 12:3:5), run for 24 h. The fringes of paper were stained with Wilson's dip. The unstained portions of interesting compounds (not shown here in full, but indicated on this image by dotted ellipses) were then eluted for further analysis. The dashed black line indicates the position of Xyl on the paper, as a visual guide for the reader.

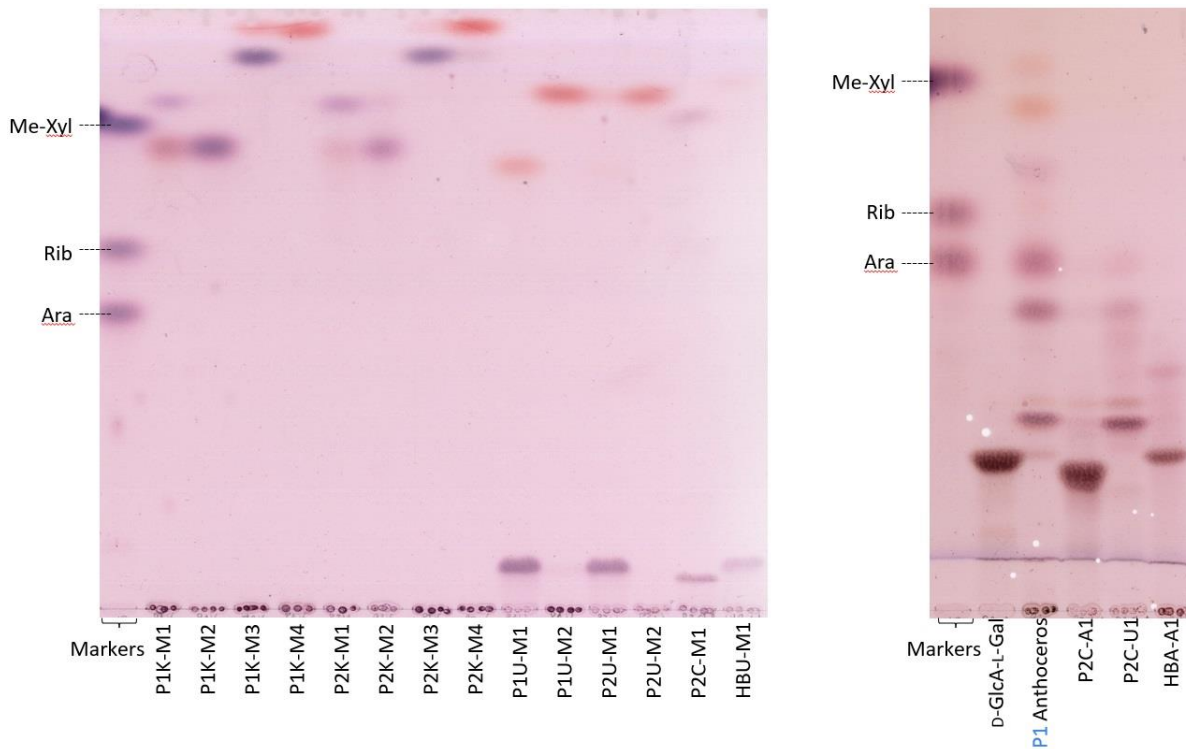


Figure 18: Separation on TLC of the isolated unidentified compounds.

Left: TLC of the fast-running compounds from PPC. Right: TLC of, from left to right : aldobiouronic acid α -D-GlcA-(1 \rightarrow 3)-L-Gal (prepared in the laboratory from *Anthoceros*), hydrolysate of P1 fraction from *Anthoceros*, and slow-running compounds on PPC. The left plate was developed in EPAW (ethyl acetate/pyridine/acetic acid/water 6:3:1:1), two ascents, on a plastic-backed silica-gel plate. The right plate was run in BAW (butan-1-ol/acetic acid/water 4:1:1), two ascents, on a plastic-backed silica-gel plate.

4.3. Further chromatographic analysis of purified, non-identified eluates from PPC

4.3.1. *Ulva* : electrophoretic and chromatographic analysis of fast-running cell-wall compounds

The two hydrolysed pectic extracts from *Ulva*, when run on PPC, both yielded two fast-migrating unidentified sugars: P1U-M1, P1U-M2, P2U-M1, and P2U-M2. When run on TLC,

the eluates were two-by-two very similar to one another: P1U-M1 resembled P2U-M1; P1U-M2 resembled P2U-M2 (Figure 18).

The eluates P1U-M1 and P2U-M1 were surprising, both by the colour they stain and the area they migrate into. With Wilson's dip on PPC, they stained orange (indicative of uronic acid, at the reducing terminus if not a monosaccharide), but migrated in the methylated sugar zone. With thymol on TLC, they stained purple (indicative of a hexose or hexuronic acid) and migrated in the uronic acid zone. When run on paper electrophoresis (PE, Figure 19), they migrated once more as a mono-charged uronic acid. They ran slightly faster than GalA, and may have been ManA, IdA or GlcA (Fry 2011). As the last two are part of the well-known ulvan, they probably correspond to the compounds from PPC (Lahaye and Robic 2007).

The two extracts displayed identical properties and are very probably identical. The situation was the same for the extract isolated from Hb, HBU-M1. HBU-M1 ran in the methylated sugars zone and stained orange on PPC, it ran in the uronic acid zone and stained purple on TLC, and it migrated like P1U-M1 and P2U-M1 on PE. It is very probably the same compound as them. All three are very probably uronic acids, in their lactonized form when run on paper chromatography, which would explain their fast migration.

P1U-M2 and P2U-M2 were, on the other hand, consistently migrating very fast, whether on paper or on TLC. They stained like rhamnose both times, although they were migrating further than rhamnose on both supports. They probably are rhamnose derivatives, such as methylated Rha.

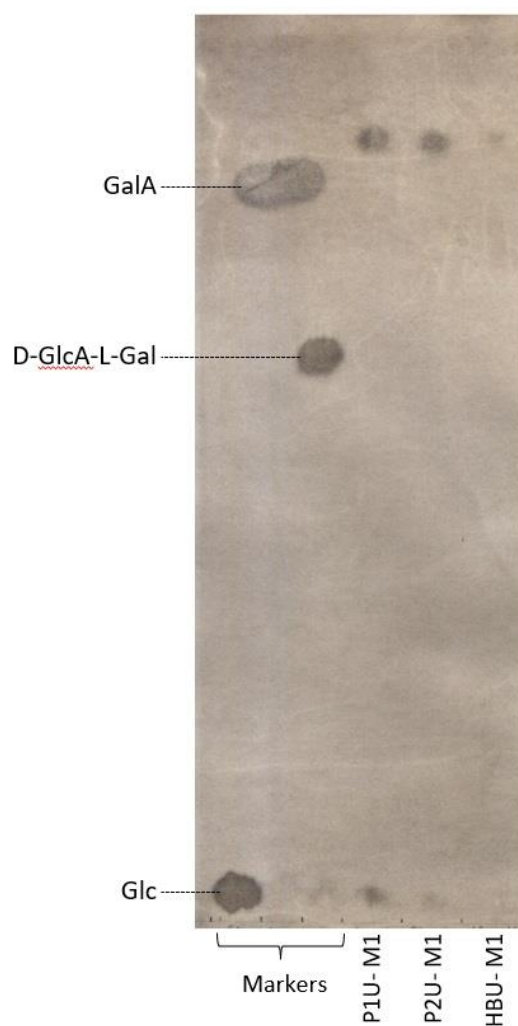


Figure 19: Analysis on paper electrophoresis of the extracts from *Ulva*. From left to right, markers (commercial GalA and Glc, and α -D-GlcA-(1 \rightarrow 3)-L-Gal prepared in the laboratory from *Anthoceros*), P1U-M1, P2U-M1 and HBU-M1, all migrating at similar speeds and slightly faster than GalA. Developed at pH 6.5 in acetic acid/pyridine/water 1:33:300, at 3 kV for 100 min, stained with AgNO₃.

4.3.2. *Anthoceros* : recognising a known cell-wall aldobiouronic acid

Hydrolysed Hb from *Anthoceros* was run on PPC, as it is the extract containing the most putative aldobiouronic acid (cf. previous Chap.). As expected, a slow-migrating compound was isolated on paper chromatography. When run on TLC, in the BAW 4:1:1 solvent system, it migrated at a similar speed to authentic α -D-glucuronosyl-(1 \rightarrow 3)-L-galactose previously isolated in the laboratory (Figure 20) (Popper *et al.* 2003). The compounds were re-hydrolysed and the co-migration assay between HBA-A1 and α -D-glucuronosyl-(1 \rightarrow 3)-L-

galactose was repeated (Figure 20). HBA-A1 yielded Glc, on top of the expected Gal and GlcA, which might come from a contamination in the sample. This assay yielded a positive result: they co-migrated. The nature of this extract is thus strongly supported.

4.3.3. *Klebsormidium* : fast-running monomers

P1 and P2 hydrolysates were run separately on PPC (Figure 17). However, in both extracts four compounds were revealed: P1K-M1, P1K-M2, P1K-M3, P1K-M4, P2K-M1, P2K-M2, P2K-M3, and P2KM4. These 8 products co-migrated two by two on paper: P1K-M1 and P2K-M1; P1K-M2 and P2K-M2, etc. When run on TLC, they once again co-migrated in the same way (Figure 18). They were pooled, producing 4 compounds (P1-2K-M1, P1-2K-M2, P1-2K-M3, and P1-2-K-M4).

P1-2K-M1 and P1-2K-M3 were separated on a preparative TLC (not shown here) in order to ensure purity, as they had seemed to contain two different sugar residues (Figure 18).

All four of these compounds are very probably deoxy and/or methylated sugars. Given their speed, by comparison with the mono-methylated Me-Xyl and the mono-deoxy sugar Rha, they might be di-deoxy or di-methylated sugars. Moreover, their colours (when stained with thymol) indicate that the slowest compound in P1-2K-M1 might be a Gal derivative (brown-staining) and the faster one might be a pentose derivative (purple staining). P1-2K-M2 stained purple, indicative of a pentose derivative again, and P1-2K-M4 stained light pink, Rha-like. In the compounds from P1-2K-M3, the main one stained purple (pentose-like) and

the second one light pink, co-migrating with P1-2K-M4 and probably being identical to it. However, their low yields kept me from performing further analysis.

4.3.4. *Chlorokybus* : Characterization of new acidic compounds

The hydrolysate of P2 from *Chlorokybus* was run on PPC, as it contained most of the putative aldobiouronic acid (Section 3.5.3.6). Three compounds were isolated: P2C-A1, P2C-U1 and P2C-M1 (Figure 18).

P2C-M1 migrated in the methylated sugars zone on PPC, but stained orange with Wilson's dip (Figure 17). When run on TLC, it displayed two compounds, both staining purple: one migrating (slowly) in the uronic acid zone, the other (fast) in the 'methylated sugar' zone (Figure 18). These two compounds were separated on preparative TLC (not shown here). However, they could be the open-chain and lactonized forms, respectively, of a single uronic acid. The former ran slower than P2U-M1 (from *Ulva*), which might either be IdoA or GlcA, and based on that evidence might have been GlcA or GalA; however, GalA does not lactonise. P2C-M1 might then be GlcA. P2C-U1 migrated with uronic acids on PPC, but stained grey-red with Wilson's dip, indicative of a pentose as a reducing terminal sugar residue (Figure 17). However, when run on TLC in BAW, P2C-U1 appeared to be a mixture of several known sugars including GlcA, Gal, and Ara and was not investigated further (Figure 18).

P2C-A1 was isolated on PPC: it stained brown with Wilson's dip (i.e. indicating a hexose as its reducing end) and it ran slightly faster than HBA-A1 (which had been identified as the dimer

α -D-GlcA-(1 \rightarrow 3)-L-Gal) (Figure 17). When run on TLC, it became clear that P2C-A1 was the putative aldobiouronic acid previously detected in *Chlorokybus* (Sections 3.5.3.6 and 4.4).

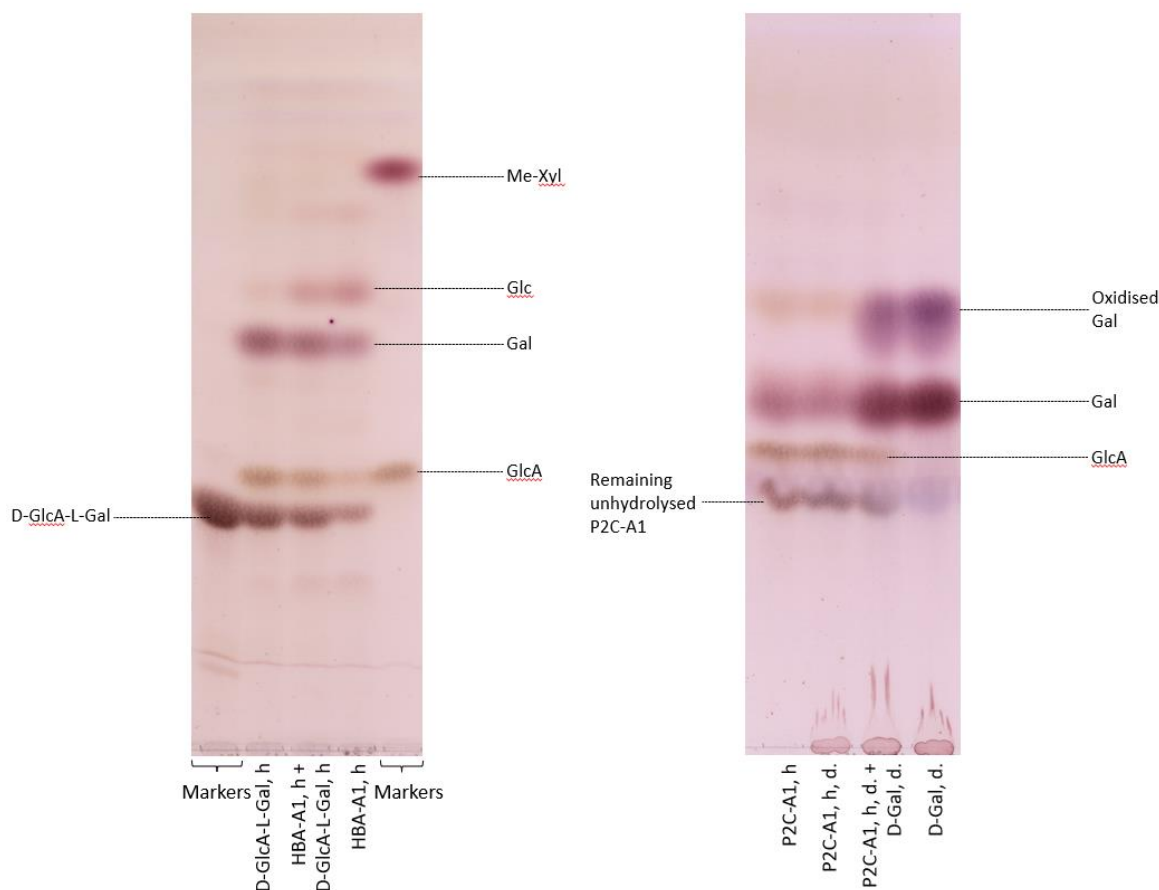


Figure 20: Separation of the hydrolysed and oxidised products from two aldobiouronic acids from *Anthoceros* and *Chlorokybus*.

Left: Co-migration of authentic α -D-glucuronosyl-(1 \rightarrow 3)-L-galactose with HBA-A1. 'h.' is for acid-hydrolysed. The TLC developed in BMW (butan-1-ol/methanol/water 3:1:1), one ascent, on a plastic silica-gel plate. Right: Co-migration of oxidised D-galactose, and hydrolysed and galactose-oxidase-incubated P2C-A1. 'h.' is for acid-hydrolysed, and 'd.' is for incubated with galactose-oxidase. TLC developed in BAW (butan-1-ol/acetic acid/water 2:1:1), one ascent, on a plastic silica-gel plate.

P2C-A1 was hydrolysed with TFA in order to check the nature of the constituent monomers.

The hydrolysate was run on TLC and yielded monomers identifiable as glucuronic acid and galactose. The product thus seemed very similar to the already known α -D-glucuronosyl-

(1→3)-L-galactose, but it did not migrate at the same speed on TLC in BAW (Figure 20). It might differ by its linkage, anomerism and/or the sugar enantiomer(s) involved.

The enantiomery of the galactose was verified. D-Galactose and L-galactose co-migrate on TLC so, in order to distinguish them from one another, the hydrolysed P2C-A1 was incubated with D-galactose oxidase, which selectively oxidises D-galactose, thus discriminating between D and L enantiomers (Popper *et al.* 2003 p. 200). It would seem that the galactose present in the extract is L-Gal, which is intriguing since this is the less common of the two enantiomers (Figure 20). The GlcA residue is assumed to be D and not L, since the second configuration is unknown in plants.

NMR spectroscopy was performed in order to characterise the glycosidic bond between D-GlcA and L-Gal (Table 4, Figure 21). It was found that the bond was 1→4, since long-range couplings are visible on the HMBC spectrum (heteronuclear multiple bond correlation, showing the interaction between distant atoms of different natures), between carbon-1 of the GlcA residue and the proton on carbon-4 of Gal in both anomers α and β , and between carbon-4 of Gal in both anomers and the proton on carbon-1 of GlcA. Thanks to the NOESY spectrum (nuclear overhauser effect spectroscopy, showing the interaction of same-nature atoms close in space (Bothwell and Griffin 2011)), it was possible to prove that the proton on carbon-1 of GlcA is in an axial position, thus the glycosidic linkage is β (and not α).

In conclusion, A1-C is made of D-GlcA and L-Gal, linked via a β -(1→4) glycosidic bond: it is the disaccharide β -D-GlcA-(1→4)-L-Gal dimer.

Table 4: ^1H and ^{13}C NMR spectral data of $\beta\text{-D-glucuronosyl-(1}\rightarrow\text{4)-L-galactose}$.

Site	δ_{C}	δ_{H}	Multiplicity	J_{HH} (Hz)	Proton-carbon long-range correlation (from HMBC spectrum)
<i>α-galactose (residue A)</i>					
A1	92.3	5.219	(d)	3.3	
A2	68.5	3.776	(dd)	3.4, 10.0	
A3	68.5	3.44-3.46	(dd)	2.6, 10.0	
A4	78.8	4.126	(d)	2.6	C1
A5	70.5	4.110	(t)	6.3	
A6a, A6b	60.2	3.762	(d)	6.3	
<i>β-galactose (residue B)</i>					
B1	96.3	4.558	(d)	7.8	
B2	72.4	3.430	(dd)	7.8, 10.0	
B3	72.2	3.564	(dd)	3.3, 10.0	
B4	77.5	4.074	(d)	3.3	C1
B5	75.0	3.713	(dd)	5.0, 7.7	
B6a	60.2	3.745	(dd)	5.0, 11.5	
B6b	60.2	3.777	(dd)	7.7, 11.5	
<i>Glucuronic acid (residue C)</i>					
C1a	102.6	4.379	(d)	8	A4
C1b	102.6	4.364	(d)	8	B4
C2	72.8	3.361	(dd)	8.0, 9.5	
C3	71.7 (or 75.2)	3.44-3.46		2nd order	
C4	75.2 (or 71.7)	3.44-3.46		2nd order	
C5	76.0	3.667		2nd order	
C6	175.5	-			

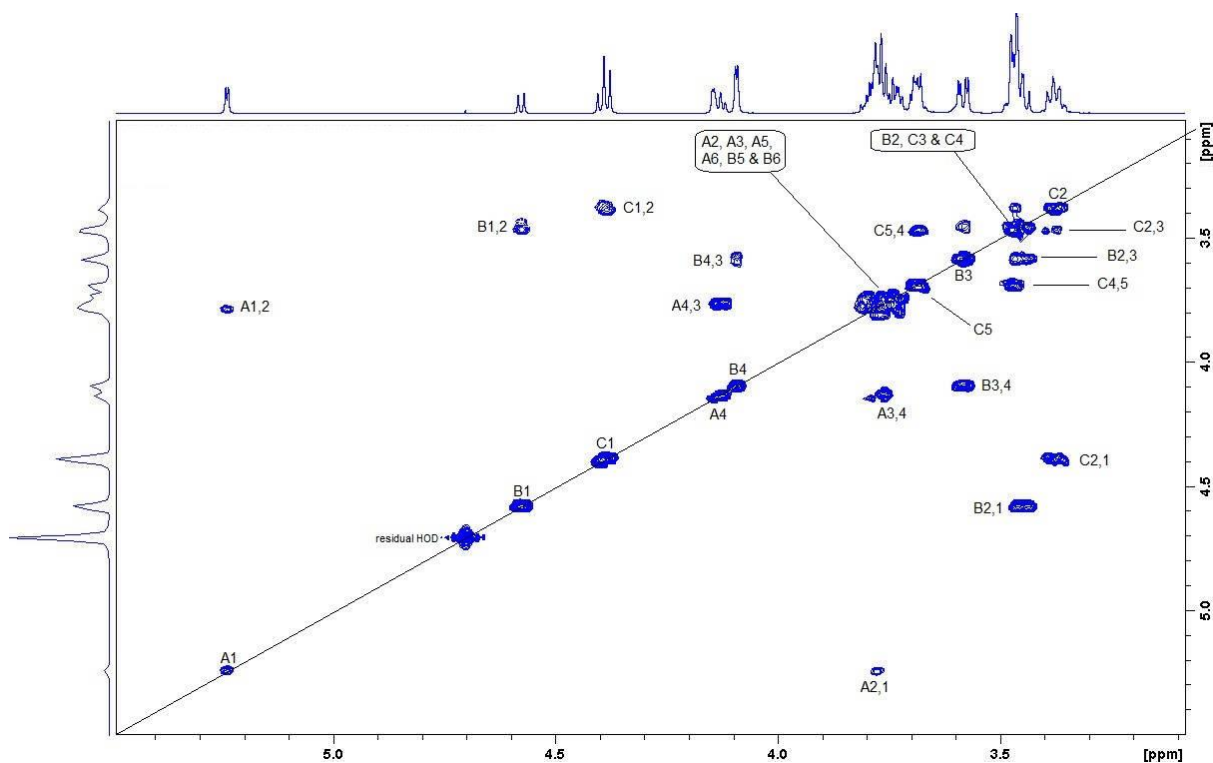


Figure 21: NMR spectra of β -D-glucuronosyl-(1 \rightarrow 4)-L-galactose.

Top graph: 1-D single-pulse 600-MHz proton NMR spectrum over the region 3.16–5.56; encompassing all visible resonances. Bottom graph: 2-D gradient-selected proton COSY NMR spectrum over the same region as previously.

4.4. Focus on *Chlorokybus* cell-wall polysaccharides

The singular sugar monomer composition of the different extracts from *Chlorokybus* attracts attention, as they do not seem to match classic plant cell wall compositions. Both the pectic and the hemicellulosic extracts were therefore analysed in further detail.

4.4.1. Pectic extract of *Chlorokybus*

Both pectic extracts from *Chlorokybus* (P1 and P2) displayed similar compositions: mainly arabinose, glucose, galactose, galacturonic acid and the dimer characterised as β -D-GlcA-(1 \rightarrow 4)-L-Gal (Section 3.5.3.6 *Chlorokybus atmophyticus*). Galacturonic acid is not organised as classical homogalacturonan, as *Chlorokybus* AIR is not sensitive to EPG (Section 3.4.2).

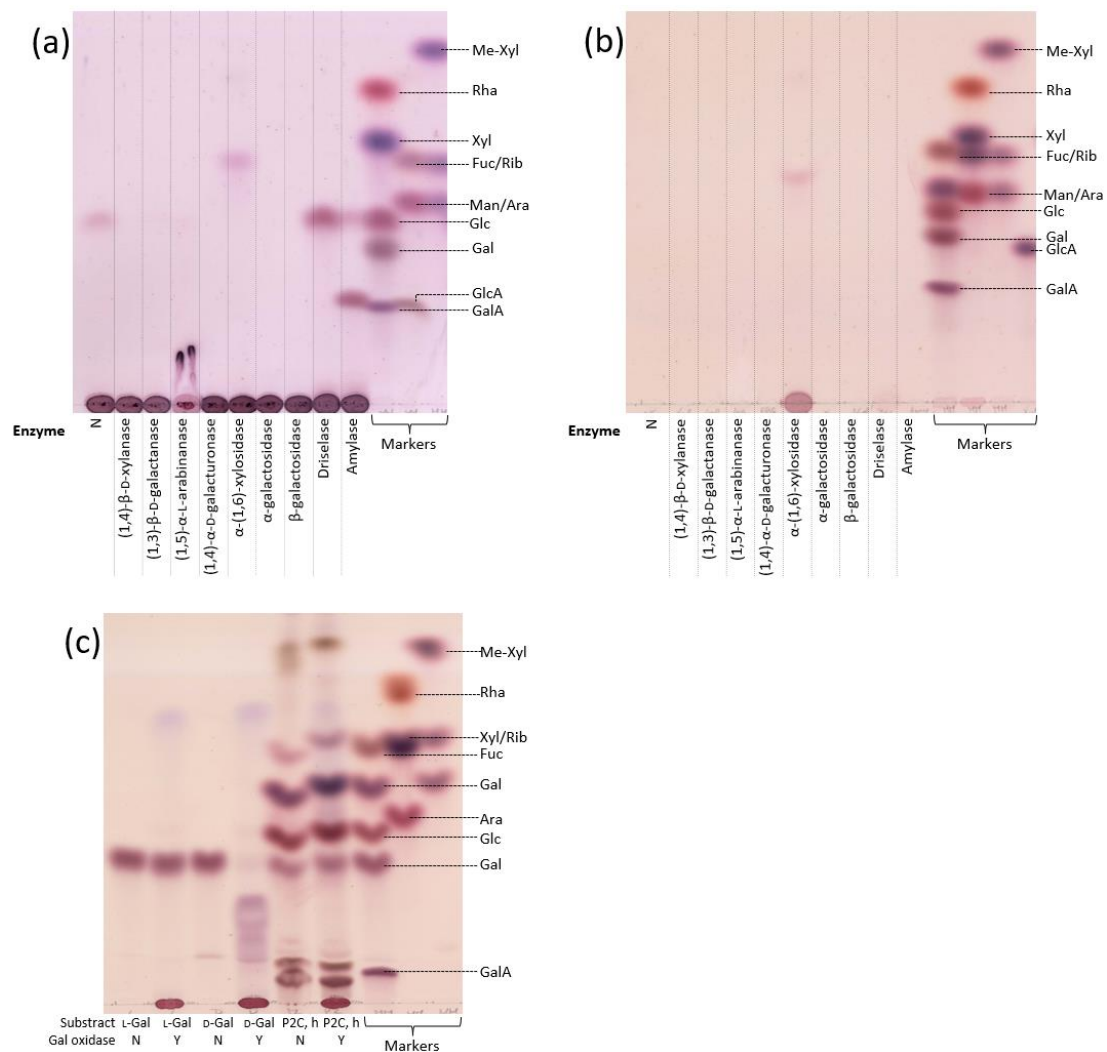


Figure 22: Enzymatic digests of P2 of *Chlorokybus*.

(a): P2 from *Chlorokybus* was assayed with a series of endo- and exo-hydrolases. 'N' indicates the absence of enzyme, meaning the polysaccharidic fraction was incubated in buffer for 72 h. (b): substrate-less controls of the same enzyme collection, 'N' indicating the incubation of buffer alone for 72 h. (c): D-galactose oxidase treatment of acid-hydrolysed P2 from *Chlorokybus* (noted 'P2C, h' on the figure) and on authentic D-Gal and L-Gal.

The TLC plates in (a) and (b) were developed twice in BAW 4:1:1, the one in (c) was developed twice in E/P/A/W 6:3:1:1.

4.4.1.1. Enzymatic assays on *Chlorokybus* 'pectin'

A series of hydrolases were applied to intact P2 extract (Figure 22). Pectic endo- and exo-enzymes were tested: (1,5)- α -L-arabinanase, (1,4)- β -D-galactanase, EPG, as well as α and β -galactosidase. In land-plant pectins, arabinanase and galactanase are expected to hydrolyse neutral pectic sidechains, whilst EPG can digest homogalacturonan (Bonnin *et al.* 2002). All enzymes yielded negative results: if P2 contains classical land-plant pectic structures, these enzymes did not hydrolyse them (Figure 22).

Hemicellulosic enzymes were also used: (1,4)- β -D-xylanase and α -(1,6)-xylosidase (respectively aimed at xylan and xyloglucan structures). They had no detectable effect on P2 of *Chlorokybus* (Figure 22). An unidentifiable band was observable on the xylosidase track; however, it was also present on the substrate-less control.

Finally, amylase (aimed at starch) and Driselase were tried. Both yielded a glucose band, and a maltose band in the case of amylase, which were not visible in the substrate-less controls (Figure 22). It is most certainly the starch present in the pectic extract that is being hydrolysed, in that case. A glucose band is also observable in the enzyme-less control: this mixture had been incubated for the longest incubation time (coinciding with those of amylase and Driselase) at the highest temperature (37°C). These conditions might have provoked the degradation of a glucose-containing polymer, presumably starch (Pigłowska *et al.*).

D-Galactose oxidase was applied to fully acid-hydrolysed P2 from *Chlorokybus*. As it is only capable of oxidising D-Gal, a positive result (disappearance of the galactose) would show that the main Gal band in P2C hydrolysate is made of the more common sugar enantiomer.

However, the oxidase did not have any effect on the pectic extract hydrolysate. This could

mean that only the L-Gal enantiomer is present in the *Chlorokybus* 'pectin', or that an unidentified compound is keeping the enzyme from acting on the hydrolysed polysaccharide fraction. However, the hydrolysate having been obtained by methods resembling the ones used for prior use of galactose-oxidase, the second hypothesis is unlikely. The Gal residues in *Chlorokybus* 'pectin' may well be L-Gal.

4.4.1.2. Separation on anion-exchange chromatography of *Chlorokybus* 'pectin'

An anion-exchange chromatography column was set up in order to assay the acidity of the potential different fractions from P2 *Chlorokybus*. The resin that was used is made of crosslinked 6% agarose beads, with quaternary ammonium (Q) strong anion exchange groups. After the samples were loaded, they were eluted with a range of pyridinium acetate buffers (11 to 1400 mM) fixed at pH 5.3 and containing 8 M urea, followed by a pH 7.0 2 M acetate buffer also containing 8 M urea, and two successive alkali solutions at 1 M and 6 M NaOH (Popper and Fry 2005).

Commercial polysaccharides, dextran and homogalacturonan, were separated on anion-exchange chromatography in order to calibrate it (Figure 23 (a)). They marked two extremes of the column, the first one being completely neutral, the second one being entirely acidic. As expected, dextran was very loosely retained on the column and was released with pyridinium acetate buffers at 44 and 88 mM. On the contrary, homogalacturonan interacted strongly with the beads and was only eluted with the latest elution buffers (1400 mM pyridinium acetate, 2 M sodium acetate and 6 M NaOH).

When loaded on the same column, P2 from *Chlorokybus* exhibited several peaks with different behaviours: the first one eluted around 700 mM pyridinium acetate buffer, and the

second one around 1 M NaOH elution buffer. When quantifying the amount of uronic acid residues present in each fraction, it was clear that the earlier peak was richer than the later one, culminating around 0.21 mg/mL uronic acids against only 0.14 mg/mL (Figure 23 (b)).

On the contrary, more sulphates groups were found in the later peak, going up to 0.22 mg/mL against only 0.07 mg/mL in the earlier one (Figure 23 (c)).

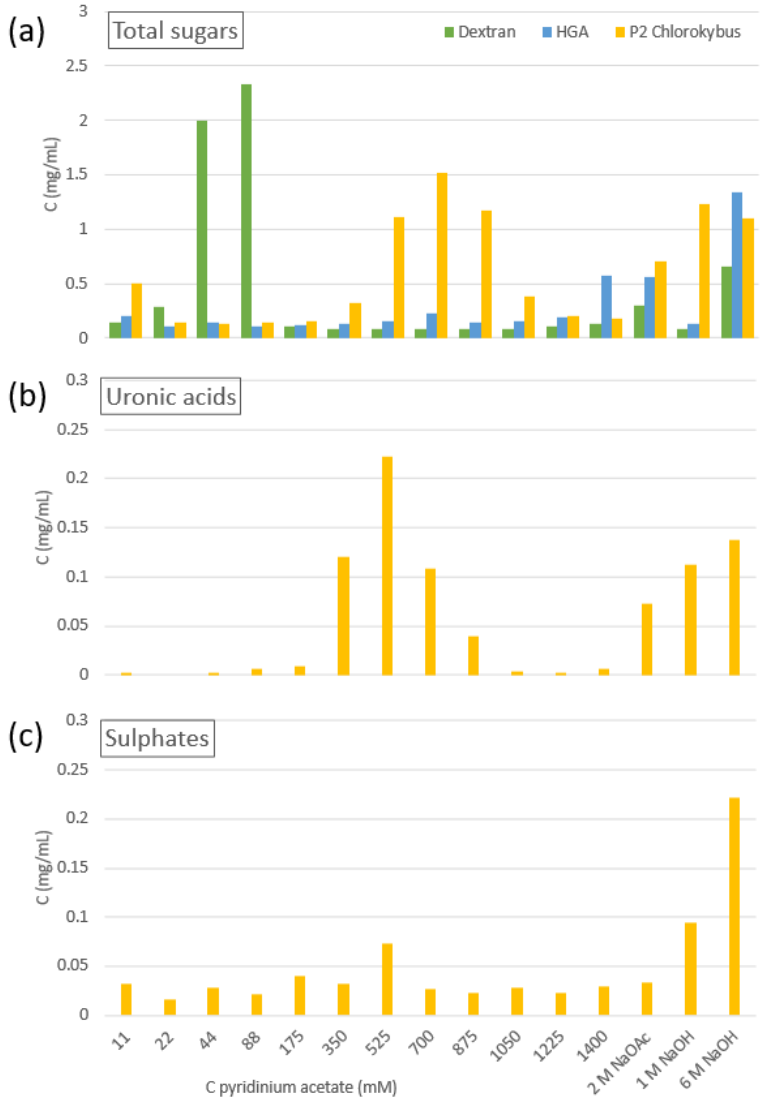
Each eluate was collected into two successive tubes, thus giving two samples per elution buffer to assay for their sugar composition. This was done via 'complete' acidic hydrolysis.

The earlier peak, centred around 525 mM pyridinium acetate, was rich in Ara and uronic acids, and contained Gal and Xyl as minor compounds. The later peak, eluted with the 2 M acetate buffer and the strong alkaline solutions, was surprisingly identical to the first one in terms of composition, apart from a Glc band visible in the 1 M NaOH fraction. For each of the later eluates, sugars were only detectable in the first sample that was collected, showing that no more polysaccharide could have been eluted in these conditions.

Other aliquots of the samples were submitted to mild acid hydrolysis. For the samples corresponding to the first peak, Ara and uronic acids were released, as well as the previously characterised α -D-GlcA-(1 \rightarrow 4)-L-Gal and several TLC-mobile oligomers. Samples from the second peak, however, were only marginally hydrolysed: they released the same compounds in much smaller quantities, and many polysaccharides remained immobile at the origin of the TLC, especially for the 6 M eluate.

Overall, separation on anion-exchange chromatography allowed for the release of two distinct fractions with similar sugar compositions, one being richer in uronic acids and susceptible to mild acid hydrolysis, the other one being richer in sulphate and containing less labile glycosidic bonds.

Only the extract Hb (not Ha) could be recovered in sufficient quantity from *Chlorokybus* AIR to allow for further analysis. On acid hydrolysis, it had been shown mainly to be made of glucose residues (Section 3.5.3.6 *Chlorokybus atmophyticus*).



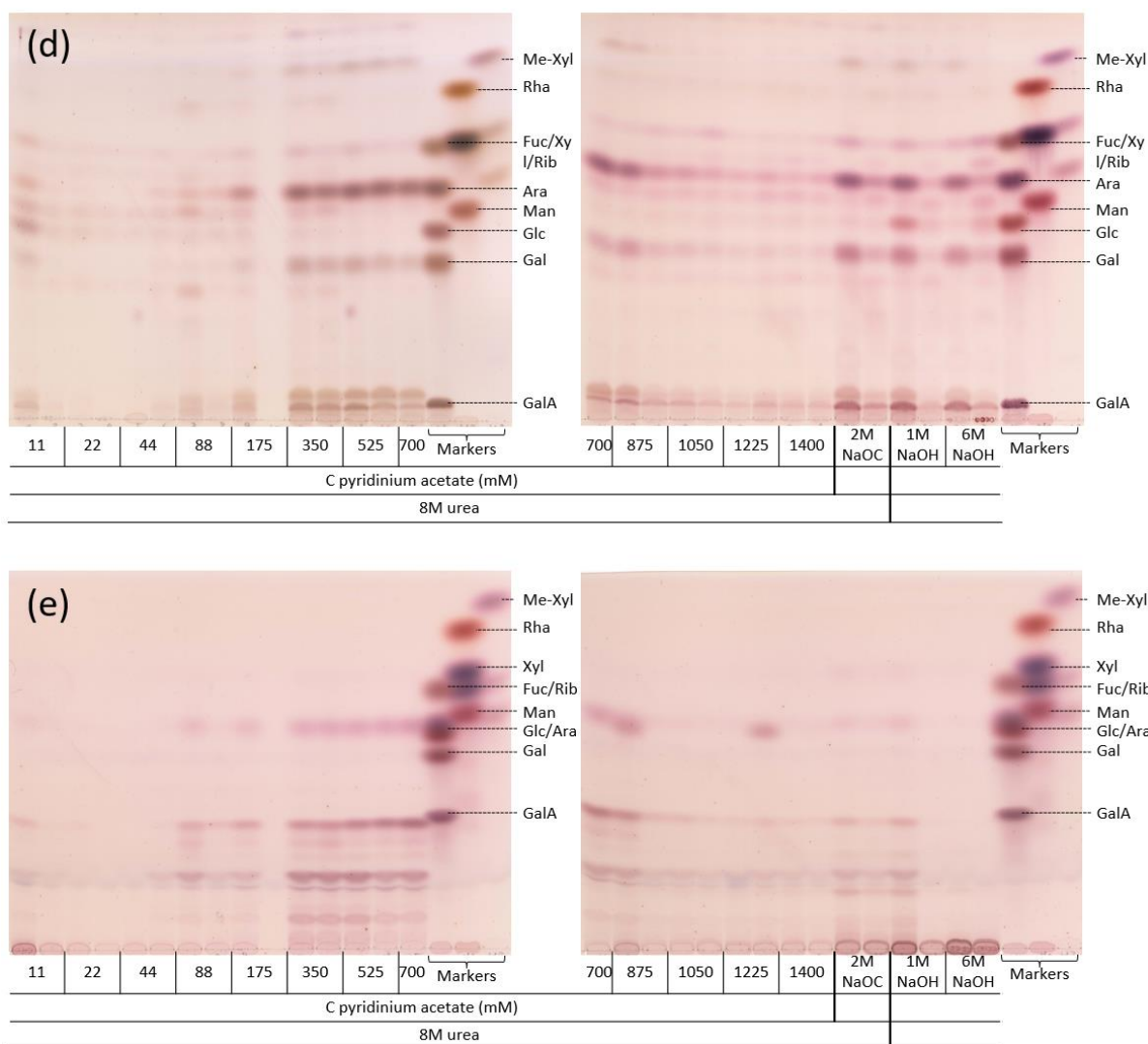


Figure 23: Separation of *Chlorokybus* P2 on anion-exchange chromatography.

(a): Concentration of total sugars in each fraction, measured by dot-blot assay on TLC plates. Dextran and homogalacturonan were run on the column as respectively neutral and acidic standards. (b): Concentration of uronic acids in each fraction of *Chlorokybus* P2, measured by *m*-hydroxybiphenyl assay after dialysis of the samples. (c): Concentration in sulphates in each fraction from *Chlorokybus* P2, measured by barium acetate assay after dialysis and complete acidic hydrolysis of the samples. (d): Hydrolysed fractions from *Chlorokybus* P2 separated on TLC. (e): Mildly hydrolysed fractions from *Chlorokybus* P2. For (d) and (e), each fraction was made of two samples collected successively. The TLC plate was developed twice in EPAW 6:3:1:1 for (d), and twice in B/A/W 4:1:1 for (e).

4.4.2. Hemicellulosic extract of *Chlorokybus*

4.4.2.1. Enzymatic assays on 'hemicellulose' from *Chlorokybus*

A range of glucan-specific enzymes was applied: endocellulase, lichenase, salivary amylase (Figure 24). Lichenan and cellulose (both commercial and extracted from *Ulva*) were used as standards for the cellulase and lichenase assays. The lichenan sample was contaminated, as it released oligomers even just in buffer. However, it was clearly hydrolysed by lichenase. Hb from *Chlorokybus* was not digestible by lichenase. The endo-cellulase assay was unsuccessful, as even the controls (cellulose and lichenan) were not hydrolysed. Amylase gave positive results, although the products released did not seem to have the same chromatographic properties as the known amylo-oligomers.

Non-glucan specific enzymes were also tested: XEG (xyloglucan-specific endoglucanase) and Driselase (a mixture of known cell wall hydrolases). Both XEG and Driselase led to the release of TLC-mobile oligomers.

The positive result from XEG was surprising, considering that it is thought only to be able to cleave the second β -(1 \rightarrow 4) linkage in Xyl- α -(1 \rightarrow 6)-Glc- β -(1 \rightarrow 4)-Glc- β -(1 \rightarrow 4)-Glc. It may be that the enzyme is also active if xylose is replaced by a glucose unit, possibly α -bonded to the rest of the polymer.

However, both Driselase and the particular XEG preparation employed are known to have a laminarinase side activity, which would enable the digestion of β -(1 \rightarrow 3)-glucan if present.

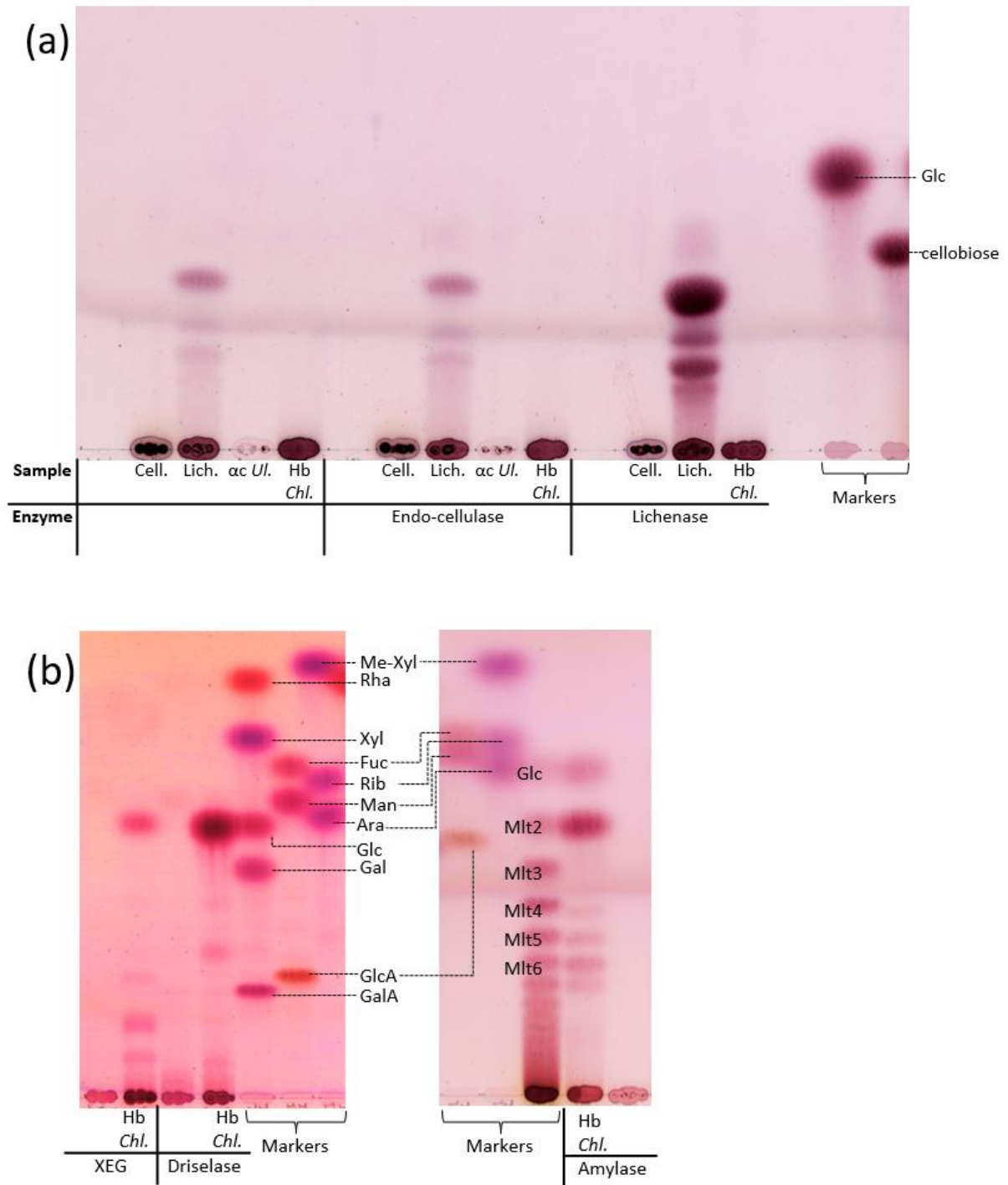


Figure 24: Enzymatic assays on Hb of *Chlorokybus*.

(a) shows both the results of endo-cellulase and lichenase assays on cellulose (Cell.), lichenan (Lich.), α -cellulose from *Ulva* spp. (ac Ul.) and hemicellulose b from *Chlorokybus* (Hb Chl.). (b) shows the results of the digestion of *Chlorokybus* Hb. by XEG, Driselase and amylase, as well as substrate-less controls for XEG and Driselase. Markers Mlt2, Mlt3, etc. stand for maltose, maltotriose, etc.

TLC (a) was developed once in BAW 2:1:1, TLC (b) was developed twice in BAW 4:1:1.

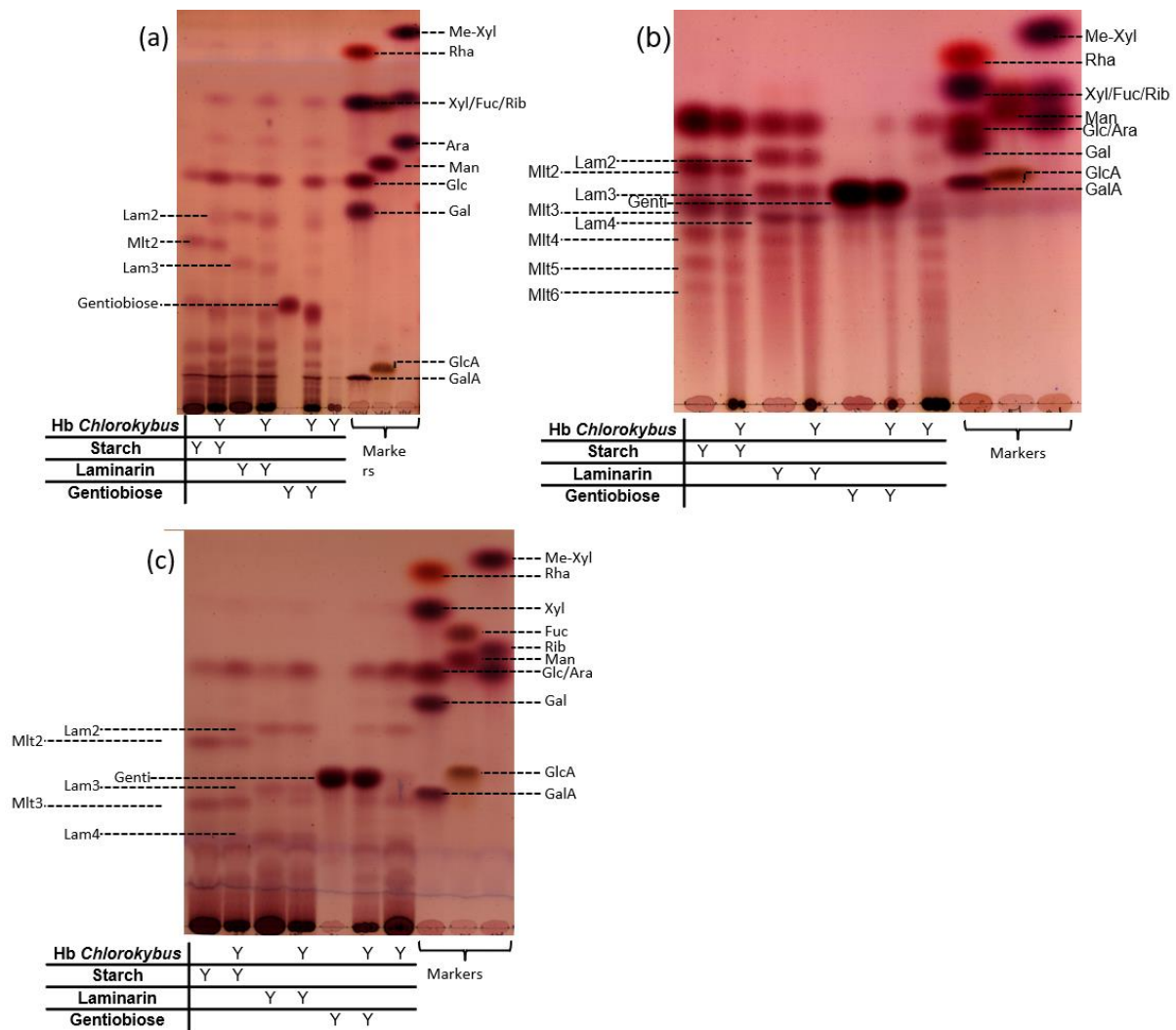


Figure 25: Mild hydrolysis assays on Hb from *Chlorokybus*, compared with starch and laminarin

All plates show co-migration assays between gentiobiose and mildly hydrolysed (0.1 M TFA, 100°C, 2 h) Hb from *Chlorokybus*, starch and laminarin. Laminarin-based oligomers are labelled Lam2, Lam3, etc., based on their polymerisation degree. Starch-based oligomers are, in the same way, labelled Mlt2, Mlt3, etc. (a): this plate was developed twice in EPAW 6:3:1:1. (b): this plate was developed once in BAW 2:1:1. (c): this plate was developed twice in BAW 4:1:1.

4.4.2.2. Mild hydrolysis assay of 'hemicellulose' from *Chlorokybus*

The above enzymatic study was complemented by a mild acid hydrolysis assay. Hb extract, alongside starch and laminarin, was hydrolysed with 0.1 M TFA, at 100°C for 2 h. This allowed for the release of series of oligomers from each of the substrates. Co-migration

assays were performed, including with gentiobiose (β -(1 \rightarrow 6)-glucobiose), in different solvent systems on TLC (Figure 25).

All substrates (starch, laminarin, *Chlorokybus* Hb) released primarily glucose, as expected. In addition, both laminarin and starch released a range of oligomers, detectable from DP2 to DP3 to 6.

Hb released a range of oligomers that were not organised as a ladder, as would have been expected from a linear polysaccharide. The fastest-migrating compound released, after glucose, co-migrated with laminaribiose in all three solvent systems tested, suggesting a β -(1 \rightarrow 3) glycosidic bond. The second hydrolysis product is more difficult to identify: it co-migrated with laminaritriose in EPAW 6:3:1:1 (Figure 25 (a)), with gentiobiose and laminaritriose (not resolved) in BAW 2:1:1 (Figure 25 (b)), and with gentiobiose in BAW 4:1:1 (Figure 25 (c)).

4.5. Conclusion

In this chapter, monomers and small oligomers that could not directly be identified were examined. The presence of the known aldobiouronic acid α -D-GlcA-(1 \rightarrow 3)-L-Gal in the bryophyte *Anthoceros* was confirmed, as were the presence of Rha derivatives and non-land-plant uronic acids in the chlorophyte *Ulva*. The fast-migrating sugars found in *Klebsormidium* could not be identified further, since their yields were too small.

The pectic extract of the early-diverging CGA *Chlorokybus* was found to contain the aldobiouronic acid β -D-GlcA-(1 \rightarrow 4)-L-Gal, which was characterised by a combination of chromatographic, chemical, enzymatic and spectroscopic methods. Going further into the

characterisation of this extract, it was found that it was not susceptible to land-plant-cell-wall-specific hydrolases. Only α -amylase and Driselase had an effect on the extract, releasing glucose and maltose, probably deriving from starch. Moreover, Gal residues could not be oxidised by D-Gal oxidase, thus they might all be L-Gal and not the usual D-Gal enantiomer. When run on anion-exchange chromatography, *Chlorokybus* P2 extract yielded two distinct fractions with similar sugar compositions, the less anionic one being richer in uronic acids and susceptible to mild acid hydrolysis, the more anionic one being richer in sulphates and more difficult to hydrolyse.

The hemicellulosic extract Hb from *Chlorokybus* was subsequently investigated, first through enzymatic assays. Even though the polymer was not susceptible to endocellulase and lichenase hydrolysis, the action of amylase, XEG and Driselase resulted into the release of several oligomers. It is known that our XEG preparation and the Driselase both have a side laminarinase activity. In order to characterise more precisely the nature of the glycosidic bonds in Hb, the extract was submitted to partial acid hydrolysis and its hydrolysate was separated on TLC in parallel with other glucans'. However, only the smallest released oligomer could be identified for sure, as laminaribiose (β -Glc-(1 \rightarrow 3)-Glc). The extract was examined spectroscopically to provide further insight into its structure.

5. *Klebsormidium fluitans* - A

fundamentally different cell wall

5.1. Introduction

In the first results chapter of this thesis (Section 3 Sugar residue composition - semi-quantitative analysis), the monosaccharide composition of a series of charophytic algae was examined. *Klebsormidium fluitans*' was particularly interesting, as it did not contain any trace of uronic acid nor of any other acidic sugars. This raises the question of the stability of the pectic matrix. In land plants, it is due to the presence of homogalacturonan, which jellifies in an "eggbox" structure thanks to the presence of calcium ions. Rhamnogalacturonans may also contribute, e.g. via boron-bridging of RG-II. Other mechanisms must take place in *Klebsormidium* for the 'pectic' polysaccharides to resist being leached into the culture medium and to guarantee cell wall integrity.

In order to tackle this, a range of studies were conducted on "pectic" extracts from *Klebsormidium*. First, the extractability of this fraction was assayed.

Additionally, a biochemical investigation was conducted on this extract. First, a series of hydrolases that are active on land-plant pectic components was tested. Then, two series of oligomers were produced, hydrolysed and analysed, leading to a closer comprehension of the cell wall structure of *Klebsormidium fluitans*.

A physical investigation on the ultrastructure and the gelling of these algal polymers remains necessary to understand the mechanisms involved in the stabilisation of the alga's cell wall.

5.2. Extractability of *Klebsormidium* 'pectin'

The pectic extract from *Klebsormidium* does not correspond to the usual composition of such extracts in land plants. It is so different that it might have very distinctive properties. The simplest one to verify is its extractability from plant AIR. Indeed, land plant pectin is extractable with ions such as oxalate: they are thought to chelate the calcium ions (which usually cross-link the homogalacturonan domains of pectin), thus disrupting the pectin network. However, chelating ions on their own do not automatically provoke the solubilisation of pectin: for example, CDTA is capable of chelating calcium ions at room temperature but fails to solubilise plant polymers. The suspension of plant AIR in buffer must be heated to efficiently solubilise pectin, probably through the disruption of additional linkages (which could be xyloglucan-pectin, or boron bridges between RG-II units).

It is worth noting that methyl-esterified and acetyl-esterified portions of homogalacturonan might also be involved in pectin gelation. However, in the absence of uronic acids, hence homogalacturonan domains, the mechanisms for pectin gelation and gel disruption in *Klebsormidium* are very probably different. Land plant pectin solubilisation happens at high temperature and moderately acidic pH (100°C, pH 4 to 4.3). The extractability of polysaccharides from *Klebsormidium* was tested at different temperatures, different pH values and in different buffers in order to discover the most favourable conditions.

5.2.1. Different temperatures and buffers

The extractability of *Klebsormidium fluitans* 'pectic' fraction was tested. Different extraction temperatures were tried: 20, 60 and 100°C. The nature of the buffer was also varied, as oxalate, acetate and formate buffers were tested. Solubilised biomass was harvested after 2 h, new buffer was added and the incubation was conducted for 16 more hours, in the same way as the production of extracts P1 and P2 was conducted (see previous chapters).

The extracted quantities, given as percentages of the initial weight of AIR, are shown in Table 5 and Figure 26 (a). It was clear that the higher the temperature, the more material was extracted. This relationship was not linear: there was a jump (with at least 20 times more material extracted) as 100°C was reached, meaning that boiling the extraction mixture is mandatory for an efficient extraction procedure.

Table 5: Extractability of *Klebsormidium* "pectin": Influence of temperature.

Extraction conditions Buffer	20°C			60°C			100°C		
	2 h	16 h	Tot.	2 h	16 h	Tot.	2 h	16 h	Tot.
Ammonium oxalate / oxalic acid	1.9	1.0	2.9	1.3	1.4	2.7	24.3	27.9	52.2
Sodium acetate / acetic acid	0.8	0.6	1.4	2.2	1.1	3.3	23.6	31.6	55.2
Sodium formate / formic acid	1.2	1.1	2.3	2.3	1.4	3.7	29.5	47.4	76.9

All the buffers were at the same concentration and the same pH, 0.2 M and pH 4.1. The supernatants were extracted after centrifugation (5000 g, 10 minutes), dialysed against water for 36 h (three to five baths), and freeze-dried. The results are given as percentages of the initial weight (5 mg).

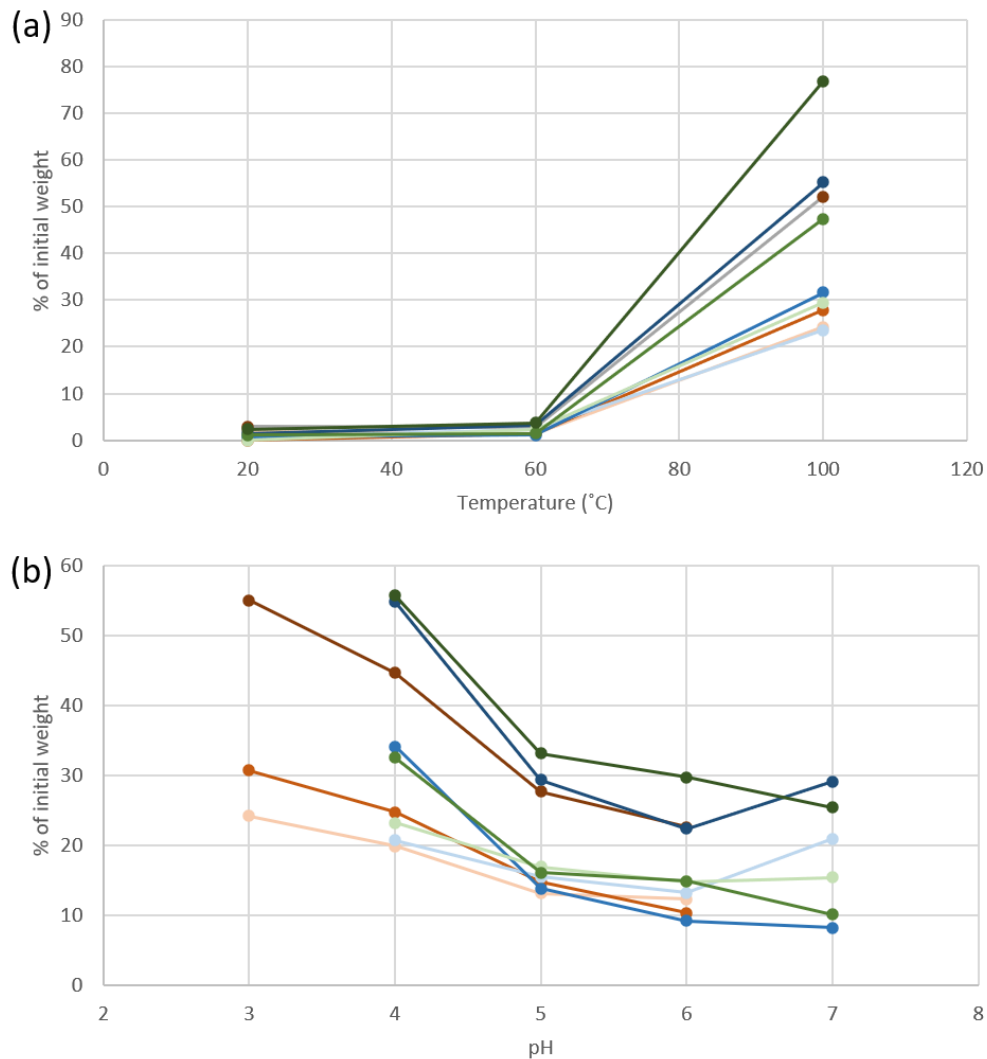


Figure 26: Extractability of *Klebsormidium 'pectin'*. Influence of temperature, buffer and pH.

(a): Influence of temperature on the extractability of *Klebsormidium 'pectin'*. (b): Influence of pH on the extractability of *Klebsormidium 'pectin'*.

All the buffers were at the same concentration and the same pH, 0.2 M and pH 4.1. The supernatants were extracted after centrifugation (5000 g, 10 minutes), dialysed against water for 36 h (three to five baths), and freeze-dried. The results are given as percentages of the initial weight (5 mg).

Concerning the influence of the nature of the buffer, it was obvious that a chelating ion is not necessary. Oxalate ($[\text{O}_2\text{C}-\text{CO}_2]^{2-}$) is characterised by its divalent nature and two pK_a values, one at 1.27 and the other at 4.28. Acetate (CH_3CO_2^-) is monovalent and its pK_a is 4.75. Formate is the smallest molecule (HCO_2^-) and displays a pK_a of 3.75. It was the most efficient

buffer for “pectin” solubilisation in *Klebsormidium*, as at least 20% more material than in oxalate or acetate was extracted. This difference in efficiencies was particularly strong after 16 hours of incubation: there was only a 20% difference after 2 h.

The composition of the extracts has been verified by hydrolysing and running them on TLC (Figure 27). There was no difference, in terms of sugar residues, between the different extracts from the different buffers. However, the temperature of extraction seemed to impact some of the fast-migrating sugars present: a purple-staining monosaccharide, migrating just faster than rhamnose, was only visible in 60°C extracts. Moreover, the loading of the 100°C extracts (weighed after dialysis and drying) was clearly insufficient.

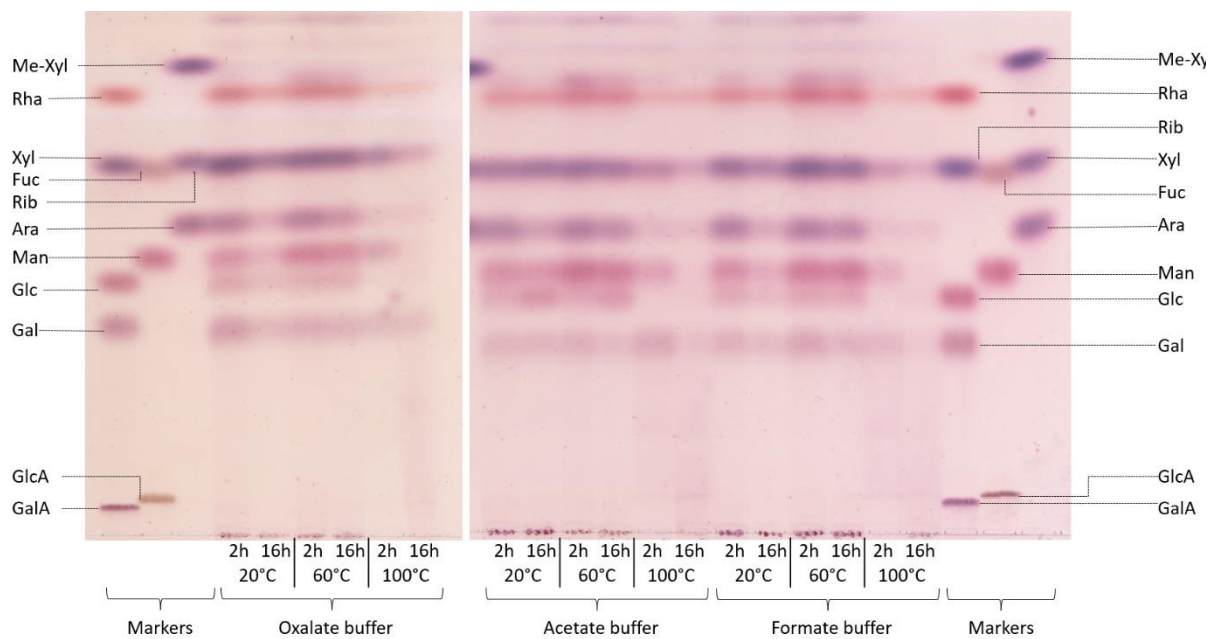


Figure 27: Separation of hydrolysed ‘pectic’ extracts from *Klebsormidium* AIR. ‘Pectic’ extracts were hydrolysed with TFA, following the usual procedure. Hydrolysates were separated on TLC, on plastic-backed silica plates developed in EPAW 6:3:1:1

5.2.2. Different pH and buffers

100°C was easily established as the temperature for extracting the maximum weight of polysaccharide from *Klebsormidium*. Hence, the following extractability assay was only conducted at this temperature.

For each acid (oxalic, acetic and formic), a series of buffers at different pH was prepared. Buffers' pH values were fixed at 3.0, 4.0, 5.0 and 6.0 in oxalate, and at 4.0, 5.0, 6.0 and 7.0 in acetate and formate.

As previously, solubilised biomass was harvested after 2 h at 100°C. New buffer was added to the pellets and the extraction was conducted for 16 more hours. The extracted polymers, given as percentages of the initial weight of AIR, are shown in Table 6 and Figure 26 (b).

For each buffer, the lower the pH, the higher the polymeric yield was. Outliers to this trend, however, are the 2-h extracts from acetate and formate buffers at pH 7.0, highlighted in orange. In the case of formate, the difference with the amount extracted after 2 h at pH 6 is incidental, and can be considered as a stagnation of the solubilisation capacity of this buffer between pH 6 and 7. In acetate, 13.2% of the initial biomass is extracted after 2 h at pH 6, whereas 20.9% is extracted after 2 h at pH 7. This difference between the two pH values might be due to beta-elimination taking place, thus making the solubilisation of sugar easier. The difference between the efficiencies of extraction of the two buffers, formate solubilising higher quantities of polymer than acetate, might be due to the size of the ions (formate smaller than acetate) or to their respective polarities (formate much more electronegative than acetate).

At pH 4, 5 and 6, formate was always more efficient than oxalate and acetate for extracting polymers. However, the yields at pH 4 were consequently lower than the ones observed during the first assay (Table 5).

The sugar composition was verified and was not found to be different from the sugar composition of the usual extracts (in oxalate, at pH 4.1 and 100°C, after 2 and 16h).

Table 6: Extractability of *Klebsormidium* "pectin": Influence of pH.

Extraction conditions	pH 3.0			pH 4.0			pH 5.0		
	2 h	16 h	Tot.	2 h	16 h	Tot.	2 h	16 h	Tot.
Ammonium oxalate / oxalic acid	24.2	30.7	55	19.9	24.7	44.6	13.1	14.7	27.7
Sodium acetate / acetic acid				20.7	34.1	54.8	15.5	13.8	29.3
Sodium formate / formic acid				23.2	32.5	55.7	16.9	16.1	33.1

Extraction conditions	pH 6.0			pH 7.0		
	2 h	16 h	Tot.	2 h	16 h	Tot.
Ammonium oxalate / oxalic acid	12.3	10.3	22.6			
Sodium acetate / acetic acid	13.2	9.2	22.4	20.9	8.2	29.1
Sodium formate / formic acid	14.8	14.9	29.7	15.4	10.1	25.4

All the extractions were conducted at the same temperature, 100°C. Other details as in Table 5.

Table 7: Enzymatic digestion of *Klebsormidium* pectic extract.

Enzyme	Target polysaccharide	Result	Product
endo-1,4- β -D-galactanase	Galactan and type I arabinogalactans (RG-I sidechain, pectin)	Neg.	
endo-1,5- α -arabinanase	Arabinan (RG-I sidechain, pectin)	Pos.	Arabinose, Prod2
endo-1,4- β -mannanase 1	Mannan, glucomannan (hemicellulose)	Neg.	
endo-1,4- β -mannanase 2	Mannan, glucomannan, arabinoxylan, Me-glucuronoxylan (hemicellulose)	Pos.	Prod4
endo-1,4- β -xylanase	Xylan, arabinoxylan & Me-glucuronoxylan (hemicellulose)	Pos.	Prod3, Prod4
lichenase	Mixed-linkage glucan (hemicellulose)	Neg.	
β -xylosidase:	Terminal Xyl residues of (hetero)xylans and xylogalacturonan	Neg.	
β -galactosidase	Terminal Gal residues of RG-I, galactoglucomannan etc.	Neg.	
α -galactosidase	Gymnosperm galactoglucomannans	Pos.	Gal, Rha
Driselase	All except RG-II and possibly AGPs	Pos.	.

*This table shows the enzymes tested against *Klebsormidium* pectin, their target polysaccharides as seen in a land-plant, whether digestion with the said enzyme yielded the release of low- M_r products or not, and where the related information can be found in this chapter. The table is divided between pectin-specific endo enzymes (Figure 28), hemicellulose-specific endo enzymes (Figure 29), exo-enzymes (Figure 30), and the multi-target Driselase (Figure 31). Neg. signifies the absence of detectable digestion product following the action of the enzyme, Pos. means the presence of digestion product following the action of the enzyme.*

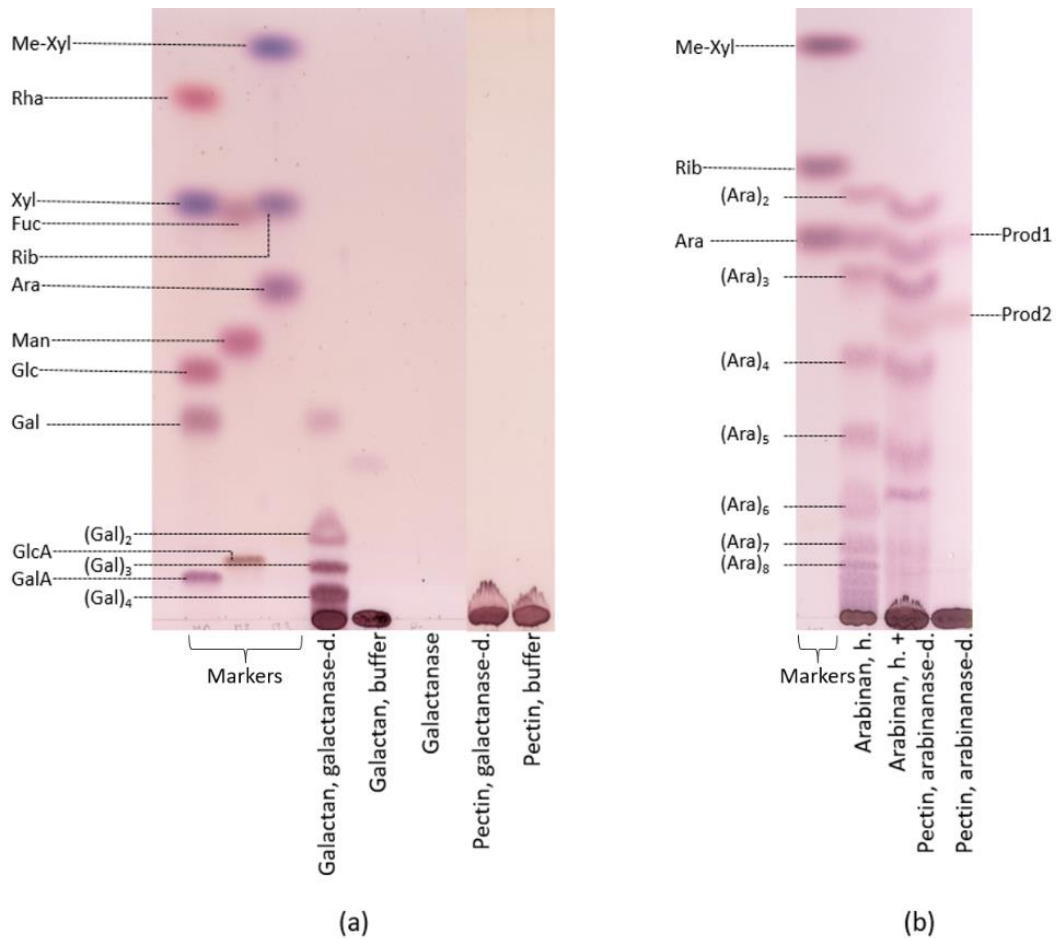


Figure 28: Enzymatic digestion of *Klebsormidium* 'pectic' extract with pectin specific enzymes.

(a): Galactanase assay and control experiments: Commercial galactan (left) and *K. fluitans* 'pectin' (right) were incubated in buffer + galactanase and in buffer only. Galactanase enzyme was incubated without a substrate and run on its own as a control. (b): Co-migration assay of mildly acid-hydrolysed arabinan and arabinanase-digested pectin. Prod.1 co-migrates with arabinose. Prod.2 does not co-migrate with any oligomer. Both assays were conducted on plastic-backed silica plates developed in EPAW 6:3:1:1. d. is for enzyme-digested, h. for acid-hydrolysed.

5.3. Enzymatic assays on *Klebsormidium* 'pectic' extracts

In order to get a clearer idea of the glycosidic bonds involved, the "pectic" extract P2 from *Klebsormidium* was tested against various enzymes that characteristically cleave bonds between neutral sugar residues in plants (Figure 29). These enzymes were selected because

they act on polysaccharides containing sugar residues known to be present in the extract of interest. Both endo and exo-enzymes were used. The first ones act by randomly cleaving the glycosidic bonds within a polysaccharide, while the second one acts from the non-reducing end. However, only a few of these enzymes were efficient on *Klebsormidium* 'pectic' extract.

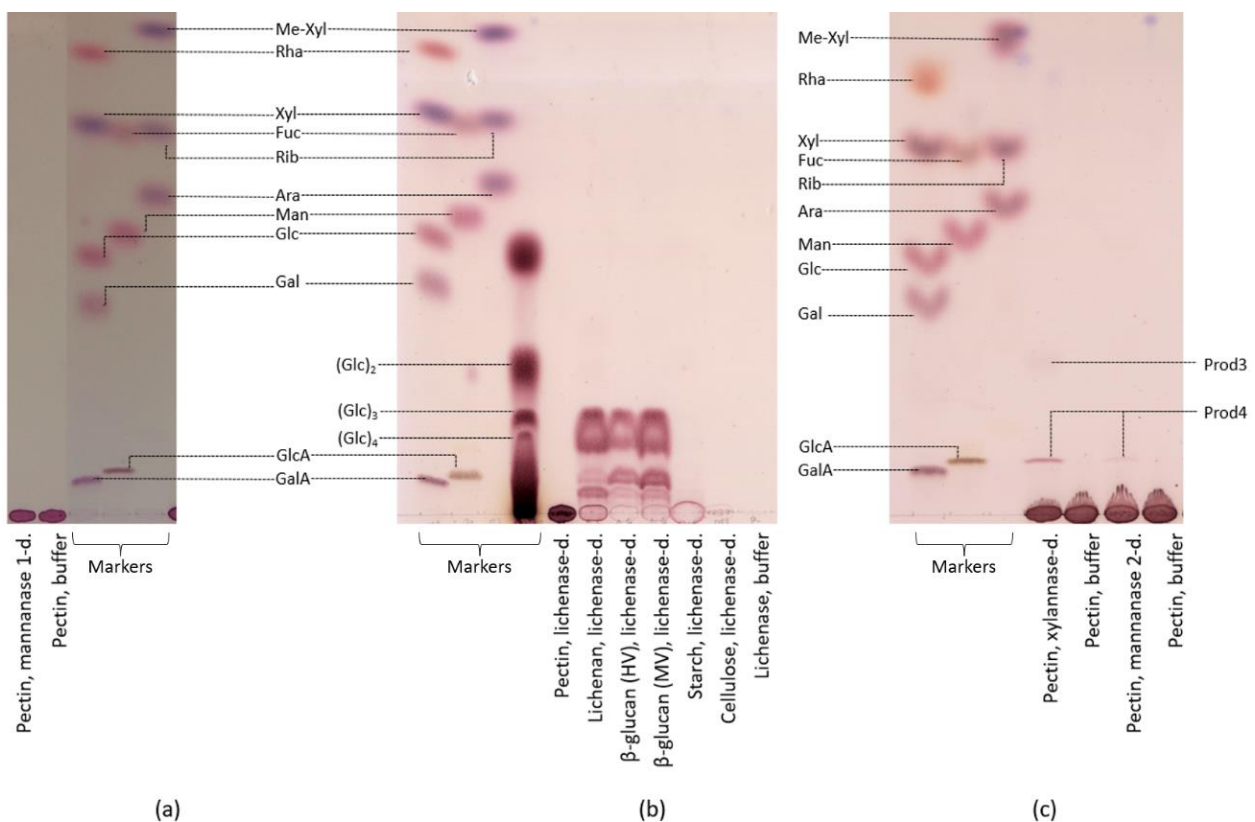


Figure 29: Enzymatic digestion of *Klebsormidium* 'pectic' extract with hemicellulose-specific enzymes.

(a): Mannanase-1 assay on pectin. Pectin has been incubated in buffer alone as control experiment. (b): Lichenase assay on *Klebsormidium* 'pectin' and a variety of glucans. Incubation of the enzyme in buffer has been performed as a negative control. A malto-oligosaccharides ladder was included with the markers (fourth lane). (c): Xylanase and mannanase-2 assay on pectin. Pectin has been incubated in both buffers as control experiments. The 3 assays were realised on plastic-backed silica plate and developed twice in EPAW 6:3:1:1. d. is for enzyme-digested.

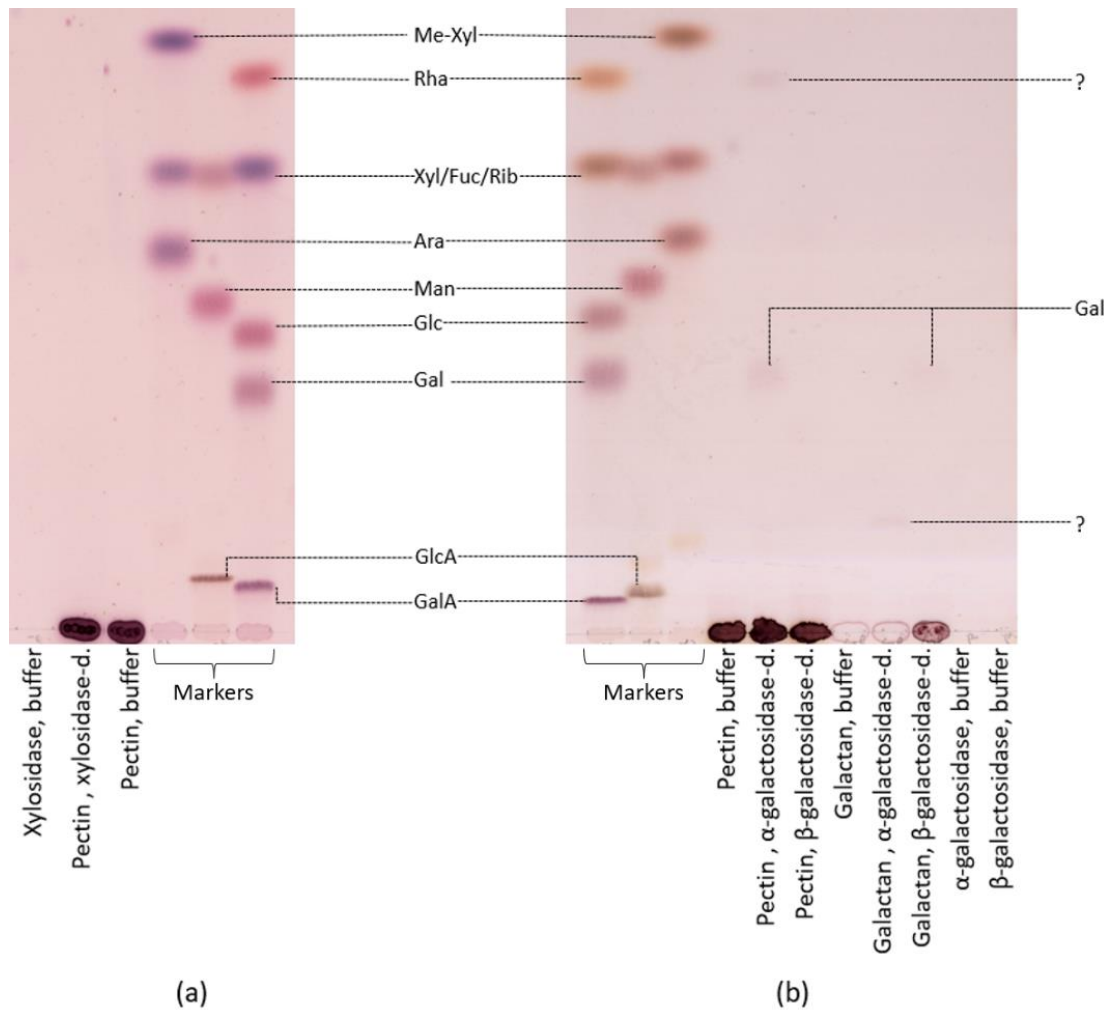


Figure 30: Enzymatic digestion of *Klebsormidium* 'pectic' extract with exo-enzymes. (a): β -xylosidase assay on pectin. Pectin and xylosidase have been incubated in buffer alone as control experiments. (b): α - and β -galactosidase assays on pectin and β -(1 \rightarrow 4)-galactan. Enzymes and substrates were incubated alone in buffer as control experiments. The 3 assays were realised on plastic-backed silica plate and developed twice in EPAW 6:3:1:1. d. is for enzyme-digested.

5.3.1. Results from pectin-specific enzymes on *Klebsormidium* 'pectic' extracts

Endo-enzymes specific to pectic domains were tested first (summary in Table 7).

It has been established in Chapter 3.4.2 that *Klebsormidium* is left unchanged after EPG digestion, as it does not contain its target glycan, homogalacturonan.

The pectic domain RG-I contains, in land plants, sidechains of arabinan and galactan. As both arabinose and galactose are fairly abundant in the studied extract, both RG-I-active galactanase and arabinanase were tested on the P2 *Klebsormidium* fraction (Figure 28). Galactanase was tested against commercial galactan, thus producing a ladder of galacto-oligomers of DP 1 to 4. In the case of galactanase, nothing was released. It was clear that unsubstituted β -(1 \rightarrow 4)-D-galactose residues, were not detectable.

The algal pectic extract did yield digestion products under arabinan action. The TLC plate (Figure 28 (b)) shows the results of arabinan partial hydrolysis on the left (an arabino-oligomers ladder, with arabinobiose remarkably migrating further than arabinose), of algal pectic extract on the right, and the superposition of these two mixtures in the middle.

Klebsormidium 'pectin' yielded two products, respectively named Prod1 and Prod2. Prod1 co-migrated with arabinose and stained purple, as expected. Prod2 also stained purple; however, it did not co-migrate with any linear arabinose oligomer. It might be a dimer of arabinose and a different sugar residue. Indeed, the arabinanase used is known to cleave the bond between two Ara residues, irrespective of whether or not they are non-reducing termini.

5.3.2. Results from hemicellulose-specific enzymes on *Klebsormidium* 'pectic' extracts

As the experiments involving the expected pectin domains yielded a very limited amount of information, the *Klebsormidium* 'pectic' extract was tested for land plant hemicellulose-specific carbohydrates (

Figure 29).

No product was detected from the analysis of the digestion products with high-specificity mannanase nor with lichenase (

Figure 29 (a) and (b)). This showed the absence of both mixed-linkage glucan and classical mannan. However, mannanase 2 (active on heteroxylans and mannans) released a digestion product, labelled Prod4 and co-migrating with GalA (

Figure 29 (c)). Digestion with xylanase yielded two products, respectively named Prod3 and Prod4 (

Figure 29 (c)). However, their nature was undefined, as they migrated in unexpected zones:

Prod3 between uronic acids and neutral sugars, Prod4 co-migrated with galacturonic acid.

However, Prod4 did not stain the same colour as GalA. Prod4 produced from mannanase 2 digestion and Prod4 produced from xylanase digestion co-migrated; as both enzymes are active on heteroxylans, this product is probably identical in both digests.

5.3.3. Results from exo-enzymes (β -xylosidase and galactosidases) on

Klebsormidium 'pectic' extracts

The non-reducing termini of *Klebsormidium* pectic extracts were investigated by enzymatic digestion (Figure 30).

β -xylosidase digestion did not release any monomer. Thus, even if the *Klebsormidium* cell wall displays xylose-containing polysaccharides, their termini are not β -linked xylose residues.

Both α and β -galactosidase actions on *Klebsordmidium* 'pectic' extract were tested. Their action upon commercial galactan (β -(1 \rightarrow 4)) was verified: as expected, only β -galactosidase provoked the release of galactose, although in surprisingly low amounts. The *Klebsordmidium* 'pectic' extract released galactose when digested with α -galactosidase. This was unexpected, since in land plants, non-reducing terminal galactosyl residues are mainly present as β -residues, for example as β -(1 \rightarrow 4)-Gal oligomers in RG-I side-chains, as (1 \rightarrow 2)-linked β -galactosyl residues in xyloglucan side-chains, or as β -(1 \rightarrow 3)-Gal oligomers in AGPs. However, terminal α -galactosyl residues are present in nature, for example in galactoglucomannans (Schröder *et al.* 2001).

A second unidentified and unexpected compound, migrating with rhamnose, was released upon digestion of pectin with α -galactosidase. It might be that Rha, linked to the backbone of the polysaccharide and the terminal Gal residue, is particularly labile once the terminal Gal residue is removed. When galactan was digested with α -galactosidase, an unidentified slow-migrating compound was released. Neither of these compounds was known in the literature, nor were they studied in this work.

5.4. Driselase dissection of *Klebsordmidium* 'pectin'

Driselase is a mixture of enzyme extracted from the fungus *Irpex lacteus*. Driselase contains a variety of enzymes which usually digests plant cell walls, amongst which α and β -galactosidase, β -glucosidase, α and β -mannosidase, α -L-arabinosidase, β -xylosidase, α -L-fucosidase, cellobiohydrolase, cellulase, β -galactanase, α -L-arabinanase, EPG, β -mannanase,

β -xylanase, and xyloglucan-specific β -glucosidase have been documented (Novotný *et al.* 2009).

5.4.1. Preliminary tests of Driselase action on *Klebsormidium* 'pectin'

Klebsormidium pectin was digested with Driselase, for various durations (Figure 31). Monosaccharides, including glucose, mannose, arabinose, and xylose, were released. Several oligosaccharides were also mobile on TLC plates, whilst many products were not effectively hydrolysed (heavy band at the origin). At the end of the digestion assay, each enzyme + 'pectin' mixture was kept at -20°C before loading on TLC, which might explain the surprising amount of digestion products visible even in the least digested mixtures.

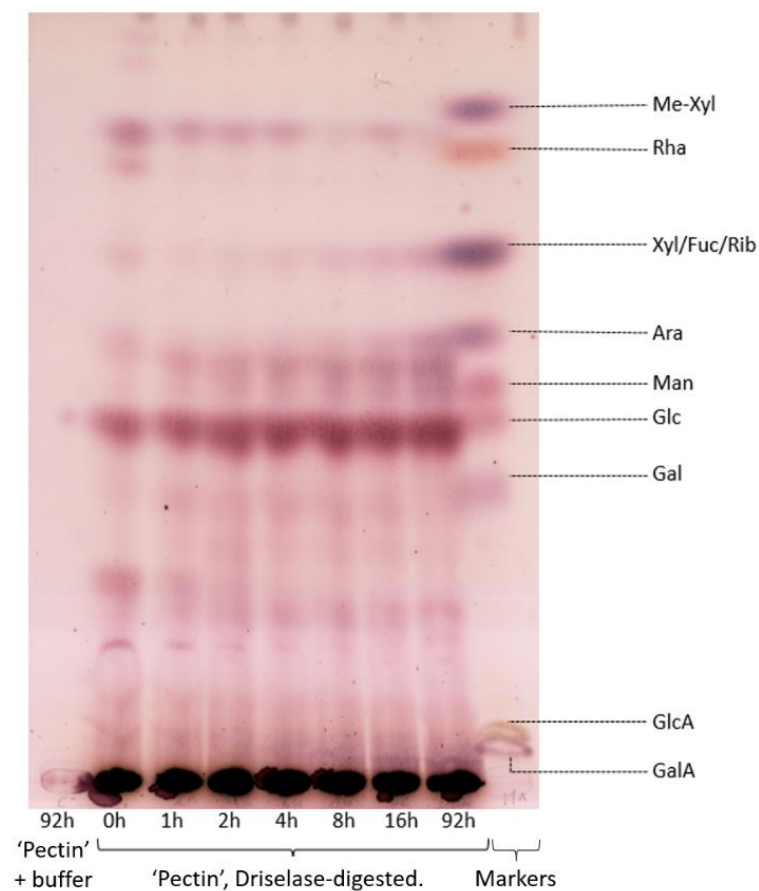


Figure 31: Driselase time-course on *Klebsormidium* 'pectin'.

Pectic extract digested with Driselase for 0 to 92 h. Pectin was also incubated in buffer as a control experiment. Driselase was incubated without substrate as a control, releasing non-detectable amounts of monomeric and oligomeric sugars (not visible here, cf. Figure 32).

5.4.2. Coupling α -amylase and Driselase for digestion of *Klebsormidium* 'pectin'

Klebsormidium pectin was successively submitted to α -amylase digestion (i.e. de-starching) and Driselase digestion. The goal was to verify that the oligosaccharides observed previously were indeed *Klebsormidium*-specific and not merely malto-oligosaccharides.

After α -amylase digestion, the mixture of enzymes and pectin was incubated in 75% ethanol: this was aimed at solubilising short oligomers and precipitating the remaining polymers.

Both the precipitate and the supernatant were incubated with Driselase, and extracted with 75% ethanol.

A total of four samples were produced:

- Fraction Sol-Sol, containing the ethanol-soluble products from amylase digestion, re-digested with Driselase and still soluble in 75% ethanol
- Fraction Sol-Res, containing the ethanol-soluble products from amylase digestion, re-digested with Driselase and found to be insoluble in 75% ethanol
- Fraction Res-Sol, containing the ethanol-insoluble products from amylase digestion, digested with Driselase and now soluble in 75% ethanol
- Fraction Res-Res, containing the insoluble residues left from both digestion steps

Each sample was run on thin-layer chromatography, in two different solvent systems (Figure 32).

5.4.2.1. Fraction Sol-Sol

Fraction Sol-Sol contained only glucose, in terms of mobile compounds. This was expected, as malto-oligosaccharides have been released by α -amylase, and they have been broken down to the monosaccharide residue by Driselase.

5.4.2.2. Fraction Sol-Res

Fraction Sol-Res was empty, as the amylase-solubilised oligomers did not become insoluble again after a second enzymatic treatment.

5.4.2.3. Fraction Res-Res

Fraction Res-Res only contained polysaccharides that stayed stuck at the origin and did not migrate at all. This is not surprising, since this fraction contains everything that could not be solubilised by amylase nor Driselase.

5.4.2.4. Fraction Res-Sol

Fraction Res-Sol is the most interesting one. It contains the monomers and oligomers released by Driselase from de-starched polysaccharides. Xylose, arabinose, glucose, and galactose could be identified. A range of oligomers of various sizes was also produced. As these compounds were not visible in the Sol-Sol fraction (apart from glucose) they necessarily have been produced by the enzymatic hydrolysis of *Klebsormidium* 'pectin' and are not the result of Driselase autolysis.

5.5. Gel permeation chromatography for starch-freed, Driselase-digested *Klebsormidium* pectin

Fraction Res-Sol, i.e. pectin freed from starch and Driselase-digested, was separated by gel permeation chromatography on Bio-Gel P-2 (see Figure 33).

In fractions 25 to 29, the main monomers could be identified (xylose, arabinose/glucose and galactose). Two short (i.e. being released from the column just before the monomers) purple-staining oligomers were visible in fractions 22 to 26, they migrated just slower than the monomers in BAW and in the monomer region in EPAW. Fractions 14 to 21 contained a series of longer oligomers, all purple-staining. The purple colour obtained with thymol-staining indicates that these oligomers contain a fair proportion of pentoses (for example, Xyl). Fractions 12 and 13 displayed heavy bands at the origin, indicating the presence of longer oligomers, soluble in ethanol but immobile on TLC.

In order to isolate each oligomer, the fractions were run individually on preparative TLC. Plates with a glass-back and a thicker silica coating were used, as they allow for heavier loadings and easier scraping, thus losing less material afterwards. Fractions 14 to 20 were separated on these thicker plates, and developed three times in EPAW 6:3:1:1.

Initially, the plates were transiently stained with iodine. This allowed for the detection and isolation of a number of compounds. However, this technique later on proved to be unreliable and erratic. Instead, the compounds were eluted off the plate as 1-cm-wide strips.

Only the first 10 cm of the plate contained sugars. This gave a total of 70 sub-fractions (ten for each SEC-fraction, see Figure 34).

5.5.1. Monomer composition of the oligomers produced by Driselase-digestion of *Klebsormidium* 'pectin'

As some of the sub-fractions were identical, they were pooled and ten samples were obtained in the end (Figure 35). Each of these ten samples was completely hydrolysed with TFA, and two main monosaccharides were obtained: xylose and rhamnose. Minor sugars that were also visible are arabinose (as a trace), and glucose in sample 2.

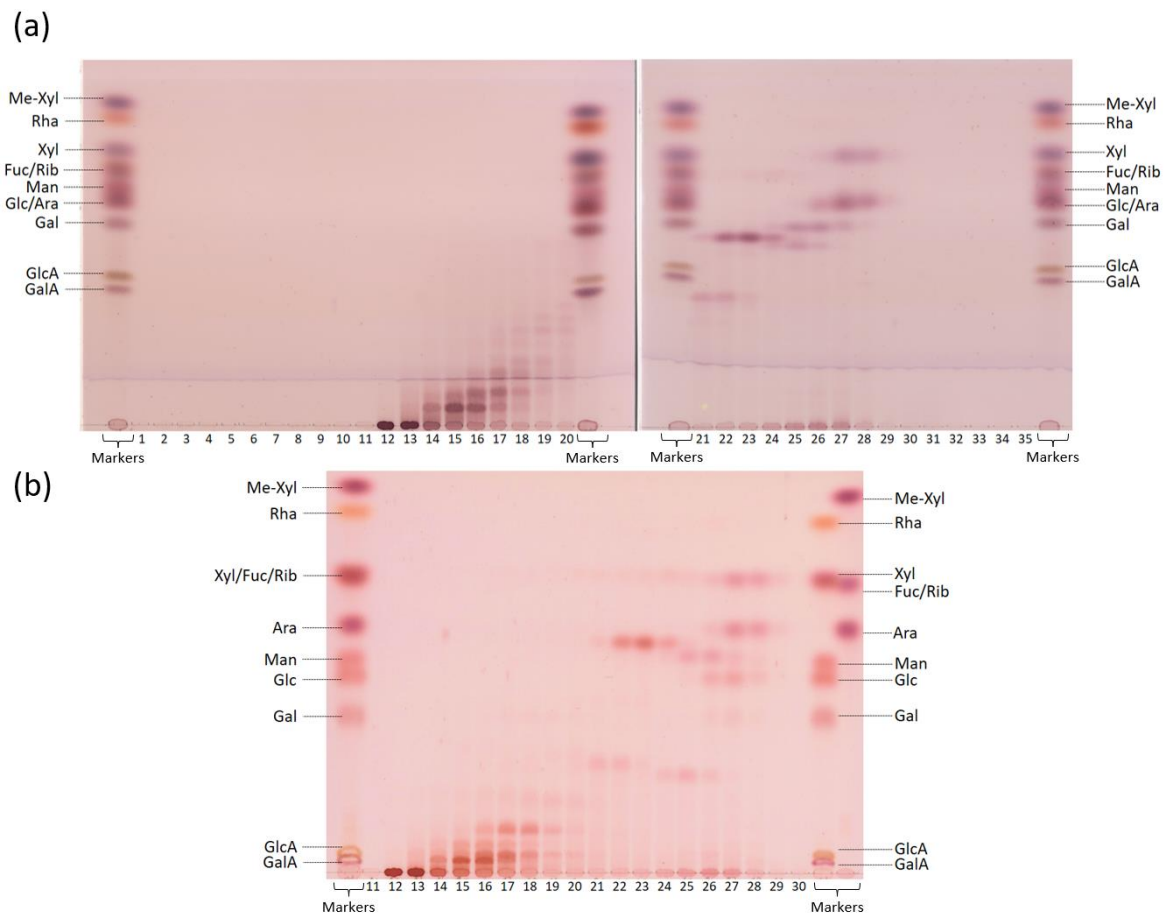


Figure 33: De-starched, Driselase-digested *Klebsormidium* 'pectin' separated by gel permeation chromatography.

Klebsormidium pectin was digested with α -amylase, the remaining ethanol-insoluble material (including that which dissolved in the aqueous amylase solution) was digested with Driselase. The new ethanol-soluble fraction was separated from the solid residue. It was separated by gel permeation chromatography on Bio-Gel P-2. Thirty-five 2-ml fractions (numbered above) were collected and run individually on TLC: developed in BAW 4:1:1 in (a), developed in EPAW 6311 in (b).

All the fractions were loaded in (a), fractions 11 to 30 were loaded in (b).

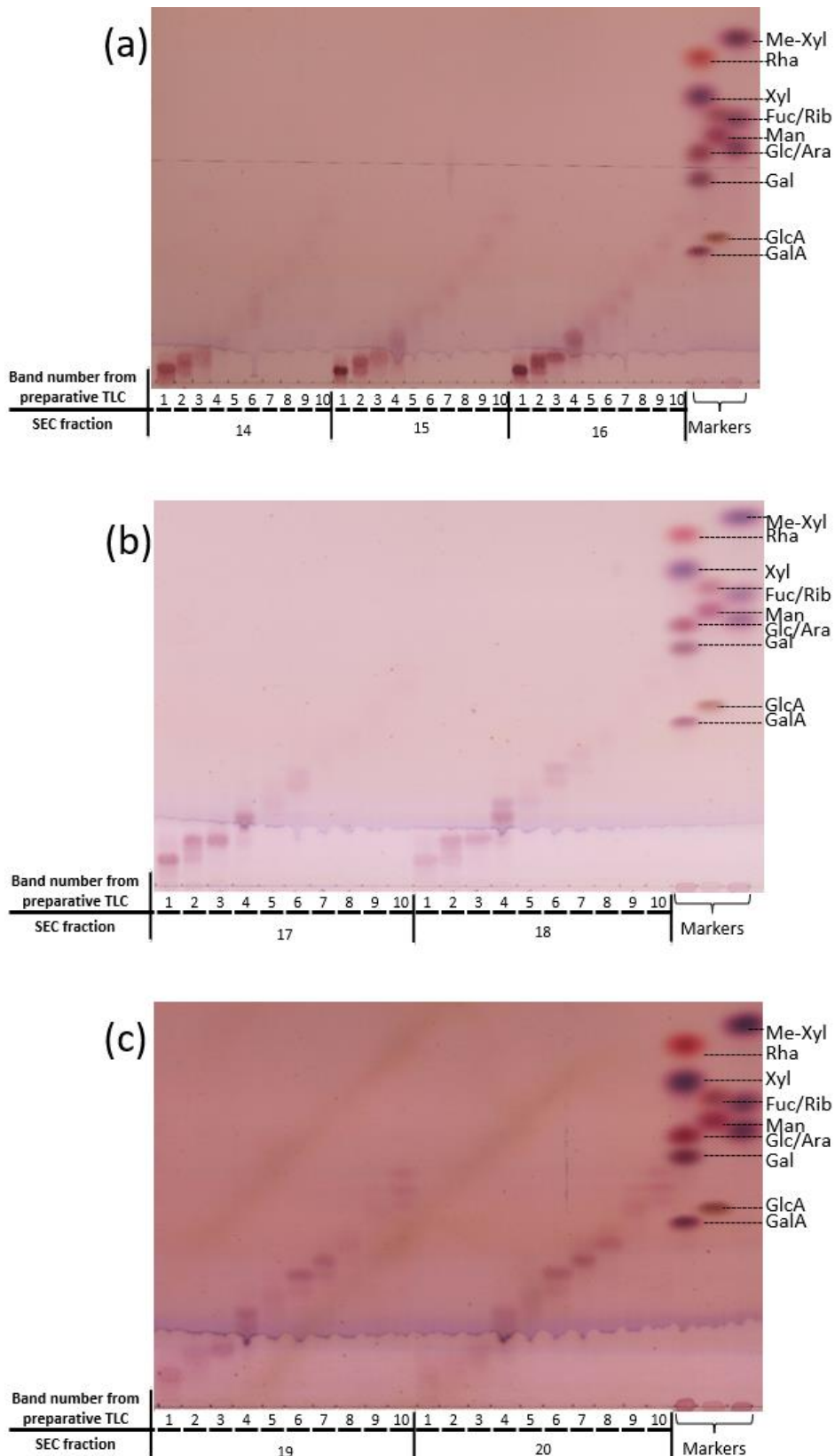


Figure 34: Analytical TLC of GP-fractions from Driselase-digested pectin from *Klebsormidium* previously separated on preparative TLC.

(a) shows each of the ten sub-fractions obtained from the separation by preparative TLC of the SEC-fractions 14, 15 and 16. (b) is the same for SEC-fractions 17 and 18, (c) is for SEC-fractions 19 and 20. The plates were developed in BAW 4:1:1.

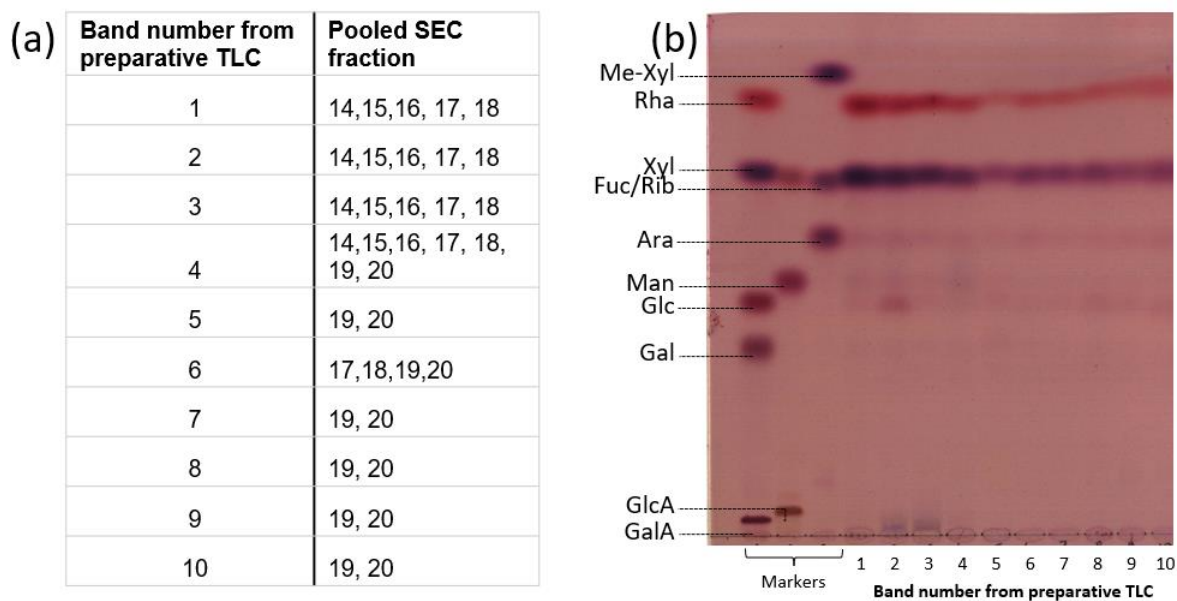


Figure 35: Monomer composition of sub-fractions from preparative TLC.

(a): The sub-fractions that had similar migration properties on TLC were grouped together. For example, the sub-fraction 1 from the SEC-fractions 14, 15, 16, 17 and 18 were pooled to make up a new compound called 1. (b): Each of the 10 fractions obtained by pooling the samples was hydrolysed.

5.5.2. Chromatographic properties of the oligomers produced by Driselase-digestion of *Klebsormidium* 'pectin'

The chromatographic properties of each sub-fraction 1-10 for SEC-fractions 14 to 20 were measured. Indeed, each 1-10 group may be a suite of linear oligosaccharides, as each one migrates faster than the previous one and they all contain the same sugar residues. If that is the case, then the successive $\log \left(\frac{1}{R_f} - 1 \right)$ of different size oligomers should fit a linear model, increasing with the degree of polymerisation of the oligomer (Powning and Irzykiewicz 1967).

However, the size of the oligomers is unknown at this stage. Instead, the sub-fraction numbers (1 to 10, from the slowest- to the fastest-migrating compound) were used. This means that, even though the absolute values of the slopes do not vary, they will be inverted (decreasing instead of increasing), and the y-intercept may be different than what it would be if calculated with the actual DP.

The front of the solvent not having been marked, it was easier to use another sugar for reference, in order to calculate a retention factor equivalent. β -methyl-xyloside was used, as it is the furthest-migrating sugar. The notation R_{MeXyl} is used to signify this.

Knowing that, the measures and calculations were realised on each plate – when the compounds were visible enough to allow for reliable measurement (Figure 36).

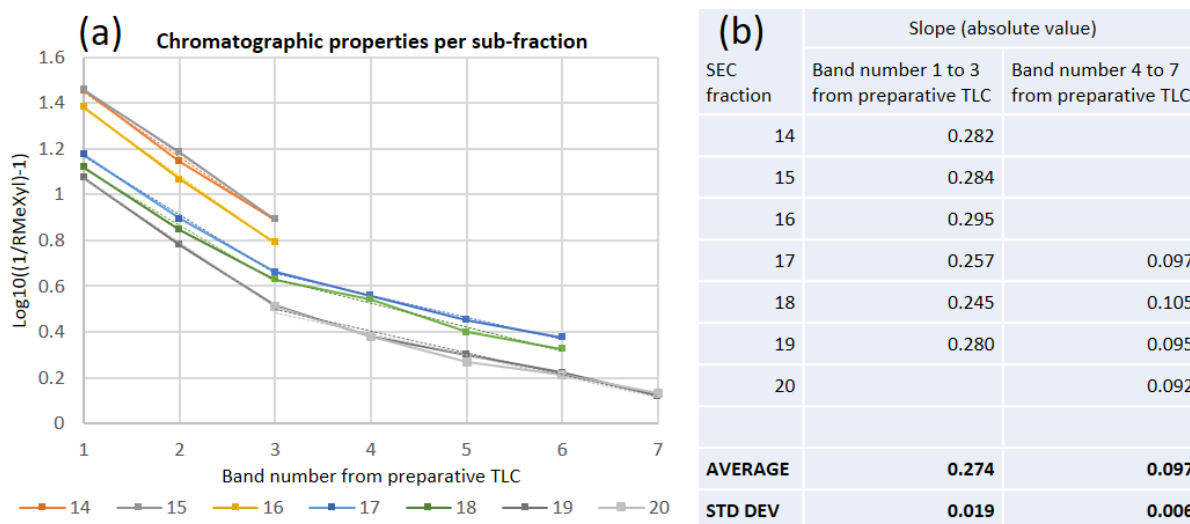


Figure 36: Chromatographic properties of sub-fractions from preparative TLC.

(a): The graph shows the measure of $\log\left(\frac{1}{R_{MeXyl}} - 1\right)$, against the band number from the preparative TLC. The values were measured on the TLC plates from the previous figure. (b): the table shows the slopes obtained by fitting a linear model onto these measures, as well as the average and standard deviation of the absolute values of these slopes for each SEC fraction.

Two different slopes were found: one slope for oligomers 1 to 3 (around 0.27), and one for oligomers 3 to 7 (around 0.1). This could indicate the oligomers 1 to 3 are each one sugar residue (always the same) shorter than the previous one, and that oligomers 3 to 7 also are each one sugar residue shorter than the previous one. As the slope is different for oligomers 1 to 3 and 3 to 7, it is possible that the nature of the sugar residue or of the glycosidic bond is different in each series.

5.5.3. Mild acid lability of the oligomers produced by Driselase-digestion of

Klebsormidium 'pectin'

Oligomer 1 was submitted to mild acid hydrolysis for various amounts of time. As it is the slowest-migrating compound of the series, it was chosen for this study as the most likely to release monomeric sugars (xylose and/or rhamnose) successively, thus displaying the intermediate oligomers produced during acidic degradation. The release of its constituent monomers was measured. If one monomer is released faster than the other one, it might mean that this monomer is usually a non-reducing terminus (a sidechain), thus only needing one hydrolysis event to be released.

The rhamnose release is much superior to the xylose release in the first 2 hours of incubation (Figure 37). However, they are about similar at the end of the incubation, as expected from the total hydrolysis of the oligomer performed earlier (Figure 35). Up until 64 minutes of incubation, only monomers are released, and smaller slow-migrating oligomers appear, very close to compound 1 on TLC. After 128 minutes of incubation, more oligomers are visible, on top of xylose and rhamnose: slow-migrating ones close to compound 1, and

faster migrating ones, appearing on TLC halfway between the GalA and the Gal markers, as well as faster ones migrating in the monomer region. This points towards rhamnose being a terminal residue, maybe forming sidechains on a xylose backbone.

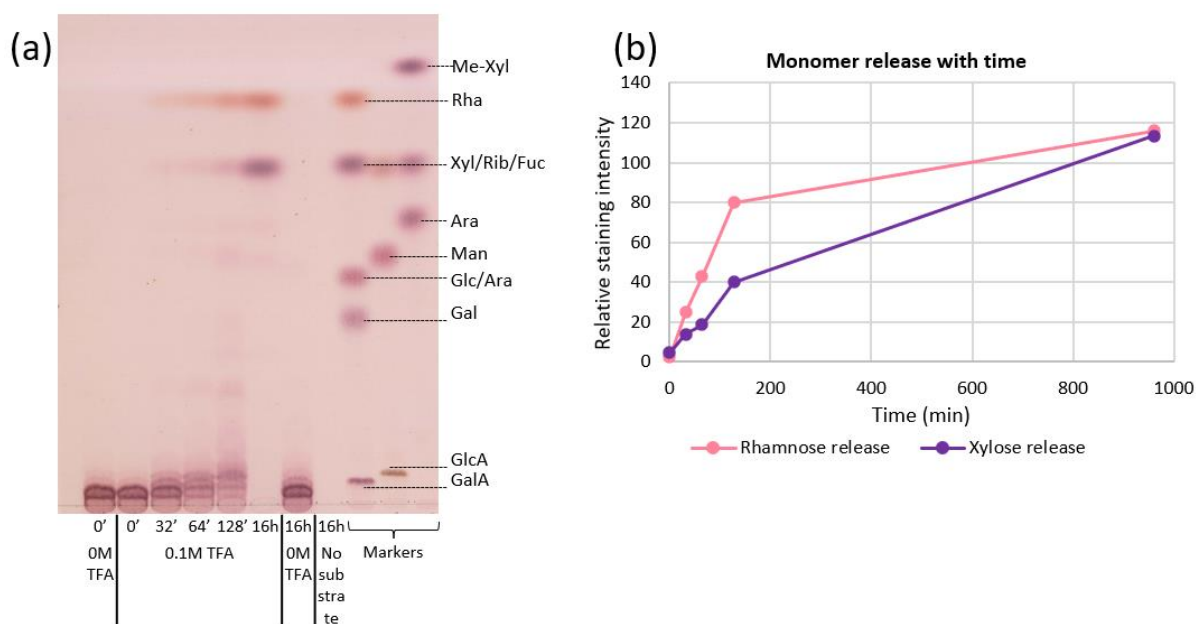


Figure 37: Acid lability of fraction 1 from preparative TLC.

Fraction 1 was submitted to mild acid hydrolysis in 0.1 M TFA at 80°C for successively 0, 32, 64, 128 minutes and 16h (960 minutes). Controls included incubation in the absence of acid, and incubation in the absence of substrate. The resulting TLC is visible in (a). The staining intensity at each stage was measured, relatively to the intensity of the marker (1.5 µg). It was plotted against the incubation duration in (b).

5.5.4. Exo-enzyme tests on the oligomers produced by Driselase-digestion of *Klebsormidium* 'pectin'

Xylose was thus not expected to be a terminal residue in the oligomer 1. Although it would be ideal to assay the efficiency of rhamnosidases, this enzyme was not available. Xylosidases were assayed instead: if the results were negative, it would be one more indication that

rhamnose was indeed a terminal residue. β -xylosidase was assayed on sample 6. As expected, the result was negative.

5.6. Partial acid hydrolysis of *Klebsormidium* 'pectin'

Klebsormidium pectin was hydrolysed with different concentrations of TFA at different temperatures. The goal was to verify how easily it can be broken down, and whether oligosaccharides can be produced by this method.

The concentrations assayed were 0, 0.5, 1 and 2 M TFA, and the temperatures tested were 20, 40, 60, 80, 100 and 120°C for 1 h. The standard hydrolysis procedure is performed with 2 M TFA at 120°C for 1 h. The products of this hydrolysis series are shown in Figure 38.

At 20 and 40°C, nothing was released but some faint traces of arabinose. Arabinose, in its furanose form, is indeed very labile.

At 60°C, traces of arabinose, xylose and rhamnose were visible. Some oligosaccharides were also detectable: they are bands migrating slower than uronic acid monosaccharide markers in BAW 4:1:1. They were also visible in EPAW 6:3:1:1, as bands migrating slightly faster than uronic acid markers. The more concentrated TFA was, the more intense monomers and oligomers bands were. However, at 20, 40 and 60°C, heavy loadings of immobile compounds could be seen at the origin.

At 80°C, all the constituent monomers of *Klebsormidium* pectin could be seen: galactose, glucose, arabinose, xylose, rhamnose and other fast-migrating monomers. Oligomer bands were detectable, in higher amounts than in the 60°C hydrolysates. The intensity of the bands

increased slightly with the concentration of TFA. Bands at the origin were still intense, though less than for lower-temperature hydrolysates. Their intensities decreased as the concentration of TFA increased.

At 100°C, all four samples looked like streaks rather than clear bands. If the constituent monomers of *Klebsormidium* pectin were still detectable, they did not appear more abundant than in the 80°C hydrolysates. The different TFA concentrations did not appear to have much effect: no polysaccharide was hydrolysed without acid, but all the other samples (0.5, 1 and 2 M TFA) were very similar to each other, with the origin band being weakly stained.

At 120°C, finally, no degradation was observed without TFA. The 3 other samples (0.5, 1 and 2 M TFA) were all identical: no immobile polysaccharide was visible at the origin, whilst all the constituent sugars were detectable in the expected proportions: galactose, glucose, mannose (weak staining), arabinose, xylose, rhamnose and traces of fast-migrating sugars.

The conditions for a maximised production of TLC-mobile oligomers were found to be 80°C at 0.5 M TFA.

5.7. Gel permeation chromatography for partially acid hydrolysed *Klebsormidium* 'pectin'

The conditions for an optimised production of oligomers were applied to a bigger quantity of pectin from *Klebsormidium* in order to produce a stock of oligomers.

The hydrolysate was separated by gel permeation chromatography on Bio-Gel P-30, which allows an efficient separation of compounds between 2,500 and 40,000 MW (i.e. oligomers between 13 and 200 units-long).

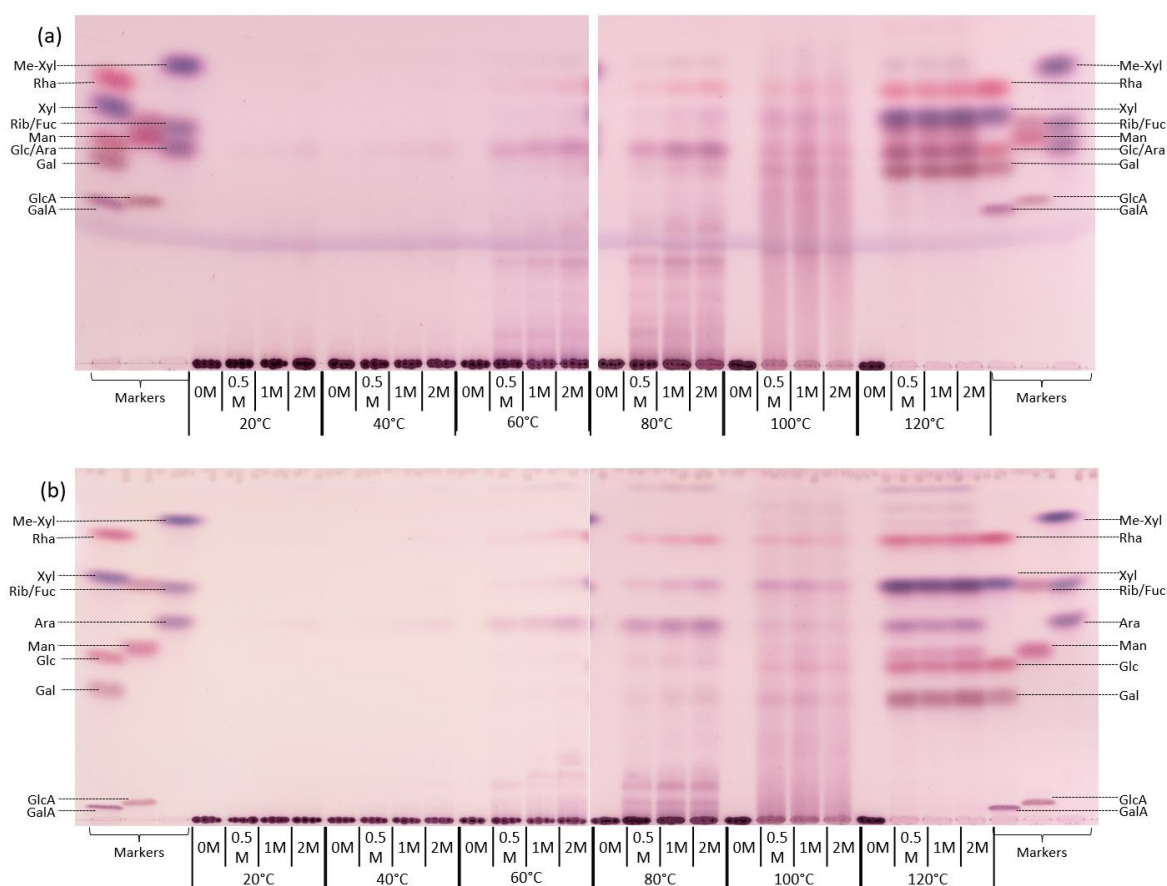


Figure 38: *Klebsormidium pectin* hydrolysis at different acid concentrations and temperatures.

Pectin was hydrolysed in different concentrations of TFA (0-2 M) at 20-120°C for 1 h. The hydrolysates were separated on TLC in two different solvent systems : (a) BAW 4:1:1, (b) EPAW 6:3:1:1.

The abundance of sugars in each fraction was evaluated by thymol-staining a very small portion of each on a TLC plate (without chromatography). The carbohydrate-positive fractions were then run analytically on TLC in order to check their contents (Figure 39 (a)).

Two peaks were clearly visible after separating the hydrolysate on Bio-Gel-P 30: un-

hydrolysed polymers came out in the void volume, around fraction 17, and a mixture of oligomers and monomers came out between fractions 40 and 55. When run individually on TLC, it was clear that compounds from fractions 16-18 were not mobile on TLC.

Monosaccharides were visible in fractions 45 to 55. As expected, the most abundant ones were rhamnose, xylose, arabinose, glucose and galactose.

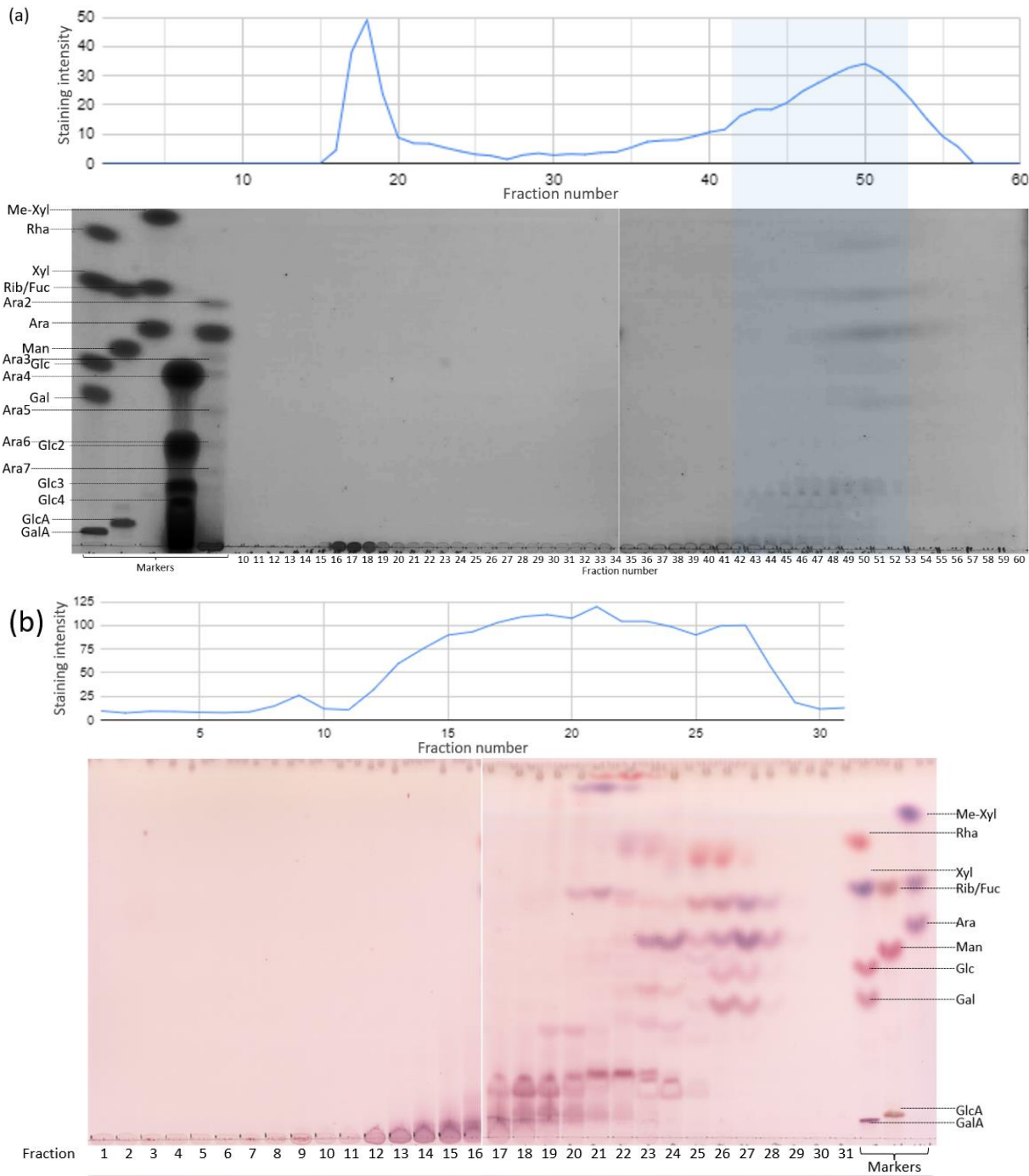
Fractions 43 to 53 seemed to contain the most TLC-mobile oligomers: these fractions were pooled and called F43-53.

F43-53 was separated on Biogel-P-2 (fractionation range between 100 and 2000 MW, i.e. between monomers and 12 units-long oligomers) (McDougall and Fry 1988). The sample was processed (Figure 39 (b)) the same way as previously. A number of monomers were visible in the latest fractions from Bio-Gel P-2: rhamnose, xylose, arabinose, glucose and galactose, as well as the two fast-migrating sugars previously observed in *Klebsormidium* pectin hydrolysates. A range of mobile oligomers was visible between the fractions 17 and 25. Previous fractions contained bigger polymers (unable to move on TLC). Fractions 17 to 27 were thus selected to be analysed.

They were run on glass-backed TLC : fractions 17 to 19 were developed three times in BAW 4:1:1, fractions 20 to 27 twice in the same solvent system.

Initially, the plates were transiently stained with iodine. This allowed for the detection and isolation of a number of compounds. However, this technique later on proved to be unreliable and erratic. Instead, the compounds were eluted off the plate as 1-cm-wide strips. Only the first 10 cm of the plate contained sugars. This gave a total of 70 sub-fractions (10 for each SEC-fraction).

As previously, the fractions were pooled by their similar chromatographic properties. Three main samples were produced: 4, 5 and 6 (Figure 40). A portion of each was hydrolysed completely and all three gave similar results: they are all made of galactose and xylose residues.



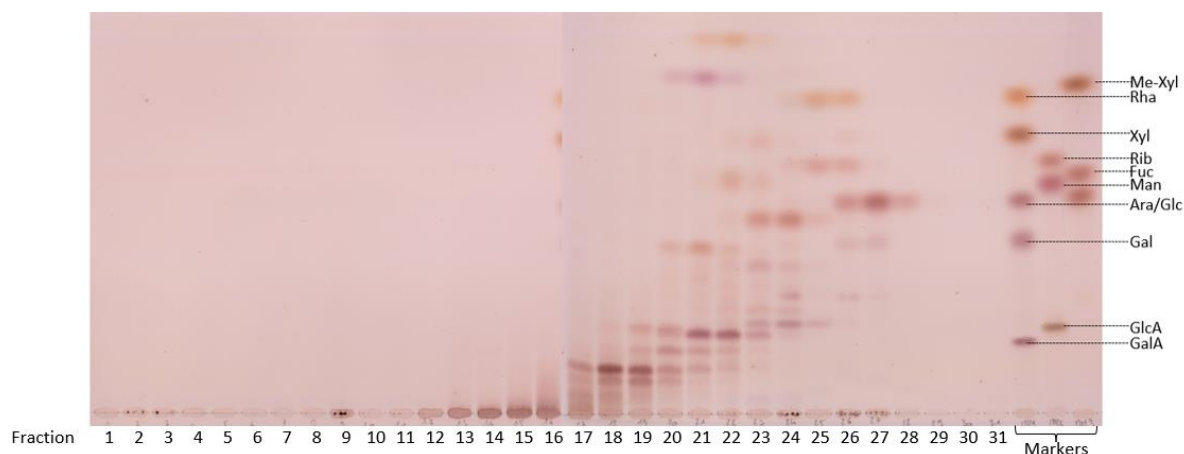
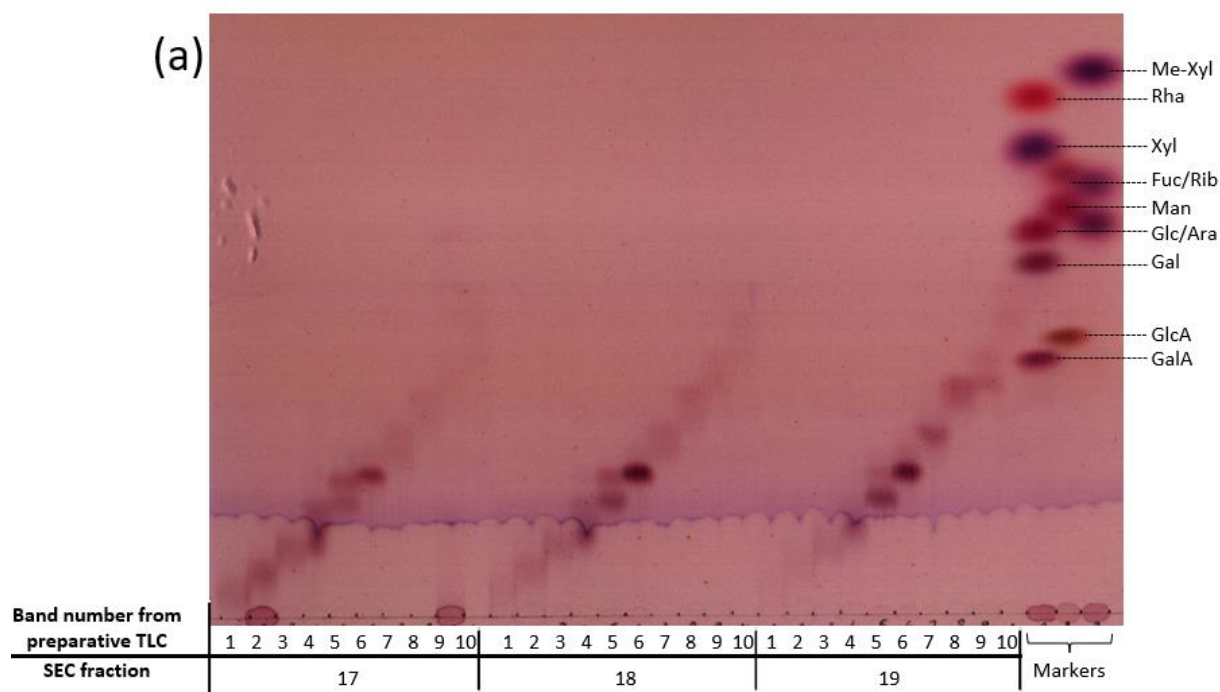


Figure 39 : Separation of *Klebsormidium* pectin hydrolysate (80°C, 0.5 M TFA) by gel permeation chromatography

(a) shows the separation of the pectin hydrolysate on Bio-Gel P-30. The top graph shows the intensity of staining of each of the fractions, when a dot was applied onto a TLC plate and it was stained thymol without chromatography. The TLC plate at the bottom shows the fractions run individually on TLC, in BAW 4:1:1. The area highlighted in blue includes fractions 43 to 53: these fractions were pooled to make sample F43-53. (b) shows the separation of F43-53 on Bio-Gel P-2. The top graph shows the intensity of staining of each of the fractions, as previously. The TLC plates show the fractions run individually on TLC. The top one was developed in EPAW 6:3:1:1, the bottom one in BAW 4:1:1.



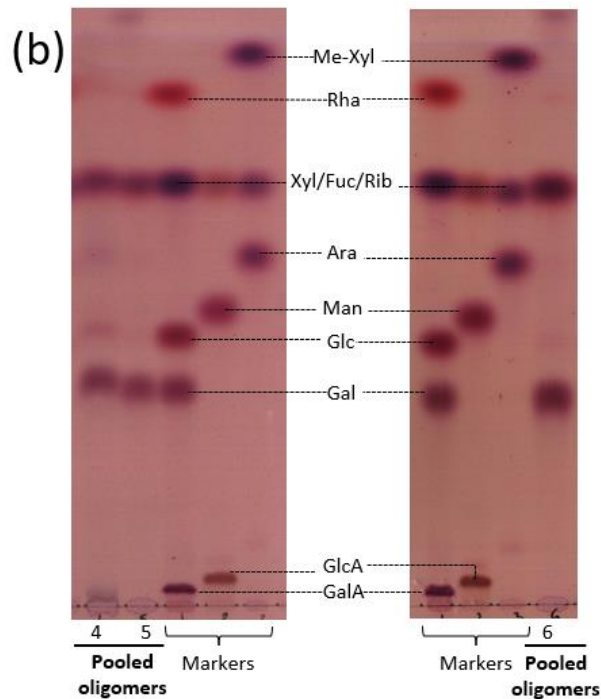


Figure 40: SEC-fractions from partially hydrolysed *Klebsormidium* pectin separated on preparative TLC, and their monomer composition revealed.

(a) shows each of the 10 sub-fractions obtained from the separation by preparative TLC of the SEC-fractions 17, 18 and 19. (b): sub-fractions 4, 5 and 6 from all three sub-fractions were pooled and submitted to complete acid hydrolysis.

(a) was developed twice in BAW 4:1:1, (b) was developed twice in EPAW 6:3:1:1.

5.7.1. Exo-enzymes assay on oligomers produced by partial hydrolysis of

Klebsormidium 'pectin'

In order to know the non-reducing terminal residue(s) of the smallest oligomer available, exo-enzymes assays were performed. β -xylosidase, as well as α and β -galactosidase were tested on sample 6 (Figure 41). All three results were negative, which led us to think that the terminal residue may be α -xylosyl.

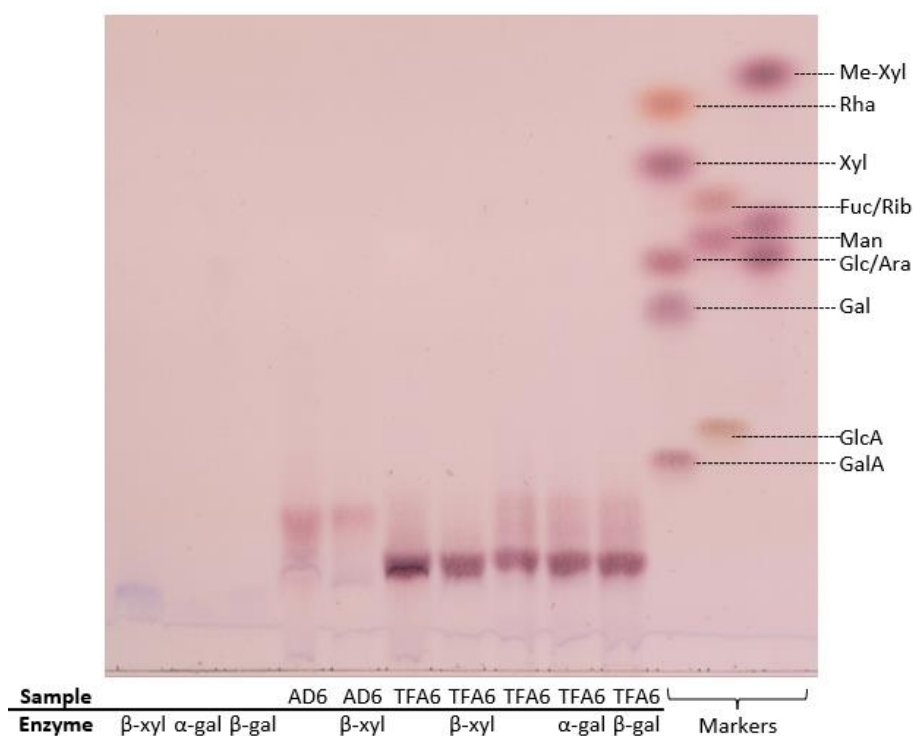


Figure 41: Exo-enzyme assays on oligomers produced by enzymatic and acidic breakdown of *Klebsormidium* 'pectin'.

Sub-fraction 6 from Driselase-treated pectin (AD6 on the figure) was assayed against β -xylosidase (β -Xyl), yielding negative results. Sub-fraction 6 from partially hydrolysed pectin (TFA6 on the figure) was assayed against β -xylosidase, α and β -galactosidase (' α -gal', ' β -gal'). Controls included incubation of enzymes without substrate, and incubation of the substrates in buffer, without the corresponding enzymes. The TLC plate was developed in BAW 4:1:1.

5.8. Reductive radioactive labelling of reducing termini of the oligomers extracted from *Klebsormidium* 'pectin'

Oligosaccharides released from the digestion of P2 with Driselase (after amylase), as well as oligosaccharides released from partial acid hydrolysis, were examined for the nature of their reducing termini. From previous work in this chapter, extracts 1 to 10 from amylase/Driselase treated P2 (written AD1 to AD10 in this paragraph) are thought to be a series of xylorhamno-oligomers

. Extracts 4 and 5 from partially hydrolysed pectin (TFA4 and TFA5 in this paragraph) contain galactose and xylose, and are probably oligomers from the same polysaccharide. These twelve extracts were submitted to borohydride reduction in order to radiolabel the reducing terminus, alongside lactose as a control (expected to yield [³H]glucitol). A range of monomers was radiolabelled first, allowing for the construction of a library of [³H]alditol markers (see 2.2.1.2 for the experimental method).

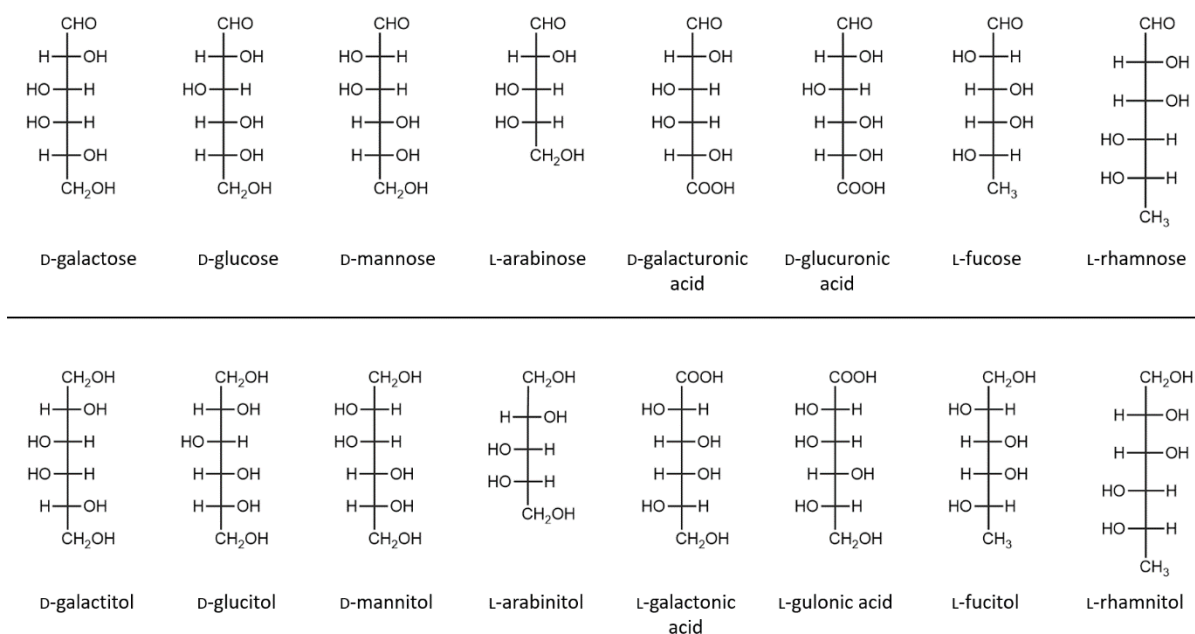


Figure 42: Structures of sugars and their sodium-borohydride-reduced counterparts.
 The top row shows the sugars that were chosen to be reduced with tritiated borohydride.
 The bottom row shows their final structure after reduction.

5.8.1. Sugar monomers radiolabelling

Galacturonic acid, glucuronic acid, galactose, glucose, mannose, arabinose, fucose, and rhamnose were submitted to reduction by radioactive sodium borohydride. The expected final structures are drawn in Figure 42. The alditols were separated twice on preparative TLC in two different solvent systems, in order to ensure purification (Figure 43). They were then

pooled into three groups to make three mixtures of reference: L-galactonic acid, D-galactitol and L-rhamnitol (from D-GalA, D-Gal and L-Rha), L-gulonic acid, D-mannitol, L-fucitol (from D-GlcA, D-Man, and L-Fuc), and D-glucitol and L-arabinitol (from D-Glc and L-Ara).

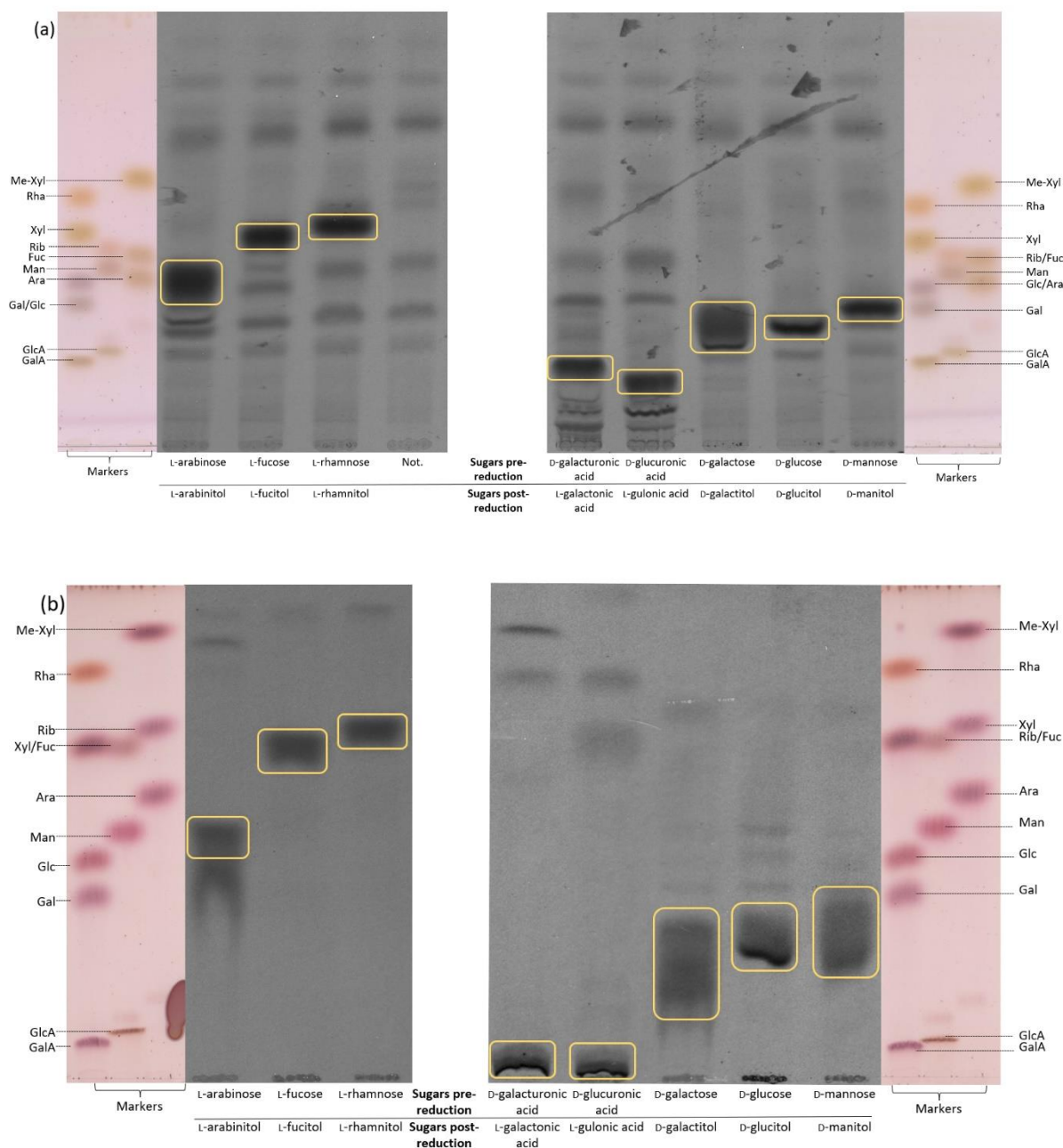


Figure 43: Preparation of $\text{NaB}[\text{}^3\text{H}]_4$ -reduced monosaccharides.

(a): Preparative TLC of $\text{NaB}[\text{}^3\text{H}]_4$ -reduced monosaccharides. The compounds ringed in yellow were eluted off the plate. (b): The compounds previously eluted were separated a second time on TLC (also ringed in yellow). (a) were run once in BAW 4/1/1 on plastic-backed TLC, scanned after four days of exposure. (b) were run twice in EPAW 6/3/1/1 on plastic-backed TLC and scanned after three days of exposure.

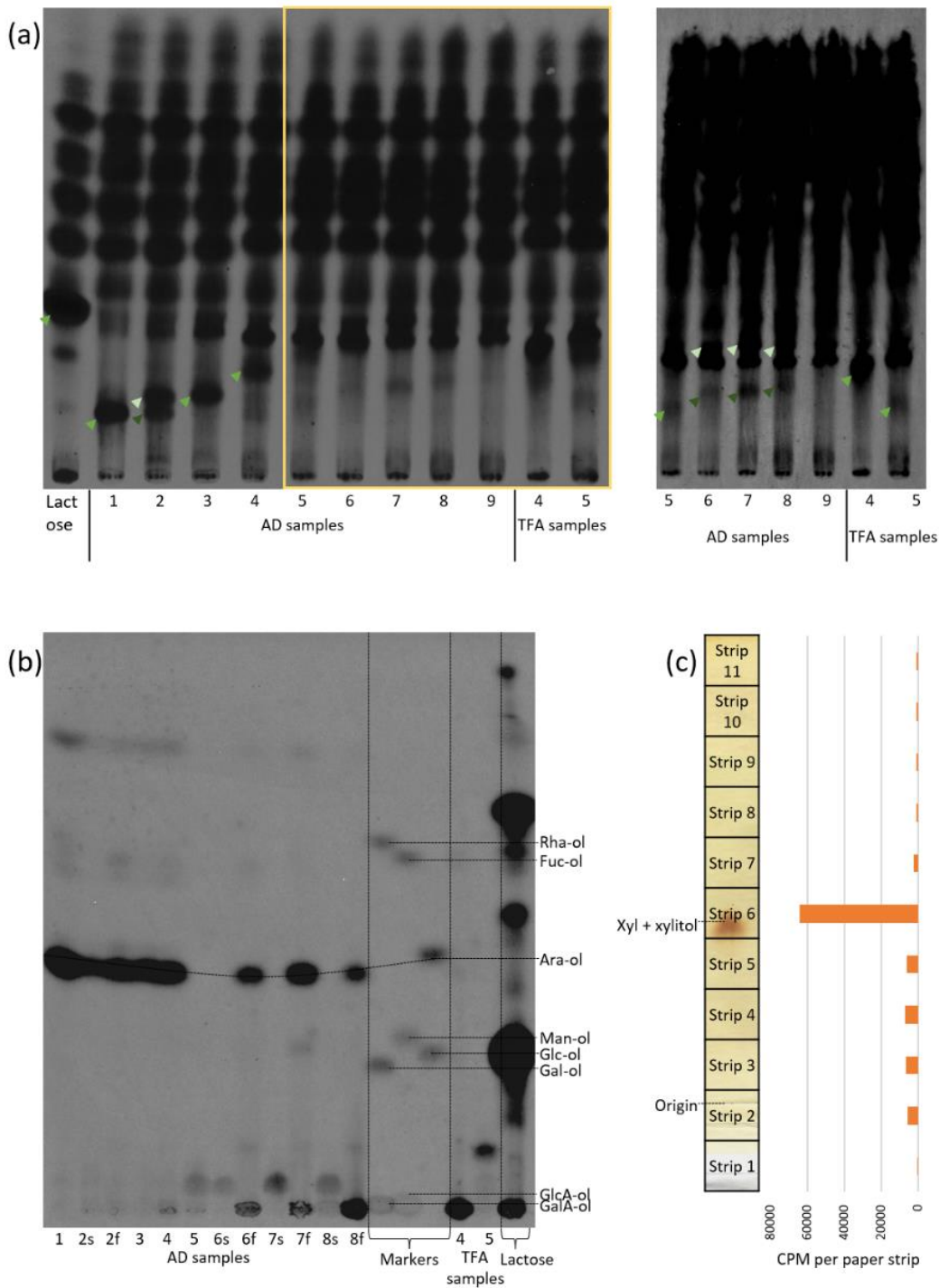


Figure 44: Purification and hydrolysis of $\text{NaB}[\text{}^3\text{H}]_4$ -reduced oligosaccharides extracted from *Klebsormidium* 'pectin'.

(a): Separation of $\text{NaB}[\text{}^3\text{H}]_4$ -reduced oligosaccharides from *Klebsormidium* and $\text{NaB}[\text{}^3\text{H}]_4$ -reduced lactose on TLC. The plate on the left was run once in BAW 211. The right half of the plate (circled in yellow) was re-run in EPAW 6311. The compounds with the green pointers were eluted off the plate. For the sample with a pale and a dark green pointer, the eluates were respectively called 'f' and 's'. (b): the eluates were TFA-hydrolysed and separated on TLC. (c): As a control experiment, Xyl was $\text{NaB}[\text{}^3\text{H}]_4$ -reduced and run on PC (BAW 12:3:5). The paper was stained, cut in 11 strips and the radioactivity in each strip was counted.

5.8.2. Sample radiolabelling

The extracts AD1 to 10, TFA4 and TFA5 were purified on TLC in the same way after sodium borohydride treatment, alongside lactose and xylose as controls (Figure 44).

Reduced xylose was run on paper chromatography. It was stained with Wilson's dip and the radioactivity in 5-cm wide paper strips was counted (Figure 44 (c)). Xyl and xylitol co-migrate in the chosen solvent system. Thus, seeing a radioactivity peak and a coloured band (which only Xyl cannot produce, since it is a reducing sugar, and xylitol is not) co-migrating confirmed that the radioactive reduction effectively happened. It was however, not complete, as the Xyl spot was visible. This was expected given the ratios of tritium to Xyl used for the reduction.

Both the reduced algal oligosaccharides and the lactose were separated preparatively on TLC (Figure 44 (a)). All samples were heavily contaminated with other products of reductive radiolabelling. However, unique bands could be recognised in reduced lactose, and AD1 to 5. In AD2, two bands were visible, which is possibly due to contaminations from AD1. The second half of the plate was re-run in another solvent system, so that the different bands appeared separated from the rest. It was this time possible to extract bands in AD 5 to 8, and in TFA 4 and 5. However, unique bands were undistinguishable in AD9 and this sample had to be discarded. Double bands were visible in AD6, 7, and 8, possible also due to some cross-contamination of the samples (originating during the elution off the preparative TLC plate).

The oligosaccharides were then hydrolysed to their constituent monomers and separated on TLC (Figure 44 (b)). When fluorographed, the radiolabelled sugar was visible and could be identified by comparison with the sugars from the [³H]alditol library.

Lactose clearly released a large amount of glucitol, which confirmed that the method was working. However, the sample was heavily contaminated with other radioactive compounds. AD1, 2s, 2f, 3, 4, 6f, 7f, and 8f all released a very visible arabinitol band. This was surprising, as they were mainly thought to contain Xyl and Rha. The other AD samples, AD5, 6s, 7s, and 8s only released faint, slowly migrating bands that could not be clearly identified. TFA4 and 5 did not release any identifiable bands either.

5.9. Conclusion

The absence of uronic acids in the *Klebsormidium* pectic extracts sparked some interest into elucidating their chemical structure and properties, as they are both unique and unknown.

The study of *Klebsormidium* 'pectin' started with a study of its extractability. It was obvious that it made no difference whether the buffer used was chelating or not, as the most effective one between oxalate, acetate and formate was the latest, which also happened to be the smallest and the most electronegative one. The extraction needs to be conducted at boiling temperature to be efficient, and the lower the pH, the higher the yield.

In a second time, the susceptibility of *Klebsormidium* P2 to land-plant hydrolases was evaluated. No sugar was released upon the actions of RG-I-specific galactanase, mannanase, lichenase, β -xylosidase, nor β -galactosidase (also RG-I-specific). However, RG-I-specific arabinanase and xylanase, as well as α -galactosidase, yielded small digestion products.

When submitted to Driselase digestion, *Klebsormidium* P2 released a series of monomers

(Gal, Glc, Ara, Xyl) and purple-staining (with thymol) oligomers, indicating the presence of pentoses.

A series of seven oligomers was prepared from the Driselase hydrolysate of de-starched *Klebsormidium* P2, all containing Xyl and Rha residues in similar amounts, and forming two series of oligomers. In each series, the next oligomer is smaller from the previous one by one sugar residue. The mild acid hydrolysis of the biggest oligomer showed that Rha are present as sidechains of a Xyl backbone.

Third, the susceptibility of *Klebsormidium* P2 to acid hydrolysis (TFA) was evaluated.

Arabinose was always found in the hydrolysates, even at low temperatures (20 and 40°C) and low acid concentrations, showing that it must be present as a labile sidechain in the polymer. At 60°C, Xyl and Rha were also released, alongside a range of oligomers: it could be that the compounds previously studied form labile sidechain attached to a more acid-resistant backbone. At 80°C, all the expected monomers (Gal, Glc, Ara, Xyl, Rha) were released, on top of distinct series of oligomers. The hydrolysis process was amplified up to complete hydrolysis at 100 and 120°C. Hydrolysing *Klebsormidium* P2 for 1h with 0.5 M at 80°C was found to produce the most oligomers. The products from this treatment were separated by gel-permeation chromatography, producing a series of 3 well-defined oligomers made of Gal and Xyl, and susceptible to neither galactosidase (α and β) nor to β -xylosidase. These oligomers could be part of the previously mentioned backbone of the 'pectic' polymer from *Klebsormidium*, or could representative of a second set of sidechains attached to a non-defined backbone.

6. Land-plant-like polymers in
charophytic algae

6.1. Introduction

A range of charophytic green algae were selected for this study, which aimed at detecting possible land-plant-like cell wall polymers. Zygnematalean algae were considered the most likely to contain such polymers, as they are the latest-diverging charophytic class. Four algae of this clade were investigated: *Spirogyra varians*, *Mesotaenium caldera*, *Zygnema circumcarinatum*, and *Netrium digitus*. Moreover, amongst these algae, two (*Mesotaenium* and *Netrium*) have been shown to contain a xyloglucan-like polysaccharide (Mikkelsen *et al.* 2021). Other late diverging charophytes, which had been studied in previous chapters, were also included: *Chara vulgaris* and *Coleochaete scutata*. Indeed, it has been previously shown in this laboratory that *Chara* contains an RG-II-like polymer. Finally, a series of early-diverging charophytes were also featured in the study, as controls: three species of *Klebsormidium* (*K. subtile*, *K. nitens*, and *K. fluitans*) and the outlier *Chlorokybus atmophyticus*.

All these algae were radiolabelled with sodium [¹⁴C]carbonate, so that we obtained radioactive biomass. The increased sensitivity due to the radioactivity should facilitate the detection of compounds by decreasing the limit of detection. The study was divided into two main parts.

The first aimed at isolating, by enzymatic means, xyloglucan-like polymers from algal cell walls. The second part of the study focused on the detection and characterization of land-plant-like RG-II in *Chara*, also based on enzymatic methods.

6.2. Live radiolabelling: Measurements

Selected algae were from 2-week-old cultures. They were radiolabelled *in vivo*, by being allowed to grow for 5 days in culture medium containing 1.0 or 1.5 MBq NaH¹⁴CO₃ (specific activity 2.31 MBq/μmol). This was followed by two days of incubation in total darkness, designed to consume [¹⁴C]starch.

6.2.1. Radioactivity in ethanolic extracts

Once the live radiolabelling was complete, the algae were washed several times: once in acidified ethanol (supernatant 1), thrice in ethanol (supernatants 2, 3 and 4) and once in acetone (supernatant A). A series of algal alcohol-insoluble residues (AIRs) was produced, containing all water- and ethanol-inextractable plant polymers, and amongst them all cell wall polysaccharides.

The amount of radioactivity released by each rinsing is visible on in Figure 45 (a): the initial ethanolic wash (supernatant 1) produced between 900 and 200 kBq for each species. The next three ethanolic rinsings contained less and less radioactivity. The final acetone rinsing (Supernatant A) was more radioactive than the previous ones, as acetone might have been able to break the last few remaining intact organelles and to extract algal lipids.

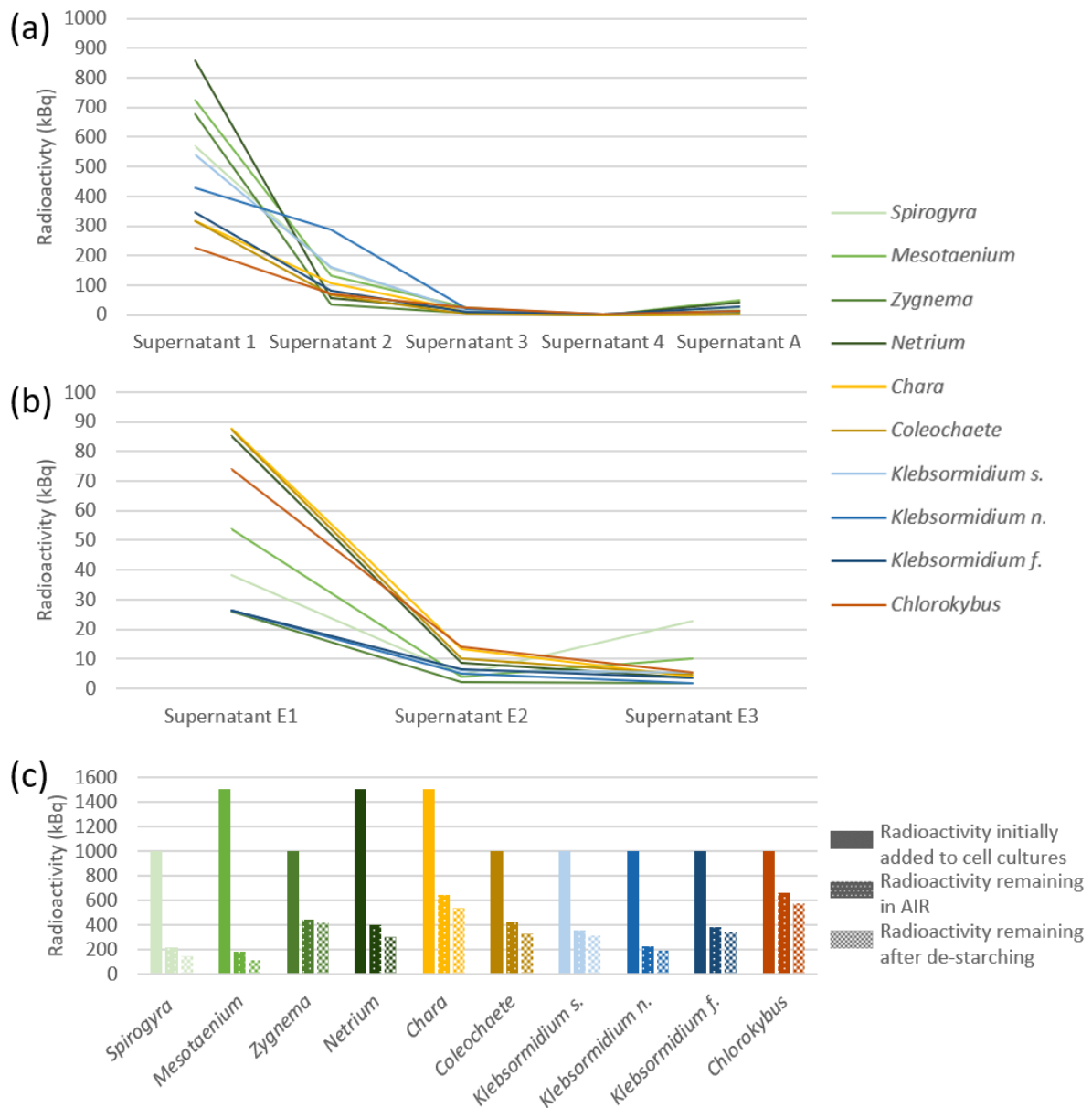


Figure 45: Radioactivity released during AIR preparation and de-starching of radiolabelled algae.

(a): for each algal species (key on the right), the amount of radioactivity released in each successive wash during AIR preparation is shown (Supernatant 1 was an acidified ethanolic rinsing, 2 to 4 were ethanolic rinsings, Supernatant A was the final acetone rinsing). (b): for each alga, the amount of radioactivity released in each wash after amylase digestion is shown. All three rinsings E1 to E3 were in 70% ethanol. (c): for each alga, the amount of initially added radioactivity is shown (plain colour), followed by the radioactivity calculated to be remaining after all five ethanolic and acetone washes (dot pattern), and the radioactivity remaining after de-starching (check pattern).

6.2.2. Radioactivity in amylase-solubilised fractions

The radiolabelled AIR was then digested with salivary amylase, and rinsed thrice with 70% ethanol, giving supernatants E1, E2 and E3. This operation aimed at solubilising and rinsing out any starch present in the residue, which would produce strong glucose bands (unrelated to cell wall components) during later analysis.

The decreasing amount of released radioactivity is visible in Figure 45 (b). For most algae, apart from *Spirogyra* and *Mesotaenium*, the supernatants were less and less radioactive. On average, E1 contained 10 times the radioactivity in E2, and E3 contained negligible amounts of radioactivity.

Figure 45 (c) summarizes these preparations steps, by showing the radioactivity added to the cultures (1,000 to 1,500 kBq), the radioactivity calculated to be remaining after AIR preparation, and the radioactivity calculated to be remaining after de-starching.

6.3. XEG digestion

6.3.1. Amounts of radioactivity extracted by XEG

XEG, or xyloglucan-specific endo-glucanase, is an enzyme capable of splitting specifically glycosidic bonds between glucosyl residues in land plant xyloglucan. By doing so, it classically releases, when applied to land plant hemicellulosic polymers, diagnostic oligomers such as the suite XXXG, XLG, XXFG and (in some cases) XLLG. Its action on algal AIR was characterised.

First, the de-starched biomass was incubated with buffer. Plant polymers were re-precipitated by the addition of acidified ethanol, and the sample was centrifuged, thus producing the supernatant B1 on the one hand and the remaining AIR on the other.

The AIR was completely dried. This process was then repeated 5 times with XEG present in the buffer, producing supernatants XEG1, XEG2, XEG3, XEG4 and XEG5.

The amount of radioactivity solubilised in acidified ethanol each time, as a percentage of the initial radioactivity in de-starched AIR, is shown in Figure 46 (a).

For all studied species, only a low proportion of the total radioactivity was extracted by XEG. The most highly radioactive fraction was B1 from *Mesotaenium* and culminated around 5.5%. Zygnematalean algae (*Spirogyra*, *Mesotaenium*, *Zygnema* and *Netrium*) were the ones that released the most radioactivity. All the other groups released similarly low quantities of ethanol-soluble compounds.

In all algae except for *Chara* and *K. subtilis*, the initial buffer rinse was the most radioactive. The extracts XEG1 to 5 (all incubated for the same duration) seemed to contain random amounts of radioactivity, as no trend was observable.

6.3.2. Analysis of XEG-solubilised oligomers

After having been quantified, the XEG-solubilised fractions from charophytic algae were examined in order to detect possible signature oligomers.

XEG1 was separated on TLC and autoradiographed (Figure 47 (a)). The plate was also scanned in order to get a clearer picture of the radioactivity profile for each extract (Figure 47 (b)).

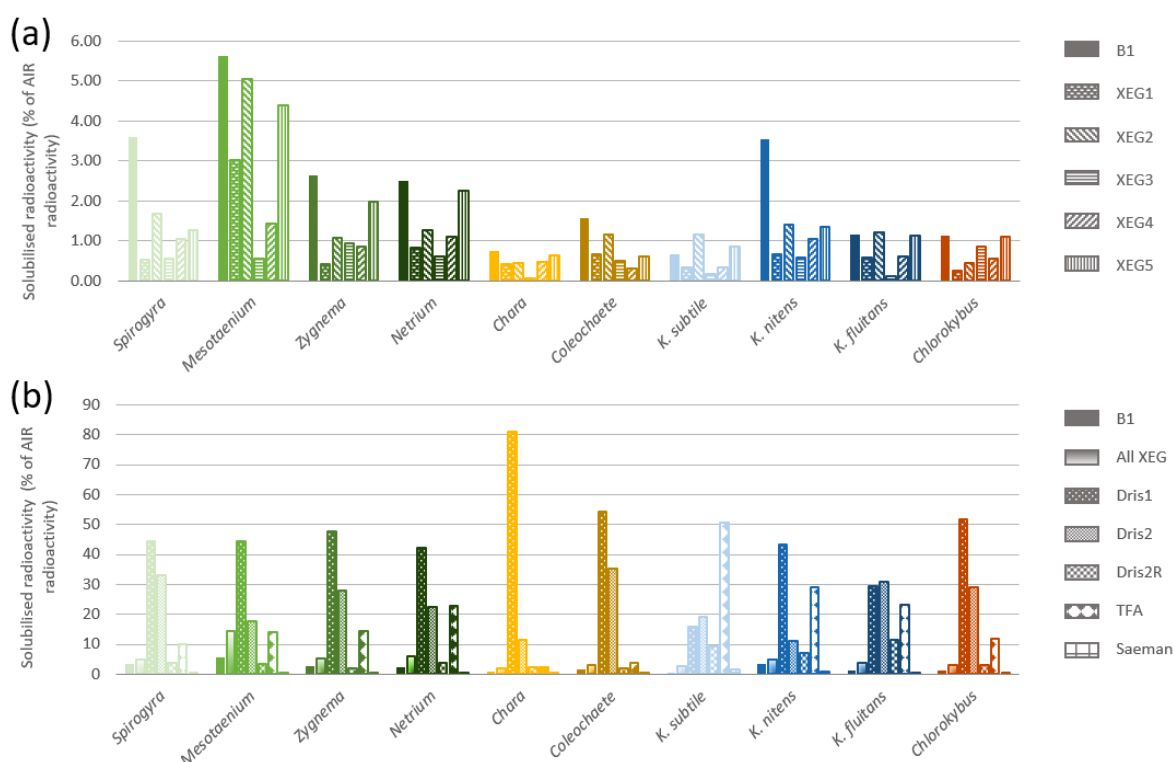


Figure 46: Radioactivity released by XEG digestion of algal AIRs.

(a): the proportion of radioactivity solubilised in each fraction by a buffer wash and XEG enzyme (B1, XEG1 to 5) for each alga per initial AIR is shown. B1 was produced by incubating algal AIR in buffer for 16h, adding acidified ethanol to 75% (0.5% v/v formic acid) and prolonging the incubation for 72 h. The sample was centrifuged at 18 g for 10 minutes, and the supernatant B1 was taken out. The remaining solid residue was dried under the fume hood for 48 h. The process was repeated with XEG-containing buffer, producing the supernatants XEG1 to XEG5. (b): the proportion of radioactivity (per initial AIR) solubilised in each fraction by buffer, enzyme digestion or acid hydrolysis is shown for each alga (B1, cumulated XEG1 to 5, Driselase as Dris1 and Dris2, buffer rinse as Dris2R, TFA and Saeman as acid hydrolysates).

All algae tested gave a major spot of chromatographically immobile, ^{14}C -labelled XEG digestion products, seen at the origin of the TLC (ringed with pale pink ovals in Figure 47 (a)). This material had evidently been produced from the insoluble algal polysaccharides by XEG digestion, yielding oligosaccharide products that were soluble in 70% ethanol (thus also water-soluble) but too large to migrate in the TLC solvent employed. All algae tested also gave several chromatographically mobile, ^{14}C -labelled XEG digestion products, potentially xyloglucan-derived fragments. These fragments varied between algal species; however, two spots were similar or identical in all ten species (ringed with pale blue ovals in Figure 47 (a)). Thus, in all cases a similar band was generated that migrated $\sim 0.6\text{--}0.8$ cm from the origin — considerably slower than the authentic nonasaccharide, XLLG (which migrated 2.5 cm), and thus potentially a large oligosaccharide(s) e.g. based on the tetradecasaccharide XXXGXXXG. An additional common product migrated to about 2.2 cm, only slightly slower than XLLG. Most of the algae produced a spot of [^{14}C]glucose (not ringed in Figure 47 (a)), especially abundant in *Chara*. Indeed, the XEG enzyme used was not completely pure, having shown, amongst others, laminarinase and amylase side-activities. By-products reported previously have included the monosaccharides glucose and galactose and short glucose oligosaccharides, but not large oligosaccharides, so the present observations are compatible with the existence of xyloglucan-related polysaccharides that are digestible by XEG but relatively resistant to hydrolysis to the products (hepta- to nonasaccharides) familiar from land-plant hemicelluloses.

Besides these common products, each alga – apart from the Zygnematalean *Spirogyra* - gave one or more additional radioactive spots, the most prominent of which are ringed in yellow in Figure 47 (a) and described in the following. Many of the algae gave spots that ran close to the positions of XLLG and XXLG (but not fully resolved from GalA, and thus of unspecified

nature), including *Zygnema*, *Netrium*, *Chara*, *Coleochaete*, *K. subtilis*, *K. fluitans* and *Chlorokybus*.

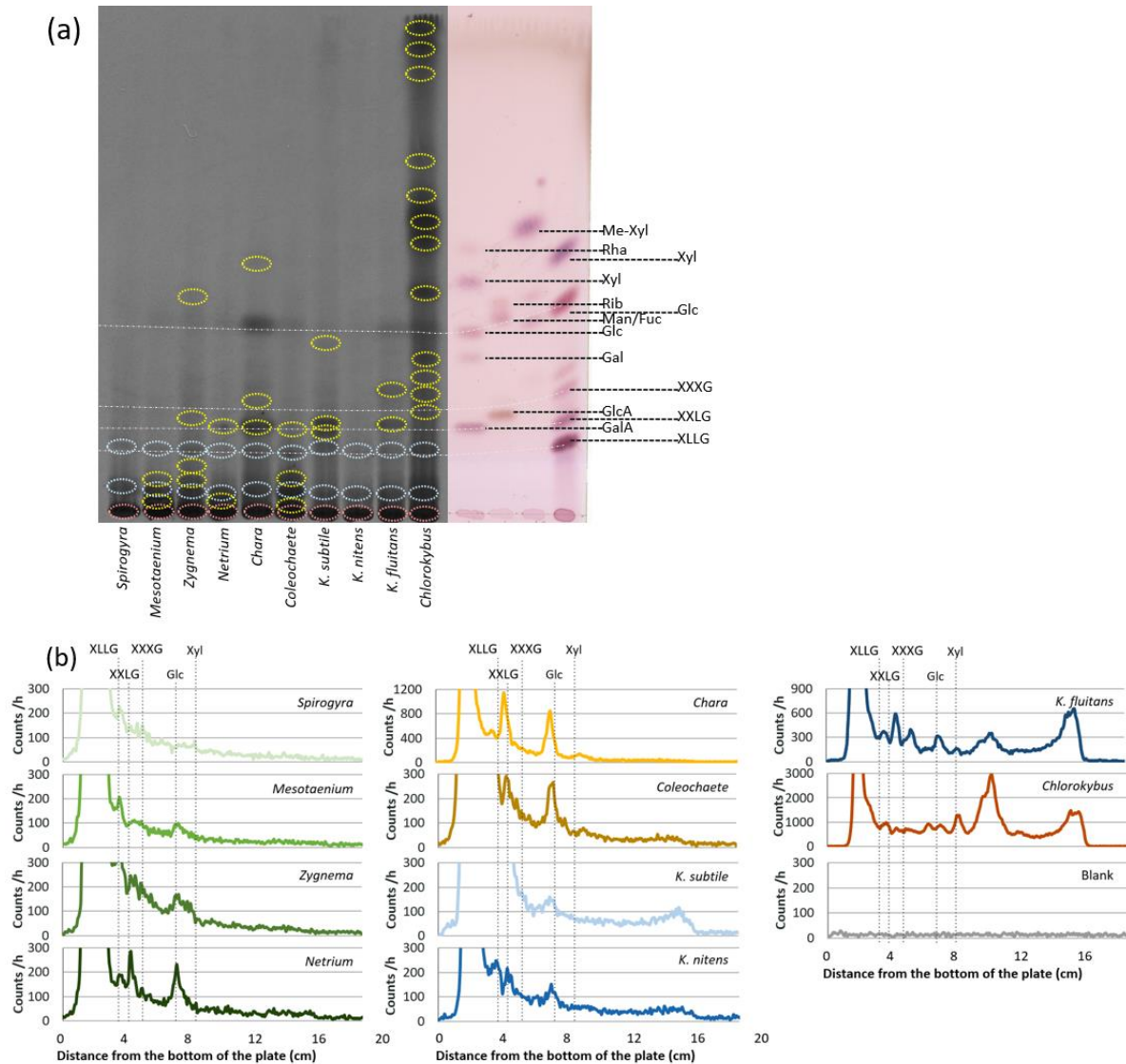


Figure 47: Separation of compounds in XEG1 extract.

XEG1 extracts were separated on plastic-backed TLC once in BAW 2:1:1. The additional markers XXXG, XXLG and XLLG are land plant xyloglucan-specific oligosaccharides. (a): autoradiography of the TLC plate after 1-week exposure. (b): radioactivity profile of each track of the above TLC plate.

Mesotaenium gave two products migrating very close to the origin, which could be variations on the potential tetradecasaccharide-based compound ringed with a blue pale oval. Other Zygnemataleans, *Zygnema* and *Netrium*, gave similar products. They also released XXLG-like oligomers, and *Zygnema* produced, in addition, a fast-migrating compound that might be similar to xylose. Interestingly, *Coleochaete* produced a similar pattern, with one band slower and one band faster than the potential tetradecasaccharide-based compound, and a smaller oligomer co-migrating with XXLG. *Chara* did not release any of the heavier oligomers previously described. However, the alga produced two interesting oligomers, one co-migrating with XXLG, and the other one slightly faster than XXXG. All three *Klebsormidium* species were fairly different from each other. *K. subtile* produced two XXLG-like oligomers, as well as a smaller compound running close to Glc and Gal. *K. nitens* did not release any new product, other than the previously described oligomers. Finally, *K. fluitans* released an XXLG-like oligomer, as well as a slightly smaller oligomer that could be a pentasaccharide. *Chlorokybus* produced at least 16 discrete products, many of them migrating faster than glucose and thus evidently small, hydrophobic compounds; these were unexpected and remain unidentified, but could possibly include acetyl esters or methyl ethers of oligosaccharides. Small oligomers could include glucose oligomers, as described in the hemicellulosic fraction of the alga (Section 7.3 *Ulva* hemicellulosic extract Hb: characterizing phyco-xyloglucan).

This analysis makes it difficult to discriminate between the algal species, as they all produced bands that can be attributed to xyloglucan-like oligomers. However, trends could be observed in particular in the similar profiles shared by the Zygnemataleans and *Coleochaete* – all late-diverging charophytes.

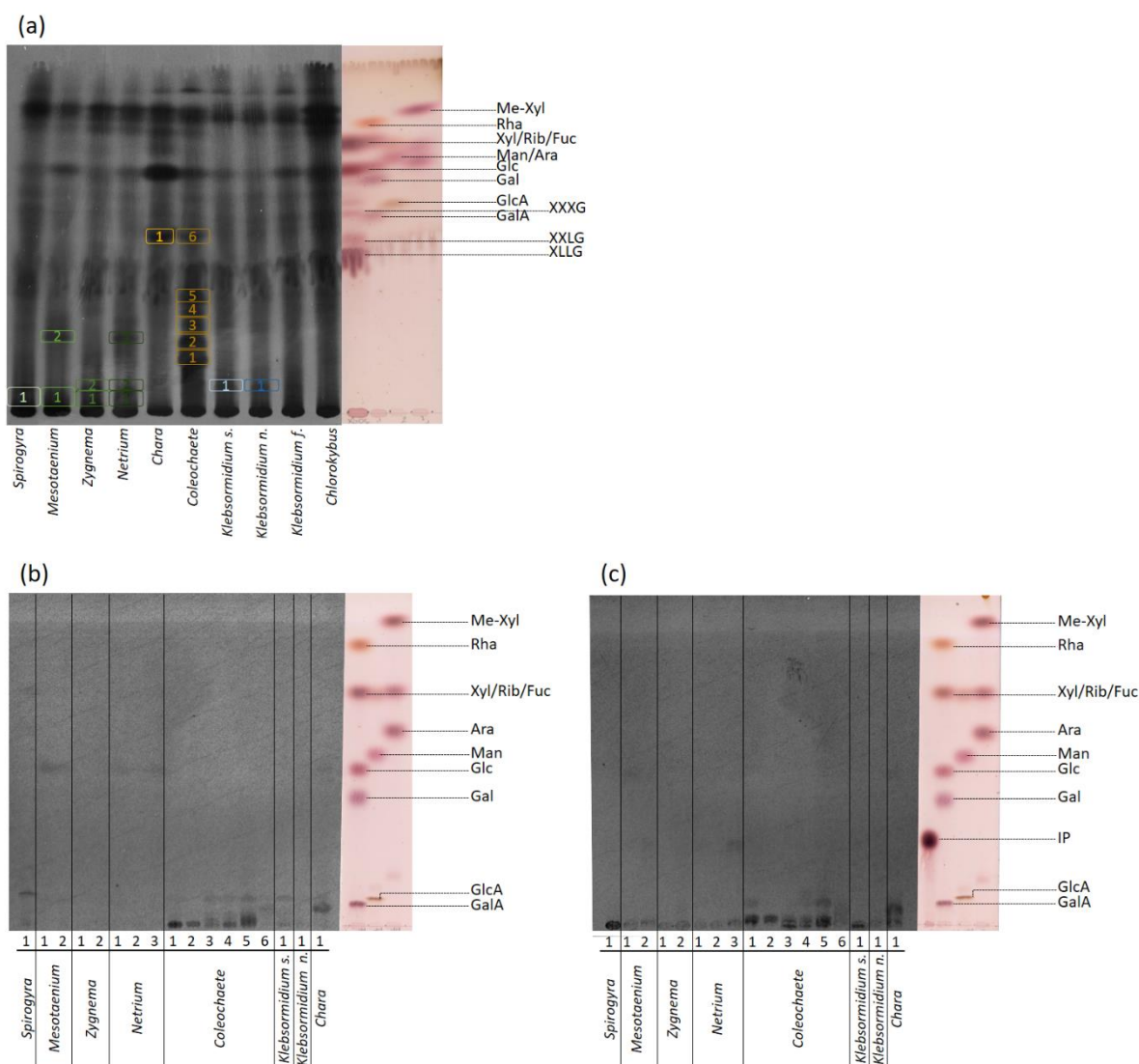


Figure 48: Separation and hydrolysis of compounds in XEG2 to 5.

XEG2, 3, 4, and 5 have been pooled together. (a): Separation of the crude pooled extracts by TLC. The bands in the coloured rectangles were eluted and analysed further. The TLC plate was developed once in BAW 2:1:1 and autoradiographed. (b): The extracts from the above plate were hydrolysed with TFA, and the hydrolysates separated on TLC. The TLC plate was developed twice in EPAW 6:3:1:1 and autoradiographed. (c): The extracts from the plate in (a) were incubated with Driselase, and the digests separated on TLC. The TLC plate was developed twice in EPAW 6:3:1:1 and autoradiographed

XEG1 was only faintly radioactive, thus making the analysis of the TLC plate difficult. To overcome this, the next four XEG digests, XEG2 to 5, were pooled and run on TLC (Figure 48 (a)). The solvent system was nominally the same, however the markers ran differently than previously. After the plate had been autoradiographed, selected compounds (ringed in colour on Figure 48) were eluted and analysed individually. They were either acid-hydrolysed

with TFA (Figure 48 (b)) or Driselase-digested (Figure 48 (c)), allowing for the identification of their constituent monomers and potentially the Driselase-resistant, xyloglucan-specific disaccharide, isoprimeverose. This analysis only worked for a few sugars, as the low radioactivity continued to be a strong limitation. All algae displayed variably strong glucose signals, as well as a heavy spot at the origin and a slightly smeared spot that approximately co-migrated with XLLG. As for XEG1, the glucose spots were attributed to the side-activities of XEG (amongst which amylase and laminarinase). The heavy origin-bound spots were oligomers small enough to be soluble in 70% ethanol, but too big to be mobile on TLC in the solvent system employed. The smeared spots that co-migrated with XLLG were, this time, clearly distinct from the GalA marker, thus taking out the possibility of these spots being uronic acids.

Additional bands were examined more closely (ringed in different colours in Figure 48 (a)): as before, most algae, apart from *K. fluitans*, *Chlorokybus*, *Chara* and *Coleochaete*, also displayed slow-migrating bands, very close to the origin line (labelled 1 and 2 in all six species). These could be attributed to longer oligomers produced by the successive rounds of XEG digestions.

It is interesting that some species did not release these slow compounds, since they did during the first round of XEG digestion (Figure 47): it might be that all the xyloglucan-like polymers were previously solubilised during that first round. Additionally, *Mesotaenium* and *Netrium* both produced unidentified intermediate-migrating bands that could be identical to the tetradecasaccharide-like (XXXGXXXG) product previously detected in all studied species. *Chara* and *Coleochaete* both showed bands that co-migrated with XLLG, once more similar to

the one detectable in all studied species in XEG1. *Coleochaete* also produced an oligomeric ladder, numbered 1 to 5 on the figure. This ladder could originate from one of the side activities of XEG or could be a suite of XEG-like oligosaccharides. Only one slow-migrating compound was eluted off the *Spirogyra* digest. Once hydrolysed with TFA, it gave a uronic acid-like compound that could not be identified with GalA or GlcA, as well as a trace of Xyl. No Driselase product was visible.

Both extracts from *Mesotaenium* gave glucose when acid-hydrolysed. After Driselase digestion however, compound 1 gave a faint trace of Glc, and compound 2 a faint trace of isoprimeverose.

None of the compounds from *Zygnema* gave detectable hydrolysis products, as the radioactivity they contained was extremely low.

All three compounds from *Netrium* gave very faint glucose signals when TFA-hydrolysed. Compounds 1 and 3 also gave a faint isoprimeverose-like signal after Driselase digestion.

The compound from *Chara* released a GalA-like compound, both from acid and enzymatic breakdown: it might be an oligosaccharide from the algal pectic fraction unexpectedly released by XEG.

All six eluates from *Coleochaete* were producing slow-migrating compounds, both after acid treatment (eluates 1 and 2 are even immobile) and after enzymatic hydrolysis.

Finally, the eluate from *K. subtilis* produced a uronic acid-like compound upon TFA hydrolysis, which was surprising given the previous work performed *K. fluitans*. The compound was immobile after Driselase digestion, indicating that it was an acidic, Driselase-resistant oligouronide.

The eluate from *K. nitens* could not be analysed after hydrolysis as its signal was too weak to be detectable.

In this experiment, an isoprimeverose-like compound was detected in at least two Zygnematalean species. A surprising number of acidic compounds were also solubilised by XEG digestion. However, this analysis might be skewed because of the unusual solvent behaviour, both for the analysis of XEG1 and XEG2-5. It makes comparisons between the two sets of chromatography difficult, although a direct comparison would have been helpful for interpreting the results of this study.

6.3.3. Post-XEG extraction analysis

6.3.3.1. Driselase dissection

After all five XEG digestions, the remaining algal residues were submitted to two consecutive digestions with Driselase. Each time, the resulting monosaccharides and oligomers were extracted with 70% ethanol, as before, thus producing extract Dris1 and Dris2.

The solid residue was then rinsed with buffer, in order to remove remaining enzymes and products, the wash being termed Dris2R.

The proportions of total radioactivity extracted each time are shown on Figure 46. Radioactivity released by XEG digestion of algal AIRs. (b). For almost all species, apart from *K. subtile* and *K. fluitans*, Dris1 was the extract containing by far the most radioactivity. It represented up to 80% of the initial de-starched AIR radioactivity in *Chara*, between 40 and

50% for the Zygnematales, *Coleochaete*, and, surprisingly, *Chlorokybus*. For the Klebsormidiales, Dris1 varied widely between under 20% for *K. subtile*, to over 40% for *K. nitens*, and 30% for *K. fluitans*.

Dris2 was, for all species apart from *K. subtile* and *K. fluitans*, far smaller than Dris1: it fell to around 30% of the initial de-starched AIR radioactivity in *Spirogyra*, *Zygnema*, *Coleochaete* and *Chlorokybus*, and even to 20% for *Mesotaenium* and *Netrium*. *Chara* and *K. nitens*' Dris2 were particularly low, falling to just above 10%. Finally, *K. subtile* and *K. fluitans* were the only species with Dris2 very slightly higher than Dris1, culminating at respectively 20 and 30% of the initial radioactivity.

The wash (Dris2R), finally, released less than 5% radioactivity for all species but the Klebsormidiales. For all three *Klebsormidium*, Dris2R contained around 10% of the initial de-starched AIR radioactivity. Dris2R was not analysed further on.

Dris1 and Dris2 were pooled in order to analyse their content. If the previous XEG digestions had gone to completion, then all the xyloglucan-like oligomers had already been released. However, if it were not the case because of unique algal xyloglucan features, Driselase might have solubilised, amongst others, isoprimeverose, which we aimed to detect.

The solubilised mono- and oligosaccharides were separated on TLC in two different solvent systems, as visible in Figure 49 (a) and (b). All algae produced extremely strong and intricate signals, which made their interpretation difficult. In the first solvent system (Figure 49 (a)), they all displayed two main bands, one slightly faster than Me-Xyl, the other migrating slightly faster than glucose. In the second solvent system (Figure 49 (b)), only the second band was still visible at this intensity. *Chara* and *Coleochaete* were particularly rich in galacturonic acid, as it is visible on both TLC plates. No isoprimeverose signal was

distinguishable. This is particularly clear in the second solvent system (EPAW), suggesting that the previous XEG digestions had indeed gone to completion.

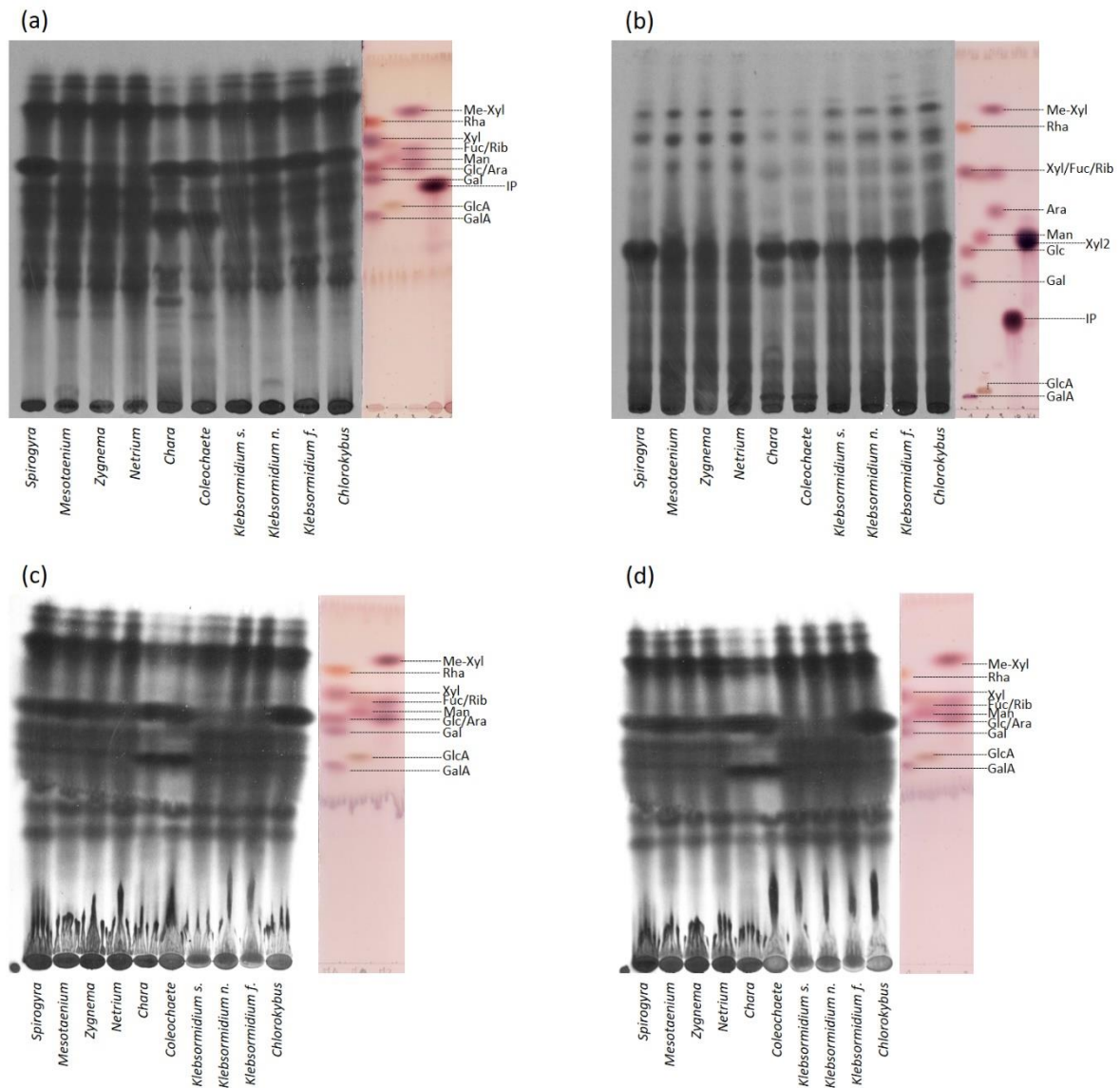


Figure 49: Driselase extracts of pre-XEG-digested AIR, and the impact of alkali treatment on these extracts.

Following digestion of the AIR with XEG and rinsing, the residues were treated with Driselase. Soluble oligomers were extracted from this digest as before, with 70% ethanol. (a): Separation of the extracts by TLC, in BAW 2:1:1. (b): Separation of the extracts by TLC, in EPAW 6:3:1:1, 2 ascents.

A portion of the Driselase extracts was then incubated with alkali, and the solution was neutralised with acetic acid. (c): Neutralised alkali-treated extracts on TLC in BAW 2:1:1. As a control, a further portion of the Driselase extracts was incubated with the equivalent concentration of 'pre-neutralised alkali' (NaOH + acetic acid). (d): Extracts in sodium acetate buffer on TLC, in BAW 2:1:1.

Strong radioactive bands with a high chromatographic mobility were detected on the BAW TLC from all algae, and we considered that these could have been uronic acid lactones. The digests were therefore treated with alkali in order to de-lactonise any uronic acids, which might clarify the signals. The products of this treatment were once more run on TLC (Figure 49 (c) and (d)). However, the signals were not clearer than before, indicating the absence of such compounds. All algae exhibited a range of unidentified products with R_{Glc} 0.35–0.60 on TLC in BAW —proposed to be moderately large Driselase-resistant oligosaccharides (considerably slower-migrating than the disaccharide, isoprimeverose).

6.3.3.2. Acid hydrolysis

In order to complete the analysis of these algal cell walls, two acid hydrolyses were performed on the residues from all previous enzymatic digestion: TFA hydrolysis followed by Saeman hydrolysis. The last is more aggressive and is able to hydrolyse any remaining enzyme- and TFA-resistant polysaccharides.

The proportions of hydrolysed sugars, for each acid treatment, are visible in Figure 46 (b). For the algae whose cell walls had been extensively hydrolysed with Driselase, it was very low: the TFA fraction represented less than 5% of the initial de-starched AIR radioactivity for *Chara* and *Coleochaete*, and around 10% for *Spirogyra*, *Mesotaenium*, *Zygnema* and *Chlorokybus*. It went up to over 20% in the Zygnematalean alga *Netrium*. For species from the *Klebsormidium* genus, it represented respectively 50, 30 and around 25% of the initial de-starched AIR radioactivity for *K. subtile*, *K. nitens* and *K. fluitans*. The peculiar cell wall architecture of the Klebsormidiales (Chapter 5) explains this lower digestibility by Driselase.

The resulting sugar mixture was separated as previously on TLC (Figure 50). The plates were much cleaner than for previous chromatograms and more interpretation was possible (Figure 49).

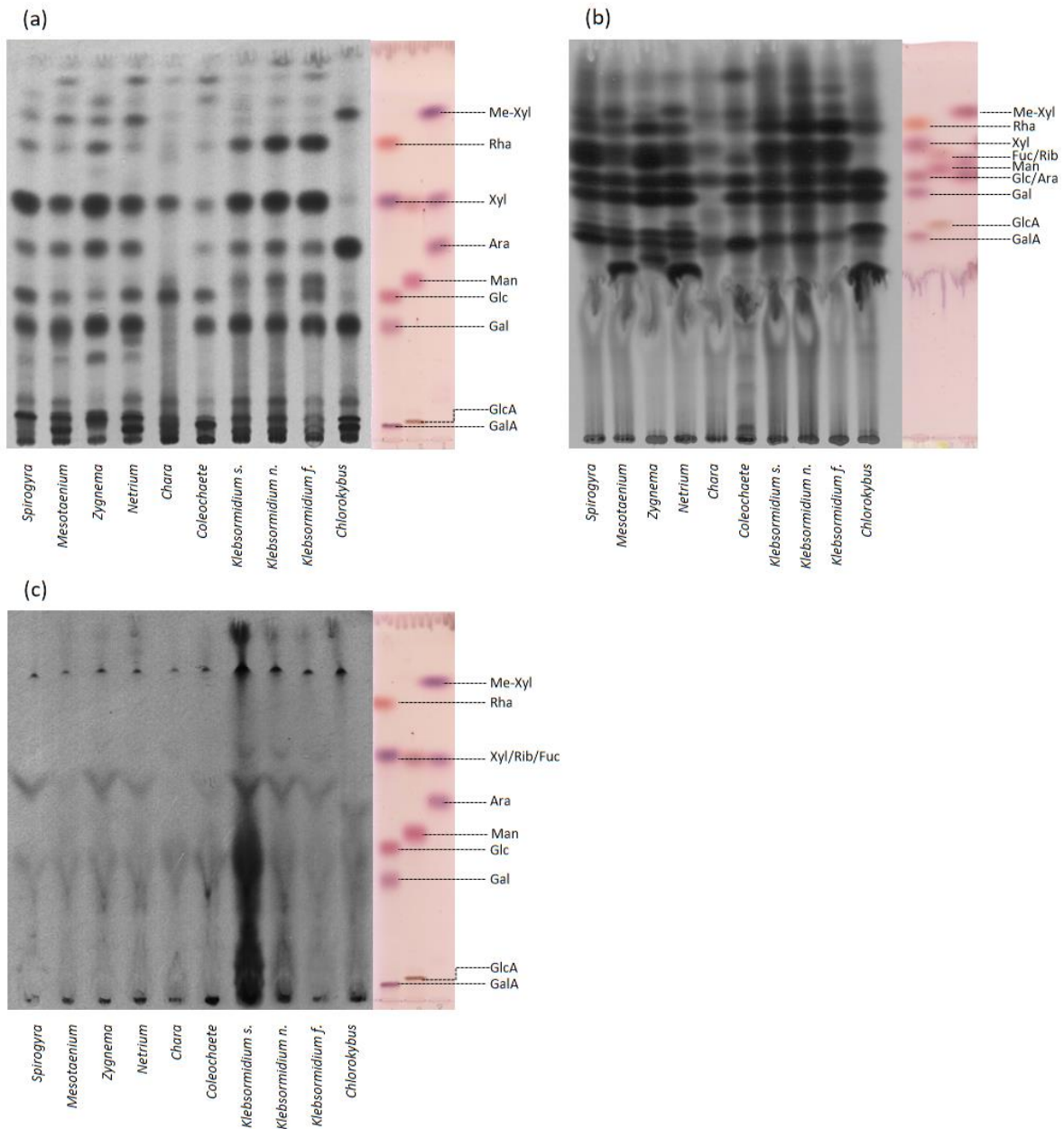


Figure 50: Acid hydrolysis of pre-digested AIRs.

Following XEG and Driselase digestions, the remaining algal residues were hydrolysed with TFA, and the soluble monosaccharides and any oligomers extracted. (a): Separation of the extracts by TLC, in EPAW 6:3:1:1, 2 ascents. (b): Separation of the extracts by TLC, in BAW 4:1:1, 2 ascents. The remaining residues were hydrolysed with sulphuric acid, following the Saeman protocol. (c): Separation of the hydrolysates by TLC, in EPAW 6:3:1:1, 2 ascents.

All four Zygnematalean algae had similar compositions: they were rich in a uronic acid (probably GalA), Gal, Glc, Ara, Xyl, and Fuc. They also all contained small amounts of Rha (particularly *Spirogyra* and *Zygnema*) and MeXyl. These monosaccharides are characteristic of land-plant pectins, as homogalacturonan and RG-I are primarily made of GalA, Gal, Ara, Rha; and of land-plant hemicellulose (Xyl, Glc) and cellulose (Glc). The high amount of Fuc is surprising. On top of that, *Mesotaenium*, *Zygnema* and *Netrium* showed bands that could be characteristic of neutral dimers and aldobiouronic acids.

Chara was mostly rich in GalA, Glc and Xyl, and was conspicuously lacking Gal and Ara. This alga is known to contain a homogalacturonan-rich fraction, and no other known pectic polymer, which explains the abundance of GalA in its cell wall hydrolysates. As previously, Xyl and Glc were attributed to the hemicellulosic and cellulosic fractions

Coleochaete cell wall hydrolysate remarkably resembled the Zygnematales', as it comprised all four main land-plant pectin monomers GalA, Gal, Ara, and Rha, as well as Glc, Fuc and Xyl as a very minor constituent. The low amounts of Xyl might be attributed to a particularly glucose-rich hemicellulosic fraction or to the total solubilisation of Xyl-containing polymers during the enzymatic treatments.

All three *Klebsormidium* species were surprising, as they presented bands characteristic of uronic acids, which had not been detected in *K. fluitans* previously (Section 3.5.3.5). They were also all rich in Gal, Man, Ara, Xyl, Fuc and Rha. *K. fluitans* also displayed a marked Glc band. These neutral sugars were all found in the pectic fraction of *K. fluitans* in the previous chapter.

Finally, *Chlorokybus* showed bands indicative of an aldobiouronic acid, previously characterised in this thesis, a uronic acid (probably GlcA), Gal, Ara and an unidentified

compound, co-migrating with Me-Xyl in EPAW and with Rha in BAW. Again, these sugars are all found in the pectic fraction from *Chlorokybus* (Section 3.5.3.6). The other cell wall fractions were shown to contain mainly Glc, which appears to have been solubilised in the previous stages of AIR digestion.

After TFA hydrolysis, the remaining solid residues (invisible to the naked eye) were hydrolysed with sulphuric acid following Saeman's protocol. It is commonly used for hydrolysing non-TFA-sensitive cell-wall polymers, in particular cellulose. In this experiment, cellulose should have been hydrolysed by Driselase in the previous extraction steps, thus the Saeman hydrolysis products should amount to very little. For all species, this final hydrolysate represented under 1% of their initial radioactivity. The products are visible in Figure 50 (c): no substantial amount of radioactive biomass was left in most species.

6.3.4. Driselase product analysis for *Chara* and *Coleochaete*

On Figure 49 (a) and (b), oligomers released by Driselase from pre-XEG-digested-AIR are shown. Both *Chara* and *Coleochaete* displayed strong bands that could correspond to uronic acids or aldobouronic acids. In order to investigate their compositions more thoroughly, Driselase extracts from both algae were analysed further by TLC. The sample was loaded as a dot near a corner of the TLC plate, and the plate was developed thrice in each direction, in two different solvents (Figure 51 (a) and (f)). The plates were exposed to film, which allowed for the detection of radioactive compounds. The vertical direction was developed in BAW

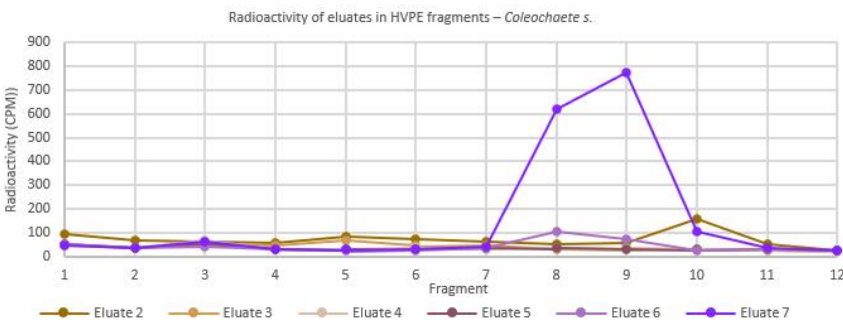
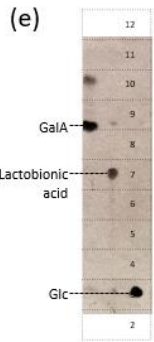
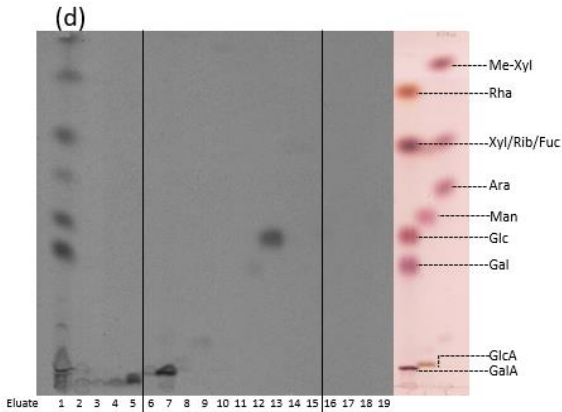
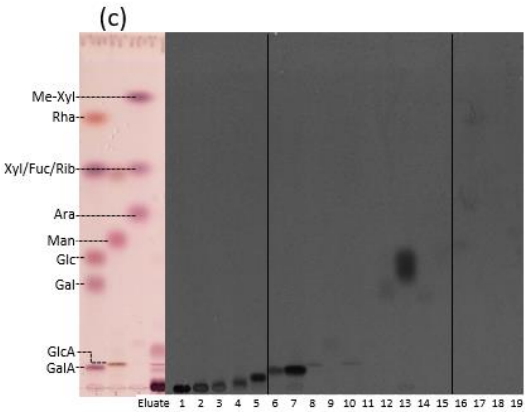
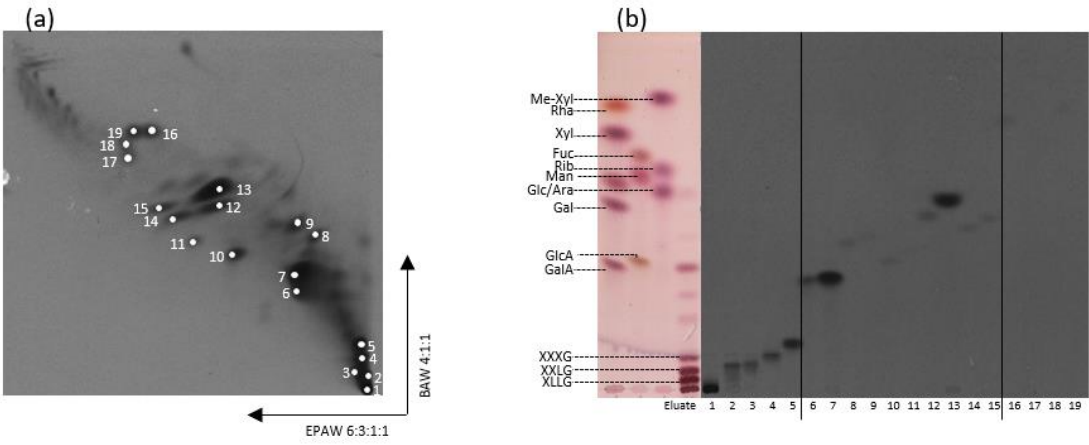
4:1:1, which allows for a clear distinction between different sizes of oligosaccharides. The horizontal direction was developed in EPAW 6:3:1:1, so that the acids and heavy compounds were clearly distinguishable from the neutral monomeric sugars.

In *Coleochaete*, 19 compounds were detected. They were then eluted off the plate and examined one by one. Compound 1 was at the origin, or the loading point: it comprises the oligosaccharides that were small enough to be soluble in ethanol but too big to be mobile on TLC, even in BAW. When re-developed in unidimensional TLC, it always stuck at the origin. When acid-hydrolysed, 1 yielded a range of uronic acids, as well as Gal, Glc, Ara, Xyl, and Rha. Compounds 2 to 5 had no to very little mobility when developed in EPAW, which is indicative of a high acidity or of a high molecular weight. They migrated around the neutral heptasaccharide zone in B/A/W. Acid hydrolysis surprisingly caused little or no change in mobility in EPAW, suggesting that compounds 2–5 contain highly acid-resistant glycosidic bonds. Compounds 2–5 could not be reliably detected after HVPE (Figure 51 (e)).

Compounds 6 and 7 migrated like monomeric uronic acids on both solvent systems, and this was still the case after they were acid-hydrolysed. On HVPE, they migrated around the GalA marker (not reliably resolved from GlcA with electrophoretogram strips of this size): 6 and 7 both are monomeric uronic acids, although they migrated further than expected in the EPAW direction on the 2D TLC. Compound 13 was identified with Glc, since it co-migrated with the corresponding marker when unhydrolysed ((b) and (c)) and when hydrolysed (d). Compound 8 to 12 and 14 to 19 were not detectable in further analysis, owing their low amounts.

In *Chara*, 15 compounds were detected and eluted off the plate. Compound 1, as previously, was the origin: when hydrolysed it released uronic acids, Glc, Man, Xyl (or Fuc, as they are

not clearly resolved) and Rha. Compounds 3, 4 and 5 migrated very slowly on EPAW, and alongside neutral heptamers on B/A/W. Upon acid hydrolysis, they kept on migrating in the uronic acids zone in EPAW, thus they probably are galacturonic acid oligomers. Compounds 8 and 9, like 6 and 7 in *Coleochaete*, were identified as monomeric uronic acids. Compound 13 was identified as glucose. The remaining eluates could not be identified, as they did not contain enough radioactivity to be detectable.



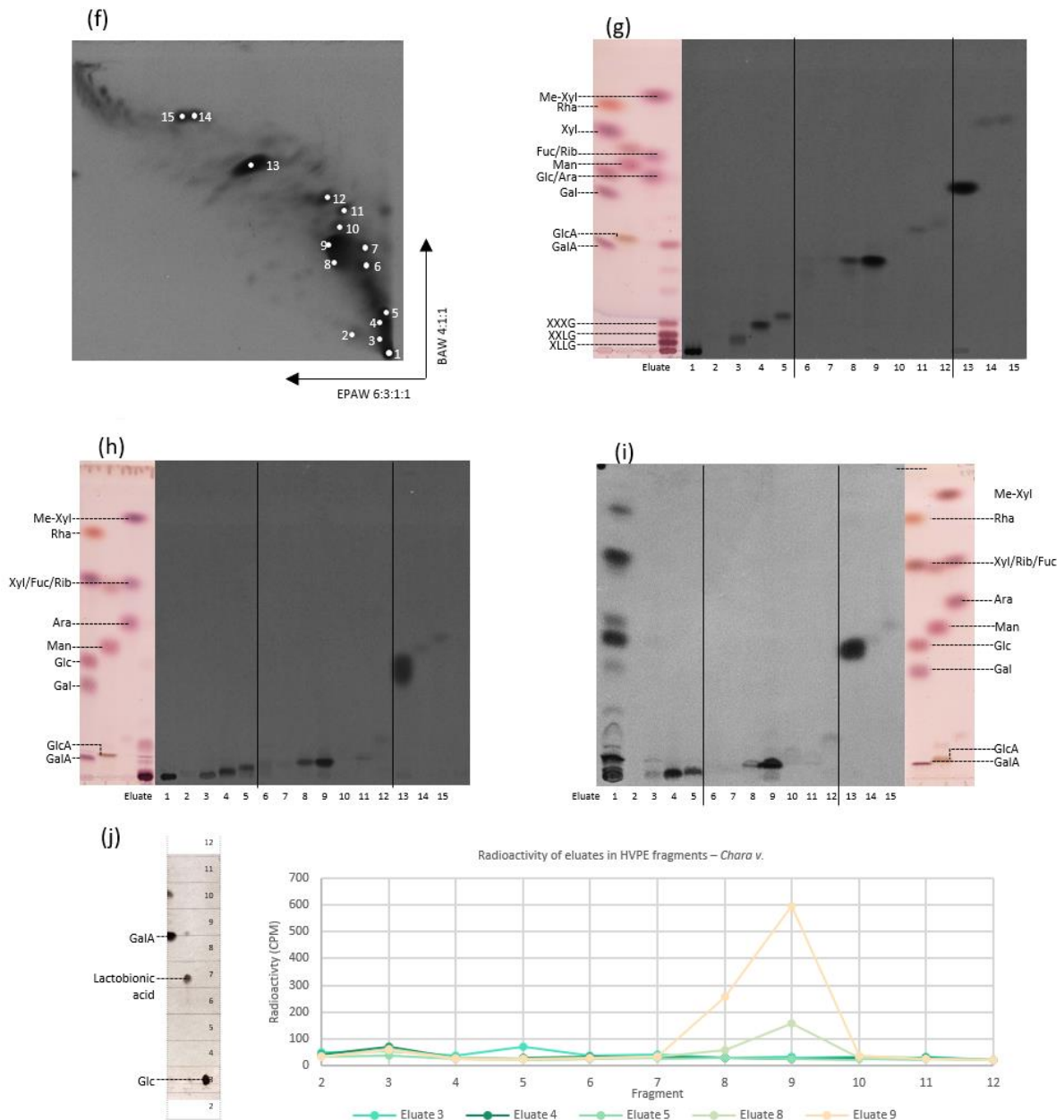


Figure 51: In-depth analysis of Driselase extracts from XEG-pre-digested *Coleochaete* and *Chara*.

XEG pre-digested AIRs were incubated with Driselase, and the soluble oligomers produced were extracted with ethanol. This extract was developed on TLC alternatively in 2 directions: 3 times in EPAW 6:3:1:1 (right to left), and 3 times in BAW 4:1:1 (bottom to top). (a): 2 dimensional TLC of *Coleochaete* extract. The radiolabelled compounds are numbered 1 to 19. (b): *Coleochaete* eluates were re-run on TLC in BAW 4:1:1. (c): *Coleochaete* eluates were re-run on TLC in EPAW 6:3:1:1, 2 ascents. (d): *Coleochaete* eluates were TFA-hydrolysed, and the hydrolysates were separated on TLC in EPAW 6:3:1:1, 2 ascents. (e): Selected *Coleochaete* eluates were separated on HVPE (pH 6.5, 3.2 kV, 60 min). The markers were stained and are visible on the left. The paper was cut in 5 cm strips, the radioactivity present on each strip was assayed by scintillation counting and is displayed on the graph on the right. (f) to (j): same process for *Chara* extracts, numbered 1 to 15.

In this study, the *Coleochaete* cell wall, post XEG-digestion, was shown to contain an abundance of uronic acids, as well as a range of RG-I specific monomers in the bigger, origin-bound oligomer, thus confirming its proximity with land plant cell walls. The presence of Glc and Xyl in the origin-bound oligomers suggests the presence of Glc and Xyl-rich oligomers that cannot be digested by XEG or common land-plant enzymes. The abundance of Glc may be due to the presence of cellulose. In *Chara*, the abundance of uronic acids was equally clear, however, less RG-I specific monomers were visible, in agreement with previous literature (Sørensen, et al. 2011). However, the presence of Man, Xyl and Glc in the origin-bound oligomers, and of Glc as a monomer, suggests, as for *Coleochaete*, the presence of non XEG- or land plant-specific-hydrolase-sensitive oligomers.

6.3.5. Enzymatic analysis of the alkali extracted fraction

A hemicellulosic fraction was extracted from fresh aliquots of each de-starched, ¹⁴C-labelled algal AIR by incubation in concentrated alkali for 72 h (6 M NaOH, 37°C). When quantified (Figure 52 (a)), this represented between 20% (*Chlorokybus*) and 3% of the initial radioactivity (*K. fluitans*). Interestingly, the proportion of extracted material was around 15% for most higher charophytes (apart from *Mesotaenium*, around 7%), whilst it was under 5% for all *Klebsormidium* species. This extraction with strong alkali removes any ester group that could functionalised sugar monomers, thus making the extracted fractions more susceptible to enzymic digestion.

These hemicellulosic extracts Hb were incubated with XEG and Driselase (non-sequentially). Oligomers produced by these treatments were, each time, extracted with acidified ethanol

as explained previously. The proportions of solubilised biomass are shown in Figure 52 (b). The products rendered ethanol-soluble by XEG are in fraction HbX: for lower charophytes, HbX contained 40 to 50% of the initial radioactivity. For higher charophytes, it varied widely: it was highest for *Chara* and *Mesotaenium* (around 35-30% of initial AIR), and lowest for *Netrium* (10%). HbD is the fraction rendered ethanol-soluble by Driselase.

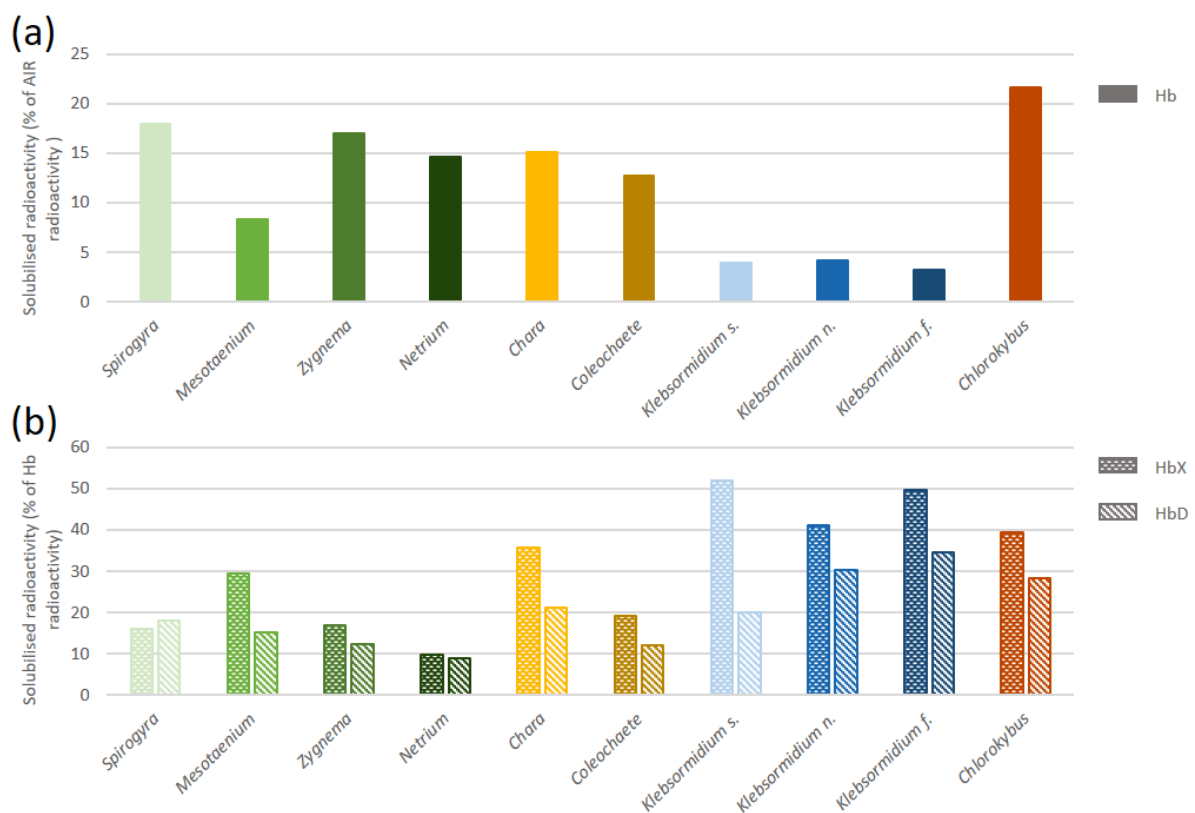


Figure 52: Quantification of alkali-extracted biomass from radiolabelled AIR, and of enzyme-released oligomers from the alkali-extracted fraction.

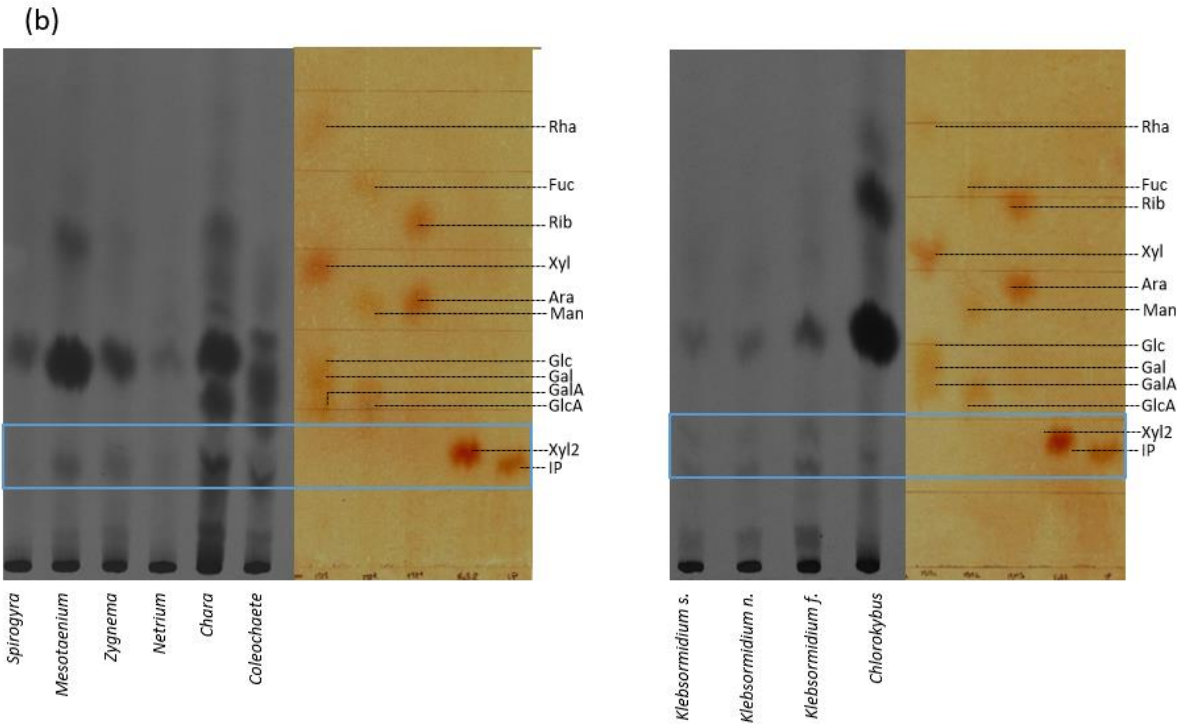
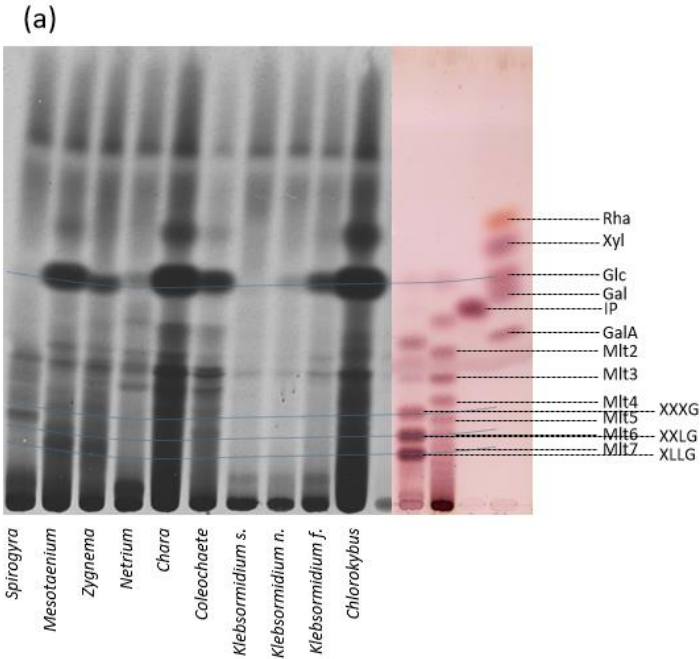
(a): proportion of radioactivity solubilised by concentrated alkali (fraction Hb, which remained soluble after neutralisation with acetic acid and dialysis against water) for each alga per initial AIR. (b): proportion of radioactivity present in HbX and HbD, i.e. released respectively by XEG and Driselase digestion of Hb, for each alga per initial Hb.

Surprisingly, it was lower than HbX for all algae except for *Spirogyra*. Once more, it was overall higher in lower charophytes than in higher ones.

HbX was run on TLC in order to spot possible xyloglucan-specific oligomers (Figure 53 (a)). All algae yielded a band (or double band) that migrated close to maltotriose — thus potentially a neutral trisaccharide. *Spirogyra* displayed no Glc band, but had a clearly visible one between XXXG and XXLG. Both *Mesotaenium* and *Zygnema* presented a fairly abundant Glc band, and a fuzzy spot around the XGO zone. *Netrium* only showed a weak Glc signal and some extremely slow-migrating compounds that could not be identified. Both *Chara* and *Coleochaete* had some strong Glc bands and oligomeric bands. The *Klebsormidium* species showed only faint oligomeric bands, although *K. fluitans* had an intense Glc band. Finally, the *Chlorokybus* track comprised heavy Glc and Xyl spots, as well as two small oligomers running faster than maltotriose. Making out bigger oligomers was difficult, as a smear was visible on the first half of the track.

HbD was separated on PC in B/A/W 12:3:5 (Figure 53 (b)). All algae had a variably strong Glc signal. In addition, *Mesotaenium* displayed an obvious Xyl band, whilst both *Chara* and *Coleochaete* showed the presence of Gal, amongst other sugars. *Chlorokybus* showed some faster-migrating sugars, probably including fucose. The strip of paper corresponding to the isoprimeverose zone (not completely resolved from xylobiose) was cut out and eluted for each alga (shown in blue on the figure). The eluates were then developed on a PC in a different solvent system (E/P/W 8:2:1, (Figure 53 (c))). The PC showed almost empty tracks for *Spirogyra* and *Netrium*. For *Mesotaenium*, *Zygnema*, *Chara*, and *Coleochaete*, a clear band was observable, migrating slightly faster than isoprimeverose though slower than xylobiose. *Coleochaete* also displayed a xylobiose-like band. All three *Klebsormidium* species displayed a xylobiose-like band plus an unidentified band that migrated between the

monosaccharides Glc and Gal. The eluates from *Chara*, *Coleochaete* and *Chlorokybus* showed radioactive material that was immobile in EPW and thus probably acidic. Overall, no isoprimeverose-like compound was observed in the present selection of algal species.



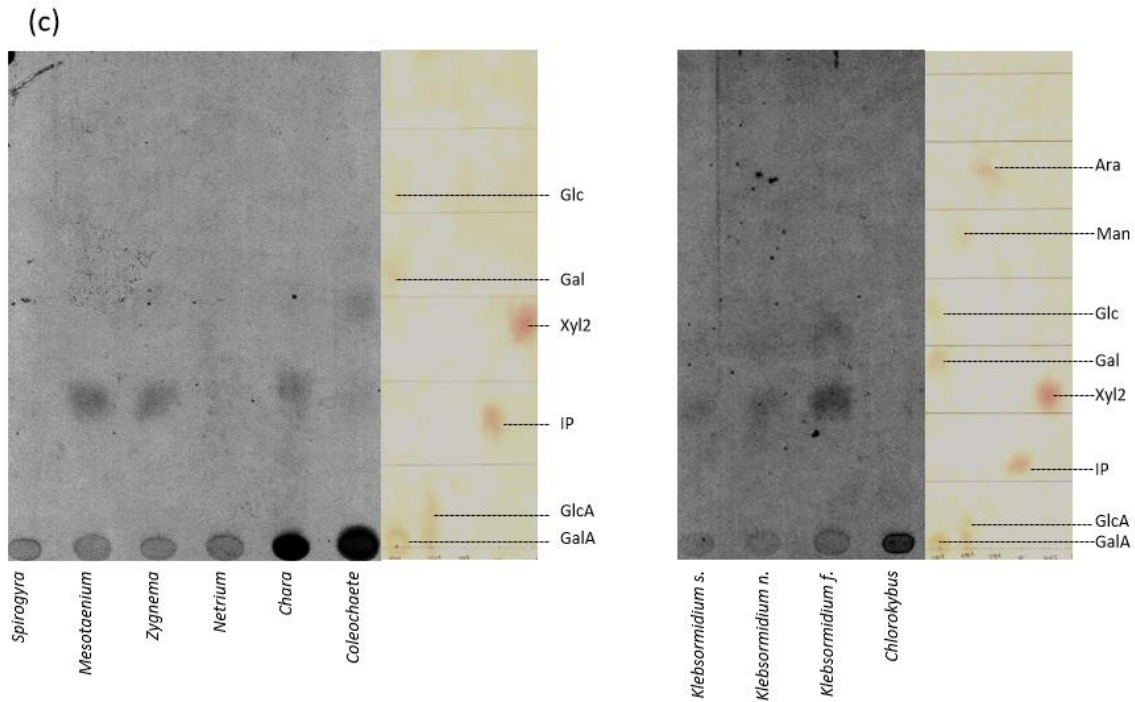


Figure 53: Chromatography of enzymatic extracts from radiolabelled Hb.

(a): HbX extracts (XEG-released oligomers from radiolabelled Hb) were separated on TLC in B/A/W 2:1:1, once, alongside xyloglucan-specific markers. The blue lines are a guide for the eye. (b): HbD extracts (Driselase-released oligomers from radiolabelled Hb) were separated by paper chromatography in B/A/W 12:3:5. The fractions in the blue box were eluted off the paper, making extracts HbD1. They comprise products co-migrating with isoprimeverose. (c): HbD1 extracts were separated by paper chromatography in E/P/W 8:2:1.

6.4. EPG assay

EPG (or endo-polygalacturonase) splits bonds in the pectic polysaccharide domain homogalacturonan, yielding oligogalacturonides. By doing so, it releases non-homogalacturonan pectic polysaccharides, such as RG-I and RG-II in land plants.

6.4.1. Amounts of extracted radioactivity by EPG

As previously done with XEG, algal AIR was first rinsed with buffer, giving the ethanol-soluble fraction B2. It was then subsequently digested with EPG 4 times in a row (EPG1 to 4), rinsed with ethanolic sodium hydroxide (fraction NaOH), re-digested with EPG (EPG5), and finally rinsed with water. The radioactivity released by each step of this process, as a proportion of the initial radioactivity in de-starched AIR, is shown in Figure 54.

Surprisingly, almost all fractions from *Spyrogyra* and *Zygnema* contained a very low amount of radioactivity (Figure 54). Only the Water fraction from *Zygnema* reached 10% of the initial radioactivity. For both *Mesotaenium* and *Netrium*, a substantial amount of radioactivity was only released after the third EPG incubation. They then both released a substantial amount of oligomers in alkali conditions. The final aqueous rinsing was the biggest fraction from *Mesotaenium*, reaching around 16% of the initial AIR radioactivity.

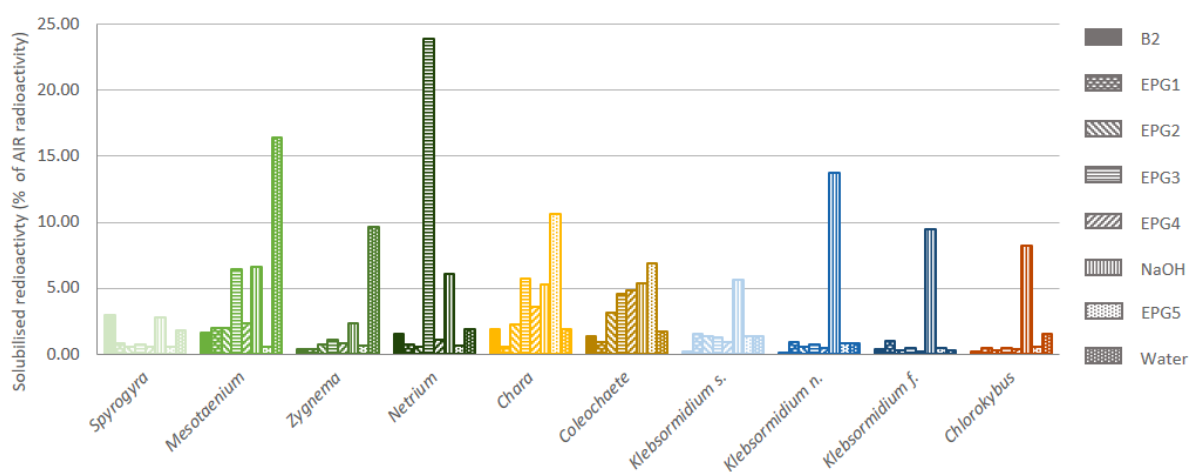


Figure 54: Quantification of EPG-extracted oligomers from radiolabelled AIR. Algal AIR was rinsed with buffer, producing extract B2. It was then digested 4 times with EPG (EPG 1 to 4), rinsed with sodium hydroxide in ethanol (NaOH), digested one more time with EPG (EPG5) and finally rinsed with water (Water). The proportion of radioactivity solubilised in each fraction for each alga per initial AIR is shown.

Chara and *Coleochaete*, displayed similar patterns: almost nothing was released during the first two EPG incubations, and the amount of released biomass was then rising with each new fraction. The final water rinsings, however, contained negligible amounts of radioactivity. Finally, as expected, it was very low for lower charophytes: all the EPG extracts represented less than 1% of the initial radioactivity. However, the NaOH fraction was each time between 5 and 15% of the initial AIR: some polymers in lower charophytes are clearly alkali-labile.

6.4.1.1. Chromatographic and electrophoretic analysis of EPG-released oligomers from *Chara*

Fractions EPG1, EPG2 and EPG3 from *Chara* were pooled and separated by size exclusion chromatography on Bio-Gel P-2. The radioactivity in each fraction was assayed and is displayed in Figure 55 (a). Both the polymer-rich and the small oligomer-rich fractions are highlighted in yellow. Fractions 29 to 40 were separated on TLC alongside oligogalacturonide markers. Small oligomers (galacturonic acid trimer) were clearly present from fraction 36, monomeric galacturonic acid was clearly visible from fraction 40. Earlier fractions (especially 29-34) contained oligomers that were too big to move on TLC (Figure 55 (b)). Fractions 31 and 35 were selected for further analysis: they were in the zone of elution that might correspond to land-plant-like RG-II. They were run by gel electrophoresis, with *Rosa* RG-II markers. The gel was then cut into strips and the radioactivity in each strip was measured, giving two graphs (Figure 55 (c)). In both cases, compounds had migrated on the gel around the markers, but none clearly co-migrated with *Rosa* RG-II.

Finally, the NaOH fraction from *Chara* was also separated on Bio-Gel P-2 as a control: it clearly contained a high proportion of heavy oligomers, lesser amounts of small oligomers and no clear RG-II like peak.

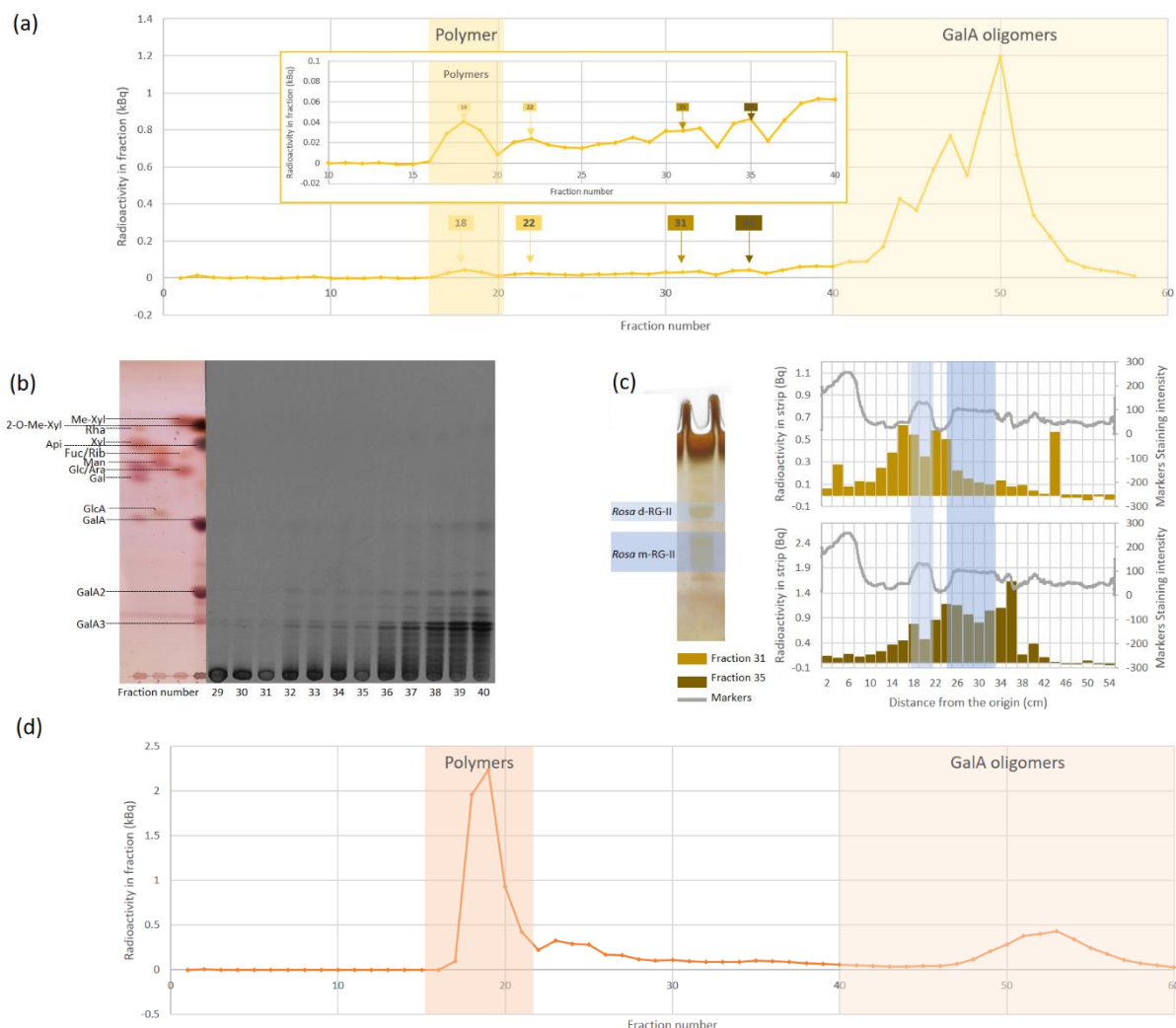


Figure 55: Analysis of EPG-digests from *Chara*.

(a): *Chara* extracts EPG1, EPG2 and EPG3 were pooled and separated by gel permeation chromatography on Bio-Gel P-2. Each fraction's radioactive content was measured. Fractions 16 to 20 contained mostly polymers, whilst fractions 40 to 60 contained mostly small oligomers (galacturonic acid-rich). The smaller graph in the yellow frame is a zoom between fractions 10 and 40. (b): fractions 29 to 40 were separated on an aluminium-backed TLC plate in B/A/W 2:1:1, thrice, alongside oligogalacturonides markers. (c): Fractions 31 and 35 were separated on gel electrophoresis, alongside *Rosa* monomeric and dimeric RG-II markers. The gels were cut in small strips, the strips were hydrolysed in TFA (1 h, 120°C), and the radioactivity in the hydrolysates was measured by scintillation counting. A profile of the radioactivity for each fraction run on gel was created. The top graph shows the profile for fraction 31, the bottom one the profile for fraction 35. On both graphs, the markers are shown as a colour profile (grey line). (d): *Chara* extract 'NaOH' (fraction from pre-EPG-digested *Chara* AIR soluble in ethanolic alkali) was separated by gel permeation chromatography on Bio-Gel P-2. Each fraction's radioactive content was measured.

6.5. Conclusion

Ten species of charophytic algae were radiolabelled in this work, and their cell wall polysaccharides analysed by enzymic methods.

Digestion of algal AIR with XEG allowed for the release of low amounts of sugar, leading to the detection of potential xyloglucan oligomers-like compounds in all species. However, the diagnostic dimer isoprimeverose could only be identified two Zygnematalean species.

Subsequent digestion of that same AIR with Driselase did not yield any more isoprimeverose, even after closer examination of the extracts from *Chara* and *Coleochaete*. The two final cell wall dissection steps performed on these samples, acid hydrolyses, allowed for the detection of pectin-specific monomers.

The fraction Hb, extracted with alkali from algal AIR, gave similar result: its digestion with XEG showed potential xyloglucan-like oligomers, but its digestion with Driselase (not subsequent) did not show any isoprimeverose.

These experiments point towards the presence of an XEG-digestible polymer in charophytic cell walls, however the absence of isoprimeverose and of structural information make it impossible to draw any definitive conclusion.

The other experiment in this chapter is focused on EPG digestion of algal cell walls: the amounts of radioactivity released by the enzyme clearly show the presence of homogalacturonan in later-diverging charophytes, and its absence in the earlier-diverging ones. Compounds resembling RG-II were found in *Chara* EPG hydrolysates, pointing towards the presence of an RG-II-like polymer in the alga.

7. *Ulva linza* cell wall: towards a
modification of previous models

7.1. Introduction

This thesis includes an investigation in a chlorophytic alga's cell wall, *Ulva* spp. *Ulva* is a common green seaweed, which sparked researchers' interest because it contains the hot-water-extractable polymer ulvan (Lahaye and Robic 2007). Ulvan is a sulphated polysaccharide, the capacity of which to form hydrogels is of particular interest for biomedical applications (Bothwell 2023). The alkali-soluble fraction of *Ulva* (or hemicellulosic fraction, by analogy with land plants' nomenclature) has been partially chemically characterised, resulting in a primitive model of its glycosidic structure (Lahaye *et al.* 1994; Ray 2006 p. 2006; Chattopadhyay *et al.* 2007). Finally, *Ulva* does contain cellulose in its cell wall, which probably plays the same reinforcing role it does in land plants' cell walls (Niklas 2004).

In this study, the different fractions of *Ulva* cell wall were extracted following the land plants protocol: the "pectic" fraction was solubilised with hot ammonium oxalate (in this case, it contained mostly ulvan), the "hemicellulosic" fraction was solubilised with 6 M sodium hydroxide, and the final residue was washed in order to isolate *Ulva* cellulose.

Upon the monosaccharides composition analysis performed previously, it was found that *Ulva*'s pectic extracts were particularly rich in rhamnose in comparison with expectations from the literature (Lahaye and Robic 2007), leading to investigating further their cell wall composition: is it classical ulvan or a variant of it? In a second time, a range of enzymes were assayed on *Ulva*'s hemicellulosic extract. Surprisingly, it was susceptible to hydrolysis by xylanase, which was against previously established structures of *Ulva*'s alkali-soluble fraction. The oligomers that were released were thus analysed, as well as the oligomers

released upon cellulase and Driselase digestion, in order to create an up-to-date model of this polysaccharidic fraction. Finally, the interaction of xylose-containing polymers and cellulose was studied.

7.2. Partial hydrolysis of *Ulva* pectic extract: characterisation of an unexpected oligomer

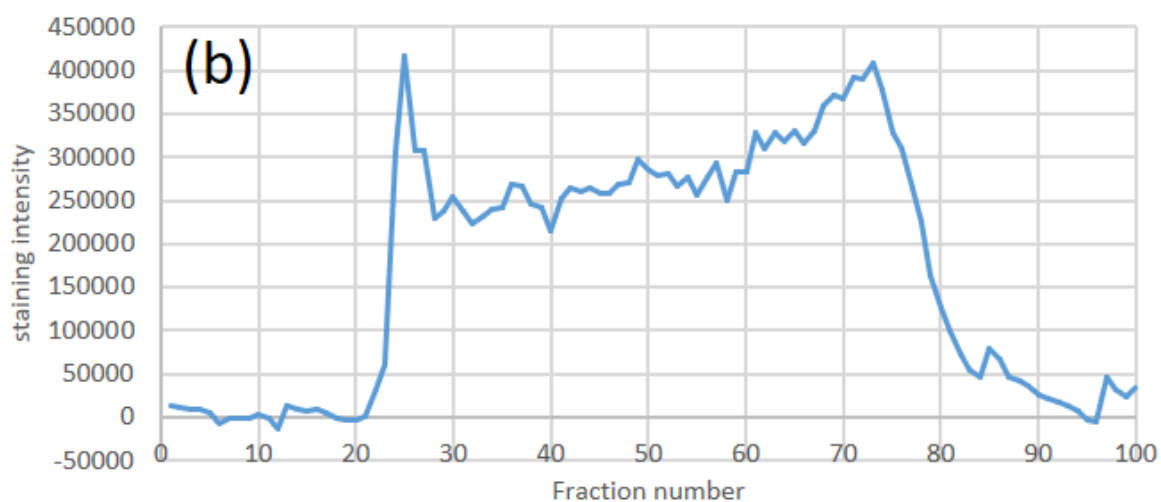
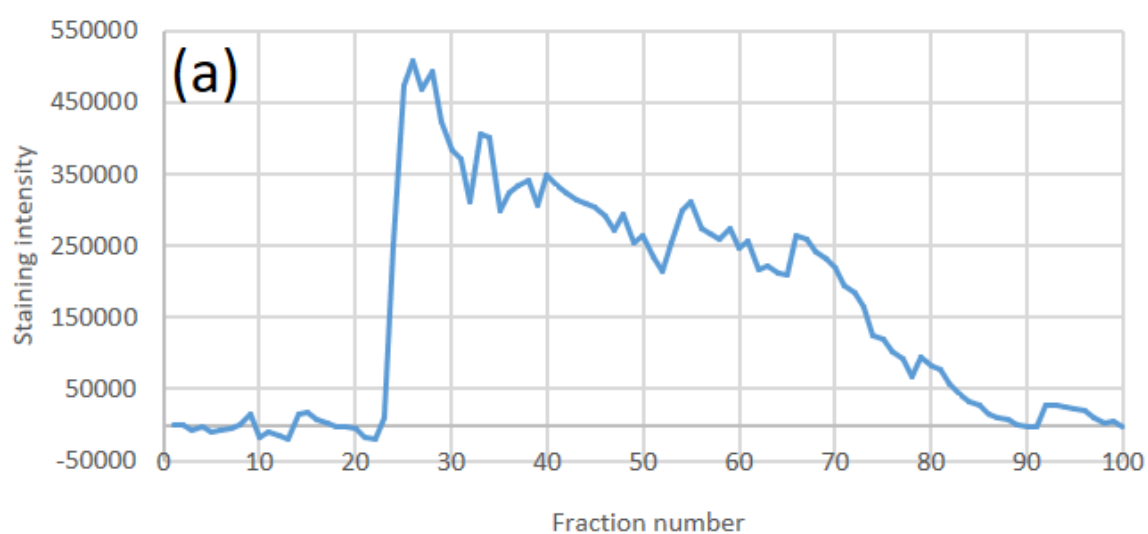
7.2.1. Gel permeation chromatography of *Ulva* 'pectin' – wide pores

Pectin extract (P2) from *Ulva* was partially hydrolysed at 80°C, in 0.1 M TFA, for 2 h. It was then separated on Bio-Gel P-30 (2500–40000 MW fractionation range), and the results compared to the filtration of un-hydrolysed P2 (Figure 56).

The un-hydrolysed fraction displayed a peak in the void volume of the column (around fraction 25): the bigger polymers, which the column did not retain, were in this fraction. The intensity of staining decreased almost linearly up to the end of the included volume, showing that polymers of all sizes were present in the column. Indeed, the extraction process of P2 from AIR may partially hydrolyse polysaccharides.

The partially hydrolysed sample also displayed a peak around fraction 25, for the same reasons as before. A second peak was visible around fraction 75, which is around where smaller oligomers and monomers are expected. A range of different sizes oligomers was detectable in between these two peaks, due to the partial hydrolysis treatment.

Fractions 25, 35, 45, 55, 65, 75 and 85 were run on TLC. The earlier ones (25 to 45) only contained heavy oligomers, immobile on TLC. Fractions 55 and 65 contained a range on undefined oligomers, which showed as a smear on TLC. Fraction 75 contained both monomers and small, well-defined oligomers. Finally, fraction 85 was almost empty (as expected from the intensity profile).



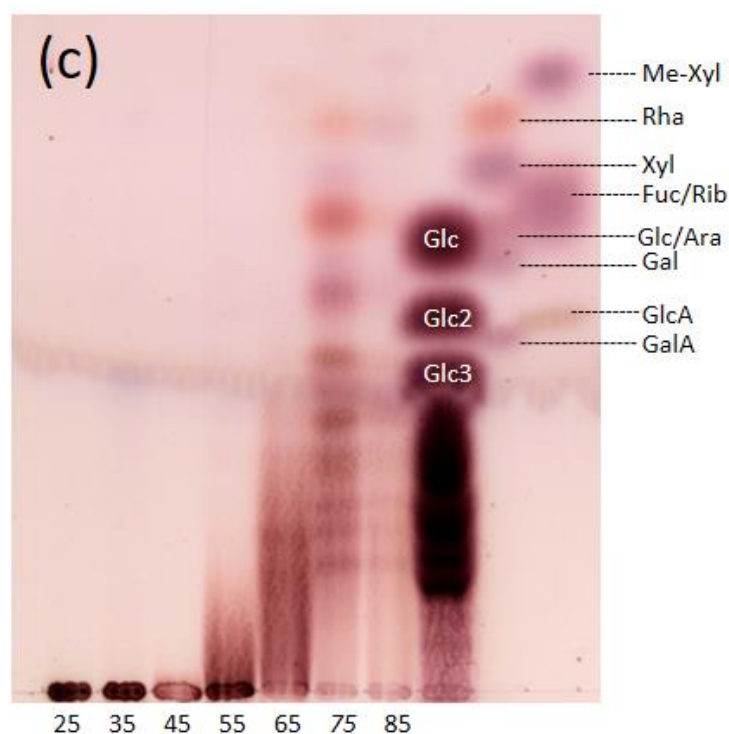


Figure 56: Gel-filtration of un-hydrolysed and partially hydrolysed pectin from *Ulva*. (a) shows the profile of staining intensity (perform by a dot-blot assay) of the different fractions from un-hydrolysed P2 eluted off the Bio-Gel P-30 column. (b) is the same for partially hydrolysed P2. (c) is the separation on TLC of a selection of fractions from (b). The smallest oligomers are visible in fraction 75.

7.2.2. Gel permeation chromatography of *Ulva* ‘pectin’– small pores

Fractions 65 to 90 were pooled together and separated on Bio-Gel P-2 (100–1800 MW fractionation range, Figure 57). There was not a prominent size of oligomers, as visible on the intensity profile. In the earlier fractions, ill-defined oligomers were visible as smears (fraction 12 to 20). In fractions 18 to 24, well-defined oligomers were detectable. Two of them were of particular interest, and were named X2 and XR. X2 is particularly abundant in fraction 23, it stains pink with thymol and migrates around the glucose marker: it is suspected that it is a dimer of rhamnose, which is a structure not known in Ulvales so far. XR is most abundant in fractions 20 and 21, it stains purple with thymol: it may be the well

known rhamnose-xylose dimer from ulvan. Finally, monomers were detectable in the later fractions, in particular rhamnose and xylose.

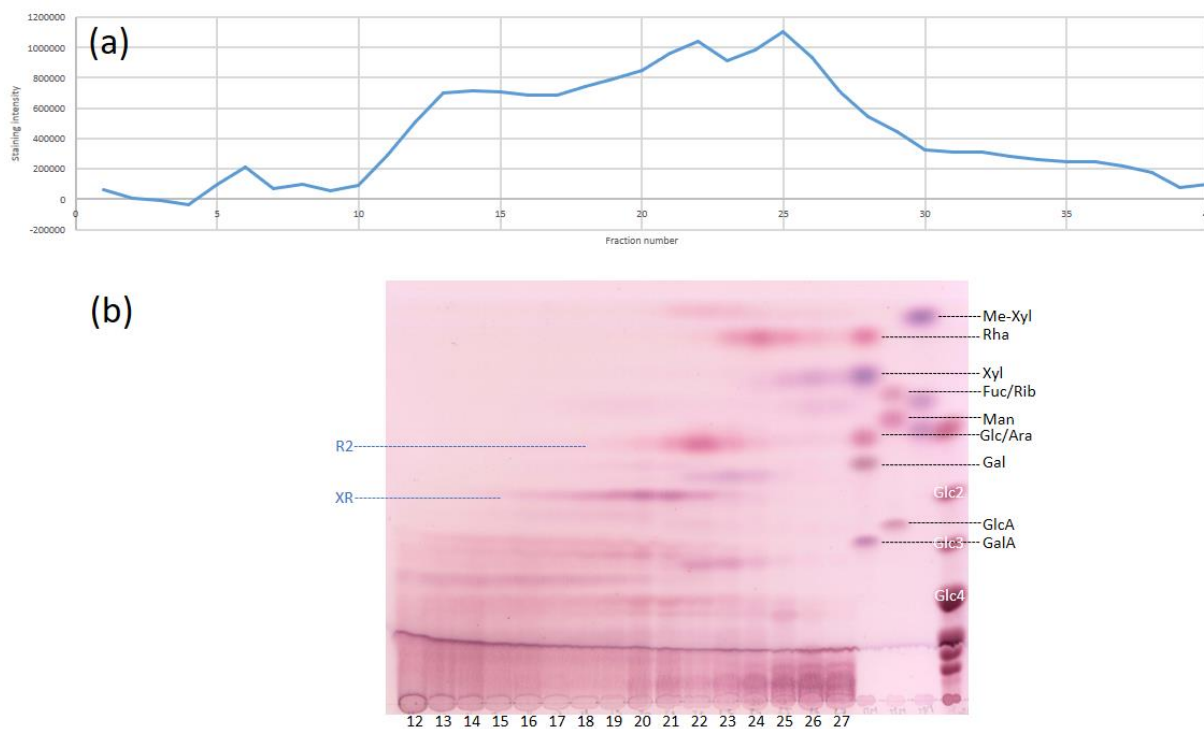


Figure 57: Gel-filtration of selected oligomers from partially hydrolysed pectin from *Ulva*. (a) shows the profile of staining intensity (perform by a dot-blot assay) of the different fractions selected from the previous gel filtration. (b) is the separation on TLC of fractions 12 to 27. The oligomers R2 and XR were of particular interest.

7.2.3. Characterisation of selected dimers extracted from *Ulva* 'pectin'

R2 and XR were isolated and fully hydrolysed to their constituent monomers (Figure 58). As expected, R2 released rhamnose and XR released rhamnose and xylose. The dimer xylose-rhamnose is already known in extracts from *Ulva* spp., and thus it was not investigated further (Lahaye and Robic 2007).

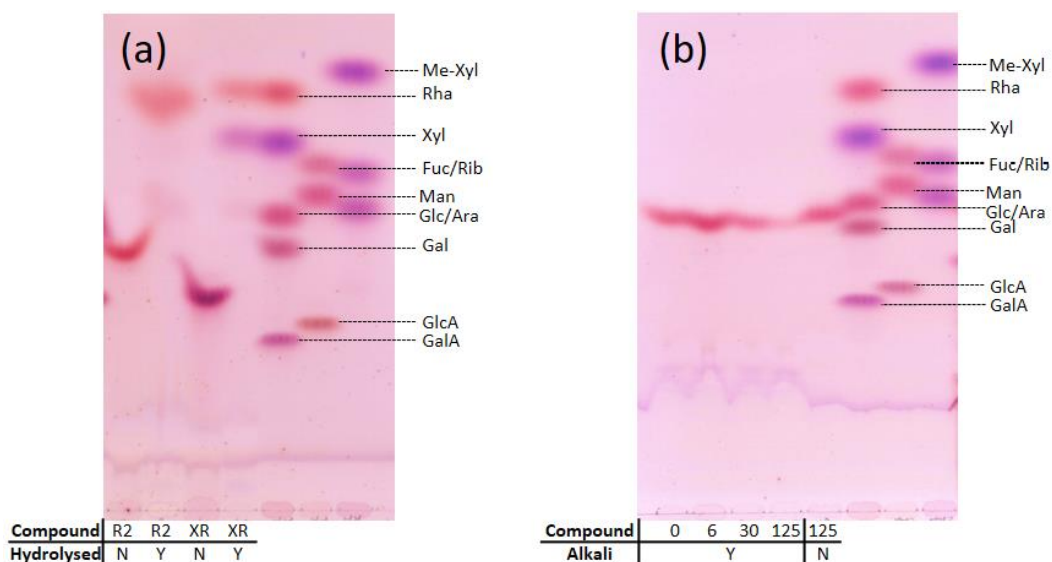


Figure 58: Hydrolysis and alkali assay of selected oligomers from *Ulva*.
 (a): the extracts X2 and XR were isolated and fully hydrolysed to their constituent monomers. (b): R2 was submitted to alkali assay. It was incubated in 0.2 M NaOH at 50°C for various amounts of time, neutralised with acetic acid, and the resulting mixture was run on TLC.

Glycosidic linkages (xylobiose)	Incubation time (minutes)			
	0	6	30	125
1→1	N	N	N	N
1→2	N	N	N	N
1→3	N	Y (Xyl)	Y (Xyl)	Y (Xyl)
1→4	N	N	Y (Xyl)	Y (Xyl)

Table 8: Degradation of xylobioses with different linkages in alkali
 Degradation of a range of xylobioses when incubated in 0.2 M NaOH at 50°C for various durations, neutralised with acetic acid, and analysed on TLC (Franková and Fry 2012). N means no sub-products are detected, Y means sub-products are detected. The names between bracket indicate the subproducts that were detected.

The rhamnose dimer however, was unknown and unexpected: no known ulvan structure contains such a dimer. An alkali assay was performed in order to check on the glycosidic

bond (Franková and Fry 2012). When this assay was tested on a range of xylobiose, (1→1) and (1→2) dimers did not release any monomer, whilst sub-products were visible after only six minutes in (1→3) and after half an hour in (1→4) dimers (Table 8). When submitted to this assay, R2 did not release any monomer nor sub-product. Thus, it is either a (1→2) rhamnobiore or a functionalised Rha residue (for example, sulphated).

The stability of Gal-4-sulphate was studied as a proxy for the hypothetical sulphated Rha (Figure 59 (a)). In acid first, in the conditions used for the production of XR and R2, the sulphate function was not impacted: if Rha was sulphated in the native extract, it would still be afterwards (Figure 59 (a) left). The stability of the sulphation was then studied in alkali, in the conditions used for the alkaline peeling experiment performed on R2 (Figure 59 (b)). Gal-4-sulphate started breaking down to Gal after 32 minutes, and 25% of the original sugar was converted to gal after 125 minutes. However, 125 minutes of incubation without alkali resulted into the breaking down of Gal-4-sulphate into multiple compounds, including Gal and a range of slower sugars. By comparison, R2 was never converted to Rha, neither after incubation in alkali nor in water. It is therefore unlikely that it would be sulphated Rha. Instead it might be a very stable dimer, very possible (1→2) rhamnobiore.

7.3. *Ulva* hemicellulosic extract Hb: characterizing phyco-xyloglucan

Some marine algae, such as red algae species, have (1→3)-xylan as their fibrillary polymer (Hsieh and Harris 2019). Is it the case of *Ulva linza*, with xylan and classical cellulose mixed together? *Ulva* spp. display a unique structure in their alkali-extractable fraction: a linear polymer made of both glucose and xylose unit, linked by β -(1→4), bonds where xylose is present every 3 to 5 monomers. The extract Hb released mainly glucose, xylose and rhamnose, as well as some uronic acids.

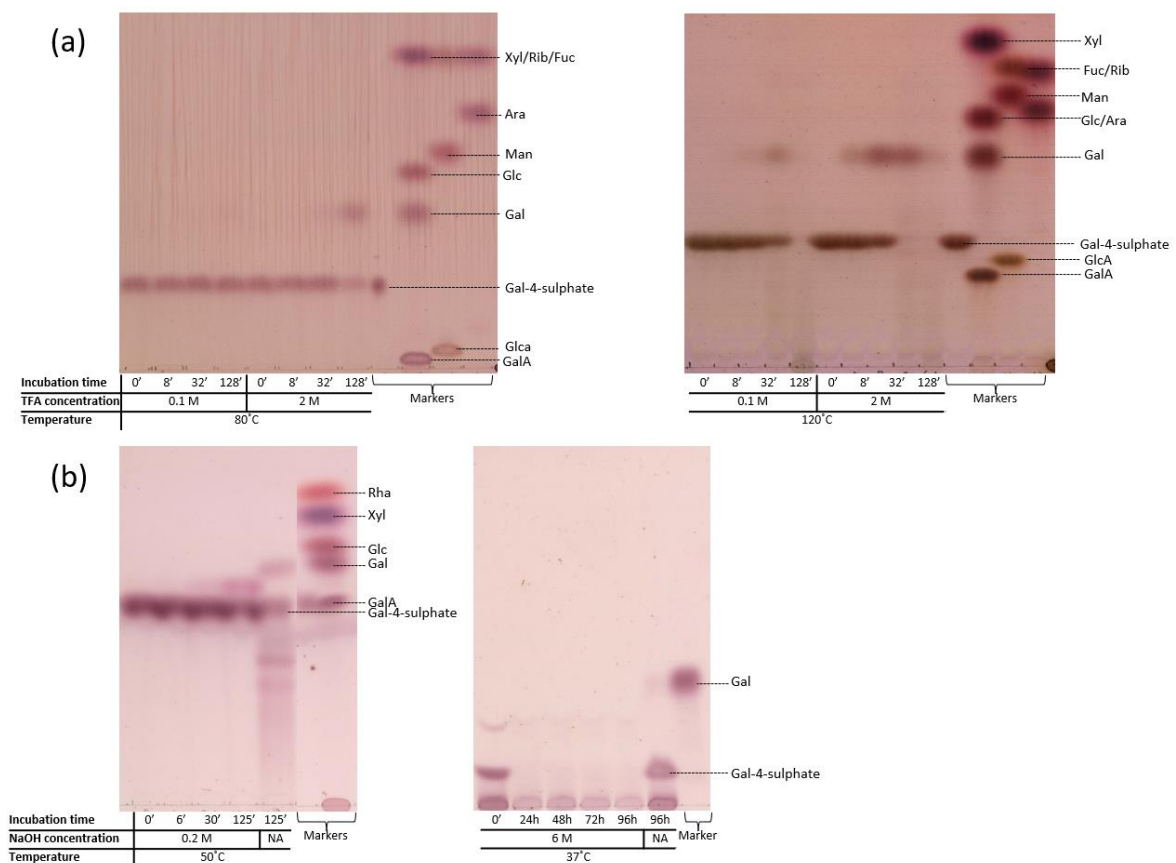


Figure 59: Stability of a commercial sulphated monosaccharide in acid and in alkali.
 (a): Gal-4-sulphate was incubated in various concentrations of TFA for 0 to 128 minutes, at 80°C (left) and 120 °C (right). (b): Gal-4-sulphate was incubated in 0.2 M NaOH for 0 to 125 minutes, at 50°C (left), and in 6 M NaOH for 0 to 96 h at 37 °C (right). All TLCs were performed on plastic-backed plate. The one showing incubations in acid at 80 °C was developed twice in E/P/A/W 6:3:1:1, all the others were developed twice in B/A/W 4:1:1.

7.3.1. Xylanase assay on *Ulva* Hb

Land-plant specific xylanase (aimed at β -(1 \rightarrow 4)-xylan) was assayed on all four extracts from *Ulva*: both hot-oxalate extracts P1 and P2, soluble alkali extract Hb, and the remaining insoluble residue α C (Figure 60 (a)). Only the extract Hb was degraded by the enzyme: it released three oligomers, named X1, X2 and X3 from the fastest to the slowest-migrating. This was surprising, since linkages between xylose monomers are not expected in *Ulva*: xylanase should not have been able to hydrolyse this extract. It may be that xylanase is not only able to cleave a β -(1 \rightarrow 4) bond between two xylose unit, but also a β -(1 \rightarrow 4) bond between a xylose and a glucose unit.

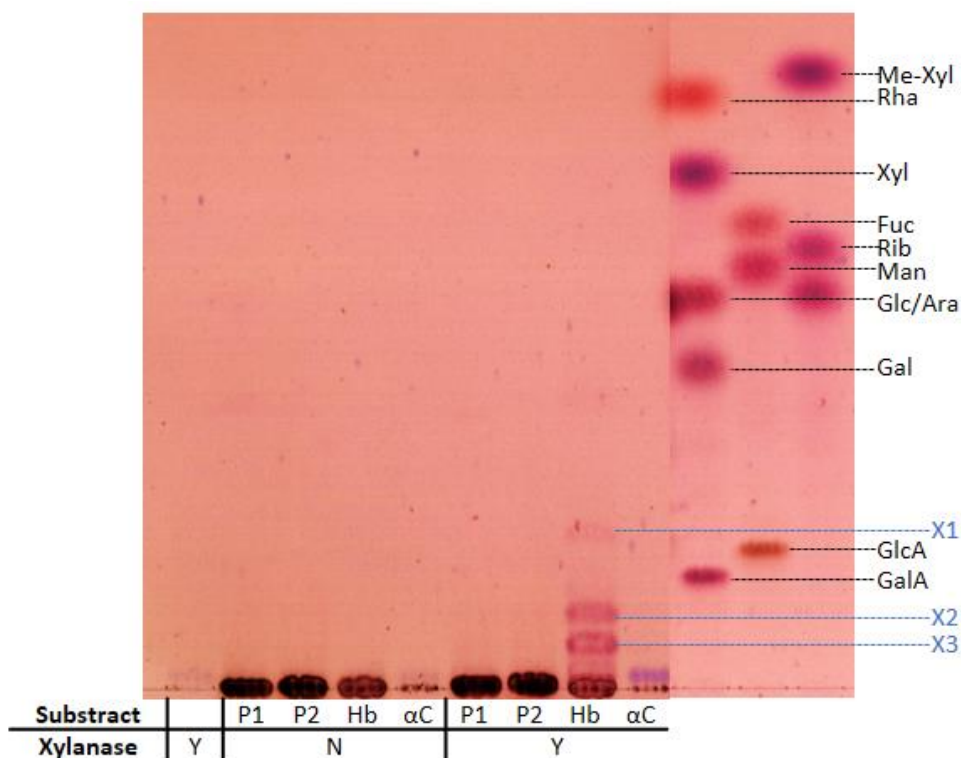


Figure 60: Xylanase assay on *Ulva* extracts.

(a): 4 extracts from *Ulva*, P1, P2, Hb and α C were tested against land-plant-specific xylanase. Hb released three oligomers, X1, X2 and X3.

X1, X2 and X3 were submitted to total acid hydrolysis and their monosaccharide compositions analysed (data not shown). They all released xylose and glucose. Both sugars appear to be present in equivalent quantities in X2 and X3, whereas xylose is less abundant in X1.

In order to gather more information about the products of hydrolysis, xylanase digestion was performed on 50 mg of hemicellulose Hb from *Ulva*. The resulting sugar mixture was separated by gel permeation chromatography (Figure 61).

The products of xylanase digestion eluted from the column in two main peaks. The first one was centred on fraction 12 and contained the polymeric structures which had not been hydrolysed. The second peak, around fraction 22, corresponded to a DP around 4. The second peak was fairly wide, as it looked like it contained multiple peaks: around fraction 22, fraction 24, fraction 26, and fraction 28.

Fractions 12 to 25 were run on TLC, in order to get a better idea of their contents. As expected, fractions 12 to 16 contained mostly polymeric material, as no sugar was migrating along the plate. From fraction 17, a range of oligomers were differentiable. However, none of them was pure enough to be analysed further.

Fractions were thus regrouped by similarity (17 to 19, 20 to 22, 23 to 29) and separated on preparative PC. Five compounds, A to E, as well as the monomers Glc and Xyl, were spotted. Interestingly, it is less oligomers than the 7 previously counted on TLC. Xyl was also not previously observable. This might be due to traces of xylanase present in the Bio-Gel fractions, breaking down the biggest oligomers. The compounds were then eluted off the paper.

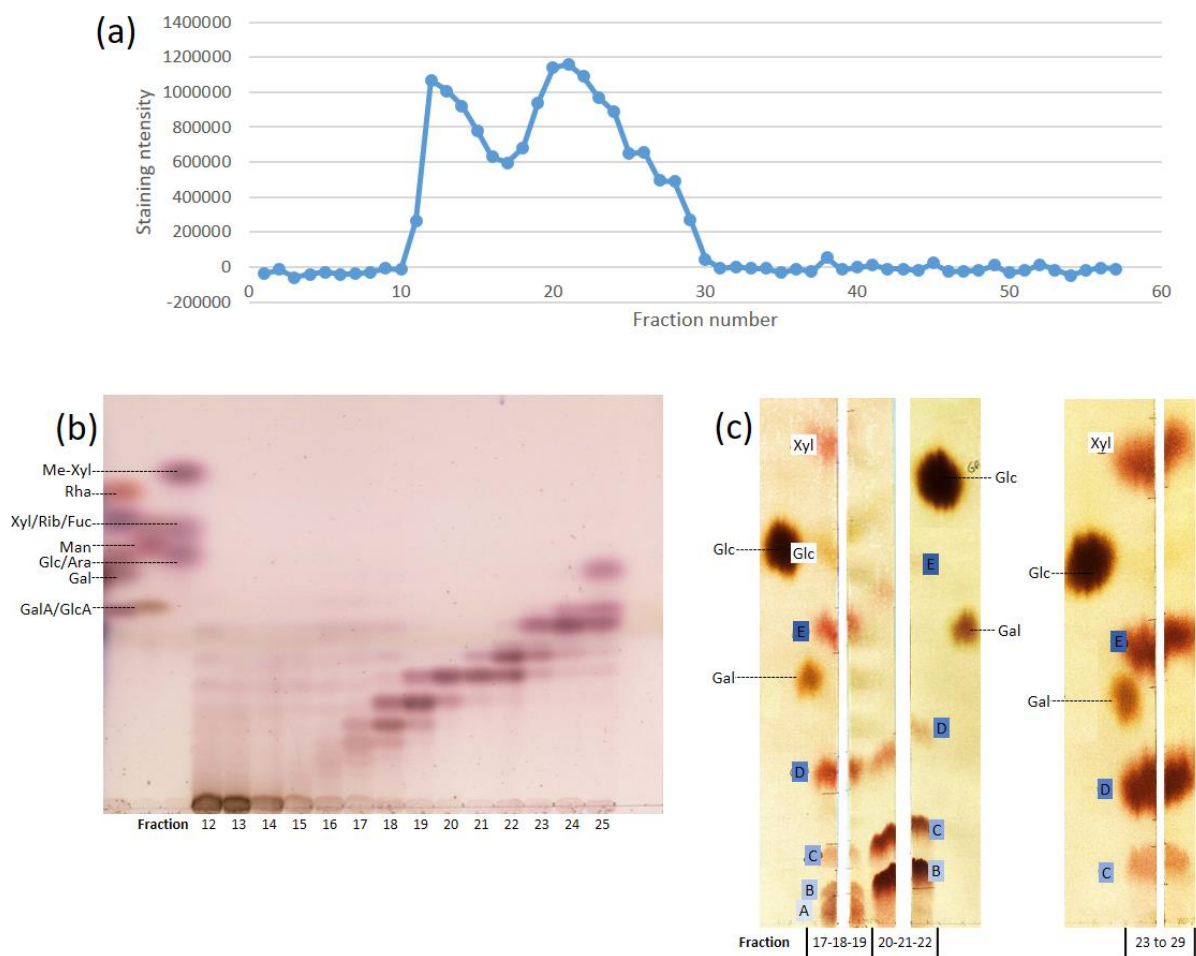


Figure 61: Bulk preparation of xylanase-digested Hb *Ulva*

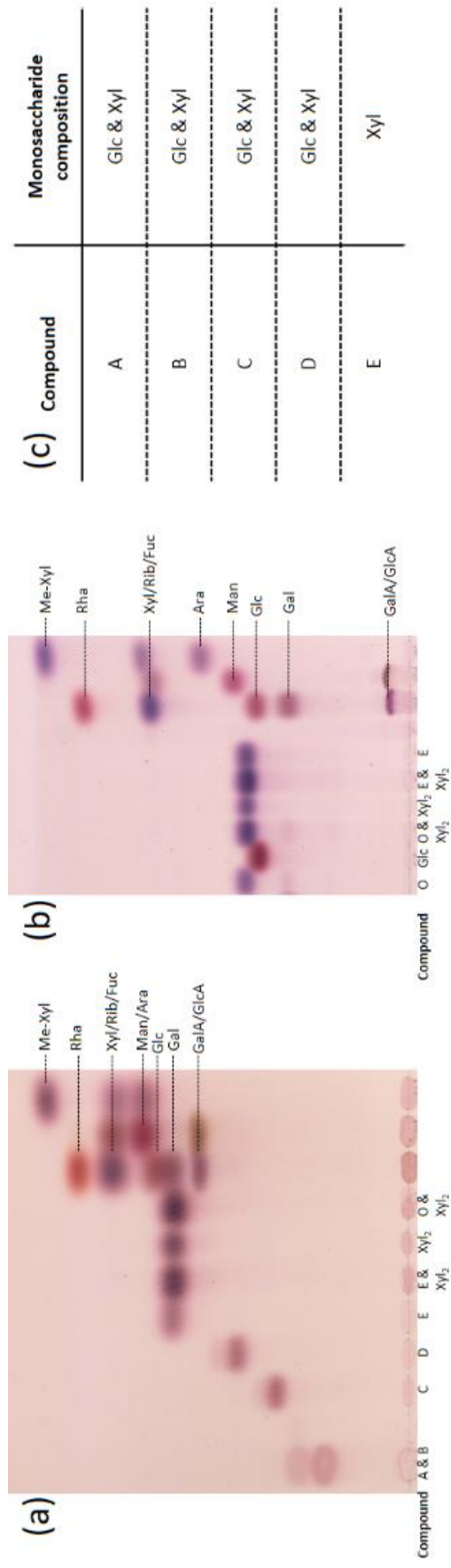
(a): *Hb Ulva* digest was separated by gel permeation chromatography on Bio-Gel P-2. The staining intensity of each fraction, proportional to the fraction's concentration, is displayed. Each fraction was 3 ml big, the void volume was 30 ml and the included volume was 90 ml. (b): Fractions 12 to 25 from Bio-Gel P-2 were separated on TLC, so the range of compounds that have been produced are visible. The TLC was performed on a plastic-back plate and developed once in B/A/W 2:1:1. (c): Fractions 17 to 19, 20 to 22, and 23 to 29, are pooled together and ran preparatively on paper chromatography. PC was ran for 72 h in B/A/W 12:3:5.

Once purified, each compound was examined more closely (Figure 62). Compound E was particularly interesting because it co-eluted with 1,4- β -xylobiose in two different solvent systems. As it was found to only contain xylose, E might be xylobiose. Compounds A to D all contained glucose and xylose, in various ratios. Compounds B, C, D, E, as well as xylobiose and cellobiose, were assayed for their alkali lability. Both xylobiose and cellobiose are made of two sugars, linked via a β -1,4 glycosidic bond. They both were 50% degraded after 30 min,

although some degradation was visible after 6 minutes for xylobiose. After 125 minutes, for both compounds, there was barely any of the initial sugar left. Compound E started isomerising and degrading after 6 minutes, reaches about 50% degradation after 30 minutes, and releases xylose. E is likely to be 1,4- β -xylobiose. Compound D started degrading after 6 minutes, producing one oligomer D' (also visible in C). After 30 minutes, D was about 50% degraded, and displayed the previously mentioned oligomer, a second one, slightly faster, and Glc. After 125 minutes, only Glc was visible. Compound D is likely to be a β -1,4-linked trimer with a Glc unit at its non-reducing end.

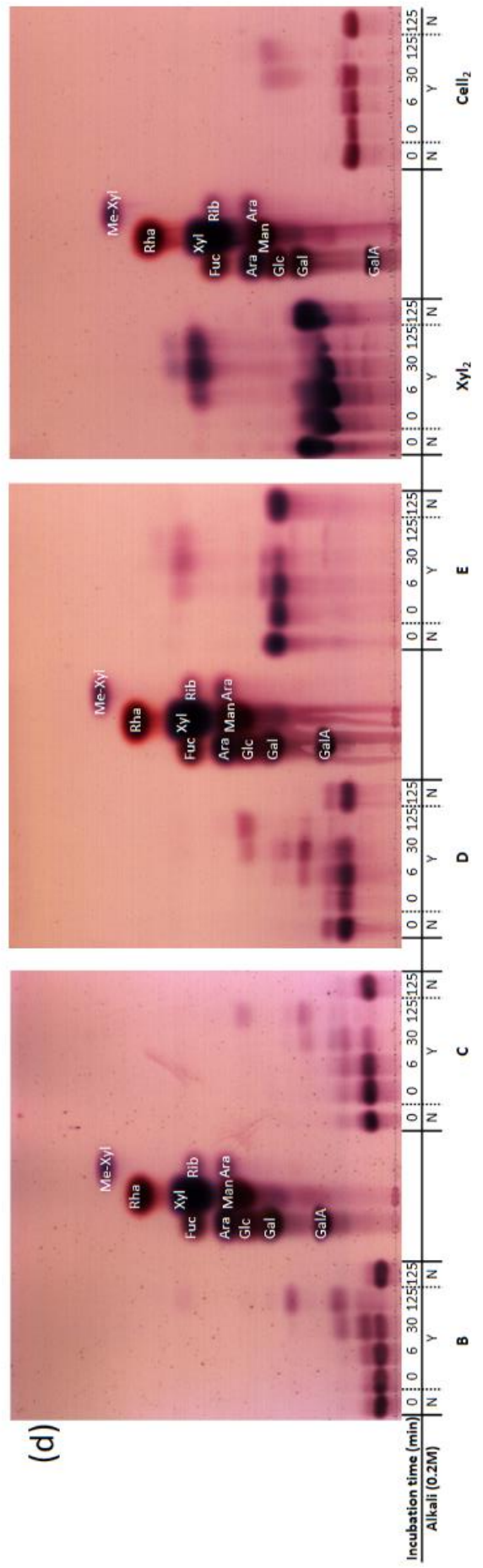
Compound C had a similar pattern of degradation, starting after 6 minutes, reaching about 50% degradation after 30 minutes, and the initial compound being gone after 125 minutes. C degraded to an oligomer that co-migrates with D, then to a second one, D', and to Glc after 125 minutes. Compound C is likely to be a β -1,4-linked tetramer with a Glc unit at its non-reducing end. Compound B had, again, a similar degradation pattern, turning into a C-like oligomer, then a D-like oligomer, then a D'-like oligomer. Compound B is likely to be a β -1,4-linked pentamer with a Glc unit at its non-reducing end.

Compounds B to E, as well as xylobiose and cellobiose as standards, were tested against glucosidase and xylosidase. Both xylobiose and cellobiose, expectedly, were hydrolysed by their corresponding enzyme (xylosidase and glucosidase) to their constituent sugar monomers (xylose and glucose). Samples B to E presented extra bands that were attributed to impurities in the extracts. B was hydrolysed to xylose and a D-like compound by xylosidase and left untouched by glucosidase. C and D were converted into glucose and xylobiose by glucosidase (and not hydrolysed by xylosidase). Finally, E was hydrolysed to xylose by xylosidase.



(c)

Compound	Monosaccharide composition
A	Glc & Xyl
B	Glc & Xyl
C	Glc & Xyl
D	Glc & Xyl
E	Xyl



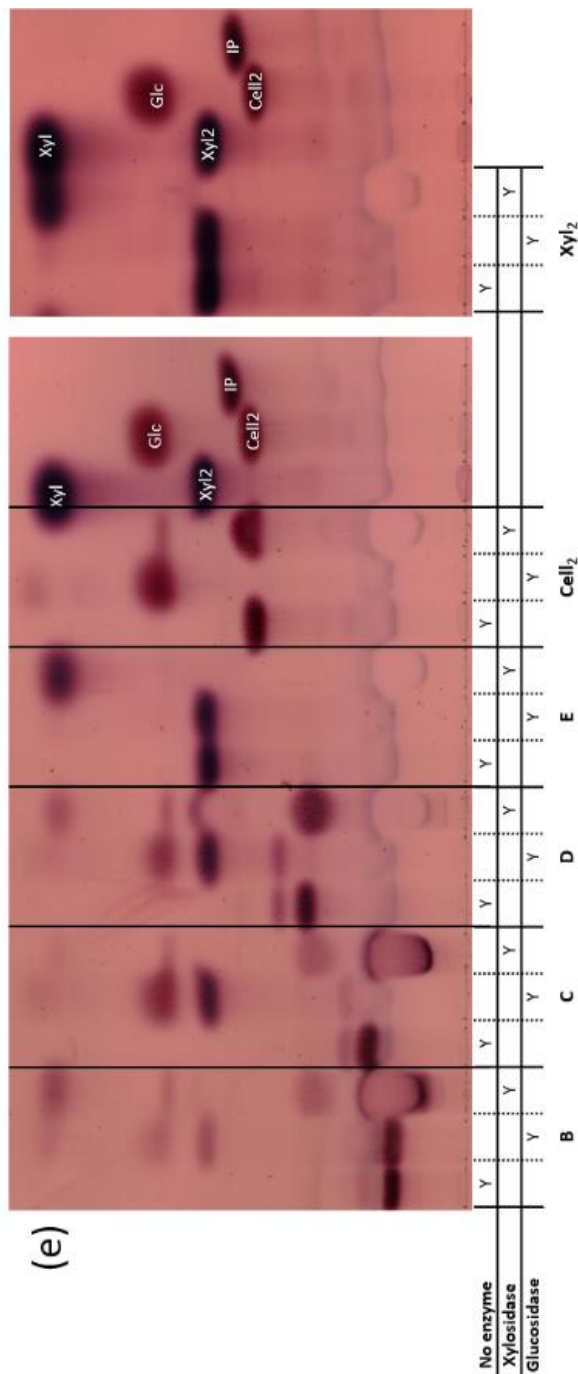


Figure 62: Analysis of the oligomers produced by xylanase digestion of Hb *Ulva*.

(a): Compounds A to E have been eluted off the paper (previous figure), they are ran by themselves. A and B are mixed on this figure. As A is not abundant enough, it will not be examined further. Compound E co-elutes with 1,4-β-xylobiose in this solvent system. (b): Co-elution assay of compound E and 1,4-β-xylobiose in a second solvent system, the result is also positive. (c): Table showing the monosaccharide compositions of all five eluates. (d): Alkali lability assay on B, C, D, E, 1,4-β-xylobiose and cellobiose. B breaks down from 30 minutes onwards, to 3 different oligomers. C also starts breaking down after 30 minutes, produces two oligomers and Glc. D breakdown starts after 6 minutes, it produces 1 oligomer and Glc. E breakdown is significant after 6 minutes, it looks like E isomerizes. E produces xylose. Xylobiose starts breaking down after 6 minutes, producing xylose. Cellobiose isomerizes from 6 minutes and breaks down from 30 minutes, producing Glc. (e): Glycosidase assay with xylosidase and glucosidase on B, C, D, E, xylobiose, and cellobiose. B is hydrolysed to xylose and a D-like compound by xylosidase, C is turned in glucose and xylobiose by glucosidase, D is hydrolysed to glucose and xylobiose in the same conditions. E is hydrolysed to xylose by xylosidase. Cellobiose is hydrolysed to glucose by glucosidase and xylobiose to xylose by xylosidase. (a) was developed once in B/A/W 2:1:1, (b) was developed twice in E/P/A/W 6:3:1:1, (c) and (d) were developed twice in B/A/W 4:1:1.

Thanks to these data, temporary structures for all four oligomers can be drawn: E is β -1,4-xylobiose, D is β -D-glucosyl-(1 \rightarrow 4)-xylobiose, C a tetramer of cellobiose β -(1 \rightarrow 4) linked to xylobiose, and B a pentamer of β -D-xylosyl-(1 \rightarrow 4)- β -D-cellobiosyl-(1 \rightarrow 4)- β -D-xylobiose (Table 9). The samples were analysed via NMR spectroscopy and all of their structures were confirmed (Appendix Table a).

Table 9: Summary of analysis of the oligomers produced by xylanase digestion of Hb *Ulva* and proposed structures.

Compound	Estimated DP	Monosaccharide composition	Reducing end	Glucosidase products	Xylosidase products	Proposed structure
B	5	Glc & Xyl	Xyl	N/A	Xyl & D	
C	4	Glc & Xyl	Glc	Glc & Xyl2	N/A	
D	3	Glc & Xyl	Glc	Glc & Xyl2	N/A	
E	2	Xyl	Xyl	N/A	Xyl	

7.3.2. Driselase assay on *Ulva* Hb

Both extract Hb (alkali-soluble) and P2 (hot oxalate-soluble) from *Ulva* were tested for Driselase digestibility (Figure 63). Driselase is commonly used to hydrolyse land plant cell walls, as it contains a wide mixture of enzymes (cellulase, a range of pectinases and hemicellulases, amongst which xylanase). As expected, P2 did not release any sugar: given how different this extract is to common land plant pectins, it was not surprising. Hb extract, however, did release a range of compounds after only 2 days: the fastest band was identified as xylose, the next 3 were named D1, D2, and D3 from the fastest to the slowest. D1 co-migrates with glucose in this solvent system. When hydrolysed, it only gave more glucose: it was then identified as such. D2 co-migrated with Xyl2 and was a similar colour, and D3 was

only slightly slower and stained pink. When hydrolysed, both D2 and D3 gave xylose and glucose, with a majority of xylose. Two slower oligomers (probably trimers) were faintly visible, but they disappeared after 5 more days of digestion and were not analysed.

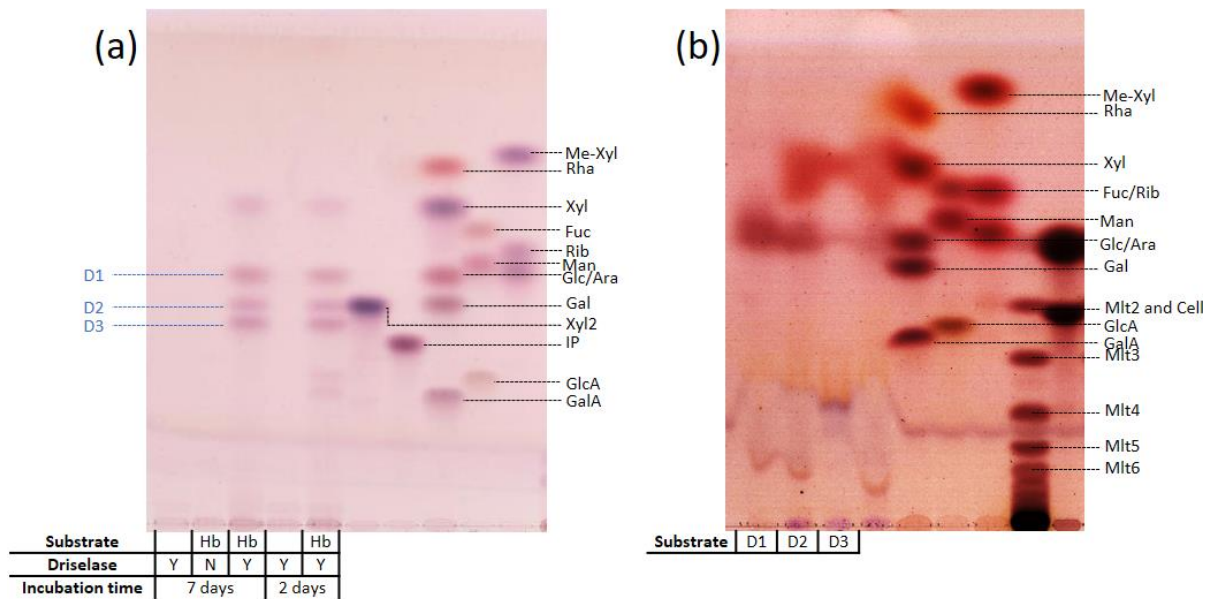


Figure 63: Driselase assay on Hb *Ulva* extract and hydrolysis of the released oligomers. (a): Hb *Ulva* was digested with Driselase for 2 and 7 days, as well as enzyme-less and substrate-less controls. Xylose, D1, D2 and D3 are released after 7 days. (b): Hydrolysis of compounds D1, D2 and D3 eluted from TLC. D1 shows only a Glc band. D2 and D3 contain xylose and glucose (xylose is the major component).

In order to gather more information about the products of hydrolysis, Driselase digestion was performed on 50 mg of hemicellulose Hb from *Ulva*.

The resulting sugar mixture is separated by gel permeation chromatography (Figure 64). As for the xylanase digestion products, the Driselase products were split between two main peaks, one containing polymeric material, centred on fraction 12, and the second containing oligomeric substances, centred on fraction 28. Fractions 23, 25, 27 and 29 were run on TLC to examine their contents. Seven compounds were clearly visible, amongst them Glc and Xyl.

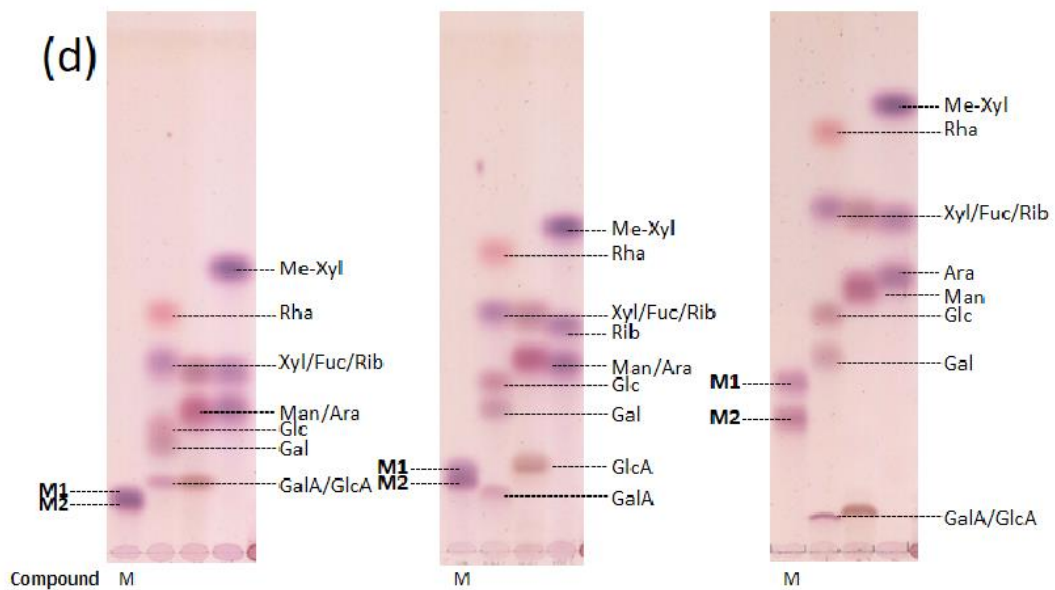
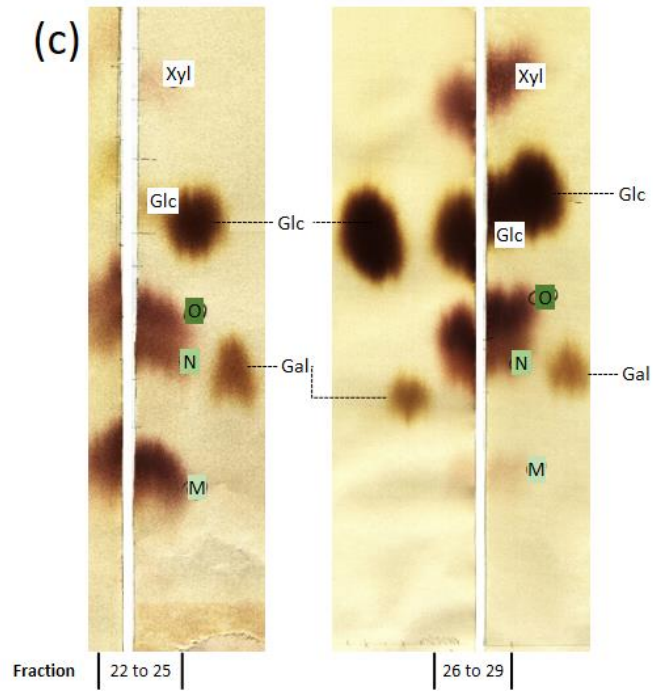
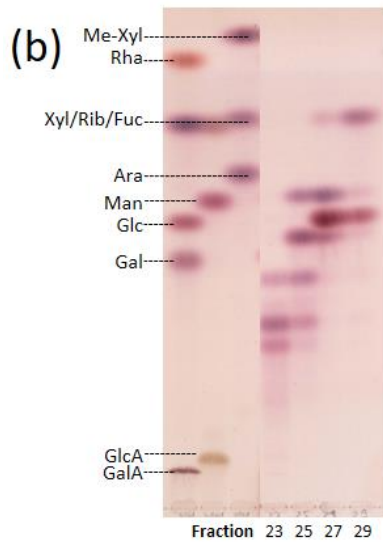
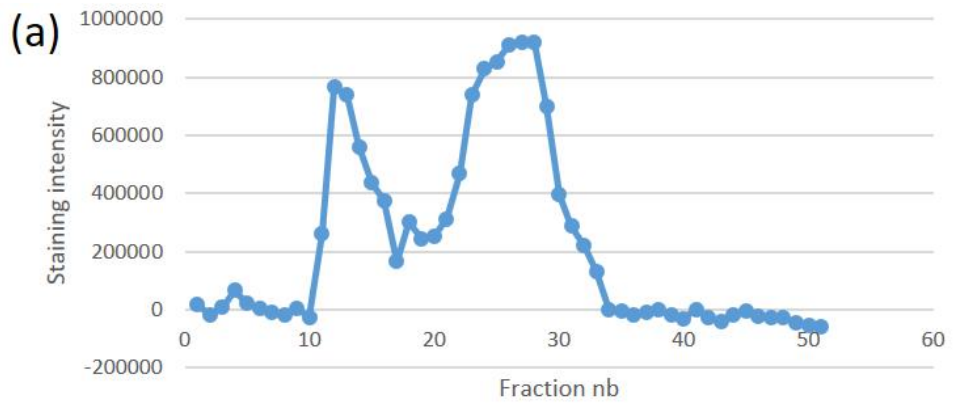


Figure 64: Bulk preparation of Driselase-digested Hb *Ulva*.

(a): Hb *Ulva* digest was separated by gel permeation chromatography on Bio-Gel P-2. The staining intensity of each fraction, proportional to the fraction's concentration, is displayed. Each fraction was 3 ml big, the void volume was 30 ml and the included volume was 90 ml. (b): Fractions 23, 25, 27, and 29, from Bio-Gel P-2 were separated on TLC, so that we can see the range of compounds that have been produced. The TLC was performed on a plastic-back plate and developed twice in E/P/A/W 6:3:1:1. (c): Fractions 22 to 25, and 26 to 29, were pooled together and run preparatively on paper chromatography. PC was ran for 72 h in B/A/W 12:3:5. (d): The compound M contained in fact two oligomers, M1 and M2. Different solvent systems were assayed for efficiently separating them, from left to right: butanol/acetic acid/ water 3:1:1, butanol/ethanol/ water 3:1:1, ethyl acetate/pyridine/propan-1-ol/acetic acid/water 5/2/2/1/1. The latest was the most efficient and was used for separating the rest of M into M1 and M2 by preparative TLC (not shown here).

As these compounds were not pure, fractions were pooled and separated together on preparative PC. Both pools (22 to 25 and 26 to 29) produced, in different ratios, 5 compounds: M, N, O, Glc, Xyl. However, M was in fact made of two oligomers, M1 and M2. They could be separated on preparative TLC after an appropriate solvent system was found, E/P/P/A/W 5:2:2:1:1 (ethyl acetate/pyridine/propan-1-ol/acetic acid/water).

Once purified, the compounds were analysed on TLC (Figure 65). Their monosaccharide compositions were analysed: M1 and O contain only xylose, while M2 and N contain both glucose and xylose. O co-migrated with xylobiose in two different solvent systems, just like E from xylanase-digested Hb *Ulva* (Figure 62 (a)).


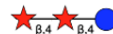
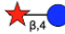

All four samples were submitted to alkali lability assay. O started degrading after 6 minutes and was about 50% degraded after 30 minutes. O released Xyl. O is probably, like E, 1,4- β -xylobiose. N is slightly slower than O. When submitted to alkali degradation, it started isomerising after 6 minutes, and was about 50% degraded after 30 minutes. As N contains both xylose and glucose, it is likely to be the dimer gluco- β -1,4-xylose. M2 also contains glucose and xylose. When degraded with alkali, M2 starts breaking down after 6 minutes,

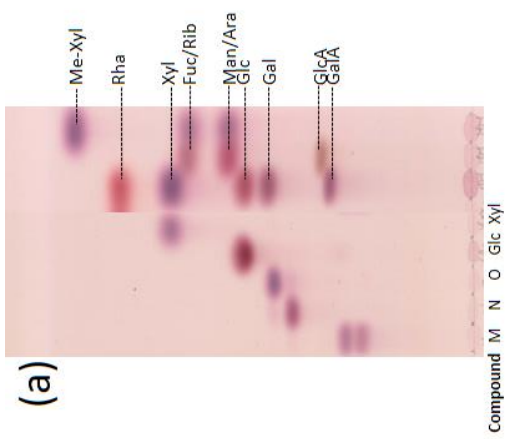
although this degradation is more visible after 30 minutes. M2 released a xylobiose-like oligomer and Xyl, thus M2 might be the β -1,4-linked trimer Xyl-Xyl-Glc. As M1 followed the exact same degradation pattern and presented the same degradation products, but contained only Xyl, M1 might be 1,4- β -xylotriose.

Compounds M1 to O, as well as xylobiose and cellobiose as standards, were tested against glucosidase and xylosidase. Both xylobiose and cellobiose, as previously, were hydrolysed by their corresponding enzyme (xylosidase and glucosidase) to their constituent sugar monomers (xylose and glucose). M1 and O were hydrolysed to xylose by xylosidase and left untouched by glucosidase. M2 and N were also hydrolysed by xylosidase and released xylose and glucose, they were not degraded by glucosidase.

Thanks to these data, temporary structures for all four oligomers can be drawn: M1 is β -1,4-xylotriose, M2 is β -D-xylobiosyl-(1 \rightarrow 4)-glucose, N is β -D-glucosyl-(1 \rightarrow 4)-xylobiose, and O is β -1,4-xylobiose (Table 10). The samples were analysed via NMR spectroscopy and all of their structures were confirmed (Table b Appendix).

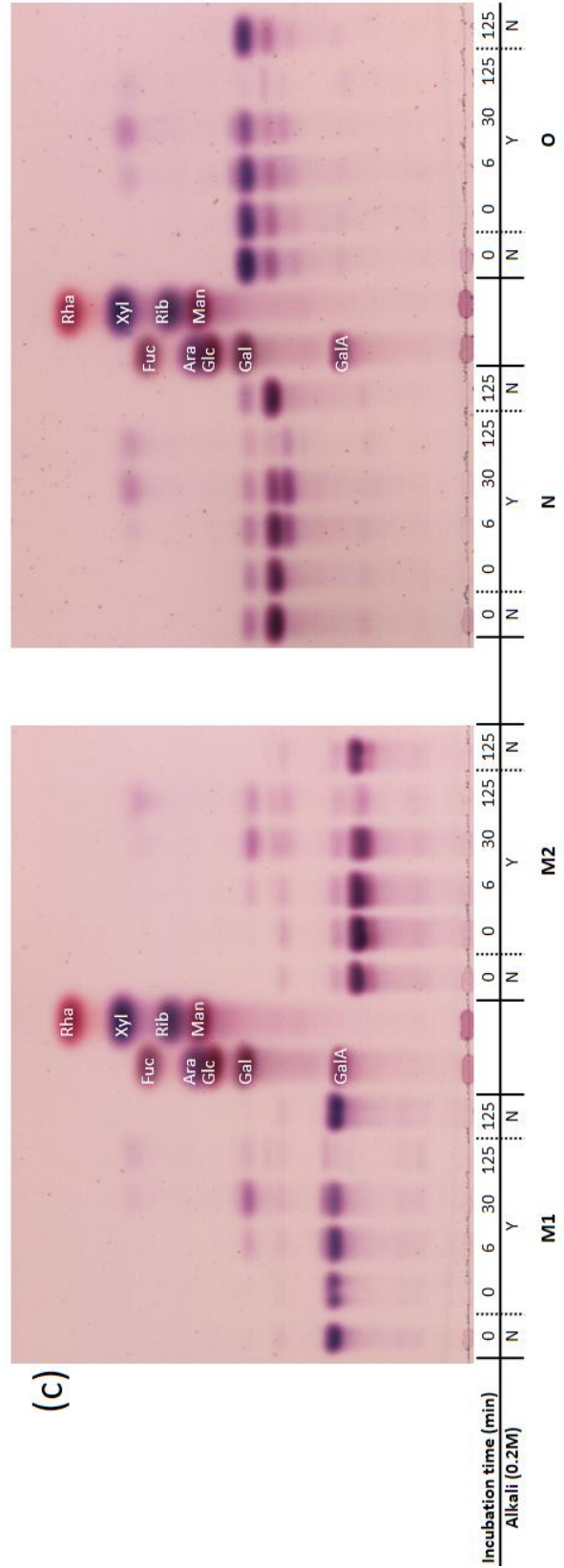
Table 10: Summary of analysis of the oligomers produced by Driselase digestion of *Hb Ulva* and proposed structures.

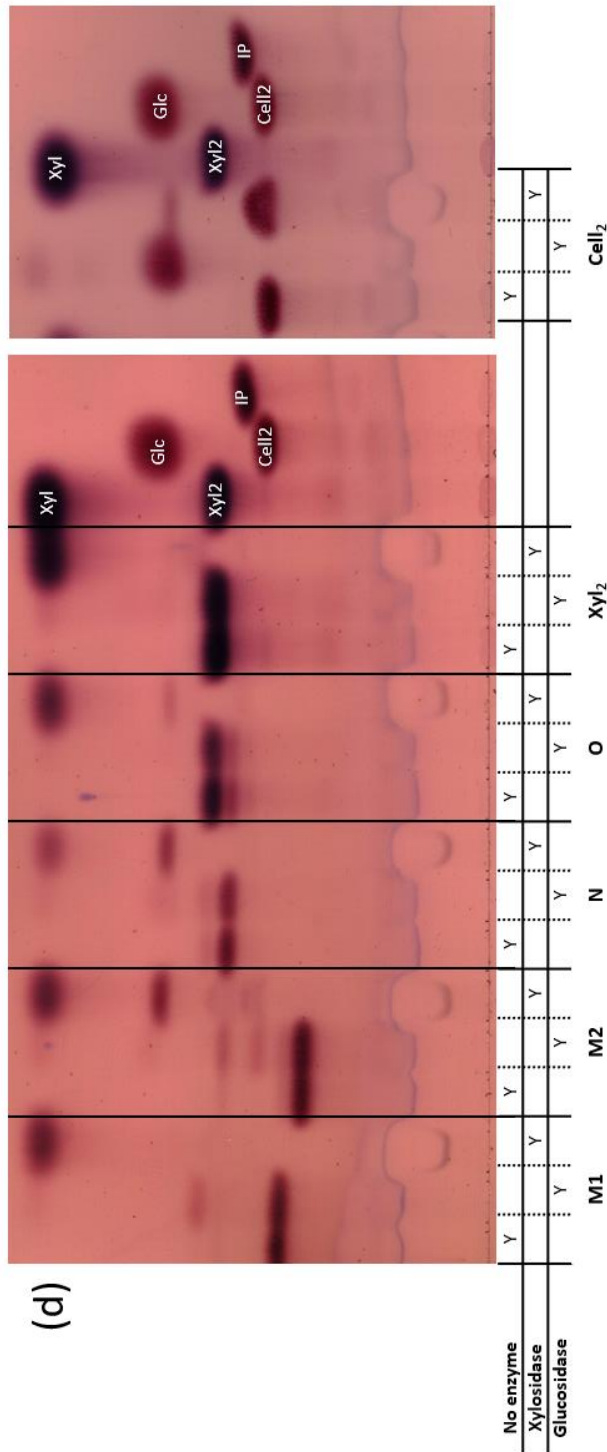
Compound	Estimated DP	Monosaccharide composition	Reducing end	Glucosidase products	Xylosidase products	Proposed structure
M1	3	Xyl	Xyl	N/A	Xyl	
M2	3	Glc & Xyl	Xyl	N/A	Glc & Xyl	
N	2	Glc & Xyl	Xyl	N/A	Glc & Xyl	
O	2	Xyl	Xyl	N/A	Xyl	



(b)

Compound	Monosaccharide composition
M1	Xyl
M2	Glc & Xyl
N	Glc & Xyl
O	Xyl





(d)

Figure 65: Analysis of the oligomers produced by Driselase digestion of Hb Ulva.

(a): Compounds M to O have been eluted off the paper (previous figure), they were run by themselves on TLC. M1 and M2 are mixed on this figure. (b): Table showing the monosaccharide compositions of all four eluates. (c): Alkali lability assay on M1, M2, N, and O. (d): Glycosidase assay with xylosidase and glucosidase on M1, M2, N, O, xylobiose, and cellobiose. (a), (c) and (d) were developed twice in B/A/W 4:1:1.

7.3.3. Cellulase assays on *Ulva* Hb

Given the previous results, it seemed natural that digestion of Hb *Ulva* with cellulase would give oligomers rich in xylose, as these ones should not be digestible by the 1,4- β -glucanase. Following this hypothesis, 50 mg of Hb were enzymatically hydrolysed and separated on Bio-Gel P-2 (Figure 66 (a)).

As previously, two main peaks were observable, one centred on fraction 12 (polymeric material) and one centred on fraction 23 (oligomeric and monomeric material). The second peak, which contained the digestion products, was the most relevant in this experiment. It was made of a main peak around fraction 22, and of a secondary peak around fraction 27. The contents of fractions 11 to 27 were examined on TLC (Figure 66 (b)). Up to fraction 17, only polymers or large oligomers were present: they all stayed stuck or very close to the origin. Fractions 18 and 19 displayed mobile sugars, but no band was clearly visible. From fraction 20 and up to fraction 28, it was easy to identify a range of oligomers with varying mobilities, each spanning about 4 fractions. In order to purify these oligomers, fractions 20 to 27 were pooled together and run on preparative PC (Figure 66 (c)). The oligomers were cut out and eluted.

Once purified, the compounds were analysed on TLC (Figure 67). Compounds R and S were not separated by paper chromatography, they had to be run in a different solvent system on TLC (ethyl acetate / pyridine / propanol / acetic acid / water 5:2:2:1:1). The monomer composition of all six compounds was tested: P, Q, S, and U all contained both glucose and

xylose, R and T contained only glucose. P was not analysed further, as only a very small amount of it was produced.

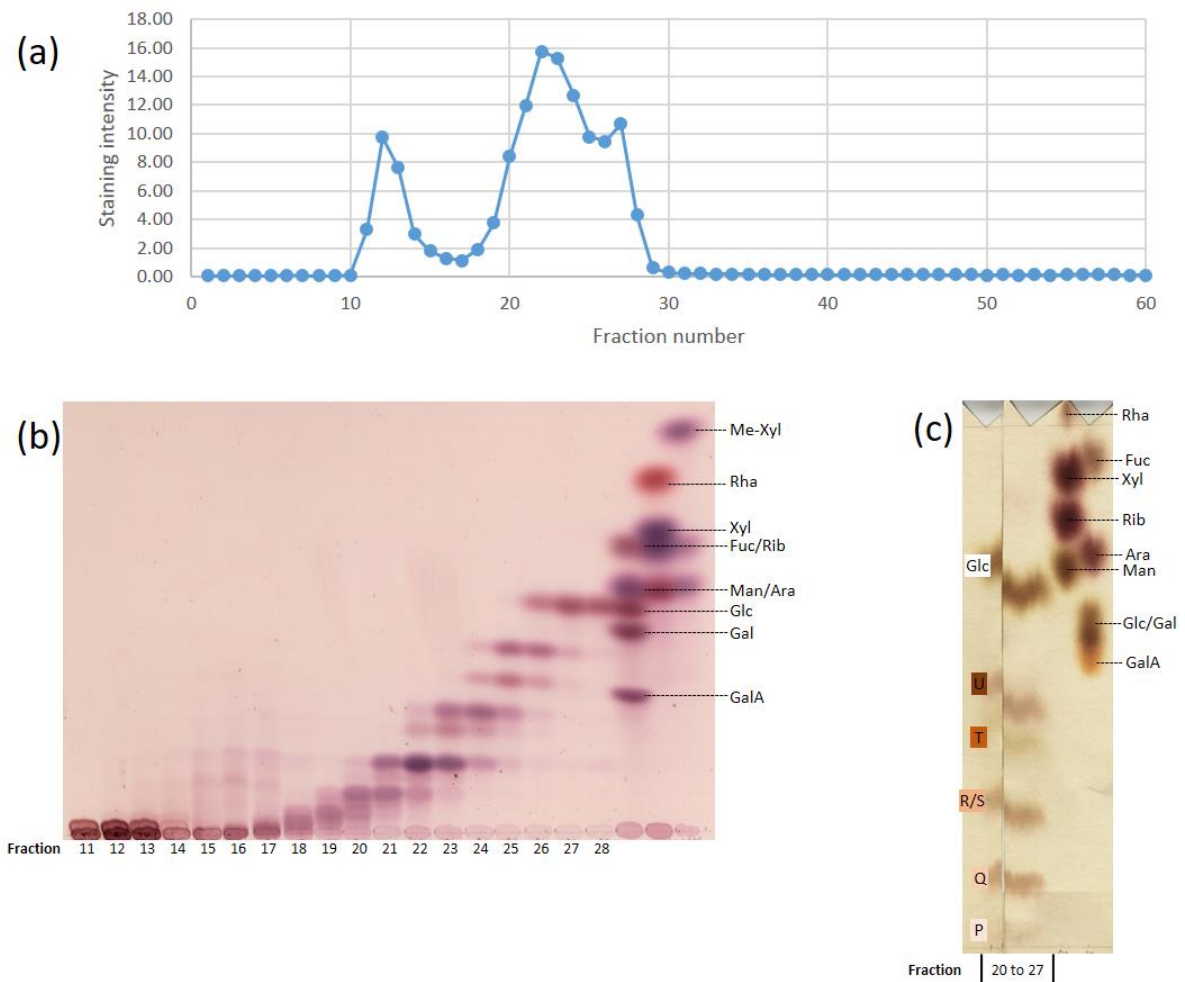


Figure 66: Bulk preparation of cellulase-digested Hb *Ulva*.

(a): Hb *Ulva* digest was separated by gel permeation chromatography on Bio-Gel P-2. The staining intensity of each fraction, proportional to the fraction's concentration, is displayed. Each fraction was 3 ml big, the void volume was 30 ml and the included volume was 90 ml. (b): Fractions 11 to 28 from Bio-Gel P-2 were separated on TLC, so that the range of compounds that have been produced was visible. The TLC was performed on a plastic-back plate and developed twice in B/A/W 4:1:1. (c): Fractions 20 to 27 were pooled together and run preparatively on paper chromatography. PC was ran for 72 h in B/A/W 12:3:5.

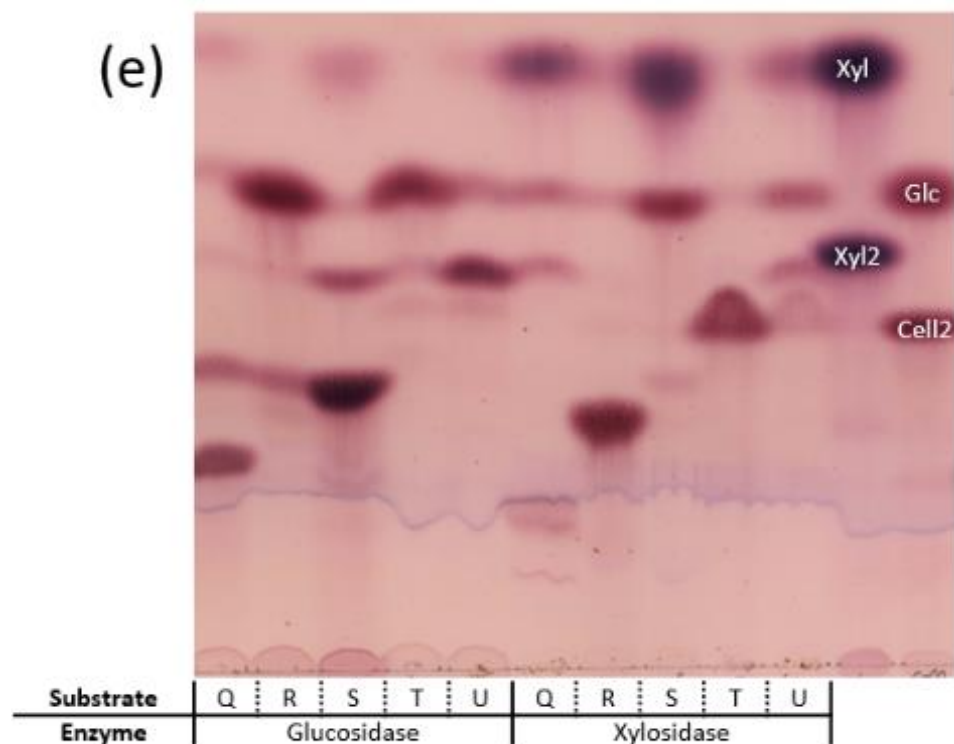


Figure 67: Analysis of the oligomers produced by cellulase digestion of Hb *Ulva*. (a): Compounds P to U were eluted off the paper (previous figure), they were run by themselves on TLC, untreated and acid-hydrolysed. R and S were mixed on this figure. (b): Left: Separation of compounds R and S on TLC in a different solvent system: ethyl acetate/pyridine/propanol/acetic acid/water 5:2:2:1:1. This analytic chromatography was repeated preparatively (not shown here). Right: R and S, acid hydrolysed. (c): Table summarising the monosaccharide compositions of all six eluates. (d): Alkali lability assay on Q, R, S, T and U. (e): Glycosidase assay with xylosidase and glucosidase on Q, R, S, T, and U. (a), (c), (d) and (e) were developed twice in B/A/W 4:1:1.


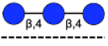
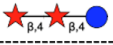
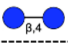
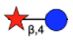
All five remaining samples were submitted to alkali lability assay. Q started degrading after 6 minutes and was about 50% degraded after 30 minutes. Xylobiose was released, as well as another heavier oligomer. R presented the same degradation rate as Q and produced a range of oligomers, the smallest of them migrating between xylobiose and cellobiose, and staining pink. S was also degraded at the same rate, and released xylobiose, xylose, as well as an isomer of S, after 30 minutes. T and U both followed the same degradation rate, producing respectively glucose and xylose residues.

Compounds Q to U were tested against glucosidase and xylosidase. As with oligomers produced by xylanase digestion of Hb, the samples were not pure and parasitic bands can be seen on the TLC scan. However, it is still possible to draw conclusions. Q, S, and U were hydrolysed to xylose and glucose by xylosidase and left intact by glucosidase. R and T were hydrolysed to glucose by glucosidase and left intact by xylosidase.

Thanks to these data, temporary structures for all five oligomers can be drawn: Q is β -D-xylotriosyl-(1 \rightarrow 4)-glucose, R is cellotriose, S is a trimer of β -D-xylobiosyl-(1 \rightarrow 4)-glucose, T is cellobiose, and U is β -D-xylosyl-(1 \rightarrow 4)-glucose (Table 11). The samples were analysed via NMR spectroscopy and most of their structures were confirmed (Table c Appendix).

However, R was not cellotriose but β -D-laminaribiosyl-(1 \rightarrow 4)-glucose, as shown by the NMR data. This fits with the features described earlier in this work.

Table 11: Summary of analysis of the oligomers produced by cellulase digestion of Hb *Ulva* and proposed structures.

Compound	Estimated DP	Monosaccharide composition	Reducing end	Glucosidase products	Xylosidase products	Proposed structure
Q	4	Glc & <u>Xyl</u>	Xyl2	N/A	<u>Xyl</u> & Glc	
R	3	Glc	?	Glc	N/A	
S	3	Glc & <u>Xyl</u>	<u>Xyl</u>	N/A	<u>Xyl</u> & Glc	
T	2	Glc	Glc	Glc	N/A	
U	2	Glc & <u>Xyl</u>	<u>Xyl</u>	N/A	<u>Xyl</u> & Glc	

7.3.4. Behaviour of xylanase and cellulase

In order to obtain more information on the previously characterised oligomers, the features of the activity of the enzymes used in this chapter were examined.

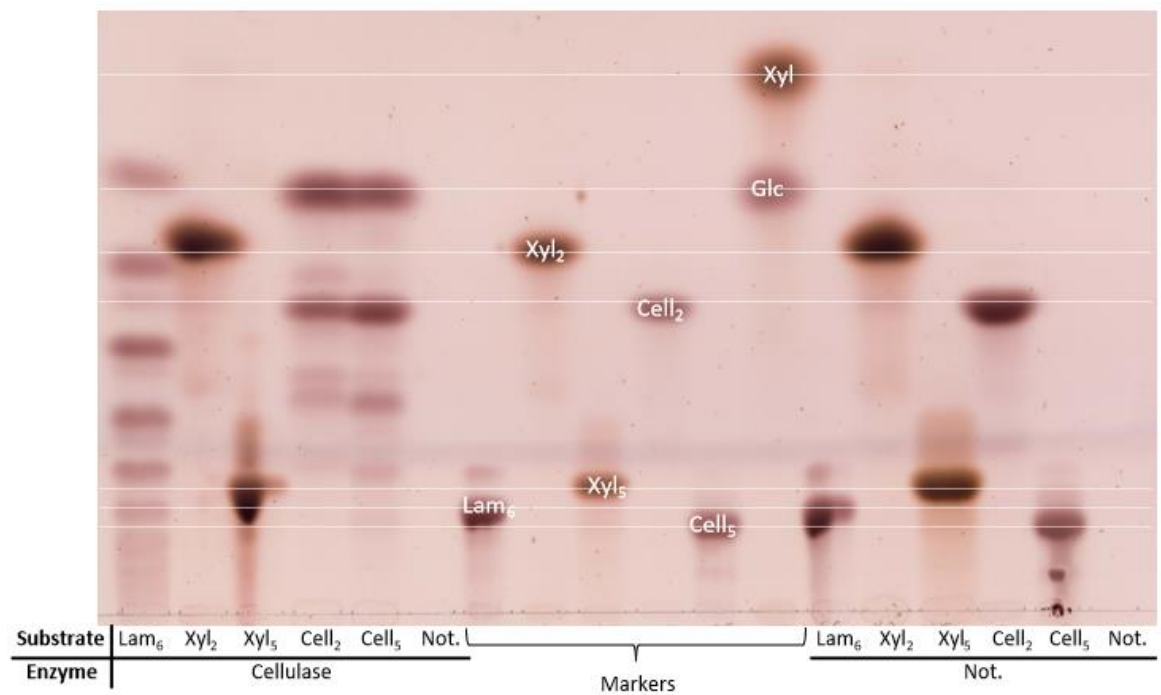
When assayed on commercial oligomers, xylanase was unable to hydrolyse glucose-based compounds (cellobiose, cellopentaose, and laminarihexaose) and xylobiose. However, it did break down xylopentaose to xylobiose and xylose (Figure 68 (a)). This data suggests that xylanase is only capable of cleaving β -(1 \rightarrow 4) bonds between Xyl residues if at least two successive residues are present on at least one side of the enzyme action site. When assayed on Driselase-produced oligomers, xylanase broke down xylotriose (M1) to xylobiose and Xyl, and β -D-xylobiosyl-(1 \rightarrow 4)-glucose (M2) to xylobiose and glucose (Figure 68 (b)). This showed that the two successive Xyl residues necessary to the enzymatic cleavage must be placed on the non-reducing side of the enzyme action site. The structures of the xylanase-produced B, C, D, and E could therefore be extended by two Xyl on their non-reducing end (Table 12).

Driselase was equally assayed on commercial oligomers (Figure 68 (a)). It hydrolysed cellobiose, cellopentaose, and laminarihexaose to glucose. Xylobiose was only partially hydrolysed to Xyl. A xylosyltransferase activity was also observed as xylotriose was produced (as a trace). In the same way, xylopentaose was hydrolysed to a series of xylo-tetraose, xylo-triose, xylo-biose and xylose. This data did not allow for any new hypothesis on the behaviour of Driselase and the study of the enzyme mixture was not carried out further.

Finally, cellulase activity on commercial oligomers was studied (Figure 68 (a)). It was not active on xylobiose nor on xylopentaose, as expected. It partially hydrolysed cellobiose to Glc, producing a trace of cellotriose from a minor glucosyltransferase activity. In the same way, cellopentaose was hydrolysed to cellotetraose, cellotriose, cellobiose and Glc. Cellulase was also able to hydrolyse laminarihexaose to a ladder of laminarino-oligomers, showing it is not β -(1 \rightarrow 4) specific. When assayed on xylanase-produced oligomers, cellulase was able to

hydrolyse β -D-xylosyl-(1 \rightarrow 4)- β -D-cellobiosyl-(1 \rightarrow 4)- β -D-xylobiose (B) to xylobiose, xyloglucose and Glc, showing it was only able to cleave the oligomer after a Glc residue. It was also able to hydrolyse β -D-cellobiosyl-(1 \rightarrow 4)- β -D-xylobiose (C) to xylobiose, cellobiose and Glc, thus confirming the previous hypothesis. However, β -D-glucosyl-(1 \rightarrow 4)-xylobiose (D) was not hydrolysed at all by cellulase: it might be that only one Glc residue on the non-reducing side of the enzyme action site is needed if the cleaving happens in the middle of an oligomer, however, if the glycosidic bond being cut is at the non-reducing end of the substrate, then two Glc residues are needed, one on each side of the cleaving site (Figure 68 (b)). Given that all the oligomers produced by cellulase digestion of Hb *Ulva* are thought to be an integral part of the polymer (and not specifically its non-reducing ends), their structures can be extended by one Glc residue at the non-reducing end (Table 9, Table 10, and Table 11).

This data allows for producing a model for the structure of the phyco-xyloglucan constitutive of Hb *Ulva* (Table 12).



(b)

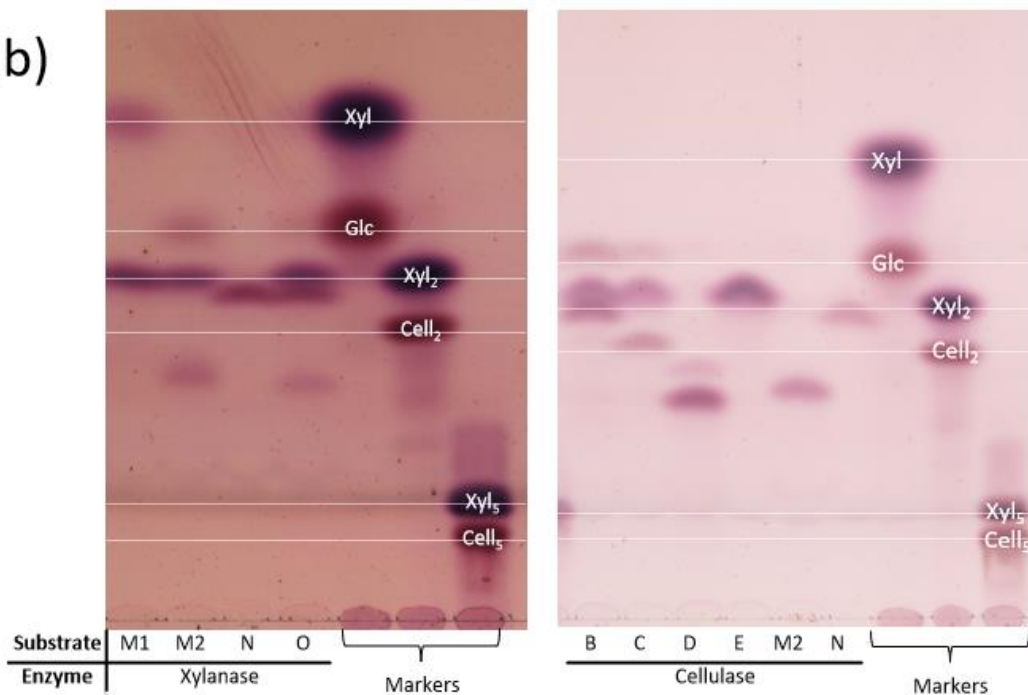


Figure 68: Study of the behaviour of xylanase, Driselase and cellulase on commercial and *Ulva*-based oligomers.

(a): Laminarihexaose, xylobiose, cellobiose, xylopentaose, cellopentaose and water were incubated with xylanase, Driselase, cellulase and buffer. (b): Xylanase was assayed on the Driselase-produced oligomers from Hb *Ulva* M1, M2, N, and O; cellulase was assayed on the xylanase-produced oligomers from Hb *Ulva* B, C, D, and E, and on Driselase-produced oligomers from Hb *Ulva* M2 and N. All TLCs were performed on plastic-backed plates and developed twice in B/A/W 4:1:1.

Table 12: Final structures of the oligomers produced enzymatically from Hb *Ulva* and proposed structure for phyco-xyloglucan.

Enzyme used to produce the oligomer	Compound	Proposed structure
Xylanase	B'	
	C'	
	D'	
	E'	
	M1	
Driselase	M2	
	N	
	O	
	All segments combined	
Cellulase	Q'	
	R'	
	S'	
	T'	
	U'	

Summary of all the structures previously described. The structures of the oligomers that could be extended thanks to supplementary analysis of the enzyme action are written X', the others are described with their previously assigned letter.

7.4. *Ulva* hemicellulosic extract Hb: study of the affinity of phyco-xyloglucan for cellulose

7.4.1. Measurement of hemicellulose/cellulose affinity

The affinity of phyco-xyloglucan for cellulose was studied, in parallel with land-plant polymers. The polysaccharides were simply incubated with Whatman paper n1, for various durations (Figure 69).

It was obvious that all polymers interacted at least to some degree with cellulose, as the measured concentration of the solution drops by 4% (mixed-linkage glucan) to 20% (Hb *Ulva*) just after mixing. Overtime, the land-plant polymers seemed to interact only weakly with the cellulose: after 72h, all their concentrations had dropped by less than 20%, with mixed-linkage glucan looking like it might be the land-plant polymer with the strongest affinity for cellulose in that length of time. In comparison, the concentration in solution of Hb *Ulva* dropped to 56% after 72h, indicating that almost half the polymer became attached to the cellulose of paper.

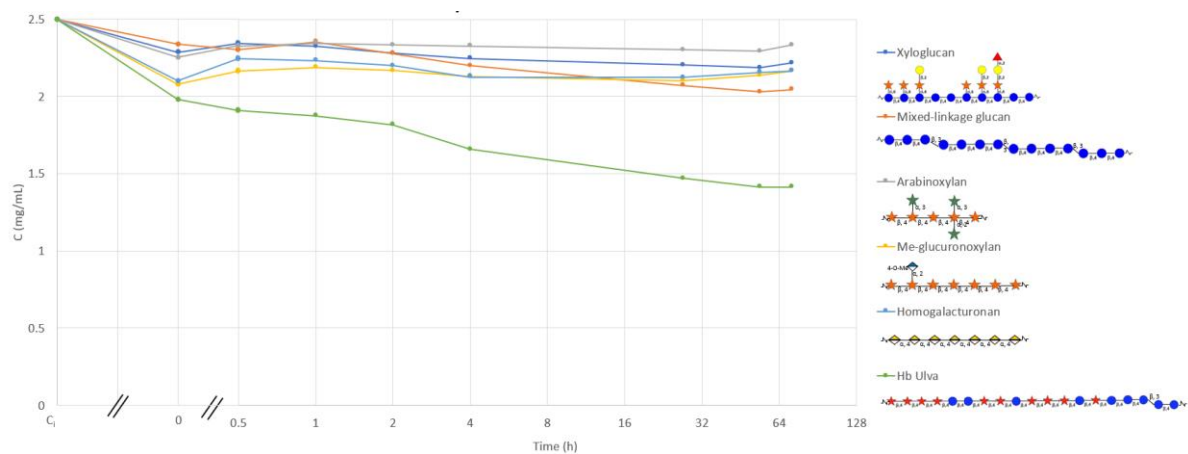


Figure 69: Study of the affinity of a range of polysaccharides for cellulose.

Polymer solutions (2 mL, $C_i=2.5$ mg/mL) were incubated with Whatman N1 paper strips (125 mg) for various amounts of time at room temperature on the rotating wheel. At each timepoint, an aliquot is taken out of solution is the incubation is continued. Timepoint 0 corresponds to a five minutes incubation to ensure the paper is wetted through before carrying on the experiment for a longer period of time.

7.4.2. Affinity of xylose for α -cellulose

α -cellulose was digested with endo-cellulase and incubated in endo-cellulase buffer as a control. Both samples were then incubated in 70% ethanol and centrifuged, giving two fractions for each: supernatant and pellets. The pellets contained, in principle, the polymers that were insoluble in ethanol: they were the sugars that could not be broken down to monomers and oligomers by cellulase or in buffer. The supernatant should contain the solubilised fraction of α -cellulose, i.e. the sugars that were digested and were hydrolysed to monomers or oligomers. Each of these fractions was acid-hydrolysed in order to examine their monomeric contents. The hydrolysates were separated on TLC. As it was difficult to read the results on the plate, profiles of staining intensity were taken and are displayed, compared by pairs: the enzyme-produced pellet and supernatant together, both supernatant (with and without enzyme), and both pellets (with and without enzyme) (Figure 70).

When treated with enzyme, cellulose released traces of xylose in the supernatant, but none in the pellets (top graph Figure 70 (c)). The phyco-xyloglucan previously characterised is digestible by cellulase, and releases xylose-rich oligomers. It is possible that this polysaccharide interacts with the cellulose micro fibrils at their surfaces, thus being very accessible to the enzyme. Moreover, cellulose is particularly resistant to the acid hydrolysis (TFA) used in this experiment, making non-cellulosic polymers even more prominent if they were present (in the pellet hydrolysate). The absence of xylose in the pellet makes it clear that xylose-containing polysaccharides were indeed solubilised in the presence of cellulase.

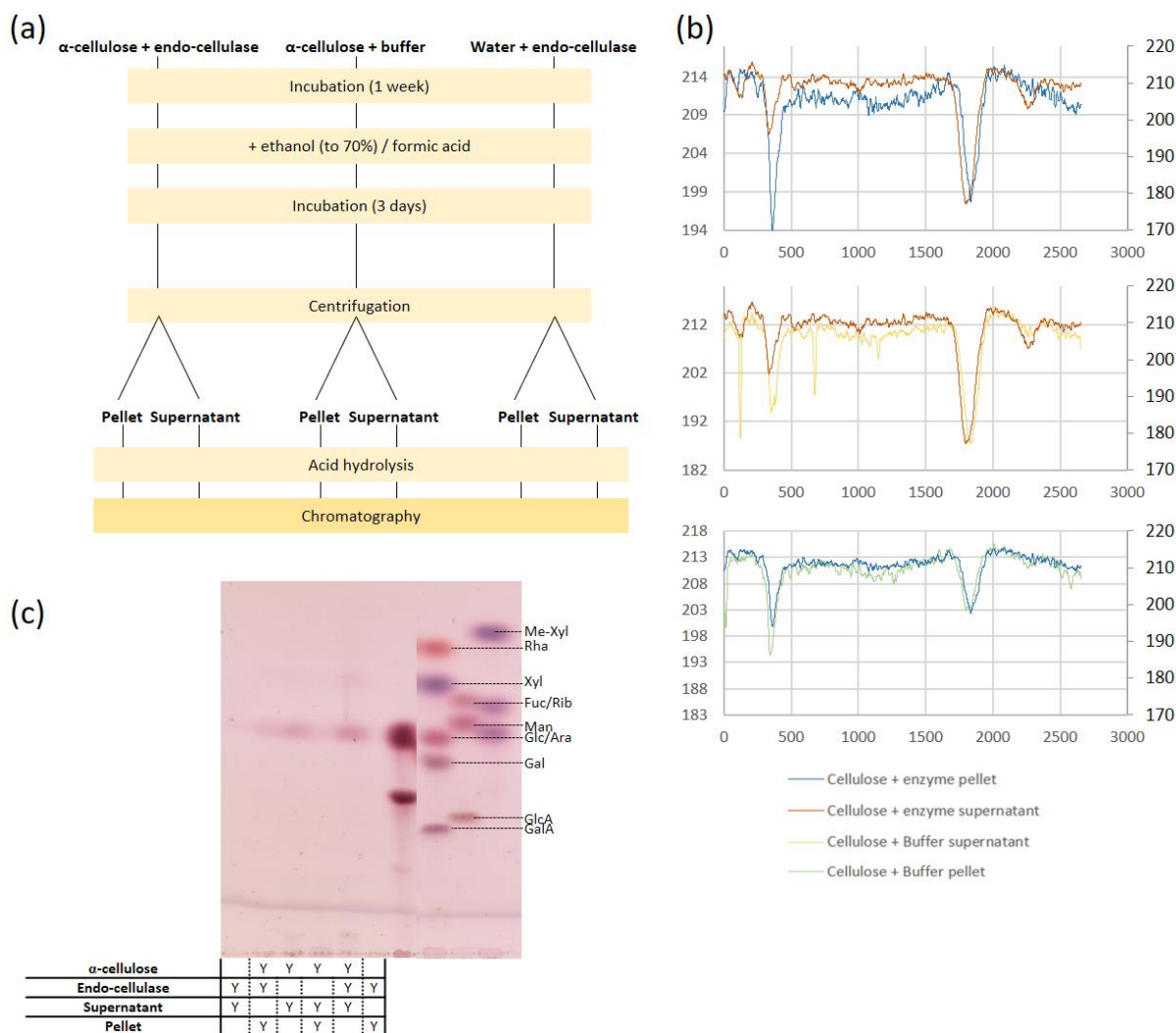


Figure 70: Assessment of the xylose content in the α -cellulose fraction from *Ulva*.

(a): α -cellulose was incubated with endo-cellulase and in endo-cellulase buffer. After the digestion was finished, the oligomers and the polymers were separated by incubation in 70% ethanol and centrifugation, giving two fractions: the supernatant and the pellets. As a control, the same protocol was applied without substrate, but with enzyme. Each of these was hydrolysed with TFA. The hydrolysates of the different fractions were separated on TLC twice in B/A/W 4:1:1. (b): Because the previous TLC was difficult to read (low loading), each track's profile was measured. They are compared two by two. Top: comparison of the supernatant and the pellet of cellulase-digested cellulose. Middle: comparison of the supernatants of cellulose incubated in buffer and with enzyme. Bottom: comparison of the pellets of cellulose incubated in buffer and with enzyme.

The profiles of the supernatants of cellulase-digested and buffer-incubated cellulose were also compared (middle graph Figure 70 (c)). Interestingly, xylose and glucose were present in both samples, even though there was more sugar in the enzymatic extract. Given that the

incubation lasted for an entire week, polymers might have been solubilised overtime, without the presence of an enzyme. Relatively to glucose, less xylose was detected in the buffer-incubated cellulose supernatant. This might be due to the fact that phyco-xyloglucan was not preferentially solubilised, as it may have been with the enzyme.

Finally, the profiles of the pellets of cellulase-digested and buffer-incubated cellulose were also compared (bottom graph Figure 70 (c)). In this case, the buffer-incubated sample displayed slightly more xylose than the enzymatically-digested one. This follows logically the trend previously described in the supernatants: with the enzyme, more xylose-containing polymers are solubilised and are present in the supernatant, without it, fewer xylose-containing polymers are solubilised and they are more prominent in the pellet.

Overall, this experiment indicates strongly the presence of phyco-xyloglucan, in the α -cellulose fraction from *Ulva*. This cellulase-digestible polymer is easily accessible to the enzyme, thus it is probably interacting with the surface of the cellulose micro fibrils.

7.5. Conclusion

The 'pectic' fraction from *Ulva* was expected to contain the well-known and well-characterised polymer ulvan, however its hydrolysate seemed to contain excessive amounts of Rha. In order to verify this, P2 from *Ulva* was submitted to mild hydrolysis and the products were separated by gel-filtration chromatography, producing two key oligomers, XR and R2. The first one, XR, was found to be the well-known Xyl-Rha dimer from ulvan. The second, however, was found to be a dimer of Rha, probably (1→2)-rhamnobiore, which had

not been found before in *Ulva* spp. This could indicate variations in ulvan structure, which may be species-specific, developmental, or seasonal, amongst others.

The 'hemicellulosic' fraction from *Ulva* was tested for its susceptibility to xylanase hydrolysis. It was found to indeed be broken down by the hydrolase, producing xylose-containing oligomers. Therefore, the process was repeated preparatively so that the oligomers could be analysed through acid hydrolysis, alkaline degradation, and glycosidase assay. This process was repeated on oligomers produced from the digestion of Hb *Ulva* with Driselase and cellulase. This led to establishing a possible structure for the alkali-extractable fraction of *Ulva*, named phyco-xyloglucan.

The interaction of phyco-xyloglucan with cellulose was studied. It was found that, in comparison with land-plant polymers, the algal polysaccharide interacted extremely strongly and extremely fast with cellulose (Zhang *et al.* 2015). Moreover, xylose was released by the cellulase digestion of the α -cellulose fraction of *Ulva*, which is an indicator for the presence of phyco-xyloglucan. Therefore, it is possible that phyco-xyloglucan interacts strongly with the surface of the cellulose microfibrils, but does not penetrate their cores, as Xyl was not found in the acid hydrolysates of non-cellulase digestible residues.

8. Discussion: Botanical significance of unique algal polysaccharides features

8.1. Charophytic and chlorophytic green algae – reminders and objectives of this thesis

Charophytic green algae, as part of the streptophytes, share a considerable number of features with land plants. They form a highly heterogeneous group whose biochemical features can be compared with those of the embryophytes (Hall and Delwiche 2007; Popper *et al.* 2011). That way, it is possible to get information on plant evolution and phylogeny. In particular, comparing charophytic and embryophytic cell walls provides an insight into the phenomena that allowed plants to conquer dry land, such as adaptation to drought or to excess UV light, or the mechanical features that allowed plants to grow vertically (Albersheim *et al.* 2011). However, charophytic cell walls remain partly mysterious: the diversity within the group, and the absence of known human use for them, have been major obstacles to their study, apart for academic purposes (McCourt *et al.* 2004; Domozych *et al.* 2016). However, some charophyte-based materials may be useful: previous studies have shown some of these algae were capable of surviving in extreme environments and may be useful as phytoremediators or pollution indicators in acidic, metal-polluted environments (Triboit *et al.* 2010; Karsten and Holzinger 2014; Sooksawat *et al.* 2016). Characterising their cell walls and scoping their properties may therefore be useful to the potential future biotechnological use of these ubiquitous green algae.

Late-diverging charophyte cell walls seem to be similar to land plants, as they display in their pectic fraction a high proportion of homogalacturonan and possibly an RG-I-like polymeric domain, as well as cellulose and a xylose and glucose-rich hemicellulosic fraction (Sørensen *et al.* 2011; O'Rourke *et al.* 2015). However, the presence of certain key land-plant polymers and polymeric domains remain mysterious. In particular, RG-II had not been detected before

in any CGA species. Xyloglucan, which was thought to be absent from charophytic cell walls, appear to be detectable via immunoassay techniques (Ikegaya *et al.* 2008), and xyloglucan-like polymers have even been characterised in *Mesotaenium caldariorum* (Mikkelsen *et al.* 2021).

Early-diverging charophyte cell walls, by comparison, remain widely ill-characterised. If a few studies have tagged homogalacturonan in *Klebsormidium* species, others have shown it was absent, alongside giving an approximate of the sugar composition of its different cell wall fractions (Sørensen *et al.* 2011; O'Rourke *et al.* 2015). Equally, *Chlorokybus* cell walls have been studied for the sugar contents in its pectic, hemicellulosic and cellulosic fractions, even though the nature of the glycosidic bonds involved remained mysterious (Sørensen *et al.* 2011; O'Rourke *et al.* 2015).

Another point of this thesis was to study the cell wall of *Ulva* spp., as this abundant “sea lettuce” is an important marine resource: it contains the biopolymer ulvan, widely known for its bioactive and rheological properties. The precise structure of ulvan varies considerably with the species; therefore focusing on unexpected features of the ulvan fraction in *U. linza* was interesting in this work (Mao *et al.* 2006; Chattopadhyay *et al.* 2007; Cassolato *et al.* 2008; Robic *et al.* 2009; Wang *et al.* 2013; Chi *et al.* 2020; Gao *et al.* 2020). Moreover, ulvan is not the only cell wall component of *Ulva* cell wall: in addition to the expected cellulose, a “hemicellulosic” fraction was extractable. This xylose and glucose-rich polymer had previously only been partially characterised, and its precise features remained completely unstudied (Lahaye *et al.* 1994; Ray 2006; Chattopadhyay *et al.* 2007).

In this work, a more precise assessment of charophytic cell wall fractions' extractabilities and compositions is provided, as well as a study of the potential presence of RG-II and xyloglucan

in CGAs. Moreover, the biochemical features of both *Chlorokybus* and *Klebsormidium* 'pectic' fractions were investigated. Finally, *Ulva* cell wall fractions were examined: ulvan for unexpected glycosidic bonds, and 'hemicellulosic' fraction for a complete chemical characterisation and an assessment of its affinity for cellulose. A visual summary is provided in Figure 71.

8.2. Extractability of polysaccharide fractions from plant AIR: general remarks

I assayed the extractability of the different cell wall fractions, pectin and hemicelluloses, in a range of charophytes (*Coleochaete scutata*, of the Coleochaetales order, *Chara vulgaris*, of the Charales, *Klebsormidium fluitans*, of the Klebsormidiales, *Chlorokybus atmophyticus*, of the Chlorokybales), as well as in the bryophyte *Anthoceros caucasicus* and in the chlorophyte *Ulva linza*. Certain patterns were identical in all six species examined: pectin represented the major part of the extracted polysaccharides, followed by hemicellulose and cellulose, plus the sometimes negligible wash fraction. This is the pattern expected in most land plant primary cell walls, supporting the hypothesis of charophytic cell walls behaving similarly to embryophytic cell walls (Albersheim *et al.* 2011 p. 20).

Interestingly, pre-treating plant AIR with alkali before extracting the different polymeric fractions led to a higher recovery of all polymers, as well as making all 'pectins' easier to extract (P1/P2 was multiplied by a factor between 2 and 4 between un-treated AIRs and alkali-pretreated ones). As the increase in the weight of released polysaccharides is connected to an increase in the weight of released pectin, it might be due to the loosening of the interactions between the different polysaccharides in the cell wall, thus making them more susceptible to subsequent extraction techniques. Another option would be the partial

alkaline peeling of polysaccharides' reducing ends, thus making the polymer chains shorter and easier to solubilise (Nieminen *et al.* 2015).

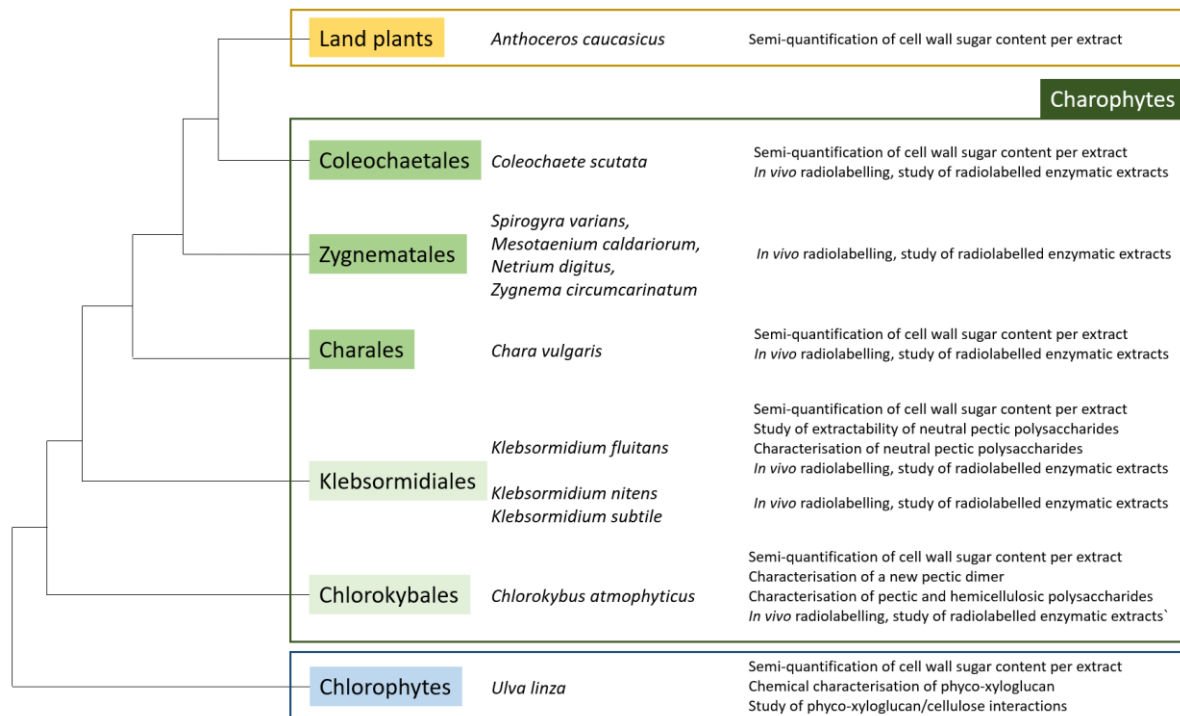


Figure 71: Extended phylogeny of the charophytic algae, showing the major pieces of work of this thesis.

Extracting starch from the AIR prior to sequential extraction had a similar effect on pectic extractability (starch was present in all six species). However, this de-starching requires first gelatinising starch by heating up the AIR to 100°C in an almost neutral buffer, prior to incubation with amylase at 60°C in the same buffer, followed by the extraction of small oligomers with 70% ethanol. As hot-water extraction is a widely known technique for solubilising pectin, it is possible that pectin was partly solubilised during the gelatinising stage of the process, before being re-precipitated with the addition of ethanol (Benassi *et al.* 2021). This would justify the substantial initial release of pectin during the first step of the sequential extraction. Moreover, more hemicellulose was recovered in all species following

this de-starching: it is possible that the first incubation at a pH higher than the physiological one loosened the hemicellulose–cellulose interactions (mostly believed to be hydrogen bonds), thus allowing a better separation of hemicellulose and cellulose and better recovery of hemicellulose (O'Rourke *et al.* 2015).

Two groups of plants were distinguishable by their cell wall biochemical features: the land-plant *Anthoceros* and the late-diverging charophytes (*Chara* and *Coleochaete*), and the chlorophyte *Ulva* and the early-diverging charophytes (*Klebsormidium* and *Chlorokybus*). Results are presented and discussed separately for each group.

8.3. Features of the polysaccharide fractions from late-diverging charophytes and bryophyte

8.3.1. Extractability of the polymeric fractions - link to their chemical nature

In the first set of plants (bryophyte and late-diverging charophytes), the pectic fractions were easier to extract, which could be indicative of looser interactions with the rest of the cell wall (hemicellulose and cellulose), or be a proof that late-diverging charophytes' and bryophytes' pectins are more sensitive to the presence of a chelating ion such as the oxalate used for the extraction (O'Rourke *et al.* 2015). This could be the case if their “pectins” were forming a gel via interactions between un-esterified GalA residues with calcium ions, forming the previously described egg-box structure. Indeed, all three species presented classical land-plant-like features, including the presence of galacturonic acid and the digestibility of the pectic fraction with EPG, irrespective of whether or not an alkaline pre-treatment was

performed (which would have de-esterified GalA residues). All taken together, these results are indicative of the presence of homogalacturonan in the pectic fractions, either un-esterified or with a very low degree of esterification. Although this was expected for *Chara*, it was more surprising for *Coleochaete* and for the bryophyte *Anthoceros* (Domozych *et al.* 2010). The implications of a low degree of esterification in algal cell walls could be the enhanced chelation of cations by GalA residues, which would strengthen the pectic gel, as these ionic interactions are stronger than the hydrophobic ones formed between esterified GalA residues (Oakenfull and Scott 1984). Homogalacturonan gels are known to play, important roles in many key plant features such as cell adhesion, regulation of cell-wall pores, and permeability (Albersheim *et al.* 2011). Their increased presence in late-diverging charophytes may be linked to their natural aqueous environment, which might bring increased stress to the cell-cell adhesion process and to the alga's mechanical integrity (due to currents for example). Moreover, the localised esterification degree of HGA plays a key role in plant development and plant growth: as cells in CGAs are not well differentiated, such fine control of their spatial biochemistry is not necessary, or vice versa (Cosgrove 2000b).

8.3.2. Presence of land-plant-like polymeric domains in 'pectic' fractions from late-diverging charophytes

The presence, albeit in varying amounts, of rhamnose, galactose, and arabinose in *Chara* and *Coleochaete* points towards the presence of RG-I, or RG-I-like, domains in the "pectin" (RG-I being characterised by galactan and arabinan sidechains on a backbone of alternating Rha and GalA) (Albersheim *et al.* 2011). These sugars were also yielded from Driselase hydrolysis,

and RG-I was detectable in *Chara* and *Coleochaete* cell walls via immunoassays, thus supporting hypothesis of the presence of RG-I in their cell walls (O'Rourke *et al.* 2015).

The potential presence of other typical pectic domains in late-diverging charophytes was examined via the Driselase hydrolysis of radiolabelled algal cell walls (from a range of Zygnematales, Coleochaetales, Charales, Klebsormidiales and Chlorokybales), which should reduce most land-plant-related cell wall compounds to monomers and small oligomers, apart from RG-II. This led to the detection of an RG-II-like polymeric fraction in *Chara* from axenic culture (although this could not be detected in wild-harvested *Chara* nor in other charophytes, even amongst the latest-diverging clade, the zygnemataleans). No such polymer has been detected before in charophytic species, to the extent of my knowledge. In land plants, RG-II is highly conserved; it is known to be cross-linked via boron bridges, thus reinforcing the gelling structure of the HGA domain close to the plasma membrane (Jarvis *et al.* 2003). The discovery of an RG-II-like structure in a CGA would lead to re-examining the synthetic pathway for RG-II and its evolution: would they have a common ancestor or have evolved distinctly? The discovery of RG-II biosynthesis-associated genes in charophytes would favour the first hypothesis (Mikkelsen *et al.* 2014). In that case, it would mean that the first bricks for RG-II synthesis were laid before the split between embryophytes and charophytes, and that they may not be associated to the terrestrialization of plants – or were pre-requisites to plant terrestrialization taking place, instead of resulting from it. A thorough review of CGA genomes, looking to detect RG-II synthase associated genes, could shed more light on the matter, as would further chemical characterisation of RG-II-like oligomers that were extracted from algal cell walls.

8.3.3. Presence of key 'hemicellulosic' polymer in late-diverging charophytes

Other evolutionary traits that were examined in this work involved the presence – or not – of xyloglucan in late-diverging-charophyte cell walls, screening, as for RG-II, zygnematalean species as well as other orders of charophytes. In all cases, digestion of radiolabelled AIR or hemicellulose with XEG yielded xyloglucan-like oligomers – with the caveat that, owing to their extremely low amounts, they could only be identified as such through their chromatographic properties, by comparing them with the key hepta-, octa- and nonasaccharides XXXG, XXLG, and XXFG, released by XEG from land-plant AIRS such as pea stems (Fry *et al.* 1993). Further characterisation would involve the analysis of their enzymatic and chemical hydrolysates, which would provide a far deeper understanding of their structures and possibly confirm that they are indeed xyloglucan-derived oligomers. As our XEG preparation possesses several side activities, such as cellulase, amylase, or laminarinase, the oligomers that were released could alternatively come from starch (which may have failed to fully solubilise during the previous amylase treatment), mixed-linkage β -glucan, or cellulose. These options are likely, as the diagnostic dimer isoprimeverose (6-O- α -D-xylopyranosyl-D-glucose) was not detectable in any species via the chromatographic analysis of enzymatic (XEG and Driselase) hydrolysates from radiolabelled algal cell walls and algal hemicelluloses. Given that immunoassays have shown the presence of xyloglucan-like polymers within CGA cell walls (Mikkelsen *et al.* 2021), it might be that an epitope of xyloglucan is present, that is not susceptible to land-plant xyloglucan-specific hydrolases. Alternatively, it could be that the immunoassay labelling lacked specificity: in spite of the high sensitivity of this method, the antibodies involved might react with the wrong target polysaccharide and give erroneous results. Thus, direct chemical characterisation is key to confirming immunoassay-based findings, and has been obtained recently for *Mesotaenium*

(a member of the Zygnematales). (Mikkelsen *et al.* 2021). The fact that I could not characterise for certain any xyloglucan-derived compound in this work might either be due to having used an insufficient quantity of radioactivity, which made their detection and characterisation difficult, or that the conditions in which the algae were grown (axenic, static, under continuous lighting) prevented them from synthesizing xyloglucan in detectable amounts.

8.4. Features of the polysaccharide fractions from early-diverging charophytes and chlorophyte

The second sub-group of plants, defined by a slower release of their 'pectic' polysaccharides, contained the early-diverging charophytes *Klebsormidium* and *Chlorokybus*, as well as *Ulva* (O'Rourke *et al.* 2015). This suggests a strong affinity of these 'pectic' polysaccharides for the rest of the cell wall matrix, maybe coming from more abundant and more resistant cross-linking between them. All three of these algae stood out because none of them released any oligomer nor monomer upon the action of EPG, even though *Chlorokybus* did contain galacturonic acid.

Moreover, both *Chlorokybus* and *Ulva* 'pectin' contained sulphates. Even if this sulphation was previously known in *Ulva*, especially in the polymer ulvan, it was new in the basal charophyte *Chlorokybus*. As cell wall polysaccharide sulphation has often been thought of as a feature of adaptation to saline environments, its presence in an aeroterrestrial alga seems counter-intuitive (Aquino *et al.* 2011). It may be a common trait to chlorophytes and streptophytes, which was eliminated after the divergence of the Chlorokybales. It might also

be that *Chlorokybus* cells, being embedded in mucilage in close contact with highly mineral environments (rock, soil), virtually also occupy highly saline environments (as mineral ions from the rock might partially dissolve in the mucilaginous matrix) thus provoking the need for similar adaptations as if they were actually living in a highly saline marine environment (Tosif *et al.* 2021). As marine algae have the ability to tailor their degree of sulphation to the salt concentration around them, measuring the variations in *Chlorokybus* sulphation with the ionic concentration of its growth medium might be a strong indicator of the common features between sulphation in the Chlorokybales and sulphation in the chlorophytes.

8.4.1. *Chlorokybus atmophyticus*: study of a primordial 'pectic' fraction

Chlorokybus was found to contain an unexpected aldobiouronic acid in its partially acid-hydrolysed pectic fraction, which was characterised as β -D-GlcA-(1→4)-L-Gal. This structure was surprisingly similar to another one characterised in the bryophyte *Anthoceros*, β -D-GlcA-(1→3)-L-Gal (Popper *et al.* 2003). In both cases, the GlcA residue was linked to the less common Gal enantiomer. However, the biochemical significance of this dimer remains mysterious and probably is radically different in *Anthoceros* and *Chlorokybus*, as β -D-GlcA-(1→3)-L-Gal is extracted from non-pectic polysaccharides in the bryophyte, whereas β -D-GlcA-(1→4)-L-Gal belongs to the oxalate-extractable, pectic-like fraction in *Chlorokybus*.

Interestingly, the rest of the Gal residues in the *Chlorokybus* cell wall were also the L-enantiomer. When assaying other land-plant-cell-wall-specific hydrolases on the *Chlorokybus* 'pectic' fraction, it was clear that none of the polymeric fractions could be hydrolysed in detectable amounts, apart from remaining contaminating starch. However, it was possible to distinguish two fractions of *Chlorokybus* pectin by ion-exchange chromatography, one being

very negatively charged, difficult to hydrolyse and containing high amounts of sulphates, and the second one being less charged, susceptible to mild acid hydrolysis and richer in uronic acids. It is possible that the strong negative charge of the first fraction is what keeps it from being easily hydrolysed, as the acidic TFA would be less likely to access the glycosidic bonds as easily if the polysaccharide's backbone is very acidic itself (Shi *et al.* 2020). Overall, it appeared clearly that the structure of the *Chlorokybus* cell wall is very far from being elucidated: even though its sugar residue composition might lead to guessing that it is land-plant-like (rich in Ara, Gal, Rha, uronic acid), it is obviously fundamentally different. Hypothetically, the *Chlorokybus* 'pectin' could be seen as a mock version of land-plant pectins, with more or less charged fractions (like HGA and RG-I for example), that interact to form a gel in the cell wall.

The hemicellulosic fraction of *Chlorokybus* was equally interesting, as it contained a large majority of Glc residues and could only be hydrolysed by enzymes with a laminarinase activity, able to hydrolyse β -(1 \rightarrow 3)-glucans by cutting the β -(1 \rightarrow 3) glycosidic bonds between successive Glc residues. Moreover, the fraction released laminaribiose upon mild acid hydrolysis, thus confirming the presence of β -(1 \rightarrow 3)-glucan stretches in the hemicellulosic fraction of *Chlorokybus*. These could come from the presence of callose in the cell wall, previously detected in both *Chlorokybus* and *Klebsormidium* (Scherp *et al.* 2001). Another option would be the presence of a mixed-linkage glucan in *Chlorokybus* cell wall, which would be yet another occurrence of MLG having evolved independently (Fry *et al.* 2008).

8.4.2. *Klebsormidium fluitans*: characterisation and implication of a neutral 'pectic' fraction

The *Klebsormidium* 'pectic' fraction was just as unique as the one from *Chlorokybus* presented above, as it did not appear to contain any uronic acid. By assaying its extractability properties, it was obvious that, even though a high temperature and a low pH made 'pectin' solubilisation more effective, as it would do in land plants, the presence of a chelating ion was not necessary. On the contrary, it appeared that the chelating nature of the ion was irrelevant, considering that the non-chelating ion formate was more effective than both bigger, less electronegative compounds oxalate (chelating) and acetate (non-chelating). As the *Klebsormidium* cell wall does not contain any GalA, the usual 'eggbox' fraction that needs to be disrupted by oxalate for pectin to be extracted is absent, thus other mechanisms are responsible for the extraction of the 'pectic' material. In this case, the efficiency of formate may be linked to its size: it might be able to disrupt more easily hypothetical hydrogen or hydrophobic bonds in the cell wall, allowing for the release of 'pectin' into solution. Another hypothesis for the enhanced efficiency of formic acid on 'pectin' extraction in *Klebsormidium* is the partial hydrolysis of the most acid-labile domains in the cell wall, usually made up by pentose-containing polysaccharidic domains, thus making the concepts of 'pectin' and 'hemicellulose' completely different from their initial definitions. Beyond these surprising extractability properties, *Klebsormidium* 'pectin' contained unique small, deoxy sugars, and was digestible by Driselase and a few other land-plant-cell-wall hydrolases (arabinanase and xylanase in particular), producing a series of monomers and oligomers, thus showing that it contains a considerable number of glycosidic bonds identical to those of land plants. The close analysis of the oligomer series released by Driselase led to characterising a pectic domain made of a Xyl backbone and Rha sidechains. This unique

structure could be seen as similar to certain hemicelluloses such as arabinoxylan (Albersheim *et al.* 2011). Following this, the mild acid hydrolysis of ‘pectin’ from *Klebsormidium* led to characterising a pectic domain containing Gal and Xyl residues, not susceptible to either galactosidase or β -xylosidase. Both domains do not seem to have much in common with known cell-wall structures from land- plants. With the assumption that they play major roles in the algal cell wall, they might be involved in a jellification mechanism through hydrophobic interactions, as certain domains of conventional pectins or AGPs seem to do (but since there is no uronic acid, it cannot be through ionic bonds, like it is with GalA-rich pectins) (Palacio-López *et al.* 2019). This non-ionic dependent mechanism may be key to why *Klebsormidium* species are capable of surviving in extremely harsh environments, such as acid mine drainages, glaciers and alpine environments (Holzinger and Pichrtová 2016). Indeed, the non-reliance of their cell wall on pH conditions or cation presence in the water makes them less likely to be affected by what are usually toxic concentrations of heavy metal ions or by particularly low pH conditions, such as the waters of the Río Tinto in Spain (a 100 km long ecosystem of geothermic origin with a pH around 2.3 and high concentration of heavy metals), or acid mine drainages in Ohio (particularly rich in aluminium, iron, manganese and zinc) (Stevens *et al.* 2001; Aguilera 2013).

8.4.3. Features of ulvan and ‘hemicellulose’ from *Ulva linza*

The chlorophyte and seaweed representative of the study, *Ulva linza*, was examined. Its oxalate-extractable fraction contained the expected ulvan signature sugars — uronic acids, Xyl, Rha— and high amounts of sulphate (Lahaye and Robic 2007). An unexpected dimer of Rha, probably (1→2)-rhamnobiore, was found in the same fraction. Rhamnans had been

detected in the past in other green seaweeds including *Ulva* species, thus the occurrence of this dimer in *Ulva linza* was not unexpected (Robic *et al.* 2009).

The analysis of the 'hemicellulosic' fraction of *Ulva linza* cell wall conducted in this thesis was, however, new: this fraction had previously only been partially chemically characterised (Lahaye *et al.* 1994; Ray 2006; Chattopadhyay *et al.* 2007). It led to the characterization of the linear polymer phyco-xyloglucan, containing stretches of xylan and glucan linked via almost exclusively β -(1 \rightarrow 4) glycosidic bonds. This similarity with cellulose structure (β -(1 \rightarrow 4)-glucan) might explain the particularly strong and fast affinity of these two polysaccharides. In the acid hydrolysate of cellulase-digested *Ulva* cellulose residue, xylose was found, possibly indicating the remaining presence of phyco-xyloglucan even after alkali extraction, and its accessibility to the enzyme. Indeed, xylose was not detectable in the acid hydrolysate of non-cellulase digested algal cellulose residue. This accessibility to the enzyme of the xylose-containing polymer is only possible if it is bound to the surface of the cellulose microfibril, rather than being interwoven within the microfibril (Bansala *et al.* 2012). This points towards an architecture of the cellulose–hemicellulose network different from the one in land plants, characterised by interactions at the surface of the microfibrils but also by the presence of hotspots where hemicellulosic domains are intertwined within the cellulose microfibrils (Cosgrove 2016). The precise nature of the interactions between phyco-xyloglucan and cellulose remains to be studied. However, because of the linear nature and considerable Glc content of phyco-xyloglucan, it may be possible that the more Glc-rich segments interact with the cellulose microfibrils as if they were an integral part to their structures, like land-plant xyloglucan being trapped within cellulose microfibrils (Pauly *et al.* 1999). The Xyl-rich segments may either interact with the cellulose microfibrils in a looser manner (fewer H-bonds between Xyl and Glc residues than between Glc residues from two

different cellulose-like molecules) or they may not interact with the cellulose fibres at all, being the tethers between the cellulose microfibrils (Lahaye and Robic 2007; Zhang *et al.* 2015). Following this, the impact of the amount of xylose on this affinity phenomenon is key: it might be an adaptive feature of the algae, modulating the mechanical properties of the cell wall via the proportion of phyco-xyloglucan directly interacting or not with cellulose. Finally, the evolutionary significance of this polymer remains to be examined: if similar structures were found throughout the whole *Ulva* genus or even the Ulvophyceae, studying their biosynthetic pathway would perhaps be key to understanding the evolution of xylose and glucose-containing plant polymers. The genes involved in it would then be an important indicator of the conservation and the evolution of the cellulose-associated polymers in plant and algal cell walls.

8.5. Conclusion

In this work, the properties and biochemical features of the cell walls of a range of charophytic green algae and of a chlorophyte were examined. The study of the polymeric fractions extractability led to marking an obvious divide between the later-diverging charophytes, and the earlier-diverging charophytes and the chlorophyte, the second group less land-plant-like than the first one. However, in spite of the later-diverging charophytes presenting similar sugar compositions to the land plants, the polymer xyloglucan could not be detected in their cell walls. This might be due to the developmental stage or the growth conditions of the samples used for the study, as other recently published work demonstrated the presence of xyloglucan in charophytic cell walls (Mikkelsen *et al.* 2021). However, the presence of RG-II, another key land-plant polymer, in *Chara*, is not ruled out. The 'pectic' structure in earlier diverging polymers was investigated. *Klebsormidium fluitans*

was unique by its absence of charge, raising multiple questions about the mechanism responsible for the integrity and the defence of the cell wall. Specific mechanisms (such as particularly strong hydrophobic interactions or hydrogen bonding) may have arisen to guarantee it in the absence of the usual uronic acids. These mechanisms may be the ones guaranteeing the survival of several *Klebsormidium* species in particularly acidic and heavy metal rich environments. *Chlorokybus* presented an original chemical composition, but its pectic fraction seemed to behave similarly to a land plant's, using different sugars and probably a different architecture. This pectic fraction also contained sulfates, like many seaweed cell walls do: this feature may be the one allowing for survival in the particularly vulnerable sarcinoid structure characteristic to *Chlorokybus*. Finally, the hemicellulosic fraction of *Ulva* spp. was examined, leading to the elucidation of the structure of phyco-xyloglucan, which displays extremely strong and fast interactions with cellulose, when compared to land plant hemicellulosic polymers. Therefore, this polysaccharide may play an important mechanical role within the algal cell wall, which may be dynamic depending on the immediate environment of the alga.

Overall, I demonstrated in this thesis the limited resemblance of higher charophyte cell walls with land plant cell walls. Via the examination of their pectic fraction, I showed that the lower charophytes had evolved independently towards a greater adaptability to survival in their respective, harsh environments. Finally, the presence of phyco-xyloglucan in *Ulva* may be a feature of the seaweed's adaptability to its own buoyant marine environment.

9. Appendix

Table a: ¹H and ¹³C NMR spectral data of xylanase-produced oligomers from Hb Ulva.

Substrate	Site	δ_c	δ_H	multiplicity	J_{HH} (Hz)
<i>E, O</i> (β -(1→4)-xylobiose) (α : β =1:2)					
	α -Xyl1-1	91.9	5.105	(<i>d</i>)	$J_{12} = 3.6$
	α -Xyl1-2	71.5	3.467		$J_{23} = **$
	α -Xyl1-3	70.9	3.671		$J_{34} = **$
	α -Xyl1-4	76.5	~3.67		$J_{45ax/eq} = **$
	α -Xyl1-5ax	58.7	3.668		$J_{5ax5eq} = **$
	α -Xyl1-5eq		3.733		
	β -Xyl1-1	96.6	4.506	(<i>d</i>)	$J_{12} = 7.9$
	β -Xyl1-2	74.0	3.171	(<i>dd</i>)	$J_{23} = 9.4$
	β -Xyl1-3	74.0	3.467	(<i>t</i>)	$J_{34} = 9.2$
	β -Xyl1-4	76.5	3.698	(<i>ddd</i>)	$J_{45ax/eq} = 10.5/5.5$
	β -Xyl1-5ax	62.9	3.300	(<i>dd</i>)	$J_{5ax5eq} = 11.5$
	β -Xyl1-5eq		3.977	(<i>dd</i>)	
	Xyl2-1	101.8	4.376, 4.378	(<i>2d</i>)	$J_{12} = 7.9$
	Xyl2-2	72.7	3.184, 3.176	(<i>2dd</i>)	$J_{23} = 9.4$
	Xyl2-3	75.6	3.349, 3.347	(<i>2t</i>)	$J_{34} = 9.2$
	Xyl2-4	69.1	3.547	(<i>ddd</i>)	$J_{45ax/eq} = 10.5/5.5$
	Xyl2-5ax	65.2	3.229	(<i>dd</i>)	$J_{5ax5eq} = 11.5$
	Xyl2-5eq		3.893	(<i>dd</i>)	
<i>D</i> (β -D-glucosyl-(1→4)-xylobiose)					
	α -Xyl1-1	91.1	5.105	(<i>d</i>)	$J_{12} = 3.7$
	α -Xyl1-2	71.5	3.493	(<i>dd</i>)	$J_{23} = 8.9$
	α -Xyl1-3	71.0	~3.70		$J_{34} = **$
	α -Xyl1-4	76.5	~3.70		$J_{45ax/eq} = **$
	α -Xyl1-5ax	58.8	~3.69		$J_{5ax5eq} = **$
	α -Xyl1-5eq		~3.76		
	β -Xyl1-1	96.4	4.531	(<i>d</i>)	$J_{12} = 7.9$
	β -Xyl1-2	73.9	3.197	(<i>dd</i>)	$J_{23} = 9.3$
	β -Xyl1-3	73.9	3.495	(<i>t</i>)	$J_{34} = 9.3$
	β -Xyl1-4	76.4	3.729	(<i>ddd</i>)	$J_{45ax/eq} = 10.5/5.5$
	β -Xyl1-5ax	62.9	3.326	(<i>dd</i>)	$J_{5ax5eq} = 11.9$
	β -Xyl1-5eq		4.004	(<i>dd</i>)	

Xyl2-1	101.6	4.428	(d)	J ₁₂ = 7.9
Xyl2-2	72.7	3.244	(dd)	J ₂₃ = 9.3
Xyl2-3	73.9	3.525	(t)	J ₃₄ = 9.3
Xyl2-4	76.4	3.794	(ddd)	J _{45ax/eq} = 10.4/5.4
Xyl2-5ax	62.9	3.336	(dd)	J _{5ax5eq} = 11.9
Xyl2-5eq		4.061	(dd)	
Glc3-1	101.1	4.482	(d)	J ₁₂ = 8.0
Glc3-2	72.8	3.221	(dd)	J ₂₃ = 9.3
Glc3-3	75.6	3.431	(dd)	J ₃₄ = 9.3
Glc3-4	69.6	3.339	(t)	J ₄₅ = 9.7
Glc3-5	76.0	3.413	(ddd)	J _{56a/b} = 2.2/6.1
Glc3-6a	60.9	3.863	(dd)	J _{6a6b} = 12.3
Glc3-6b		3.669	(dd)	

C (β-cellobiosyl-(1→4)-xylobiose)

α-Xyl1-1	92	5.130	(d)	J ₁₂ = 3.7
α-Xyl1-2	71.3	3.492	(dd)	J ₂₃ = 8.8
α-Xyl1-3	70.9	3.698†		J ₃₄ = **
α-Xyl1-4	76.3	3.699†		J _{45ax/eq} = **
α-Xyl1-5ax	58.6	3.685†		J _{5ax5eq} = **
α-Xyl1-5eq		3.756		
β-Xyl1-1	96.5	4.530	(d)	J ₁₂ = 7.9
β-Xyl1-2	74.0	3.196	(dd)	J ₂₃ = 9.3
β-Xyl1-3	73.8	3.494	(t)	J ₃₄ = 9.3
β-Xyl1-4	76.3	3.728	(ddd)	J _{45ax/eq} = 10.7/5.3
β-Xyl1-5ax	62.9	3.326	(t)	J _{5ax5eq} = 12.0
β-Xyl1-5eq		4.003	(dd)	
Xyl2-1	101.6	4.426, 4.430	(d)	J ₁₂ = 7.8
Xyl2-2	72.6	3.243	(dd)	J ₂₃ = 9.3
Xyl2-3	73.7	3.526	(t)	J ₃₄ = 9.1
Xyl2-4	76.3	3.792	(ddd)	J _{45ax/eq} = 10.5, 5.4
Xyl2-5ax	62.9	3.336	(dd)	J _{5ax5eq} = 11.9
Xyl2-5eq		4.062	(dd)	
Glc3-1	100.9	4.506	(d)	J ₁₂ = 8.0
Glc3-2	72.6	3.264	(dd)	J ₂₃ = 9.0

Glc3-3	74.1	3.574	(t)	J ₃₄ = 9.1
Glc3-4	78.6	3.597	(t)	J ₄₅ = 9.7
Glc3-5	74.8	3.545		J _{56a/b} = 2.3, 5.4
Glc3-6a	60	3.929	(dd)	J _{6a6b} = 12.4
Glc3-6b		3.758	(dd)	
Glc4-1	102.6	4.447	(d)	J ₁₂ = 8.0
Glc4-2	73.1	3.285	(dd)	J ₂₃ = 9.4
Glc4-3	75.5	3.450	(t)	J ₃₄ = 9.2
Glc4-4	69.5	3.361	(t)	J ₄₅ = 9.8
Glc4-5	76.0	3.427	(ddd)	J _{56a/b} = 2.3/5.8
Glc4-6a	60.6	3.857	(dd)	J _{6a6b} = 12.4
Glc4-6b		3.678	(dd)	

B (β-D-xylosyl-(1→4)- β-D-cellobiosyl-(1→4)- β-D-xylobiose)

α-Xyl1-1	91.9	5.130	(d)	J ₁₂ = 3.7
α-Xyl1-2	71.4	3.491	(dd)	J ₂₃ = 9.2
α-Xyl1-3	70.9	~3.69		J ₃₄ = **
α-Xyl1-4	76.5	~3.69		J _{45ax/eq} = **
α-Xyl1-5ax	58.8	~3.69		J _{5ax5eq} = **
α-Xyl1-5eq		3.758		
β-Xyl1-1	96.5	4.530	(d)	J ₁₂ = 8.0
β-Xyl1-2	74.0	3.196	(dd)	J ₂₃ = 9.2
β-Xyl1-3	73.9	3.494	(t)	J ₃₄ = 9.3
β-Xyl1-4	76.4	3.727	(ddd)	J _{45ax/eq} = 10.5/5.5
β-Xyl1-5ax	63.0	3.325	(dd)	J _{5ax5eq} = 11.6
β-Xyl1-5eq		4.003	(dd)	
Xyl2-1	101.6	4.427, 4.429	(d)	J ₁₂ = 7.9
Xyl2-2	72.7	3.242	(dd)	J ₂₃ = 9.2
Xyl2-3	73.7	3.525	(t)	J ₃₄ = 9.2
Xyl2-4	76.3	3.792	(ddd)	J _{45ax/eq} = 10.3/5.5
Xyl2-5ax	63.0	3.335	(dd)	J _{5ax5eq} = 11.9
Xyl2-5eq		4.061	(dd)	
Glc3-1	100.9	4.505	(d)	J ₁₂ = 7.9
Glc3-2	72.7	3.264	(dd)	J ₂₃ = 8.8
Glc3-3	73.9	3.574		J ₃₄ = **
Glc3-4	78.4	3.588		J ₄₅ = **
Glc3-5	74.8	3.547		J _{56a/b} = 2.0/5.4

Glc3-6a	59.5	3.927	(<i>dd</i>)	$J_{6a6b} = 12.2$
Glc3-6b		3.759	(<i>dd</i>)	
Glc4-1	102.4	4.461	(<i>d</i>)	$J_{12} = 7.9$
Glc4-2	73.1	3.258	(<i>d</i>)	$J_{23} = 9.2$
Glc4-3	73.7	3.451		$J_{34} = 9.3$
Glc4-4	78.0	3.361		$J_{45} = 9.7$
Glc4-5	74.1	3.425	(<i>ddd</i>)	$J_{56a/b} = 2.0/5.8$
Glc4-6a	59.9	3.856	(<i>dd</i>)	$J_{6a6b} = 12.2$
Glc4-6b		3.678	(<i>dd</i>)	
Xyl5-1	103.3	4.361	(<i>d</i>)	$J_{12} = 7.9$
Xyl5-2	73.1	3.236	(<i>dd</i>)	$J_{23} = 9.2$
Xyl5-3	75.6	3.388	(<i>t</i>)	$J_{34} = 9.2$
Xyl5-4	69.2	3.576	(<i>ddd</i>)	$J_{45ax/eq} = 10.5$
Xyl5-5ax	65.1	3.254	(<i>dd</i>)	$J_{5ax5eq} = 5.5$
Xyl5-5eq		3.927	(<i>dd</i>)	

† from HSQC spectrum

** unresolved (signal overlap)

Table b: ¹H and ¹³C NMR spectral data of Driselase-produced oligomers from Hb Ulva.

Substrate	Site	δ_c	δ_H	multiplicity	J_{HH} (Hz)
<i>M1 (xylotriose) ($\alpha:\beta=1:2$)</i>					
	α -Xyl1-1	91.8	5.129	(d)	$J_{12} = 7.8$
	α -Xyl1-2	71.5	3.401	(dd)	$J_{23} = **$
	α -Xyl1-3	70.9	~ 3.69		$J_{34} = **$
	α -Xyl1-4	76.5	~ 3.69		$J_{45ax/eq} = **$
	α -Xyl1-5ax	58.6	~ 3.69		$J_{5ax5eq} = 11.8$
	α -Xyl1-5eq		3.76		
	β -Xyl1-1	96.4	4.529	(d)	$J_{12} = 7.8$
	β -Xyl1-2	74.1	3.106	(dd)	$J_{23} = 9.4$
	β -Xyl1-3	73.7	3.493	(t)	$J_{34} = 9.2$
	β -Xyl1-4	76.5	3.724	(ddd)	$J_{45ax/eq} = 10.5/5.5$
	β -Xyl1-5ax	63	3.323	(dd)	$J_{5ax5eq} = 11.5$
	β -Xyl1-5eq		4	(dd)	
	Xyl2-1	101.7	4.421, 4.424	(2d)	$J_{12} = 7.8$
	Xyl2-2	72.7	3.234, 3.246	(2dd)	$J_{23} = 9.3$
	Xyl2-3	73.8	3.498, 3.500	(t)	$J_{34} = 9.2$
	Xyl2-4	76.5	3.735		$J_{45ax/eq} = 10.5/5.3$
	Xyl2-5ax	63	3.323	(dd)	$J_{5ax5eq} = 11.5$
	Xyl2-5eq		4.051	(dd)	
	Xyl3-1	101.7	4.405	(d)	$J_{12} = 7.8$
	Xyl3-2	72.7	3.202	(dd)	$J_{23} = 9.3$
	Xyl3-3	76.5	3.373	(t)	$J_{34} = 9.3$
	Xyl3-4	69.1	3.57	(ddd)	$J_{45a/e} = 10.5/5.5$
	Xyl3-5ax	65.2	3.25	(dd)	$J_{5ax5eq} = 11.8$
	Xyl3-5eq		3.92	(dd)	
<hr/>					
<i>M2, S (β-D-xylobiosyl-(1\rightarrow4)-glucose) ($\alpha:\beta=1:2$)</i>					
	α -Glc-1	91.8	5.163	(dd)	$J_{12} = 3.8$
	α -Glc-2	71.3	3.502	(dd)	$J_{23} = 9.9$
	α -Glc-3	71.0	3.734	(t)	$J_{34} = 9.0$
	α -Glc-4	78.3	3.552	(dd)	$J_{45} = 10.2$
	α -Glc-5	70.2	3.880		$J_{56a/b} = 2.0/4.2$
	α -Glc-6a	59.8	3.825		
	α -Glc-6b		3.793		

β -Glc-1	95.7	4.595	(d)	$J_{12} = 8.0$
β -Glc-2	74.1	3.208	(dd)	$J_{23} = 9.2$
β -Glc-3	74.0	3.532		$J_{34} = 9.3$
β -Glc-4	78.3	3.563	(t)	$J_{45} = 9.3$
β -Glc-5	73.7	3.527		$J_{56a/b} = 2.1/4.5$
β -Glc-6a	59.8	3.892	(dd)	$J_{6a6b} = 12.2$
β -Glc-6b		3.745	(dd)	
Xyl2-1	103.1	4.386,4.388	(d)	$J_{12} = 7.9$
Xyl2-2	73.1	3.238, 3.273	(dd)	$J_{23} = 9.4$
Xyl2-3	74.8	3.514, 3.517	(t)	$J_{34} = 9.3$
Xyl2-4	76.6	3.739	(td)	$J_{45ax/eq} = 10.5/5.5$
Xyl2-5ax	62.9	3.327	(dd)	$J_{5ax5eq} = 11.9$
Xyl2-5eq		4.063	(dd)	
Xyl3-1	101.9	4.404	(d)	$J_{12} = 7.9$
Xyl3-2	72.7	3.202	(dd)	$J_{23} = 9.4$
Xyl3-3	75.6	3.373	(t)	$J_{34} = 9.3$
Xyl3-4	69.2	3.570	(td)	$J_{45ax/eq} = 10.6/5.5$
Xyl3-5ax	65.1	3.253	(dd)	$J_{5ax5eq} = 11.6$
Xyl3-5eq		3.916	(dd)	

N,U (β -D-glucosyl-(1 \rightarrow 4)-xylobiose) (α : β =1:2)

α -Glc-1	91.8	5.162	(d)	$J_{12} = 3.8$
α -Glc-2	71.3	3.501	(dd)	$J_{23} = 9.8$
α -Glc-3	71.2	3.733	(dd)	$J_{34} = 9.0$
α -Glc-4	78.3	3.541	(d)	$J_{45} = 9.9$
α -Glc-5	70.1	3.88	(ddd)	$J_{56a/b} = 2.0/4.2$
α -Glc-6a	59.9	3.825	(dd)	$J_{6a6b} = 12.2$
α -Glc-6b		3.794	(dd)	
β -Glc-1	95.7	4.594	(d)	$J_{12} = 8.0$
β -Glc-2	74.0	3.205	(t)	$J_{23} = 8.8$
β -Glc-3	74.5	~3.55		$J_{34} = **$
β -Glc-4	78.3	~3.55		$J_{45} = **$
β -Glc-5	74.5	~3.55		$J_{56a/b} = 2.0/4.9$
β -Glc-6a	59.9	3.894	(dd)	$J_{6a6b} = 12.2$
β -Glc-6b		3.746	(dd)	

Xyl-1	103.3	4.365	(d)	$J_{12} = 7.9$
Xyl-2	73.1	3.246	(t)	$J_{23} = 9.3$
Xyl-3	75.6	3.389	(t)	$J_{34} = 9.2$
Xyl-4	69.3	3.577	(ddd)	$J_{45ax/eq} = **/5.4$
Xyl-5ax	65.2	3.254	(dd)	$J_{5ax5eq} = 11.7$
Xyl-5eq		3.93	(dd)	

** unresolved (signal overlap)

Table c: ¹H and ¹³C NMR spectral data of cellulase-produced oligomers from Hb Ulva.

Substrate	Site	δ_c	δ_H	multiplicity	J_{HH} (Hz)	HMBC
<i>Q</i> (β -D-xylotriosyl-(1 \rightarrow 4)-glucose) (α : β =1:1)						
	α -Glc-1*	91.9	5.161	(d)	$J_{12} = 3.8$	
	α -Glc-2	71.4	3.500	(dd)	$J_{23} = 9.8$	
	α -Glc-3	71.1	3.733	(t)	$J_{34} = 9.1$	
	α -Glc-4	78.2	3.551	(t)	$J_{45} = 10.0$	α -Glc-C4 / Xyl2-H1
	α -Glc-5	70.2	3.879	(ddd)	$J_{56a/b} = 2.2/4.5$	
	α -Glc-6a*	59.8	3.822	(dd)	$J_{6a6b} = 12.3$	
	α -Glc-6b*		3.792	(dd)		
	β -Glc-1*	95.8	4.593	(d)	$J_{12} = 8.1$	
	β -Glc-2	74.0	3.207	(dd)	$J_{23} = 9.0$	
	β -Glc-3	74.6	3.532	(t)	$J_{34} = 9.1$	
	β -Glc-4	78.2	3.563	(t)	$J_{45} = 9.4$	β -Glc-C4 / Xyl2-H1
	β -Glc-5	74.6	3.524	(ddd)	$J_{56a/b} = 2.0/5.0$	
	β -Glc-6a	59.8	3.891	(dd)	$J_{6a6b} = 12.2$	
	β -Glc-6b		3.744	(dd)		
	Xyl2-1*	103.2	4.385, 4.387	(d)	$J_{12} = 7.8$	Xyl2-C1 / Glc-H4(α & β)
	Xyl2-2	73.2	3.271, 3.278	(dd)	$J_{23} = 9.4$	
	Xyl2-3	73.7	3.515, 3.518	(t)	$J_{34} = 9.2$	
	Xyl2-4	76.4	3.743	(td)	$J_{45ax/eq} =$ $10.5/5.1$	Xyl2-C4 / Xyl3-H1
	Xyl2-5ax	62.9	3.326	(t)	$J_{5ax5eq} = 11.7$	
	Xyl2-5eq		4.063, 4.064	(dd)		
	Xyl3-1*	101.5	4.425, 4.427	(d)	$J_{12} = 7.8$	
	Xyl3-2	72.7	3.237	(dd)	$J_{23} = 9.3$	
	Xyl3-3	73.7	3.499	(t)	$J_{34} = 9.2$	Xyl3-C4 / Xyl4 -H1
	Xyl3-4	76.4	3.732	(td)	$J_{45ax/eq} = 9.2/5.3$	
	Xyl3-5ax	62.9	3.323	(dd)	$J_{5ax5eq} = 11.8$	
	Xyl3-5eq		4.051	(dd)		

Xyl4-1*	101.8	4.404	(d)	J ₁₂ = 7.9
Xyl4-2	72.7	3.202	(dd)	J ₂₃ = 9.3
Xyl4-3*	75.5	3.372	(t)	J ₃₄ = 9.2
Xyl4-4	69.2	3.569	(ddd)	J _{45ax/eq} = 10.5/5.5
Xyl4-5ax	65.2	3.252	(t)	J _{5ax5eq} = 11.7
Xyl4-5eq*		3.915	(dd)	

R (β-laminarinobiosyl-(1→4)-glucose)

α-Glc1-1	91.7	5.169	(dd)	J ₁₂ = 3.8	
α-Glc1-2	70.9	3.522	(dd)	J ₂₃ = 10.0	
α-Glc1-3	71.2	3.766	(t)	J ₃₄ = 8.7	
α-Glc1-4	78.3	3.596	(t)	J ₄₅ = 9.4	α-Glc1-C4 / Glc2-H1
α-Glc1-5	69.8	3.894	(ddd)	J _{56a/b} = 2.5/4.7	α-Glc1-C5 / α-Glc1-H1
α-Glc1-6a	59.7	3.834	(dd)	J _{6a6b} = 12.4	
α-Glc1-6b		3.806	(dd)		
β-Glc1-1	95.6	4.606	(d)	J ₁₂ = 8.0	β-Glc1-C1 / β-Glc1-H2
β-Glc1-2	73.8	3.226	(dd)	J ₂₃ = 9.2	
β-Glc1-3	74.0	3.569	(t)	J ₃₄ = 8.9	
β-Glc1-4	78.3	3.607	(t)	J ₄₅ = 9.8	β-Glc1-C4 / Glc2-H1
β-Glc1-5	74.8	3.542	(ddd)	J _{56a/b} = 2.0/5.0	
β-Glc1-6a	59.6	3.904	(dd)	J _{6a6b} = 12.3	
β-Glc1-6b		3.755	(dd)		
β-Glc2-1	102.1	4.488	(d)	J ₁₂ = 7.9	Glc2-C1 / Glc1- H4(α&β), Glc2-H2
β-Glc2-2	72.9	3.464, 3.471	(2dd)	J ₂₃ = 9.4	
β-Glc2-3	83.6	3.708, 3.711	(2t)	J ₃₄ = 8.3	Glc2-C3 / Glc3-H1, Glc2-H2, Glc2-H4
β-Glc2-4	67.7	~3.46	(ob)	J ₄₅ = **	
β-Glc2-5	75.4	~3.45	(ob)	J _{56a/b} = 2.2/**	
β-Glc2-6a	60.3	3.870		J _{6a6b} = 12.4	

β -Glc2-6b		3.7	(2dd)			
		4.697,				Glc3-C1 /
β -Glc3-1	102.7	4.699	(dd)	$J_{12} = 7.9$		Glc2-H3,
β -Glc3-2	73.3	3.295	(dd)	$J_{23} = 9.5$		Glc3-H2
β -Glc3-3	73.4	3.466	(t)	$J_{34} = 9.4$		
β -Glc3-4	69.4	3.350	(t)	$J_{45} = 9.7$		
β -Glc3-5	75.8	3.424	(ddd)	$J_{56a/b} = 2.2/6.2.0$		
β -Glc3-6b	60.5	3.866	(dd)	$J_{6a6b} = 12.3$		
β -Glc3-6a		3.666	(dd)			

** unresolved (signal overlap)

10. Bibliography

Aguilera A. 2013. Eukaryotic Organisms in Extreme Acidic Environments, the Rio Tinto Case. *Life*: 363–374.

Ahmad HM, Rahman M-R, Ali Q, Awan S. 2015. Plant cuticular waxes: a review on functions, composition, biosynthesis mechanism and transportation. *Life Science Journal* **12**: 60–67.

Aigner S, Remias D, Karsten U, Holzinger A. 2013. Unusual phenolic compounds contribute to ecophysiological performance in the purple-colored green alga *Zygonium ericetorum* (Zygnematophyceae, Streptophyta) from a high-alpine habitat (R Bassi, Ed.). *Journal of Phycology* **49**: 648–660.

Al Hinai TZS, Vreeburg RAM, Mackay L, Murray L, Sadler IH, Fry SC. 2021. Fruit softening: evidence for pectate lyase action in vivo in date (*Phoenix dactylifera*) and rosaceous fruit cell walls. *Annals of Botany* **128**: 511–525.

Albersheim P, Darvill A, Roberts K, Sederoff R, Staehelin A. 2011. *Plant cell walls*. Garland Science. New York: Taylor and Francis Group.

Anderson CT. 2016. We be jammin': an update on pectin biosynthesis, trafficking and dynamics. *Journal of Experimental Botany* **67**: 495–502.

Aquino RS, Grativol C, Mourão PAS. 2011. Rising from the Sea: Correlations between Sulfated Polysaccharides and Salinity in Plants. *PLoS ONE* **6**: e 18862.

Ashline DJ, Lapadula AJ, Liu Y-H, et al. 2007. Carbohydrate structural isomers analyzed by sequential mass spectrometry. *Analytical chemistry* **79**: 3830–3842.

Bansala P, Vowell BJ, Hall M, Realff MJ, Lee JH, Bommarius AS. 2012. Elucidation of cellulose accessibility, hydrolysability and reactivity as the major limitations in the enzymatic hydrolysis of cellulose. *Bioresource technology* **107**: 243–250.

Bartels D, Baumann A, Maeder M, et al. 2017. Evolution of plant cell wall: Arabinogalactan-proteins from three moss genera show structural differences compared to seed plants. *Carbohydrate polymers* **163**: 227–235.

Bauer S. 2012. Mass Spectrometry for Characterizing Plant Cell Wall Polysaccharides. *Frontiers in Plant Science* **3**: 45.

Bauer S, Vasu P, Persson S, Mort AJ, Somerville CR. 2006. Development and application of a suite of polysaccharide-degrading enzymes for analyzing plant cell walls. *Proceedings of the National Academy of Sciences* **103**: 11417–11422.

Benassi L, Alessandri I, Vassalini I. 2021. Assessing Green Methods for Pectin Extraction from Waste Orange Peels. *Molecules* **26**: 1766.

Bonnin E, Dolo E, Le Goff A, Thibault J-F. 2002. Characterisation of pectin subunits released by an optimised combination of enzymes. *Carbohydrate Research* **337**: 1687–1696.

Bonnin E, Garnier C, Ralet M-C. 2014. Pectin-modifying enzymes and pectin-derived materials: applications and impacts. *Applied microbiology and biotechnology* **98**: 519–532.

- Borowitzka MA, Beardall J, Raven JA. 2016.** *The physiology of microalgae*. Springer.
- Borsuk AM, Roddy AB, Th  roux-Rancourt G, Brodersen CR. 2022.** Structural organization of the spongy mesophyll. *New Phytologist* **234**: 946–960.
- Bothwell JH. 2023.** *Seaweeds of the World: A Guide to Every Order*. Princeton Nature.
- Bothwell JH, Griffin JL. 2011.** An introduction to biological nuclear magnetic resonance spectroscopy. *Biological Reviews* **86**: 493–510.
- Bruggink C, Maurer R, Herrmann H, Cavalli S, Hoefler F. 2005.** Analysis of carbohydrates by anion exchange chromatography and mass spectrometry. *Journal of Chromatography A* **1085**: 104–109.
- Busi MV, Barchiesi J, Mart  n M, Gomez-Casati DF. 2014.** Starch metabolism in green algae. *Starch-St  rke* **66**: 28–40.
- Caffall KH, Mohnen D. 2009.** The structure, function, and biosynthesis of plant cell wall pectic polysaccharides. *Carbohydrate research* **344**: 1879–1900.
- Carafa A, Duckett JG, Knox PJ, Ligrone R. 2005.** Distribution of cell-wall xylans in bryophytes and tracheophytes: new insights into basal interrelationships of land plants. *New Phytologist* **168**: 231–240.
- Carpita NC, Filisetti-Cozzi TMCC. 1991.** Measurement of Uronic Acids without Interference from Neutral Sugars. *Analytical biochemistry* **197**: 157–162.
- Carpita NC, Gibeaut DM. 1993.** Structural models of primary cell walls in flowering plants: consistency of molecular structure with the physical properties of the walls during growth. *The Plant Journal* **3**: 1–30.
- Cassab GI. 1998.** Plant cell wall proteins. *Annual review of plant biology* **49**: 281–309.
- Cassolato JEF, Nosed   MD, Pujol CA, Pellizzari FM, Damonte EB, Duarte MER. 2008.** Chemical structure and antiviral activity of the sulfated heterorhamnan isolated from the green seaweed *Gayralia oxysperma*. *Carbohydrate research* **343**: 3085–3095.
- Cavalier DM, Lerouxel O, Neumetzler L, et al. 2008.** Disrupting two *Arabidopsis thaliana* xylosyltransferase genes results in plants deficient in xyloglucan, a major primary cell wall component. *The Plant Cell* **20**: 1519–1537.
- Chattopadhyay K, Mandal P, Lerouge P, Driouich A. 2007.** Sulphated polysaccharides from Indian samples of *Enteromorpha compressa* (Ulvales, Chlorophyta): Isolation and structural features. *Food Chemistry* **104**: 928–935.
- Chen J, Liang R, Liu W, et al. 2014.** Extraction of pectin from *Premna microphylla* turcz leaves and its physicochemical properties. *Carbohydrate polymers* **102**: 376–384.
- Cheng S, Xian W, Fu Y, et al. 2019.** Genomes of Subaerial Zygnematophyceae Provide Insights into Land Plant Evolution. *Cell* **179**: 1057-1067.e14.

- Cherno NK, Dudkin MS, Areshidze IV. 1976.** Pectin substances of *Chara aculeolata*. *Chemistry of Natural Compounds* **12**: 633–635.
- Chi Y, Li H, Wang Pei, et al. 2020.** Structural characterization of ulvan extracted from *Ulva clathrata* assisted by an ulvan lyase. *Carbohydrate Polymers* **229**: 115497.
- Chormova D, Messenger DJ, Fry SC. 2014.** Boron bridging of rhamnogalacturonan-II, monitored by gel electrophoresis, occurs during polysaccharide synthesis and secretion but not post-secretion. *The Plant Journal* **77**: 534–546.
- Clarke AE, Anderson RL, Stone BA. 1979.** Form and function of arabinogalactans and arabinogalactan-proteins. *Phytochemistry* **18**: 521–540.
- Cook ME, Graham LE. 2017.** Chlorokybophyceae, Klebsormidiophyceae, Coleochaetophyceae In: Archibald JM, Simpson AGB, Slamovits CH, eds. *Handbook of the protists*. Springer Cham, 185–204.
- Cosgrove DJ. 1993.** How Do Plant Cell Walls Extend? *Plant Physiology* **102**: 1–6.
- Cosgrove DJ. 2000a.** Expansive growth of plant cell walls. *Plant Physiology and Biochemistry* **38**: 109–124.
- Cosgrove DJ. 2000b.** Loosening of plant cell walls by expansins. *Nature* **407**: 321–326.
- Cosgrove DJ. 2014.** Re-constructing our models of cellulose and primary cell wall assembly. *Current opinion in Plant Biology* **22**: 122–131.
- Cosgrove DJ. 2015.** Plant expansins: diversity and interactions with plant cell walls. *Current opinion in plant biology* **25**: 162–172.
- Cosgrove D. 2016.** Catalysts of plant cell wall loosening. *F1000Research* **5 (F1000 Faculty Rev):119**.
- Cosgrove DJ, Jarvis MC. 2012.** Comparative structure and biomechanics of plant primary and secondary cell walls. *Frontiers in plant science* **3**: 204.
- Cracraft J, Donoghue MJ. 2004.** *Assembling the tree of life*. Oxford University Press.
- Delwiche CF, Cooper ED. 2015.** The evolutionary origin of a terrestrial flora. *Current Biology* **25**: R899-910.
- Delwiche CF, Graham LE, Thomson N. 1989.** Lignin-like compounds and sporopollenin coleochaete, an algal model for land plant ancestry. *Science* **245**: 399–401.
- Dhanoa PK, Sinclair AM, Mullen RT, Mathur J. 2006.** Illuminating subcellular structures and dynamics in plants: a fluorescent protein toolbox. *Botany* **84**: 515–522.
- Dick-Pérez M, Zhang Y, Hayes J, Salazar A, Zabolina OA, Hong M. 2011.** Structure and interactions of plant cell-wall polysaccharides by two- and three-dimensional magic-angle-spinning solid-state NMR. *Biochemistry* **50**: 989–1000.

- Domozych DS, Bagdan K. 2022.** The cell biology of charophytes: Exploring the past and models for the future. *Plant Physiology* **190**: 1588–1608.
- Domozych D, Ciancia M, Fangel JU, Mikkelsen MD, Ulvskov P, Willats WGT. 2012.** The cell walls of green algae: a journey through evolution and diversity. *Frontiers in plant science* **3**: 82.
- Domozych DS, Domozych CE. 2014.** Multicellularity in green algae: upsizing in a walled complex. *Frontiers in plant science* **5**: 649.
- Domozych D, Popper ZA, Sørensen I. 2016.** Charophytes: evolutionary giants and emerging model organisms. *Frontiers in plant science* **7**: 1470.
- Domozych DS, Serfis A, Kiemle SN, Gretz MR. 2007.** The structure and biochemistry of charophycean cell walls: I. Pectins of *Penium margaritaceum*. *Protoplasma* **230**: 99–115.
- Domozych DS, Sørensen I, Pettolino FA, Bacic A, Willats WGT. 2010.** The cell wall polymers of the charophycean green alga *Chara corallina*: Immunobinding and biochemical screening. *International journal of plant sciences* **171**: 345–361.
- Domozych DS, Sørensen I, Popper ZA, et al. 2014.** Pectin metabolism and assembly in the cell wall of the charophyte green alga *Penium margaritaceum*. *Plant Physiology* **165**: 105–118.
- Domozych DS, Sørensen I, Willats WGT. 2009.** The distribution of cell wall polymers during antheridium development and spermatogenesis in the Charophycean green alga, *Chara corallina*. *Annals of botany* **104**: 1045–1056.
- Domozych DS, Wells B, Shaw PJ. 1991.** Basket Scales of the Green Alga, *Mesostigma Viride*: Chemistry and Ultrastructure. *Journal of Cell Science* **100**: 397–407.
- Ebringerová A. 2005.** Structural diversity and application potential of hemicelluloses. *Macromolecular Symposia* **232**: 1–12.
- Eder M, Lütz-Meindl U. 2008.** Pectin-like carbohydrates in the green alga *Micrasterias* characterized by cytochemical analysis and energy filtering TEM. *Journal of Microscopy* **231**: 201–214.
- Eder M, Lütz-Meindl U. 2010.** Analyses and localization of pectin-like carbohydrates in cell wall and mucilage of the green alga *Netrium digitus*. *Protoplasma* **243**: 25–38.
- Eder M, Tenhaken R, Driouich A, Lütz-Meindl U. 2008.** Occurrence and characterization of arabinogalactan-like proteins and hemicelluloses in *Micrasterias* (Streptophyta) (1). *Journal of Phycology* **44**: 1221–1234.
- Elster J, Degma P, Kováčik L, Valentová L, Šramková K, Pereira AB. 2008.** Freezing and desiccation injury resistance in the filamentous green alga *Klebsormidium* from the Antarctic, Arctic and Slovakia. *Biologia* **63**: 843–851.

- Fraeye I, Colle I, Vandevenne E, et al. 2010.** Influence of pectin structure on texture of pectin–calcium gels. *Innovative food science & emerging technologies* **11**: 401–409.
- Franková L, Fry SC. 2012.** Trans-alpha-xylosidase, a widespread enzyme activity in plants, introduces (1->4)-alpha-D-xylobiose side-chains into xyloglucan structures. *Phytochemistry* **78**: 29–43.
- Frei E, Preston RD. 1964.** Non-cellulosic structural polysaccharides in algal cell walls I. Xylan in siphonous green algae. *Proceedings of the Royal Society of London. B.* **160**: 293–313.
- Fry SC. 1983.** Feruloylated pectins from the primary cell wall: their structure and possible functions. *Planta* **157**: 111–123.
- Fry SC. 1995.** Polysaccharide-Modifying Enzymes in the Plant Cell Wall. *Annual Review of Plant Physiology and Plant Molecular Biology* **46**: 497–520.
- Fry SC. 2000.** *The Growing Plant Cell Wall: Chemical and Metabolic Analysis*. Reprint Edition, The Blackburn Press.
- Fry SC. 2001.** Plant cell wall biosynthesis. *e LS*.
- Fry SC. 2011.** Cell wall polysaccharide composition and covalent crosslinking In: *Annual Plant reviews*. Blackwell Publishing Ltd., 1–42.
- Fry SC. 2017.** Cell walls. *Encyclopedia of Applied Plant Sciences* **1**: 161–173.
- Fry SC. 2020.** High-Voltage Paper Electrophoresis (HVPE) In: Popper ZA, ed. *The Plant Cell Wall. Methods in Molecular Biology*. NY: Humana, New York, 2149.
- Fry SC, Nesselrode BHWA, Miller JG, Mewburn BR. 2008.** Mixed-linkage (1→3,1→4)-β-d-glucan is a major hemicellulose of Equisetum (horsetail) cell walls. *New phytologist* **179**: 104–115.
- Fry SC, York WS, Albersheim P, et al. 1993.** An unambiguous nomenclature for xyloglucan-derived oligosaccharides. *Physiologia Plantarum* **89**: 1–3.
- Gao X, Qu H, Shan S, et al. 2020.** A novel polysaccharide isolated from Ulva Pertusa: Structure and physicochemical property. *Carbohydrate Polymers* **233**: 115849.
- Gawkowska D, Cybulska J, Zdunek A. 2018.** Structure-related gelling of pectins and linking with other natural compounds: A review. *Polymers* **10**: 762.
- Geitmann A. 2023.** Seeing clearly – Plant anatomy through Katherine Esau’s microscopy lens. *Journal of Microscopy*: 1–13.
- Ghaffar SH, Fan M. 2013.** Structural analysis for lignin characteristics in biomass straw. *Biomass and bioenergy* **57**: 264–279.
- Gilbert HJ. 2010.** The Biochemistry and Structural Biology of Plant Cell Wall Deconstruction. *Plant Physiology* **153**: 444–455.

- Gow NAR, Latge J-P, Munro CA. 2017.** The fungal cell wall: structure, biosynthesis, and function. *Microbiology Spectrum* **5**.
- Graham LE, Arancibia-Avila P, Taylor WA, Strother PK, Cook ME. 2012.** Aeroterrestrial Coleochaete (Streptophyta, Coleochaetales) models early plant adaptation to land. *American journal of botany* **99**: 130–144.
- Gyure RA, Konopka A, Brooks A, Doemel W. 1987.** Algal and bacterial activities in acidic (pH 3) strip mine lakes. *Applied and Environmental Microbiology* **53**: 2069–2076.
- Hall JD, Delwiche CF. 2007.** In the shadow of giants: systematics of the charophyte green algae In: Brodie J, Lewis J, eds. *Unraveling the Algae: the Past, Present, and Future of Algal Systematics*. CRC Press, 155–169.
- Harholt J, Moestrup Ø, Ulvskov P. 2016.** Why plants were terrestrial from the beginning. *Trends in Plant Science* **21**: 96–101.
- Henry RJ. 2005.** *Plant diversity and evolution: genotypic and phenotypic variation in higher plants*. Cabi Publishing.
- Herburger K, Holzinger A. 2015.** Localization and quantification of callose in the streptophyte green algae *Zygnema* and *Klebsormidium*: correlation with desiccation tolerance. *Plant and Cell Physiology* **56**: 2259–2270.
- Herburger K, Ryan LM, Popper ZA, Holzinger A. 2018.** Localisation and substrate specificities of transglycanases in charophyte algae relate to development and morphology. *Journal of Cell Science* **131**: 203–208.
- Herburger K, Xin A, Holzinger A. 2019.** Homogalacturonan Accumulation in Cell Walls of the Green Alga *Zygnema* sp. (Charophyta) Increases Desiccation Resistance. *Frontiers in Plant Science* **10**.
- Heredia-Guerrero JA, Benítez JJ, Domínguez E, et al. 2014.** Infrared and Raman spectroscopic features of plant cuticles: a review. *Frontiers in plant science* **5**: 305.
- Holzinger A, Pichrtová M. 2016.** Abiotic stress tolerance of charophyte green algae: new challenges for omics techniques. *Frontiers in plant science* **7**: 678.
- Hsieh YSY, Harris PJ. 2019.** Xylans of Red and Green Algae: What Is Known about Their Structures and How They Are Synthesised? *Polymers* **11**: 354.
- Ikegaya H, Hayashi T, Kaku T, Iwata K, Sonobe S, Shimmen T. 2008.** Presence of xyloglucan-like polysaccharide in *Spirogyra* and possible involvement in cell–cell attachment. *Phycological Research* **56**: 216–222.
- Jamet E, Albenne C, Boudart G, Irshad M, Canut H, Pont-Lezica R. 2008.** Recent advances in plant cell wall proteomics. *Proteomics* **8**: 893–908.
- Jamet E, Canut H, Boudart G, Pont-Lezica RF. 2006.** Cell wall proteins: a new insight through proteomics. *Trends in plant science* **11**: 33–39.

- Jarvis MC, Briggs SPH, Knox P. 2003.** Intercellular adhesion and cell separation in plants. *Plant, Cell & Environment* **26**: 977–989.
- Jedvert K, Heinze T. 2017.** Cellulose modification and shaping—a review. *Journal of Polymer Engineering* **37**: 845–860.
- Jensen JK, Busse-Wicher M, Poulsen CP, et al. 2018.** Identification of an algal xylan synthase indicates that there is functional orthology between algal and plant cell wall biosynthesis. *New Phytologist* **218**: 1049–1060.
- Jiao C, Sørensen I, Sun X, et al. 2020.** The *Penium margaritaceum* Genome: Hallmarks of the Origins of Land Plants. *Cell* **181**: 1097-1111.e12.
- Jork H, Funk W, Fischer W, Wimmer H. 1994.** *Thin layer chromatography: reagents and detection methods*. Weimheim: WCH.
- Kailemia MJ, Ruhaak LR, Lebrilla CB, Amster IJ. 2014.** Oligosaccharide analysis by mass spectrometry: a review of recent developments. *Analytical chemistry* **86**: 196–212.
- Kaplan DL (Ed.). 1998.** *Biopolymers from Renewable Resources*. Berlin, Heidelberg: Springer.
- Kaplan F, Lewis LA, Wastian J, Holzinger A. 2012.** Plasmolysis effects and osmotic potential of two phylogenetically distinct alpine strains of *Klebsormidium* (Streptophyta). *Protoplasma* **249**: 789–804.
- Karsten U, Herburger K, Holzinger A. 2016.** Living in biological soil crust communities of African deserts—physiological traits of green algal *Klebsormidium* species (Streptophyta) to cope with desiccation, light and temperature gradients. *Journal of plant physiology* **194**: 2–12.
- Karsten U, Holzinger A. 2014.** Green algae in alpine biological soil crust communities: acclimation strategies against ultraviolet radiation and dehydration. *Biodiversity and conservation* **23**: 1845–1858.
- Karsten U, Lütz C, Holzinger A. 2010.** Ecophysiological performance of the aeroterrestrial green alga *Klebsormidium crenulatum* (Charophyceae, Streptophyta) isolated from an alpine soil crust with an emphasis on desiccation stress. *Journal of Phycology* **46**: 1187–1197.
- Karsten U, Pröschold T, Mikhailyuk T, Holzinger A. 2013.** Photosynthetic performance of different genotypes of the green alga *Klebsormidium* sp. (Streptophyta) isolated from biological soil crusts of the Alps. *Algological Studies* **142**: 45–62.
- Karunaratne DN. 2012.** *The complex world of polysaccharides*. BoD—Books on Demand.
- Kaya M, Sousa AG, Crépeau M-J, Sørensen SO, Ralet M-C. 2014.** Characterization of citrus pectin samples extracted under different conditions: influence of acid type and pH of extraction. *Annals of botany* **114**: 1319–1326.
- Keegstra K. 2010.** Plant Cell Walls. *Plant Physiology* **154**: 483–486.

- Keegstra K, Talmadge KW, Bauer WD, Albersheim P. 1973.** The structure of plant cell walls: III. A model of the walls of suspension-cultured sycamore cells based on the interconnections of the macromolecular components. *Plant physiology* **51**: 188–197.
- Kiemle SN. 2010.** *Extracellular matrix of the charophycean green algae.*
- Kim U-J, Eom SH, Wada M. 2010.** Thermal decomposition of native cellulose: influence on crystallite size. *Polymer Degradation and Stability* **95**: 778–781.
- Kirkwood S. 1974.** Unusual polysaccharides. *Annual review of biochemistry* **43**: 401–417.
- Kitzing C, Pröschold T, Karsten U. 2014.** UV-induced effects on growth, photosynthetic performance and sunscreen contents in different populations of the green alga *Klebsormidium fluitans* (Streptophyta) from alpine soil crusts. *Microbial ecology* **67**: 327–340.
- Kochumalayil JJ, Berglund LA. 2014.** Water-soluble hemicelluloses for high humidity applications—enzymatic modification of xyloglucan for mechanical and oxygen barrier properties. *Green Chemistry* **16**: 1904–1910.
- Kremer C, Pettolino F, Bacic A, Drinnan A. 2004.** Distribution of cell wall components in *Sphagnum* hyaline cells and in liverwort and hornwort elaters. *Planta* **219**: 1023–1035.
- Lahaye M, Jegou D, Buleon A. 1994.** Chemical characteristics of insoluble glucans from the cell wall of the marine green alga *Ulva lactuca* (L.) Thuret. *Carbohydrate research* **262**: 115–125.
- Lahaye M, Robic A. 2007.** Structure and functional properties of ulvan, a polysaccharide from green seaweeds. *Biomacromolecules* **8**: 1765–1774.
- Lampugnani ER, Khan GA, Somssich M, Persson S. 2018.** Building a plant cell wall at a glance. *Journal of Cell Science* **131**: jcs207373.
- Lazaridou A, Biliaderis CG, Micha-Screttas M, Steele BR. 2004.** A comparative study on structure-function relations of mixed-linkage (1→3),(1→4) linear β -D-glucans. *Food Hydrocolloids* **18**: 837–855.
- Lee S-J, Saravanan RS, Damasceno CMB, Yamane H, Kim B-D, Rose JKC. 2004.** Digging deeper into the plant cell wall proteome. *Plant physiology and Biochemistry* **42**: 979–988.
- Lewis LA, McCourt RM. 2004.** Green algae and the origin of land plants. *American journal of botany* **91**: 1535–1556.
- Ligrone R, Duckett JG, Renzaglia KS. 2012.** Major transitions in the evolution of early land plants: a bryological perspective. *Annals of botany* **109**: 851–871.
- Linskens H-Ferdinand, Jackson JF (Eds.). 1989.** *Plant Fibers.* Berlin, Heidelberg: Springer.

- Liu H-M. 2016.** Embracing the pteridophyte classification of Ren-Chang Ching using a generic phylogeny of Chinese ferns and lycophytes. *Journal of Systematics and Evolution* **54**: 307–335.
- Lopes Leivas C, Iacomini M, Cordeiro LMC. 2016.** Pectic type II arabinogalactans from starfruit (*Averrhoa carambola* L.). *Food Chemistry* **199**: 252–257.
- Malinovsky FG, Fangel JU, Willats WGT. 2014.** The role of the cell wall in plant immunity. *Frontiers in plant science* **5**: 178.
- Mao W, Zang X, Li Y, Zhang H. 2006.** Sulfated polysaccharides from marine green algae *Ulva conglobata* and their anticoagulant activity. *Journal of Applied Phycology* **18**: 9–14.
- Matsunaga T, Ishii T, Matsumoto S, et al. 2004.** Occurrence of the primary cell wall polysaccharide rhamnogalacturonan II in pteridophytes, lycophytes, and bryophytes. Implications for the evolution of vascular plants. *Plant Physiology* **134**: 339–351.
- Mattox KR, Stewart KD. 1984.** Classification of the green algae: a concept based on comparative cytology In: Irvine D, John DM, eds. *Systematics of the Green Algae*. London, 29–72.
- McCann MC, Roberts K. 1991.** Architecture of the primary cell wall In: Lloyd CW, ed. *The Cytoskeletal Basis of Plant Growth and Form*. London: Academic Press, 109–129.
- McCleary BV, McKie VA, Draga A, Rooney E, Mangan D, Larkin J. 2015.** Hydrolysis of wheat flour arabinoxylan, acid-debranched wheat flour arabinoxylan and arabino-xylo-oligosaccharides by β -xylanase, α -L-arabinofuranosidase and β -xylosidase. *Carbohydrate research* **407**: 79–96.
- McCourt RM, Delwiche CF, Karol KG. 2004.** Charophyte algae and land plant origins. *Trends in Ecology & Evolution* **19**: 661–666.
- McDougall GJ, Fry SC. 1988.** Inhibition of Auxin-Stimulated Growth of Pea Stem Segments by a Specific Nonasaccharide of Xyloglucan. *Planta* **175**: 412–16.
- Mikkelsen MD, Harholt J, Ulvskov P, et al. 2014.** Evidence for land plant cell wall biosynthetic mechanisms in charophyte green algae. *Annals of botany* **114**: 1217–1236.
- Mikkelsen MD, Harholt J, Westereng B, et al. 2021.** Ancient origin of fucosylated xyloglucan in charophycean green algae. *Communications Biology* **4**: 754.
- Minic Z. 2008.** Physiological roles of plant glycoside hydrolases. *Planta* **227**: 723–40.
- Míguez F, Holzinger A, Fernandez-Marin B, García-Plazaola JI, Karsten U, Gustavs L. 2020.** Ecophysiological changes and spore formation: two strategies in response to low-temperature and high-light stress in *Klebsormidium* cf. *flaccidum* (Klebsormidiophyceae, Streptophyta). *Journal of Phycology* **56**: 649–661.

- Moller I, Sørensen I, Bernal AJ, et al.** High-throughput mapping of cell-wall polymers within and between plants using novel microarrays. *The Plant journal : for cell and molecular biology* **50**: 118–128.
- Moon RJ, Martini A, Nairn J, Simonsen J, Youngblood J. 2011.** Cellulose nanomaterials review: structure, properties and nanocomposites. *Chemical Society Reviews* **40**: 3941–3994.
- Moore JP, Farrant JM, Driouich A. 2008.** A role for pectin-associated arabinans in maintaining the flexibility of the plant cell wall during water deficit stress. *Plant Signaling & Behavior* **3**: 102–104.
- Morris GA, Ralet M-C. 2012.** The effect of neutral sugar distribution on the dilute solution conformation of sugar beet pectin. *Carbohydrate polymers* **88**: 1488–1491.
- Nagao M, Matsui K, Uemura M. 2008.** Klebsormidium flaccidum, a charophycean green alga, exhibits cold acclimation that is closely associated with compatible solute accumulation and ultrastructural changes. *Plant, cell & environment* **31**: 872–885.
- Nagy G, Peng T, Pohl NLB. 2017.** Recent liquid chromatographic approaches and developments for the separation and purification of carbohydrates. *Analytical Methods* **9**: 3579–3593.
- Naidu DS, Hlangothi SP, John MJ. 2018.** Bio-based products from xylan: A review. *Carbohydrate polymers* **179**: 28–41.
- Ndeh D, Rogowski A, Cartmell A, et al. 2017.** Complex pectin metabolism by gut bacteria reveals novel catalytic functions. *Nature* **544**: 65–70.
- Necchi OJ. 2016.** *River Algae*. Springer.
- Nelson DL, Cox MM, Lehninger AL. 2008.** *Principles of biochemistry*. Freeman New York.
- Ngouémazong DE, Kabuye G, Fraeye I, et al. 2012.** Effect of debranching on the rheological properties of Ca²⁺ pectin gels. *Food Hydrocolloids* **26**: 44–53.
- Nieminen K, Testova L, Paananen M, Sixta H. 2015.** Novel insight in carbohydrate degradation during alkaline treatment. *Holzforschung* **69**: 667–675.
- Niklas KJ. 2004.** The cell walls that bind the tree of life. *Bioscience* **54**: 831–841.
- Nishiyama T, Sakayama H, de Vries J, et al. 2018.** The Chara Genome: Secondary Complexity and Implications for Plant Terrestrialization. *Cell* **174**: 448–464.e24.
- Nothnagel AL, Nothnagel EA. 2007.** Primary cell wall structure in the evolution of land plants. *Journal of Integrative Plant Biology* **49**: 1271–1278.
- Novotný C, Cajthaml T, Svobodová K, Susla M, Sasek V. 2009.** Irpex lacteus, a White-Rot Fungus with Biotechnological Potential - A Review. *Folia Microbiologica* **54**: 375–390.

- Oakenfull D, Scott A. 1984.** Hydrophobic Interaction in the Gelation of High Methoxyl Pectins. *Food Science* **49**: 1093–1098.
- Omarsdottir S, Petersen BO, Paulsen BS, Togola A, Duus JØ, Olafsdottir ES. 2006.** Structural characterisation of novel lichen heteroglycans by NMR spectroscopy and methylation analysis. *Carbohydrate research* **341**: 2449–2455.
- O'Neill MA, Ishii T, Albersheim P, Darvill AG. 2004.** Rhamnogalacturonan II: structure and function of a borate cross-linked cell wall pectic polysaccharide. *Annual Review of Plant Biology* **55**: 109–139.
- Oosterveld A, Beldman G, Voragen AGJ. 2002.** Enzymatic modification of pectic polysaccharides obtained from sugar beet pulp. *Carbohydrate polymers* **48**: 73–81.
- O'Rourke C, Gregson T, Murray L, Sadler IH, Fry SC. 2015.** Sugar composition of the pectic polysaccharides of charophytes, the closest algal relatives of land-plants: presence of 3-O-methyl-D-galactose residues. *Annals of botany* **116**: 225–236.
- Palacio-López K, Sun L, Reed R, et al. 2020.** Experimental Manipulation of Pectin Architecture in the Cell Wall of the Unicellular Charophyte, *Penium margaritaceum*. *Frontiers in Plant Science* **11**.
- Palacio-López K, Tinaz B, Holzinger A, Domozych DS. 2019.** Arabinogalactan proteins and the extracellular matrix of charophytes: a sticky business. *Frontiers in Plant Science* **10**: 447.
- Park YB, Cosgrove DJ. 2012.** A revised architecture of primary cell walls based on biomechanical changes induced by substrate-specific endoglucanases. *Plant Physiology* **158**: 1933–1943.
- Pauly M, Albersheim P, Darvill A, York WS. 1999.** Molecular domains of the cellulose/xyloglucan network in the cell walls of higher plants. *The Plant journal : for cell and molecular biology* **20**: 629–639.
- Peña MJ, Darvill AG, Eberhard S, York WS, O'Neill MA. 2008.** Moss and liverwort xyloglucans contain galacturonic acid and are structurally distinct from the xyloglucans synthesized by hornworts and vascular plants. *Glycobiology* **18**: 891–904.
- Permann C, Herburger K, Felhofer M, Gierlinger N, Lewis LA, Holzinger A. 2021.** Induction of Conjugation and Zygosporangium Cell Wall Characteristics in the Alpine *Spirogyra mirabilis* (Zygnematophyceae, Charophyta): Advantage under Climate Change Scenarios? *Plants* **10**.
- Permann C, Herburger K, Nierdermeir M, Felhofer M, Gierlinger N, Holzinger A. 2021.** Cell wall characteristics during sexual reproduction of *Mougeotia* sp. (Zygnematophyceae) revealed by electron microscopy, glycan microarrays and RAMAN spectroscopy. *Protoplasma* **258**: 1261–1275.
- Piglowska M, Kurc B, Rymaniak L, Lijewski P, Fuc P.** Kinetics and Thermodynamics of Thermal Degradation of Different Starches and Estimation the OH Group and H₂O Content on the Surface by TG/DTG-DTA. *Polymers (Basel)* **12**: 357.

- Piršelová B, Matušíková I. 2013.** Callose: the plant cell wall polysaccharide with multiple biological functions. *Acta Physiologiae Plantarum* **35**: 635–644.
- Ponnusamy VK, Nguyen DD, Dharmaraja J, et al. 2019.** A review on lignin structure, pretreatments, fermentation reactions and biorefinery potential. *Bioresource technology* **271**: 462–472.
- Popper ZA. 2006.** The cell walls of pteridophytes and other green plants—a review. *The Fern Gazette* **17**: 315–332.
- Popper ZA. 2008.** Evolution and diversity of green plant cell walls. *Current opinion in plant biology* **11**: 286–292.
- Popper ZA, Fry SC. 2003.** Primary cell wall composition of bryophytes and charophytes. *Annals of botany* **91**: 1–12.
- Popper ZA, Fry SC. 2004.** Primary cell wall composition of pteridophytes and spermatophytes. *New Phytologist* **164**: 165–174.
- Popper ZA, Fry SC. 2005.** Widespread occurrence of a covalent linkage between xyloglucan and acidic polysaccharides in suspension-cultured angiosperm cells. *Annals of Botany* **96**: 91–99.
- Popper ZA, Michel G, Hervé C, et al. 2011.** Evolution and diversity of plant cell walls: from algae to flowering plants. *Annual review of plant biology* **62**: 567–590.
- Popper ZA, Sadler IH, Fry SC. 2003.** α -d-Glucuronosyl-(1 \rightarrow 3)-L-galactose, an unusual disaccharide from polysaccharides of the hornwort *Anthoceros caucasicus*. *Phytochemistry* **64**: 325–335.
- Popper ZA, Sadler IH, Fry SC. 2004.** 3-O-Methylrhamnose in lower land plant primary cell walls. *Biochemical Systematics and Ecology* **32**: 279–289.
- Popper ZA, Tuohy MG. 2010.** Beyond the green: understanding the evolutionary puzzle of plant and algal cell walls. *Plant physiology* **153**: 373–383.
- Powning RF, Irzykiewicz H. 1967.** Separation of chitin oligosaccharides by thin-layer chromatography. *Journal of Chromatography A* **29**: 115–119.
- Prabhu M, Chemozanov A, Gottlieb R, et al. 2019.** Starch from the sea: The green macroalga *Ulva ohnoi* as a potential source for sustainable starch production in the marine biorefinery. *Algal Research* **37**: 215–227.
- Ray B. 2006.** Polysaccharides from *Enteromorpha compressa*: Isolation, purification and structural features. *Carbohydrate polymers* **66**: 408–416.
- Ray B, Lahaye M. 1995.** Cell-wall polysaccharides from the marine green alga *Ulva "rigida"* (Ulvales, Chlorophyta). Extraction and chemical composition. *Carbohydrate Research* **274**: 251–261.

- Reina-Pinto JJ, Yephremov A. 2009.** Surface lipids and plant defenses. *Plant Physiology and Biochemistry* **47**: 540–549.
- Rinaudo M. 2004.** Role of substituents on the properties of some polysaccharides. *Biomacromolecules* **5**: 1155–1165.
- Rindi F, Guiry MD, López-Bautista JM. 2008.** Distribution, morphology, and phylogeny of Klebsormidium (Klebsormidiales, Charophyceae) in urban environments in Europe. *Journal of Phycology* **44**: 1529–1540.
- Rippin M, Borchhardt N, Karsten U, Becker B. 2019.** Cold Acclimation Improves the Desiccation Stress Resilience of Polar Strains of Klebsormidium (Streptophyta). *Frontiers in microbiology* **10**: 1730.
- Robic A, Sassi J-F, Dion P, Lerat Y, Lahaye M. 2009.** Seasonal variability of physicochemical and rheological properties of ulvan in two *Ulva* species (Chlorophyta) from the Brittany coast. *Journal of phycology* **45**: 962–973.
- Rose JKC. 2003.** *The plant cell wall*. CRC Press.
- Rose JKC, Lee S-J. 2010.** Straying off the highway: trafficking of secreted plant proteins and complexity in the plant cell wall proteome. *Plant Physiology* **153**: 433–436.
- Rydahl MG, Kračun SK, Fangel JU, et al. 2017.** Development of novel monoclonal antibodies against starch and ulvan - implications for antibody production against polysaccharides with limited immunogenicity. *Scientific Reports* **7**: 9326.
- Ryšánek D, Holzinger A, Škaloud P. 2016.** Influence of substrate and pH on the diversity of the aeroterrestrial alga Klebsormidium (Klebsormidiales, Streptophyta): a potentially important factor for sympatric speciation. *Phycologia* **55**: 347–358.
- Saeman JF, Moore WE, Mitchell RL, Millett MA. 1954.** In: *Tappi*.336–343.
- Sahoo D, Seckbach J. 2015.** *The algae world*. Springer.
- Sarkar P, Bosneaga E, Auer M. 2009.** Plant cell walls throughout evolution: towards a molecular understanding of their design principles. *Journal of experimental botany* **60**: 3615–3635.
- Scheller HV, Ulvskov P. 2010.** Hemicelluloses. *Annual review of plant biology* **61**: 263–289.
- Scherp P, Grotha R, Kutschera U. 2001.** Occurrence and phylogenetic significance of cytokinesis-related callose in green algae, bryophytes, ferns and seed plants. *Plant Cell Reports* **20**: 143–149.
- Schröder R, Nicolas P, Vincent SJF, Fischer M, Reymond S, Redgwell RJ. 2001.** Purification and characterisation of a galactoglucomannan from kiwifruit (*Actinidia deliciosa*). *Carbohydrate Research* **331**: 291–306.

- Schultink A, Liu L, Zhu L, Pauly M. 2014.** Structural diversity and function of xyloglucan sidechain substituents. *Plants* **3**: 526–542.
- Sénéchal F, Wattier C, Rustérucci C, Pelloux J. 2014.** Homogalacturonan-modifying enzymes: structure, expression, and roles in plants. *Journal of Experimental Botany* **65**: 5125–5160.
- Serrano M, Coluccia F, Torres M, L’Haridon F, Métraux J-P. 2014.** The cuticle and plant defense to pathogens. *Frontiers in plant science* **5**: 274.
- Séveno M, Voxeur A, Rihouey C, et al. 2009.** Structural characterisation of the pectic polysaccharide rhamnogalacturonan II using an acidic fingerprinting methodology. *Planta* **230**: 947–957.
- Shi H, Wan Y, Li O, et al. 2020.** Two-step hydrolysis method for monosaccharide composition analysis of natural polysaccharides rich in uronic acids. *Food Hydrocolloids* **101**: 105524.
- Showalter AM. 1993.** Structure and function of plant cell wall proteins. *The Plant Cell* **5**: 9–23.
- Škaloud P, Lukešová A, Malavasi V, Ryšánek D, Hřčková K, Rindi F. 2014.** Molecular evidence for the polyphyletic origin of low pH adaptation in the genus *Klebsormidium* (Klebsormidiophyceae, Streptophyta). *Plant Ecology and Evolution* **147**: 333–345.
- Somerville C, Bauer S, Brininstool G, et al. 2004.** Toward a systems approach to understanding plant cell walls. *Science* **306**: 2206–2211.
- Sooksawat N, Meetam M, Kruatrachue M, Pokethitiyook P, Inthorn D. 2016.** Equilibrium and kinetic studies on biosorption potential of charophyte biomass to remove heavy metals from synthetic metal solution and municipal wastewater. *Bioremediation journal* **20**: 240–251.
- Sørensen I, Fei Z, Andreas A, Willats WGT, Domozych DS, Rose JKC. 2013.** Stable transformation and reverse genetic analysis of *Penium margaritaceum*: a platform for studies of charophyte green algae, the immediate ancestors of land plants. *The Plant Journal* **77**: 339–351.
- Sørensen I, Pettolino FA, Bacic A, et al. 2011.** The charophycean green algae provide insights into the early origins of plant cell walls. *The Plant Journal* **68**: 201–211.
- Spiridon I, Popa VI. 2008.** Hemicelluloses: major sources, properties and applications In: Naceur Belgacem M, Gandini A, eds. *Monomers, polymers and composites from renewable resources*. Elsevier, 289–304.
- Stevens AE, McCarthy BC, Vis ML. 2001.** Metal Content of *Klebsormidium*-Dominated (Chlorophyta) Algal Mats from Acid Mine Drainage Waters in Southeastern Ohio. *The Journal of the Torrey Botanical Society* **128**: 226–233.
- Stewart KD, Mattox KR. 1975.** Comparative cytology, evolution and classification of the green algae with some consideration of the origin of other organisms with chlorophylls a and b. *The Botanical Review* **41**: 104–135.

- Sticklen MB. 2008.** Plant genetic engineering for biofuel production: towards affordable cellulosic ethanol. *Nature Reviews Genetics* **9**: 433–443.
- Stiger-Pouvreau V, Bourgoignon N, Deslandes E. 2016.** Carbohydrates from seaweeds In: *Seaweed in health and disease prevention*. Elsevier, 223–274.
- Tosif MM, Najda A, Bains A, et al. 2021.** A Comprehensive Review on Plant-Derived Mucilage: Characterization, Functional Properties, Applications, and Its Utilization for Nanocarrier Fabrication. *Polymers (Basel)* **13**: 1066.
- Triboit F, Laffont-Schwob I, Demory F, et al. 2010.** Heavy metal lability in porewater of highway detention pond sediments in South-Eastern France in relation to submerged vegetation. *Water, Air, & Soil Pollution* **209**: 229–240.
- Van Oostende-Triplet C, Guillet D, Triplet T, Pandzic E, Wiseman PW, Geitmann A. 2017.** Vesicle dynamics during plant cell cytokinesis reveals distinct developmental phases. *Plant Physiology* **174**: 1544–1558.
- Van Sandt VST, Stieperaere H, Guisez Y, Verbelen J-P, Vissenberg K. 2007.** XET activity is found near sites of growth and cell elongation in bryophytes and some green algae: new insights into the evolution of primary cell wall elongation. *Annals of Botany* **99**: 39–51.
- Vorwerk S, Somerville S, Somerville C. 2004.** The role of plant cell wall polysaccharide composition in disease resistance. *Trends in plant science* **9**: 203–209.
- Wang T, Hong M. 2016.** Solid-state NMR investigations of cellulose structure and interactions with matrix polysaccharides in plant primary cell walls. *Journal of experimental botany* **67**: 503–514.
- Wang D, Kanyuka K, Papp-Rupar M. 2023.** Pectin: a critical component in cell-wall-mediated immunity. *Trends in Plant Science* **28**: 10–13.
- Wang S, Li L, Li H, et al. 2020.** Genomes of early-diverging streptophyte algae shed light on plant terrestrialization. *Nature Plants* **6**: 95–106.
- Wang T, Phyto P, Hong M. 2016.** Multidimensional solid-state NMR spectroscopy of plant cell walls. *Solid state nuclear magnetic resonance* **78**: 56–63.
- Wang X, Zhang Z, Yao Z, Zhao M, Qi H. 2013.** Sulfation, anticoagulant and antioxidant activities of polysaccharide from green algae *Enteromorpha linza*. *International journal of biological macromolecules* **58**: 225–230.
- Willför S, Sundberg K, Tenkanen M, Holmbom B. 2008.** Spruce-derived mannans—A potential raw material for hydrocolloids and novel advanced natural materials. *Carbohydrate Polymers* **72**: 197–210.
- Wolf S, Hématy K, Höfte H. 2012.** Growth control and cell wall signaling in plants. *Annual review of plant biology* **63**: 381–407.

Xin A, Fei Y, Molnar A, Fry SC. Cutin:cutin-acid endo-transacylase (CCT), a cuticle-remodelling enzyme activity in the plant epidermis. *The Biochemical journal* **478**: 777–798.

Zhang N, Li S, Xiong L, Hong Y, Chen Y. 2015. Cellulose-hemicellulose interaction in wood secondary cell-wall. *Modelling and Simulation in Materials Science and Engineering* **23**: 85–100.

Zhou Y, Kobayashi M, Awano T, Matoh T, Takabe K. 2018. A new monoclonal antibody against rhamnogalacturonan II and its application to immunocytochemical detection of rhamnogalacturonan II in Arabidopsis roots. *Bioscience, Biotechnology, and Biochemistry* **82**: 1780–1789.

Zykwinska A, Thibault J-F, Ralet M-C. 2007. Organization of pectic arabinan and galactan side chains in association with cellulose microfibrils in primary cell walls and related models envisaged. *Journal of experimental botany* **58**: 1795–1802.

Zykwinska A, Thibault J-F, Ralet M-C. 2008. Competitive binding of pectin and xyloglucan with primary cell wall cellulose. *Carbohydrate polymers* **74**: 957–961.